A microstructural study of
Musselwhite Mine and Hammond Reef shear-zone-hosted gold deposits

By

Maura J. Kolb

A thesis submitted in partial fulfillment of the requirements for the degree of:

Master of Science in Geology

2010

Lakehead University

955 Oliver Road

Thunder Bay, ON P7B 5E1

Abstract

Musselwhite Mine and Hammond Reef are shear-zone-hosted gold deposits located in Northwestern Ontario, in the Western Superior Province of the Canadian Shield. A detailed microscopic investigation of three gold-hosting lithologies from Musselwhite Mine and Hammond Reef demonstrate close similarities in the microstructures which host gold and the relative timing of gold mineralization. The gold deposit at Musselwhite Mine is hosted by metamorphosed banded iron formation, while Hammond Reef is hosted by metamorphosed tonalite. Despite the difference in rock types, Musselwhite Mine and Hammond Reef are similar in that that they are located proximal to regional shear zones, have undergone regional metamorphism and are dominated by ductile deformation. Although these two deposits are hosted by completely different lithologies the microstructures which host gold are very similar, indicating structural control on mineralization at a microscopic scale.

The most common gold-hosting microstructures in these gold deposits result from heterogeneous deformation. Gold mineralization commonly occurs in fractures in competent minerals such as garnet and pyrite in every lithology in this study. These gold-hosting fractures do not extend throughout the matrix but are restricted to the competent minerals because the competent minerals are resistant to the ductile deformation around them. Gold mineralization is also associated with other deformation-induced microstructures, such as strain shadows. Gold mineralization is hosted by metamorphic minerals at both Musselwhite Mine and Hammond Reef. Gold inclusions occur at Musselwhite Mine in such metamorphic minerals as grunerite and garnet and at Hammond Reef gold inclusions occur in metamorphic muscovite. Also gold mineralization commonly occurs on plane defects, for example on grain boundaries.

Relative timing of gold mineralization is shown to have occurred during ongoing metamorphism and deformation. Inclusions within metamorphic minerals indicate that gold mineralization must have occurred before or during metamorphism, while gold mineralization associated with deformational features indicate gold mineralization to have occurred during or after deformation. This thesis demonstrates close similarities between the relative timing of gold mineralization as well as the microstructures which host gold at Musselwhite Mine and Hammond Reef.

Acknowledgements:

This thesis is dedicated to my family. Thank you for all your love and support.

First a great thanks goes to my advisor Dr. Mary Louise Hill for seeing my potential and pushing me to strive for excellence. The Geology department at Lakehead University is filled with many helpful and intelligent people, I have many to thank for their willingness to answer my questions and point me in the right direction. Thank you Dr. Andrew Conly for your help with the XRD analysis, Dr. Stephen Kissin for your knowledge of pyrite etching and Dr. Shannon Zurevinski for your patience and time spent on the SEM with me. A very special thank you goes to Anne Hammond who made an enormous number of thin sections for this study and helped with the pyrite etching.

I would like to thank Goldcorp Canada Limited- Musselwhite Mine and the Atikokan Mineral Development Initiative for their financial support of this project through research agreements with my supervisor Dr. Mary Louise Hill. Thank you to the geology team at Musselwhite Mine especially Rohan Millar, Jim Edwards, Anne Carraud, John Biczok, Sheri Lyon and Steve Zub; it was a pleasure to work with you over the summer. I learned so much from the experience; thank you for all the guidance. I want to thank both Musselwhite Mine and Brett Resources- Hammond Reef for providing access to their properties and the ability to sample drill core. Thank you to everyone at Musselwhite Mine and at Hammond Reef who helped me in my quest to collect samples and better understand the geology of these two deposits.

I want to thank my geologist and non-geologist friends for helping me keep my sanity over the past two years, it wouldn't have been the same without you! Anya and Isabelle thanks for all the late nights in the CB building as well as the hours of cooking, eating and drinking at home. Thank you to Adam, Victoria, Bobby, Lindsay and Christine you have all been unbelievable and Sam random Mondays were the best.

Table of Contents:

List of Figures:

List of Tables:

Chapter 1: Introduction

1.1: Objective

The objective of this thesis is to examine microscopically the role of deformation and metamorphism in gold mineralization for shear-zone-hosted gold deposits. This was accomplished through detailed microscopic investigation of three gold-hosting lithologies from Musselwhite Mine and Hammond Reef in Northwestern Ontario. The main focus is to document microstructures associated with gold mineralization in different lithologies from different shear-zone-hosted gold deposits. Although Musselwhite Mine and Hammond Reef are similar in that they are located adjacent to regional shear zones, have undergone regional metamorphism and are dominated by ductile deformation, the deposits are hosted by completely different lithologies. Because the rock types of these deposits differ so completely, attention to the physical similarities between microstructural control on gold mineralization is important. An outcome of this thesis is the identification of microstructures significant to the occurrence of gold in shear-zone hosted gold deposits. McCuaig and Kerrich (1998) suggest that gold mineralization may be associated with "structural traps" on the macroscopic scale created in rheologically favorable lithologies for orogenic gold deposits. In this study, the most common gold-hosting microstructures are the product of heterogeneous deformation on the microscopic scale in and adjacent to minerals with different response to strain.

In addition, microstructures observed in each study lithology are compared and used to constrain relative timing of gold mineralization for these deposits. The results of this thesis show close similarities between the two shear-zone-hosted deposits in the microstructures which host gold and the relative timing of gold mineralization. This thesis may contribute to the search for and understanding of other shear-zone-hosted gold deposits.

1.2: Study areas

Musselwhite Mine and Hammond Reef are located in the Western Superior Province of the Canadian Shield. They are located in Ontario, Canada, northwest of Lake Superior (Fig. 1.2.1). The Superior Province ranges in age from ~3.2-2.5 Ga and is the largest Archean craton in the world (Thurston et al. 1991) (Fig. 1.2.2). This craton is thought to be made up of a series of accreted continental fragments which today represent the complex structures and diverse rock types of the Superior Province (e.g. Card 1990; Percival et al. 2006). Musselwhite Mine and Hammond Reef are shear-zone-hosted gold deposits proximal to steeply dipping, major regional structures separating rock of different ages (Stott et al. 2007 and Stone 2009) (Fig. 1.2.2). Such regional structures are thought to be important to gold mineralization as they act as long term conduits for fluid movement and are synchronous with regional metamorphism and often volcanism (e.g. Eisenlohr et al. 1989; Groves 1993; Mikucki 1998).

1.2.1 Musselwhite Mine (Location and Access)

Musselwhite Mine is an active underground gold mine, which has been in operation since 1997 and today is owned entirely by Goldcorp Inc. The mine has a large camp housing hundreds of workers, with many offices and a mill on site. Musselwhite Mine is located about 500 km north of Thunder Bay, Ontario (Fig. 1.2.1). Musselwhite Mine's nearest neighboring town is Pickle Lake which is about 100 kilometers south of the mine. The mine can be accessed by road using the TransCanada (Highway 17) and secondary dirt roads Highways 599 and 808. It is a lengthy trip by road and the most common access is by air, on private charters departing from Thunder Bay International Airport.

Figure 1.2.1 Musselwhite Mine and Hammond Reef are located in Northwestern Ontario, Canada. Map shows study location in North America, with detailed map of Northwestern Ontario.

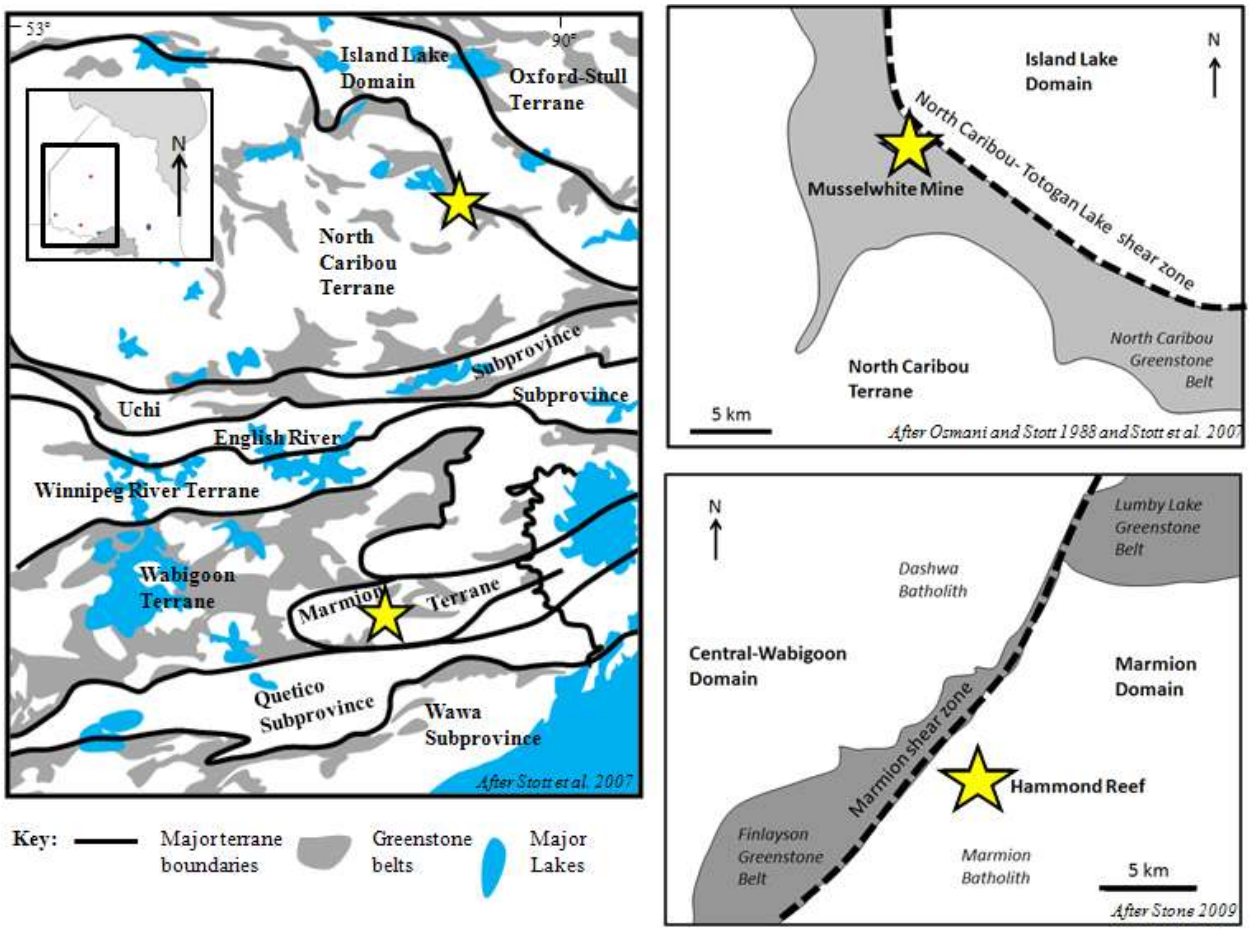

Figure 1.2.2: Simplified Geology of the study areas.

(A)The simplified geological map depicts greenstone belts in northwestern Superior Province and the major terrane boundaries interpreted by Stott et al. (2007). Musselwhite Mine is located to the north depicted a yellow star, while Hammond Reef is located to the south depicted a yellow star. Musselwhite Mine occurs within the North Caribou Terrane and Hammond Reef occurs within the Marmion Terrane as defined by Stott et al. (2007). Note the Marmion Terrane has since been subdivided by Stone (2009).

(B) The simplified regional geology of Musselwhite Mine after Osmani and Stott (1988) and Stott et al. (2007). The grey represents the North Caribou greenstone belt and the dashed line represents the North Caribou –Totogan Lake shear zone which is also the terrane boundary.

(C) The simplified regional geology of Hammond Reef, after Stone (2009). The grey represents the Finlayson and Lumby Lake greenstone belts and the dashed line represents the domain boundary which overlaps with the Marmion shear zone.

1.2.2 Hammond Reef exploration property (Location and Access)

Hammond Reef was actively mined in the late 1800s, and today it is a prospective property currently owned by Osisko Mining Corporation. Hammond Reef is located about 200 km west of Thunder Bay (Fig. 1.2.1) and is much less remote than Musselwhite Mine. The town of Atikokan is about 25 km southwest of the Hammond Reef property. The deposit is located near the shores of Marmion Lake and can be accessed by boat or by road from Highway 11 and the secondary road Highway 623 followed by dirt logging roads. In March of 2010 Osisko announced a friendly take-over bid of Brett Resources, the previous owners of the Hammond Reef property, which was accepted May 2010. Osisko has offices in the town of Atikokan as well as a camp on the property.

1.3: Regional Geology

1.3.1: Musselwhite Mine regional geology

Musselwhite Mine is located within the North Caribou greenstone belt in the North Caribou Terrane (Breaks et al. 2001) (Fig. 1.2.2). The North Caribou greenstone belt is a collage of 2.98-2.87 Ga metamorphosed volcanic and sedimentary rocks (Hollings and Kerrich 1999 and references therein). The mine is located adjacent to the North Caribou-Totogan Lake shear zone which divides the region (Osmani and Stott 1988) (Fig. 1.2.2). The Island Lake Domain lies to the north of the shear zone with the North Caribou Terrane to the south (Rayner and Stott 2005; Stott et al. 2007).

The dominant foliation at Musselwhite Mine strikes northwest and is steeply dipping, nearly vertical (Fig.1.3.1). The deposit is hosted by an Algoma-type banded iron formation (Moran

2008) within the greenstone belt (Fig. 1.3.1). The banded iron formation is folded; these folds are tight, shallowly plunging sheath folds.

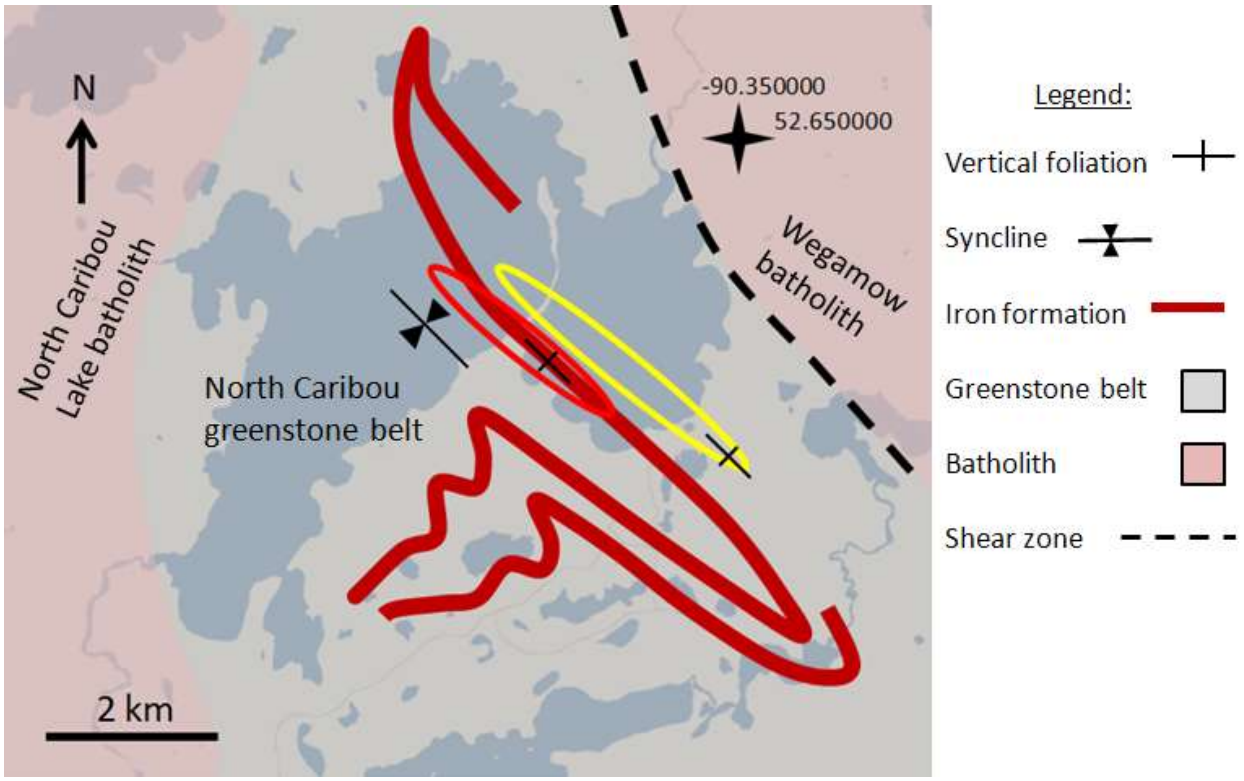

Figure 1.3.1 Geologic map of Musselwhite Mine after Osmani and Stott (1988), Breaks et al. (2001) and Stott et al. (2007). The red oval represents the area where samples of Lithology 1, the garnet-grunerite-biotite schist, were taken. The yellow oval represents the area where samples of Lithology 2, the grunerite schist, were taken.

On the deposit scale, rocks are metamorphosed to amphibolite facies (Hall and Riggs 1986, Breaks et al. 2001, Otto 2002, Stinson 2010). Recent work by Stinson (2010) used metamorphic mineral assemblages of pelitic rocks proximal to the ore bodies to determined peak metamorphic temperatures to be greater than 500 °C. These results are consistent with previous estimations using metamorphic isograds and geothermometry (Hall and Riggs 1986; Breaks et al. 2001; Otto 2002; Isaac 2009).

1.3.2: Hammond Reef

Hammond Reef is hosted by the 3.0 Ga Marmion batholith (Tomlinson et al. 2003; Tomlinson et al. 2004; Stone 2010 and references therein), which is primarily tonalite in composition. The gold deposit is located on the western edge of the batholith in the Marmion Terrane (Stone 2009 and Stone 2010) (Fig. 1.2.2). Hammond Reef is proximal to the Marmion shear zone which strikes roughly northeast (Stone 2009 and Stone 2010). At the deposit scale the quartzofeldspathic schist is often highly sheared in the same orientation as the shear zone. The foliation strikes on average about 65° and dips moderately to the southeast between 70-45° (Fig 1.3.2).

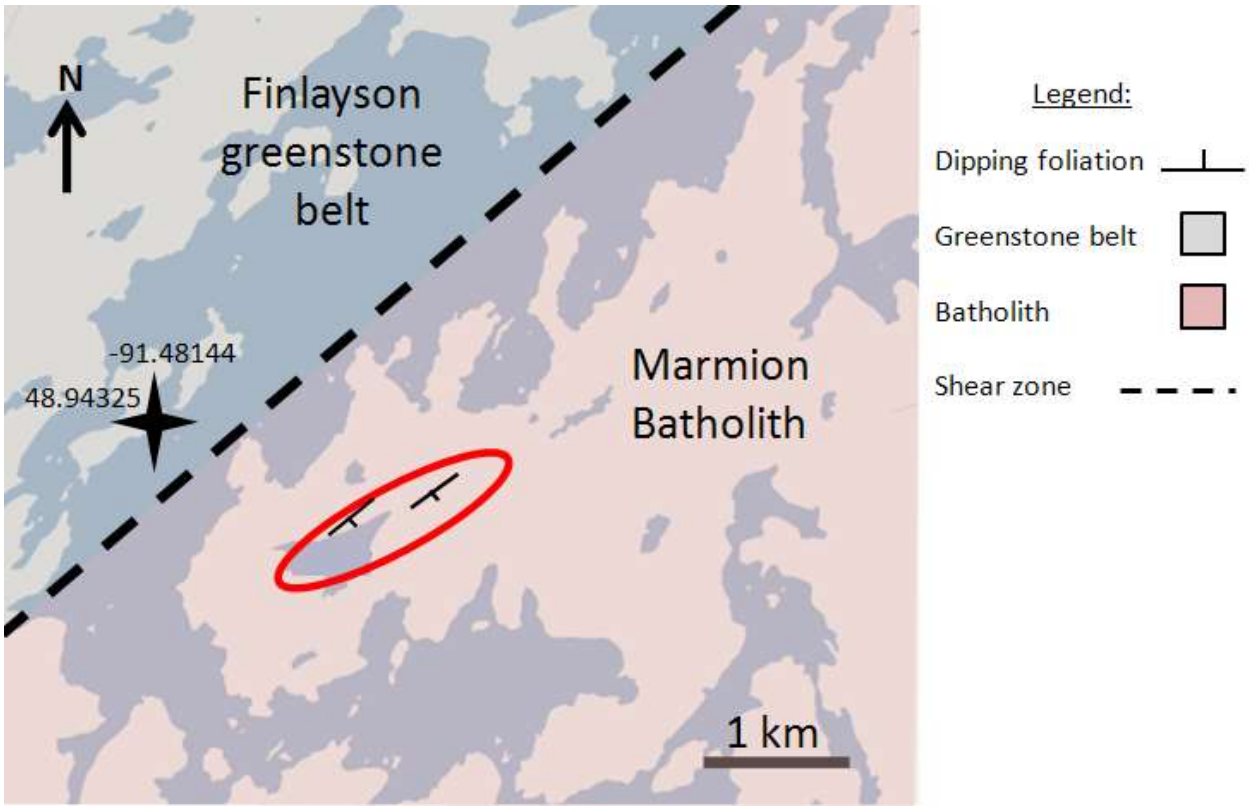

Figuer 1.3.2 Geologic Map of Hammond Reef region after Stone (2009) and Stone (2010). The red circled area depicts the A zone and 41 zone where samples were collected for this study.

To the west of the Marmion shear zone lies the 2.93 Ga Finlayson greenstone belt (Tomlinson et al. 2003). The rock at Hammond Reef appears to be in the greenschist facies of metamorphism like the Finlayson greenstone belt to the west (Easton 2000; Tomlinson et al. 2003). Recent work by Stone (2009) separated the Marmion Terrane into many different age domains. Adjacent to the Hammond Reef property is the division between the Central Wabigoon Domain and the Marmion Domain which occurs along the Marmion shear zone seen in Fig. 1.3.2 and 1.3.3.

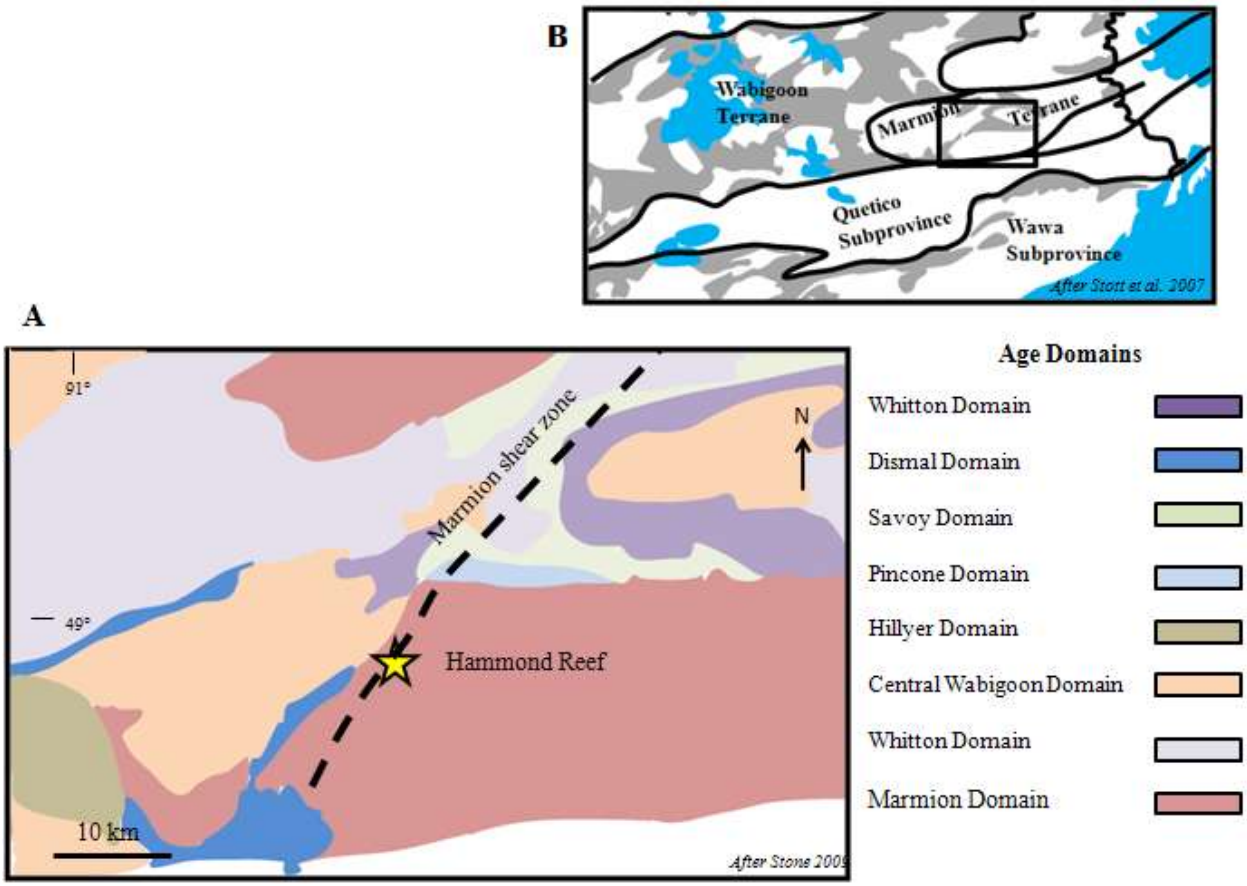

Figure 1.3.3 Age domains near Hammond Reef. Map A depicts the age domains by Stone (2009) near the Hammond Reef gold deposit. Hammond Reef is adjacent to the Marmion shear zone which separates the Marmion Domain from the Central Wabigoon Domain (Stone 2009). The location of this map with respect to the major terrane boundaries defined by Stott et al. (2007) shown in B. Age domains listed youngest to oldest.

1.4: Microstructure

This study relies on the results from many experimental studies which have examined deformation mechanisms in common rock-forming minerals. These experiments simulate temperature and pressure which would occur in naturally deformed rocks, allowing us to better understand mechanisms by which minerals deform. The biggest limitation of experimental studies is stain rate. In nature strain rates are much slower, and deformation can occur over millions of years, while in experimental deformation scientists substitute very fine grain aggregates and higher strain rates. Experimental studies have been conducted for such minerals as quartz (e.g. Carter et al. 1964; Hirth and Tullis 1992; Gleason and Tullis 1995; Post et al. 1996; Hirth et al. 2001; Stipp et al. 2002), feldspar (e.g. Marshall and McLaren 1977; Tullis and Yund 1985; Egydio-Silva and Mainprice 1999; Lapworth et al. 2002; Rybacki and Dresen 2004), and garnet (Ando et al. 1993; Voegele et al. 1998a,b; Wang and Ji 1999; Ji et al. 2003; Storey and Prior 2005). Different deformation mechanisms dominate over particular ranges of temperature and differential stress conditions. At any particular range of temperature and differential stress conditions, deformation mechanisms differ for different minerals (e.g. Gregg 1985; Berger and Stunitz 1995; Rybacki and Dresen 2004; Rutter and Brodie 2004; Storey and Prior 2005; Rahimi-Chakdel et al.2006). Crystal structure controls how a mineral will respond to deformation and under what conditions each deformation mechanism will dominate for that particular mineral (Passchier and Trouw 2005 and references therein). The deformation mechanisms important in this study include: deformation or mechanical twinning, brittle fracture, grain-scale diffusive mass transfer with grain boundary sliding and dislocation creep.

In the low temperature and low differential stress realm, deformation or mechanical twinning and kinking are most likely to dominate because other more efficient deformation mechanisms

require higher temperatures. Deformation twinning will occur in commonly twinned minerals like feldspar and calcite but is restricted to specific crystallographic planes and directions (Eggleton and Buseck 1980; White and Barnett 1990). Kinking resembles twinning but is not restricted to the specific directions and planes. Also kinking is common in many different minerals such as quartz, feldspars, amphiboles, kyanite and pyroxene (Bell et al.1986; Wu and Groshang 1991; Nishikawa and Takeshita 1999, 2000). Deformation twinning and kinking are not very efficient deformation mechanisms because they do not eliminate very much of the stress on the crystal.

At high differential stress and relatively low temperatures minerals tend to fracture in response to deformation (Passchier and Trouw 2005). Brittle fracturing occurs when the stress exceeds the brittle strength. Different minerals have different strengths and some require higher stress to fracture compared to others. This deformation mechanism can sometimes be seen in addition to mechanical twinning and kinking.

Grain-scale diffusive mass transfer operates by diffusion of vacancies in the crystal lattice. This diffusion occurs either on grain boundaries (Coble creep) or throughout the crystal lattice (Narbarro-Herring creep). This mechanism is thought to especially occur in fine grained rocks where grain boundary sliding occurs (Schmid et al. 1977; Behrmann 1983). In grain boundary sliding the voids between crystals sliding past each other are thought to be prevented by solid state diffusive mass transfer and/or solution and precipitation through grain boundary fluids (Bouller and Gueguen 1975; Stunitz and Fitz Gerald 1993; Paterson 1995; Fliervoet et al. 1997; Kruse and Stunitz 1999). This deformation mechanism does not leave clear microstructural evidence behind.

Dislocation creep is the most important mechanism because it most effectively enables ductile deformation in rocks. Dislocations are line defects which are within the crystal lattice (Passchier and Trouw 2005). Dislocation creep is the movement of dislocations in the crystal lattice and involves two types of movement, dislocation glide and dislocation climb. Dislocations have distinct orientations with respect to the crystal lattice and move only in specific crystallographic planes and directions. These specific slip planes and directions are referred to as slip systems. The specific slip system active in a crystal depends on the orientation and magnitude of the stress field acting on the crystal.

Dislocation glide occurs when the dislocation breaks the ionic bond holding it in place and bonds with the next closest atom in the crystal lattice. Dislocation glide can only move along the active slip system. The problem with this movement is that the dislocations in the crystal can build up on that particular system. Also slip systems can intersect in a crystal lattice causing tangles and build up of dislocations. When dislocations build up and/or tangle they cause strain hardening which can lead to fracturing. With dislocation glide the dislocations can only "move" along in the slip plane where they originated, but with slightly higher temperature work hardening can be avoided by dislocation climb.

Dislocation climb allows the dislocation to essentially jump up a level in the crystal lattice. This occurs at higher temperatures when vacancies are able to move through the crystal lattice. When a vacancy arrives next to a dislocation, the dislocation can climb out of its slip plane. Because the movement of vacancies in a crystal lattice requires more energy than breaking and forming ionic bonds, dislocation climb requires higher temperatures than dislocation glide. With dislocation climb work hardening is diminished. Dislocation glide and climb work together and allow ductile deformation to continue using the least amount of energy possible.

Undulose extinction, irregular grain boundaries and subgrains are all microstructural evidence of dislocation creep. Also dislocation creep is the only deformation mechanism which gives the crystals a preferred crystallographic orientation.

Dislocation creep creates typical textures in monomineralic rocks depending primarily on temperature. Bulging recrystallization or regime 1 occurs at the lowest temperatures, it occurs in quartz between ~280-400°C (Drury et al.1985; Hirth and Tullis 1992; Shigematsu 1999; Hirth et al. 2001; Stipp et al. 2002). In regime 1, locally the grain boundary can bulge into the neighboring crystal with higher dislocation density. This bulged area can form a new small independent crystal. The microtexture preserved in the rock is large grains with tiny grains around them.

Subgrain rotation recrystallization or regime 2 occurs when dislocations are continuously added to subgrain boundaries (Hirth and Tullis 1992; Nishikawa and Takeshita 2000; Hirth et al. 2001; Nishikawa et al. 2004). In order for this to occur dislocation climb must be working well allowing dislocations to easily climb from one lattice plane to another. The angle between the crystal lattice on either side of the subgrain boundary increases until the subgrain becomes an individual grain. The misorientation of these subgrains is called subgrain rotation, giving this process its name. Regime 2 occurs in quartz over a range 400-500°C (Hirth and Tullis 1992; Hirth et al. 2001; Tullis 2002). The microtexture indicative of this process is large grains surrounded by smaller grains the same size as remaining subgrains.

At higher temperatures grain boundary migration recrystallization or regime 3 dislocation creep occurs. Regime 3 occurs at temperatures higher than 500°C in quartz. Grain boundary migration only occurs at high temperatures where grain boundaries can sweep through entire crystals to remove dislocations and possibly subgrains (Guillope and Poirier 1979; Urai et al. 1986; Hirth

and Tullis 1992; Hirth et al. 2001; Stipp et al. 2002). Old grains are difficult to distinguish, unlike in regime 1 and 2 where they are the largest crystals surrounded by new grains. In regime 3, crystal size becomes more uniform. Because at higher temperatures dislocation glide and dislocation climb work together work hardening is eliminated (e.g. Hirth and Tullis 1992; Hirth et al. 2001; Stipp et al. 2002 and Tullis 2002).

Another texture can overprint the microstructures indicating deformation by dislocation creep. This texture is cause by the process of grain boundary area reduction. Grain boundary area reduction occurs when elevated temperatures persist after deformation has ceased or strain has diminished. Grain boundaries are a type of planar defect; decreasing the grain boundary area decreases the area of this defect. Defects represent internal free energy which the crystal wants to decrease. Straight grain boundaries and large grain size reduce the area of these planar defects. Dislocation creep also reduces the internal free energy and does so more efficiently than grain boundary area reduction. For this reason grain boundary area reduction only dominates once deformation has ceased or diminished.

Some minerals require high temperatures in order to deform in any ductile manner while others deform by ductile deformation mechanisms at comparably low temperatures (Winter 2010). For example garnet requires high temperatures of 600-800 °C to deform by dislocation creep (Voegele et al. 1998a,b; Wang and Ji 1999) while quartz deforms by dislocation creep at relatively low temperatures of 300-400°C (Barber and Wenk 1991; Hirth and Tullis 1992; Tullis 2002; Stipp et al. 2002). The dominant deformation mechanism depends primarily on the individual mineral‟s strength, deformation conditions and surrounding mineralogy.

In polymineralic rocks minerals can behave differently than in monomineralic rocks. In polymineralic deformation the behavior of minerals is more complex (Jordan 1987; Handy 1989;

1992; Bons and Urai 1994; Handy et al. 1999; Stunitz and Tullis 2001; Tullis 2002). The strength of the different minerals plays an important role in how they will behave. For example, in a quartz and feldspar rock at medium to high grade temperatures both quartz and feldspar will deform by dislocation creep assisted by diffusion and form monomineralic bands (Culshaw and Fyson 1984; Mackinnin et al. 1997; Hippertt et al. 2001). Tullis (2002) describes textural changes in unlike neighboring minerals.

Microstructures can be useful tools in understanding the progressive deformation in rocks. In this thesis, great significance is given to observing textures associated with different deformation mechanisms in different minerals.

Chapter 2: Methods

2.1 Sampling:

One hundred and eighty four samples in total were collected from Musselwhite Mine and Hammond Reef study areas, from drill core, outcrop and underground. At Musselwhite Mine, 136 samples were collected from two different gold-hosting lithologies, while at Hammond Reef, 48 samples were collected from the dominant gold-hosting lithology. For both deposits, the chosen lithologies host gold mineralization which is structurally controlled; these ore bodies trend in the same direction as the strike of foliation. Samples were taken from various ore zones hosted by each study lithology as well as areas outside the zones of gold mineralization. Because the aim of this study is to better explain the importance of deformation in gold mineralization, a wide variety of samples were collected ranging from highly gold mineralized to samples containing only trace amounts of gold. Samples were taken scattered along the strike of the deposits. All samples collected are listed in Appendices A, B and C with location and other details provided.

2.2 Petrography and microstructural analysis:

All samples collected were prepared into polished thin sections for petrographic and microstructural analysis. Thin sections were not orientated when taken from drill core. Metamorphic mineral assemblages, modal abundance and metamorphic fabrics were documented. The detailed microstructural analysis focused primarily on documenting microstructures associated with gold, although description of fabric and textures of common minerals was also taken into account.

2.3 X-ray Diffraction (XRD):

XRD analysis was used to determine the fine grained alteration present in the Hammond Reef samples. Two highly altered samples were selected for XRD analysis. Samples were powdered to 70 microns and an aluminum sample holder was used.

Samples were analyzed using Phillps X-Ray Diffractometer XPert MPD with a Cu anode in the Lakehead University Instrumentation Laboratory. The generator voltage used was 40 kV with generator current of 30 mA. Patterns were collected throughout an angular range of 6 to 96 (2ɵ), with a step size of 0.0260 and scan step time of 7.15 seconds.

The obtained diffraction patterns were matched using PANalytical, X'Pert HighScore Plus. This software automatically provides best-fit matches for the diffraction patterns. The CIF (crystallographic information files) came from the ICDD (International Center for Diffraction Data) database.

2.4 Scanning Electron Microscope analysis (SEM):

After petrographic and microstructural analysis, 10 samples were chosen to a) confirm gold mineralization and b) identify mineral compositions. Selected samples were carbon coated, then mineral composition was determined using X-ray energy-dispersion spectrometry (EDS) using the JEOL JSM 5900 LV scanning electron microscope (SEM) at the Lakehead University Instrumentation Lab. Spectra were acquired using detector resolution of 133eV, an accelerating voltage of 20 keV and beam current of 0.465 nA with a 60 second analysis period.

For the quantitative analysis of silicate minerals pyroxene and amphibole standards used include: wollastonite (Ca, Si), jadeite (Na, Al), benitoite (Ba, Ti), orthoclase (K) and Mn-hortonite (Mg, Fe, Si, Mn). Spectra were analyzed using LINK ISIS software. Elements were reported as oxides with total iron being reported as FeO. Back-scattered electron (BSE) images were acquired with the LINK ISIS-AUTOBEAM system. SEM results can be found in Appendix D.

2.5 Pyrite etching:

Twenty samples from Hammond Reef were selected for acid etching to test for zonation in pyrite. This method is often used to observe growth patterns in pyrite, most commonly for pyrite formed in low temperature environments. This method can also be used to etch compositional zonation.

Two different solutions were attempted using, 1:1 HNO_3 to H_2O and 100% acid. Acid solution was applied to thin sections under a fume hood using an eye dropper and allowed to sit for 60 seconds. Thin sections were then rinsed with distilled water twice and immediately examined under the microscope for zonation. This process for etching pyrite is described in Craig and Vaughan (1994).

Chapter 3: Description of Lithologies

3.1: Lithology 1, Musselwhite Mine, garnet-grunerite schist

Lithology 1 is the main ore-hosting lithology at Musselwhite Mine. It is known at the mine as unit 4EA, part of the Northern Iron Formation. This unit is made up of quartz, garnet, grunerite, hornblende, biotite, muscovite, plagioclase, magnetite, pyrrhotite and gold. Samples of the garnet-grunerite-schist (Lithology 1) were taken from the PQ Deeps and the Moose zones at Musselwhite Mine (Fig. 1.3.1). More detailed description of the locations and samples taken can be found in Appendix A.

Lithology 1 is differentiated into bands of like minerals, such as quartz-rich, garnet-biotite-rich, garnet-amphibole-rich and garnet-amphibole-biotite-rich. This banded texture can be attributed to a number of possible contributing factors including metamorphic differentiation and strain partitioning as well as initial differentiation in bedding. Moran (2008) determined this lithology to be metamorphosed Banded Iron Formation with a clastic input. Ductile deformation has impacted the banded texture of the iron formation. Bands are often discontinuous and appear like shearband boudins (Passchier and Trouw 2005). But these shearband boudins appear more complicated as if they have been folded and/or deformed.

The fabric of Lithology 1 is a spaced foliation using the classification scheme from Winter (2010) and references therein. Bands are smooth (meaning straight) to rough (meaning slightly curved and spaced out) with areas of parallel foliation and anastomosing foliation. In this lithology, mine geologists have noticed a correlation between the foliation style and gold mineralization; samples in this study support this correlation. Samples with poor gold mineralization generally have distinct smooth foliation which is nearly parallel; richer gold

mineralization is associated with rough and anastomosing foliation. Because Lithology 1 is foliated metamorphic rock, it is referred to as garnet-grunerite schist in this study, a lithologic name consistent with the new IUGS guidelines for naming metamorphic rocks (Fettes and Desmons 2007).

3.1.1: Quartz-rich bands

The quartz-rich bands of Lithology 1 appear as two different types, quartz-only and quartz-dominated bands. The quartz-dominated bands include other minerals, most often grunerite and pyrrhotite but can include biotite or hornblende.

Where quartz bands contain only quartz, textures observed are typical for quartz at amphibolite facies metamorphism. Quartz exhibits irregular grain boundaries, undulose extinction and uniform grain size; this texture has been described by Hirth and Tullis (1992) as regime 3 dislocation creep. Fig. 3.1.1 and Fig. 3.1.2 show this common texture observed in quartz from Lithology 1 from samples 909-008 and 909-003 respectively, both in cross-polarized transmitted light. Notice the irregular grain boundaries and undulose extinction in both examples. Also within these quartz-rich areas, note the nearly uniform grain size. When quartz occurs with other phases in the quartz-dominated bands the texture is changed; quartz still exhibits undulose extinction and where it is bounded by other quartz crystals, irregular boundaries are often observed, but grain size varies. Quartz grains are typically smaller where bounded by other mineral phases. Tullis (2002) links this texture with less efficient deformation in polymineralic rocks. In sample 310-638, an area which appears as a quartz band in hand sample is actually quartz-rich with grunerite and hornblende scattered throughout. A bleb of gold occurs on the grain boundaries between the hornblende and quartz (Fig. 3.1.3).

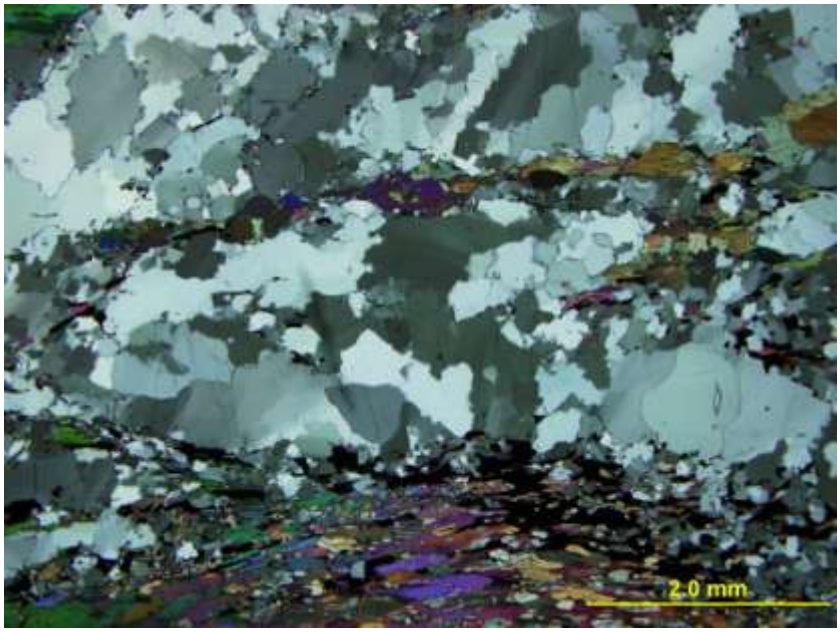

Figure 3.1.1: Sample 909-008 (008-001). This photomicrograph in cross-polarized transmitted light shows the typical texture of quartz at Musselwhite Mine. Quartz exhibits irregular grain boundaries and undulose extinction, which are evidence of dislocation creep. The grains are very similar to the experimentally defined quartz textures of regime 3 dislocation creep.

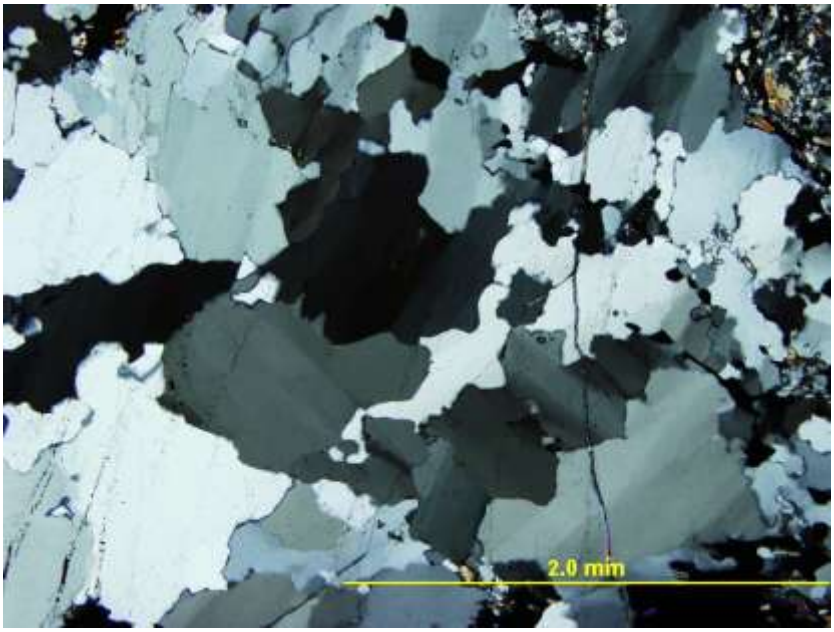

Figure 3.1.2: Sample 909-003 (003-001). This photomicrograph is in cross-polarized transmitted light. Notice the irregular grain boundaries and undulose extinction exhibited by the quartz. The grain size of the quartz is nearly uniform, except to the right side where other mineral phases occur.

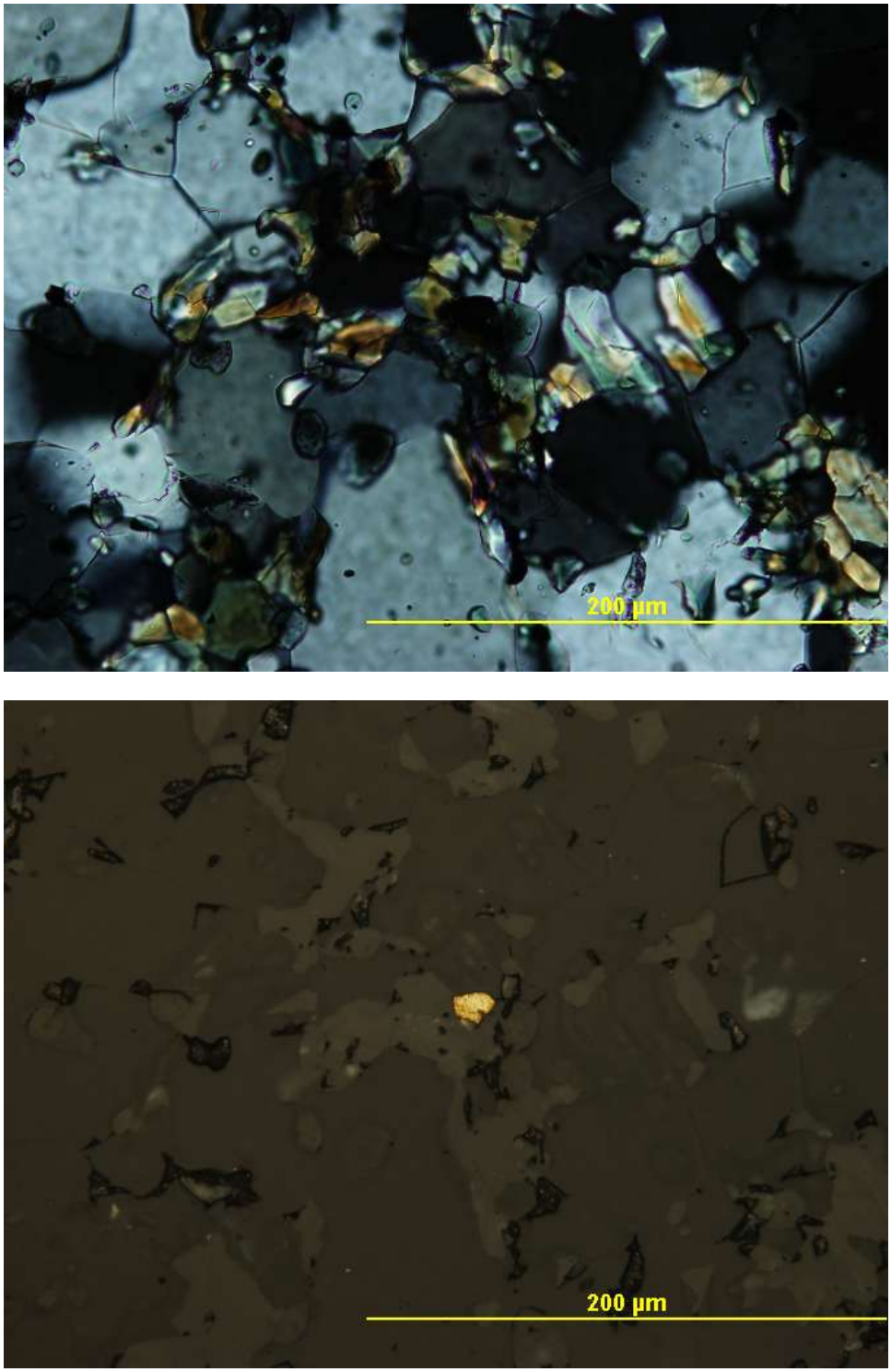

Figure 3.1.3: Sample 310-638 (638-001). This is a quartz-rich band with scattered grunerite and hornblende crystals which can be seen in cross polarized transmitted light (top photomicrograph). A bleb of gold occurs on the grain boundaries seen in the bottom photomicrograph in reflected plane polarized light. *Note both photomicrographs are taken in same area.

3.1.2: Garnet-biotite-rich bands

The garnet-biotite-rich bands are interesting because of the very different response to strain each of these minerals exhibits. Garnet is very resistant to ductile deformation; it will deform brittlely unless very high temperatures are involved, much higher than those achieved during metamorphism at Musselwhite Mine. In contrast, biotite easily deforms by ductile deformation at amphibolite facies metamorphism. Due to this contrast, strain partitioning would have occurred during deformation. Because biotite is easily deformed at amphibolite facies, it accommodated the bulk of the strain. This phenomenon has been studied by many other researchers, especially in gneiss where certain bands may accommodate more of the strain than others (Handy 1990, Tullis 2002, Holyoke and Tullis 2006a).

3.1.3: Garnet-amphibole bands

The garnet amphibole bands are most commonly dominated by the amphibole grunerite, with hornblende being slightly less common. Amphiboles are more resistant to ductile deformation than biotite, which implies that these bands are more resistant to ductile deformation (e.g. Berger and Stunitz 1995). Metamorphism is thought to aid in deformation because of the increased mobility of atoms during metamorphism. These garnet-amphibole bands would have been undergoing metamorphism during deformation which would have aided in their deformation, but to what extent is unknown. A typical example of these garnet-amphibole bands can be seen in Fig. 3.1.4. Large garnet crystals make up more than half the band with grunerite lining and filling nearly all the space between these garnet crystals. Grunerite is commonly twinned but sometimes curiously bent and shifted twins occur, like some of the twins seen in Fig. 3.1.5. These twins may be complex or deformed growth twins or could possibly be deformation twins.

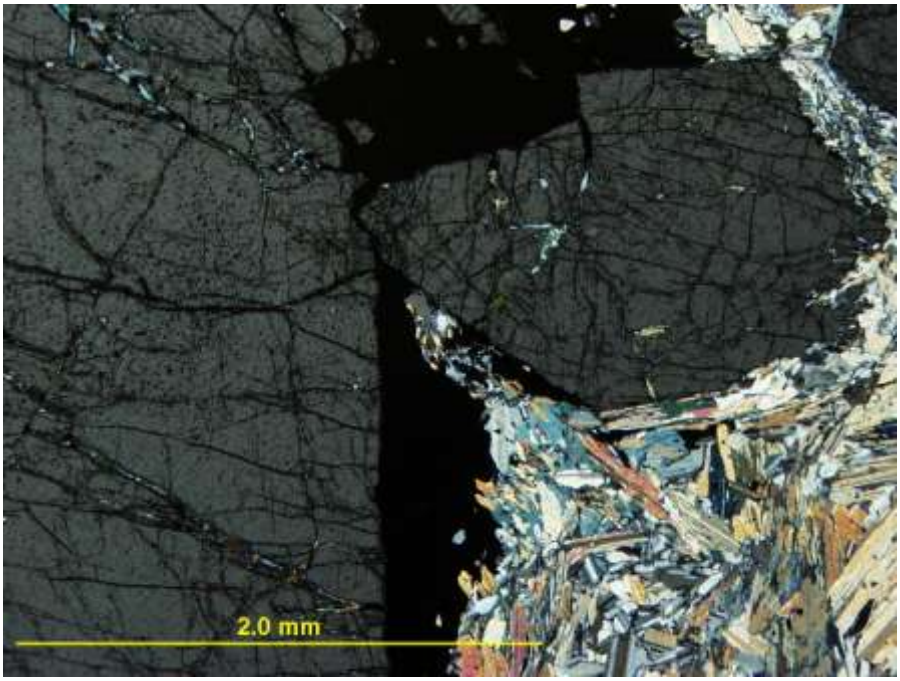

Figure 3.1.4 808-113 (113-001). Extinct garnet crystals appear with multiply twinned grunerite; the opaque mineral in this photomicrograph in cross-polarized transmitted light is pyrrhotite.

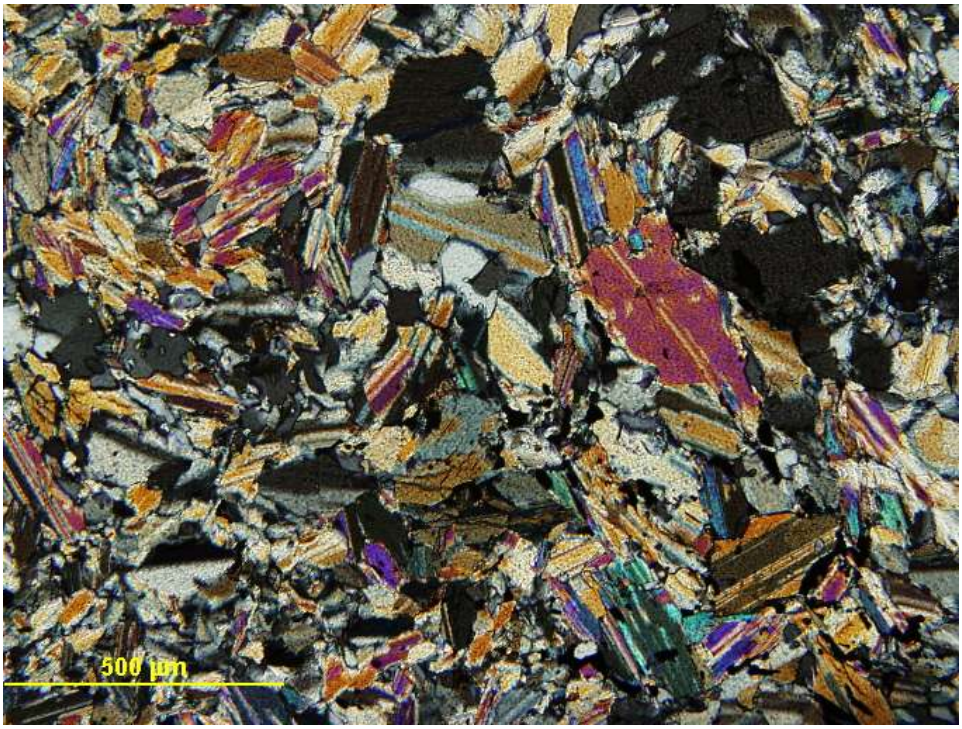

Figure 3.1.5 Sample 310-618 (618-011). This photomicrograph in cross-polarized transmitted light shows twinned grunerite crystals. Most of the twins appear straight and continuous yet others appear bent and/or discontinuous and may be deformation twins or deformed twins.

3.1.4: Garnet-amphibole-biotite bands

The deformation in garnet-amphibole-biotite bands is the most complex due to having the most different mineral phases. The modal mineralogy of these bands vary considerably. Fig. 3.1.6, sample 909-002 is biotite-rich with grunerite and shows an example of anastomosing foliation around the garnet crystals with an inclusion of gold in the garnet crystal. Many garnet crystals are rich with inclusions; sample 909-001 has garnet rich with grunerite and quartz inclusions (Fig. 3.1.7). This particular example is from a garnet-amphibole-biotite band.

3.1.5: Pyrrhotite textures

In Lithology 1 from Musselwhite Mine, pyrrhotite appears as blebs, stringers and vein-like or fracture filling. Blebs and stingers are the most common pyrrhotite texture seen in the garnet-grunerite schist (Lithology 1). Sometimes the stringer textures of pyrrhotite contain inclusions; this texture appears poikiloblastic. Poikiloblastic textures are often observed in the metamorphic minerals garnet and staurolite. Craig and Vaughan (1994) describe this texture as common in metamorphosed sulfides and can be caused by the growth of the mineral during metamorphism and/or the annealing process caused by elevated temperatures during metamorphism.

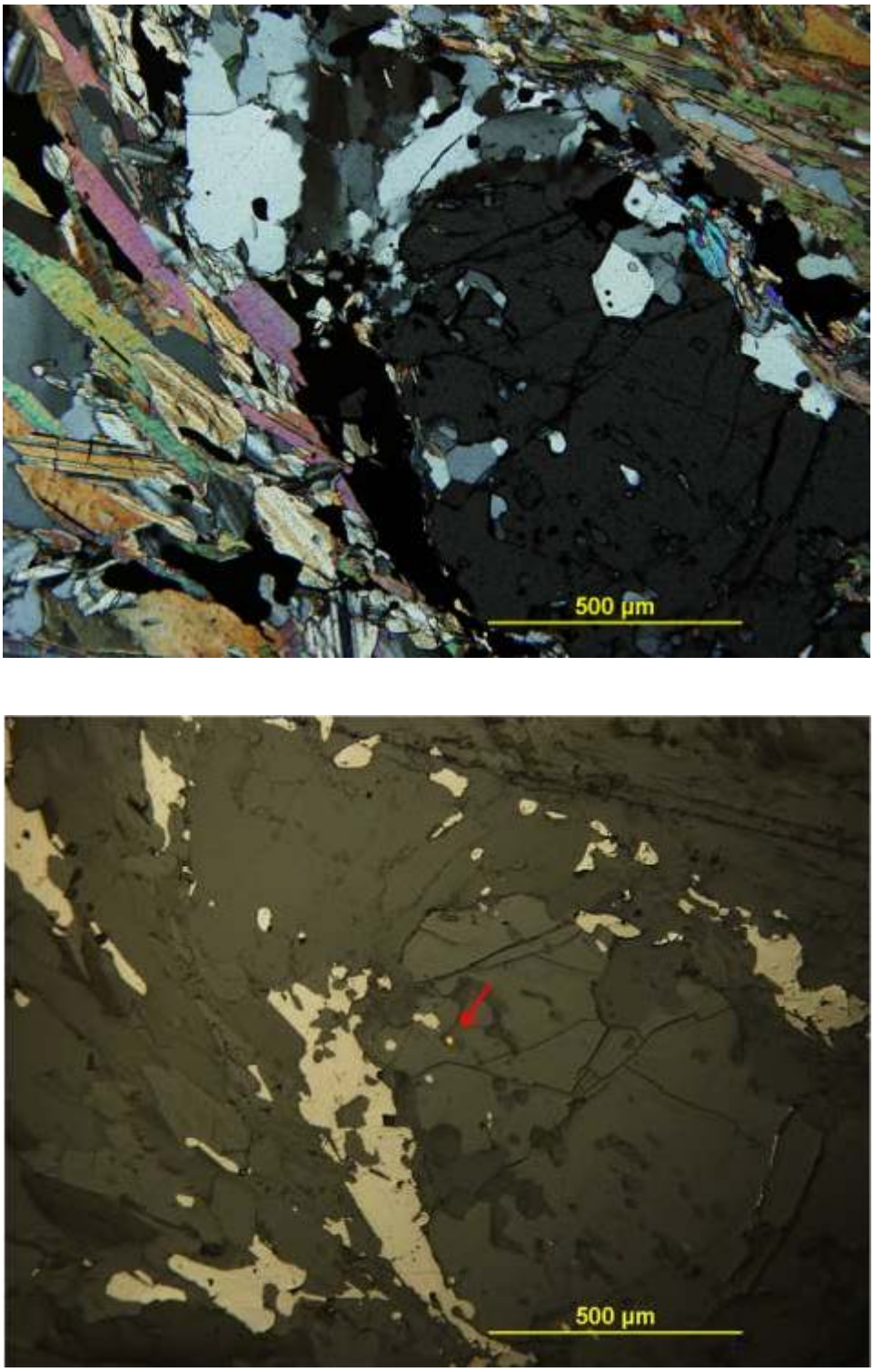

Figure 3.1.6 Sample 909-002 (002-003) The top photomicrograph in cross-polarized transmitted light gives a typical example of anastomosing foliation around the garnet crystals, while the bottom photomicrograph depicts a typical inclusion of gold within the same garnet crystal (in plane polarized reflected light).

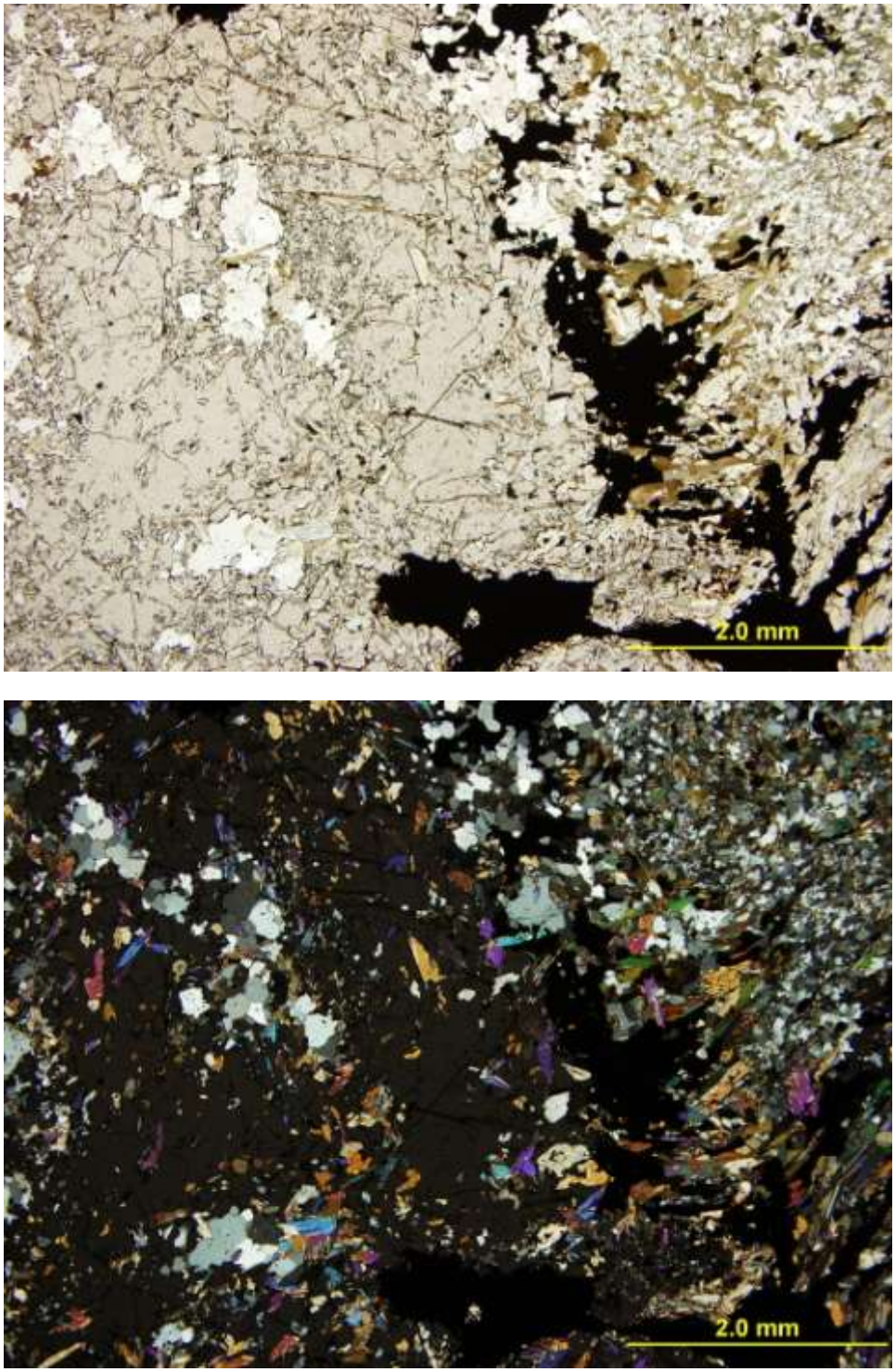

Figure 3.1.7 Sample 909-001 (001-003). This particular example is from a garnet-amphibole-biotite band. The garnet crystal is rich with grunerite and quartz inclusions, it appears slightly pink in plane polarized transmitted light in the top photomicrograph and extinct in cross-polarized transmitted light in the bottom photomicrograph. The green-brown biotite is best seen in the top plane-polarized transmitted light photomicrograph.

3.2: Lithology 2, Musselwhite Mine, grunerite schist

Lithology 2 is a secondary ore-hosting lithology at Musselwhite Mine that is not currently being mined. This lithology mainly consists of quartz, grunerite and magnetite with locally more complex mineralogy. At Musselwhite Mine this lithology is referred to as 4A; in this study it will be referred to as grunerite schist. Samples for this study come from the Southern Iron Formation although this type of iron formation also occurs in the Northern Iron Formation where Lithology 1, the garnet-grunerite schist is the main gold-hosting lithology.

Samples of the grunerite-schist (Lithology 2) were taken from the Ranger, Red Wing and Thunderwolves zones at Musselwhite Mine. Fig. 1.3.1 is a map of the mine; the yellow oval depicts the area where samples were taken. More detailed description of the locations and samples can be found in Appendix B.

Similar to Lithology 1, the garnet-grunerite schist, the foliation is again spaced, ranging from rough to smooth being sometimes parallel but also often anastomosing. A distinct relationship between texture of the fabric and intensity of gold mineralization is not apparent for this lithology, although it too has mineralogically distinct bands comparable to Lithology 1.

In drill core, the grunerite schist (Lithology 2) from Musselwhite Mine appears banded with quartz-rich bands and grunerite-rich bands; sometimes magnetite is present in the grunerite-rich bands. In detail this lithology is more complex, with carbonate-grunerite-rich bands which sometimes host clinopyroxene (hedenbergite) and blue-green amphibole (ferrotschermakite and ferroactinolite) (Appendix C). Also, sulfide textures vary throughout the grunerite schist. Thin sections were made to examine each type of band and textures observed in Lithology 2 with two goals in mind, the first to document each type of band and the second to see which bands and

textures are associated with gold mineralization. In this section each type of band will be described separately.

3.2.1: Quartz-rich bands

Quartz-rich bands in the grunerite schist commonly exhibit boudinage structures. These structures occur in-filled with pyrrhotite and/or magnetite and even lined with grunerite. Sometimes generations of quartz veining can be inferred in these areas, and often these veins are overprinted by ductile deformation. Quartz typically appears with very irregular grain boundaries, undulose extinction with nearly uniform grain size. An example of this quartz texture can be seen in cross-polarized transmitted light in Fig. 3.2.1. This texture in quartz has been described by other researchers (e.g. Hirth and Tullis 1992; Tullis 2002; Stipp et al. 2002) and also occurs in quartz-only bands from Lithology 1, the garnet-grunerite schist at Musselwhite Mine.

In Lithology 2, the grunerite schist, another quartz texture also occurs. Quartz grains sometimes appear to have less serrated, straighter boundaries like the examples in Figs. 3.2.2 and 3.2.3 from samples 210-239 and 210-542. This texture can occur when elevated temperatures persist after deformation has ceased; with less or no strain, dislocation creep stops and grain boundary area reduction dominates (Passchier and Trouw 2005).

Strain partitioning seems to be a likely cause of the various textures observed in quartz from Lithology 2. Areas undergoing metamorphism allow more efficient ductile deformation than those which are not metamorphosing, (e.g. Bell 1985; Clark and Fisher 1994; Lagoeiro et al.

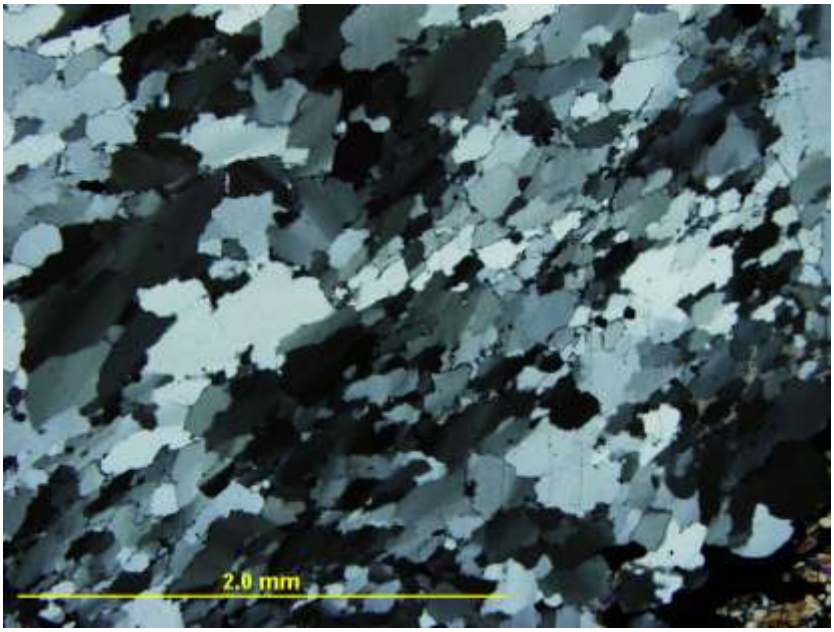

Figure 3.2.1: Sample 210-542 (542-009). Quartz has very irregular grain boundaries and undulose extinction. This photomicrograph is in cross-polarized transmitted light.

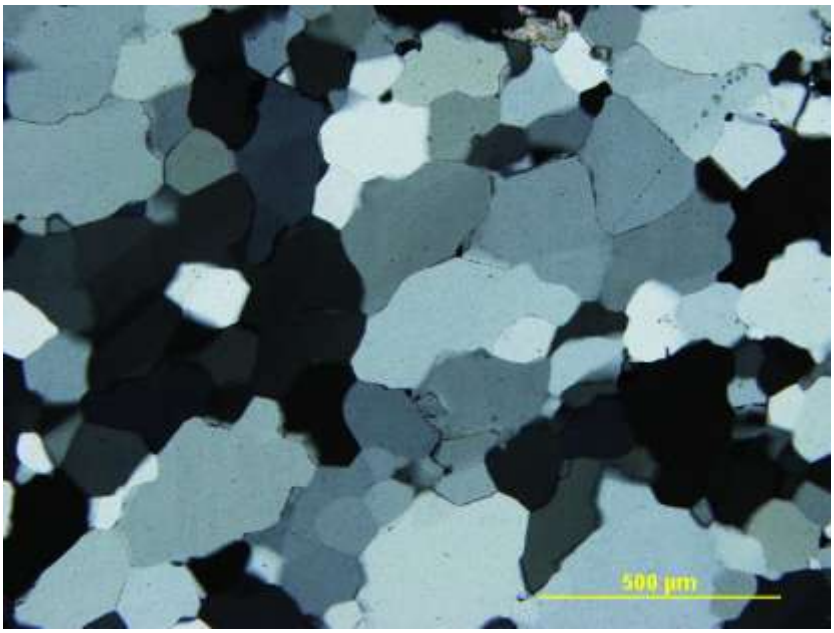

Figure 3.2.2: Sample 210-239 (239-003). Here in cross-polarized transmitted light the quartz grains appear less serrated, with straighter boundaries, this texture can occur when elevated temperatures persist after deformation has ceased or decreased. With less or no strain, the recovery process which creates the serrated/irregular grain boundaries gives way to recrystallization which allows grain boundary area reduction.

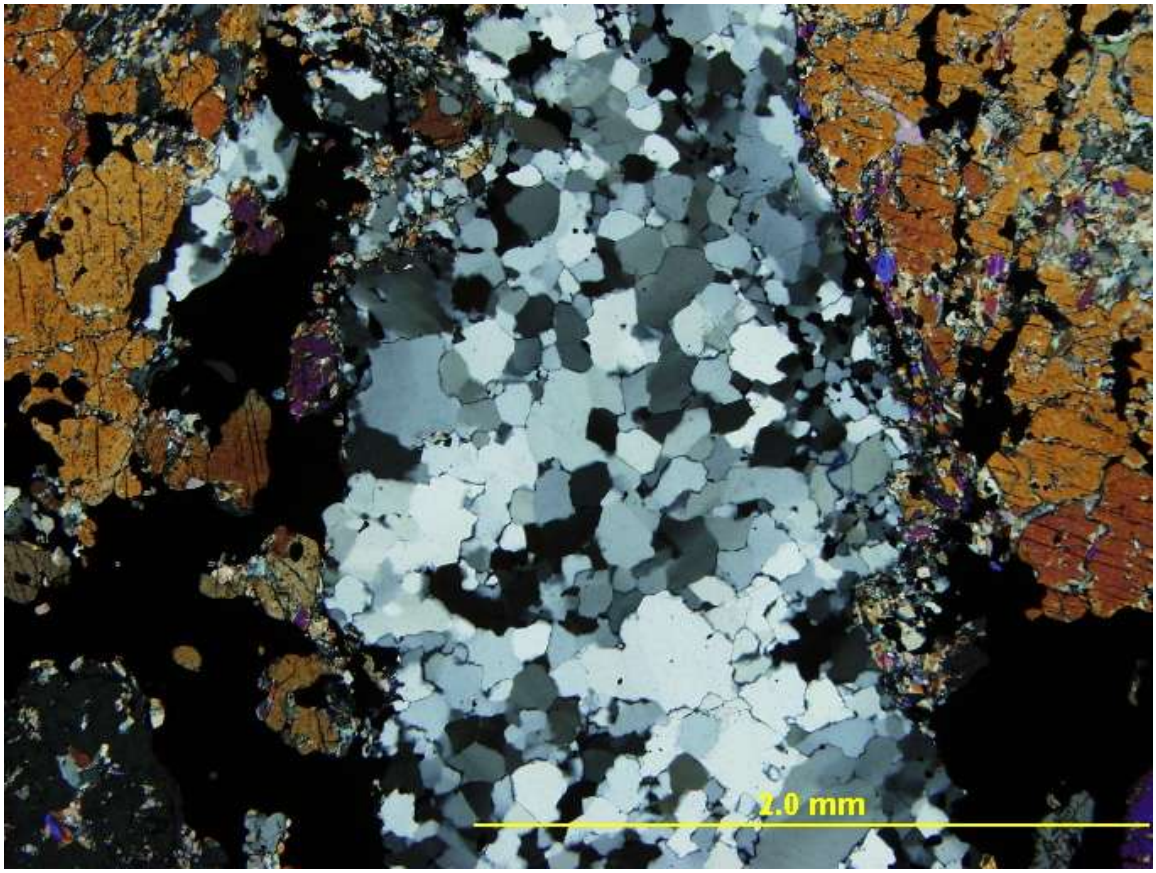

Figure 3.2.3 Sample 210-542 (542-005). This photomicrograph is in cross-polarized transmitted light, note the recrystallization texture in quartz (center), the boundaries appear only slightly irregular. Clinopyroxene, carbonate, and grunerite appear on either side; the opaque mineral is pyrrhotite.

2003; Bell et al. 2004; Holyoke and Tullis 2006a;b). The monomineralic quartz-rich bands are not undergoing metamorphism and are likely taking up less of the strain than other nearby bands which are undergoing metamorphism. A good explanation for the occurrence of both quartz textures (one indicating continuous strain during high temperatures and the other indicating little or no strain during high temperatures) is the heterogeneous nature of the strain and a complex strain partitioning of the grunerite schist (Lithology 2) at Musselwhite Mine. It is interesting to note that sometimes more than one quartz texture occurs within the same thin section, Figs. 3.2.1 and 3.2.3 show both quartz textures in one thin section.

3.2.2: Grunerite-rich bands

As to be expected Lithology 2, the grunerite schist, commonly has grunerite-rich bands. These bands typically are defined by very fine grained grunerite with or without quartz and magnetite. A typical example can be seen in Fig. 3.2.4 with grunerite and opaque magnetite. These bands have a very distinct texture with very fine grained crystals. The grunerite defines a strong foliation, which is smooth and parallel. Magnetite appears scattered through the grunerite as well in thin bands.

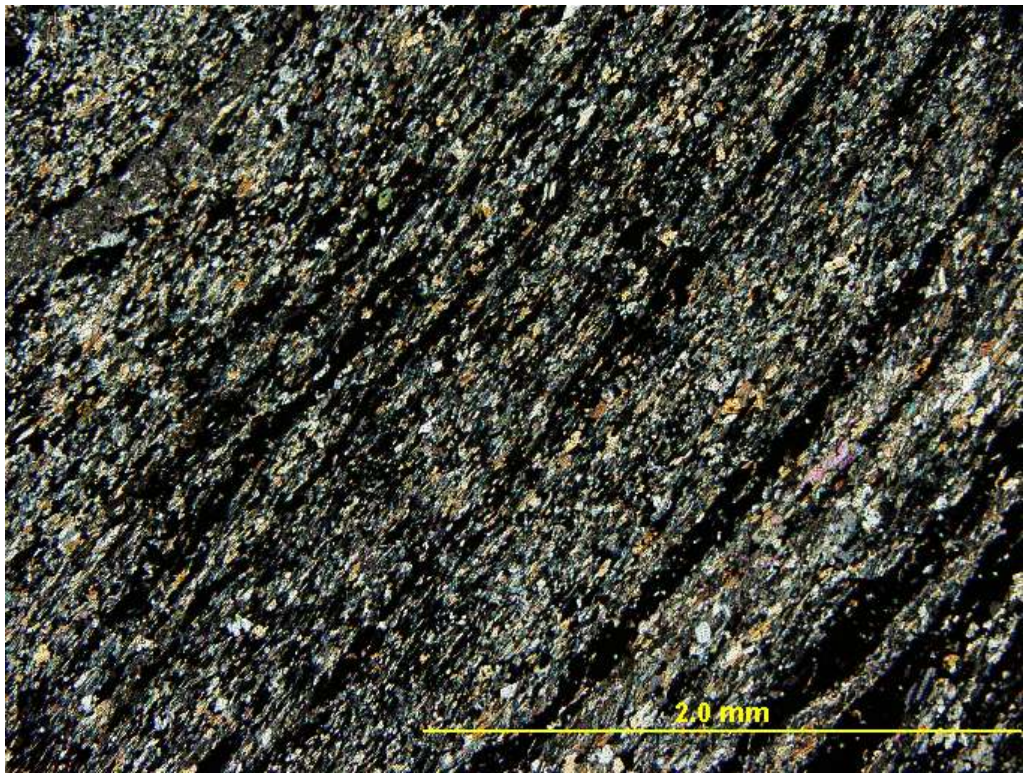

Figure 3.2.4 Sample 210-209 (209-002). Grunerite-rich band with opaque magnetite in cross polarized transmitted light.

3.2.3: Carbonate-grunerite-rich bands

Carbonate is sometimes observed at Musselwhite Mine and in this study is commonly observed associated with grunerite. Minor carbonate is observed in specific sections of grunerite-rich bands, but in the carbonate-grunerite-rich bands, carbonate appears much more consistently and in much larger amounts with quartz and magnetite becoming minor components if present at all, like in sample 210-217 (Fig. 3.2.5).

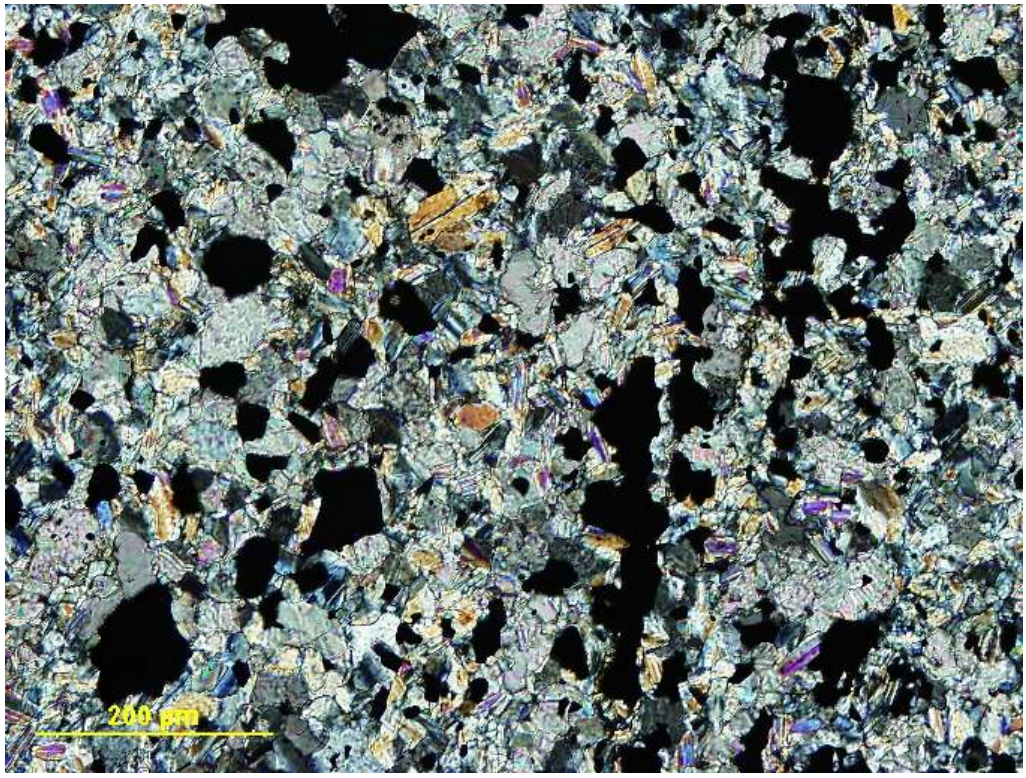

Figure 3.2.5 Sample 210-217 (217-001). Typical example of a carbonate-grunerite-rich band in cross-polarized transmitted light. Carbonate and grunerite are fine grained; the opaque specks are pyrrhotite and magnetite.

These bands can be more complex, sometimes including clinopyroxene and blue-green amphibole in addition to grunerite. The clinopyroxene was determined to be hedenbergite using semi-quantitative SEM analysis (Appendix C). The blue-green amphiboles were determined to

be two types of iron-rich amphiboles, ferroschermakite and ferroactinolite. The hedenbergite can be seen in Fig. 3.2.3, while the ferroactinolite can be seen in Fig. 3.2.6. These minerals have been found in association with other BIF-hosted gold deposits (McCuaig and Kerrich 1998 and references therein).

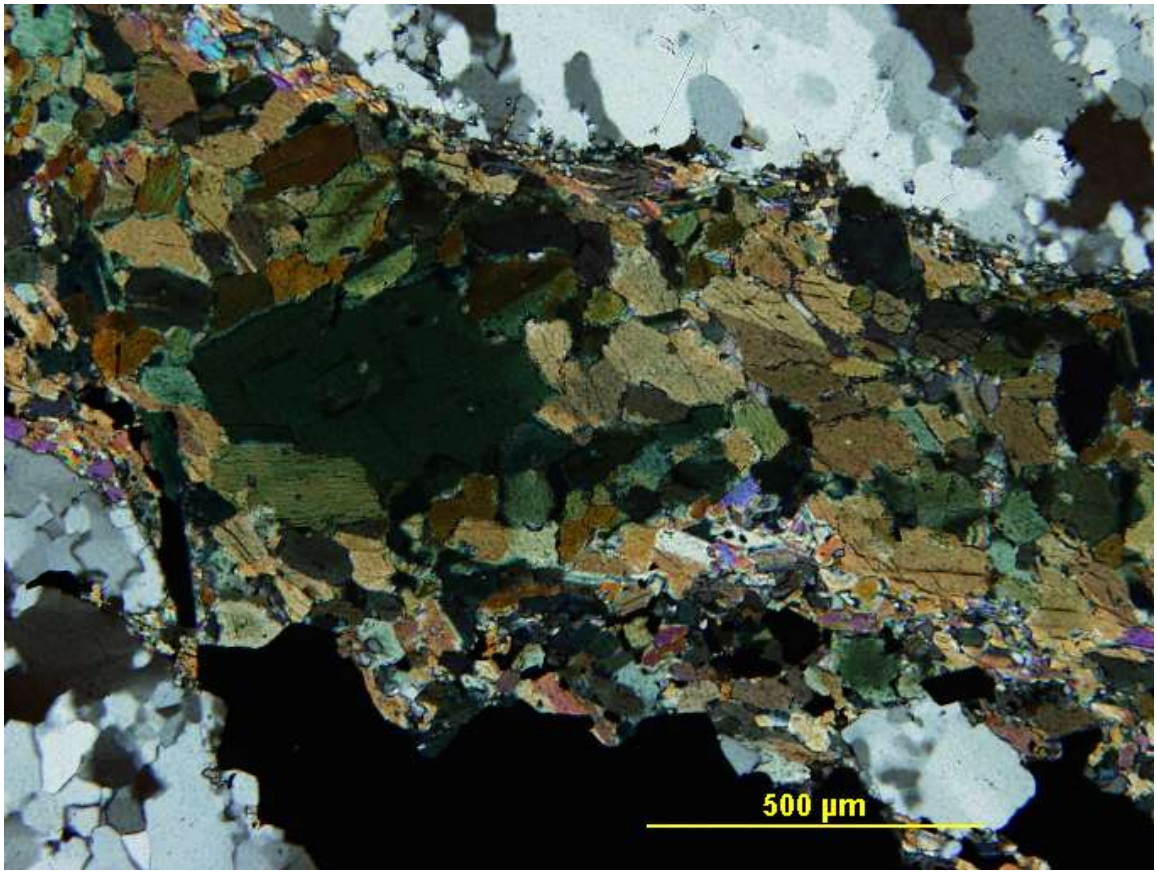

Figure 3.2.6 Sample 210-513 (513-016). The green amphibole on the left of this photomicrograph (cross-polarized transmitted light) is ferroactinolite and the green-brown amphibole also making up this band is ferroschermakite.

3.2.5: Pyrrhotite textures

Pyrrhotite is the most common sulfide mineral at Musselwhite Mine. In Lithology 2, pyrrhotite occurs in three textures. Pyrrhotite is often observed as massive veins, which commonly appear

within quartz-rich areas. Pyrrhotite also occurs as stringers usually oriented parallel with the foliation or other bands. Sometimes pyrrhotite occurs in a massive poikiloblastic texture, where it completely surrounds mineral inclusions, enveloping them in pyrrhotite. Minerals commonly surrounded by pyrrhotite are carbonate, grunerite, quartz and feldspar, see Fig. 3.2.7. The latter two textures of pyrrhotite occur at times with arsenopyrite. The arsenopyrite crystals are subhedral; many of them appear ragged and/or fractured.

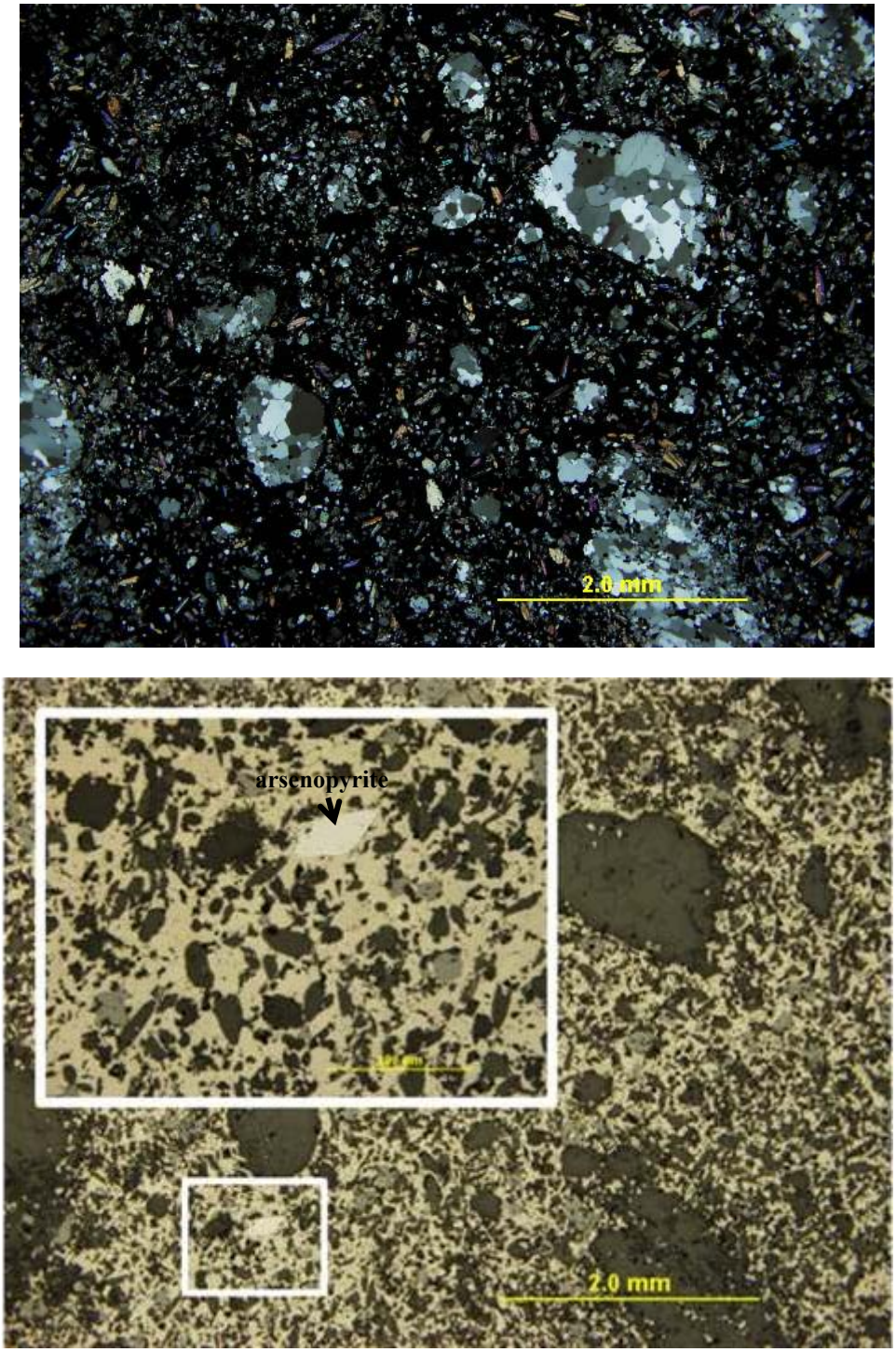

Figure 3.2.7 Sample 210-203 (203-001) Pyrrhotite dominates this sample; its poikiloblastic texture surrounds the other minerals, quartz, carbonate and grunerite (which can be noted in the top cross-polarized transmitted). Scattered throughout the pyrrhotite are blebs of grey colored magnetite as well as silver to white colored, subhedral arsenopyrite crystals (bottom photomicrograph in plane-polarized reflected light). The boxed-in area is zoomed to a higher magnification to better show the arsenopyrite and magnetite.

3.3: Lithology 3, Hammond Reef, quartzofeldspathic schist

Hammond Reef is hosted by the Marmion batholith which is a metamorphosed tonalite. In this study it is referred to as quartzofeldspathic schist, Lithology 3. This unit is primarily made up of quartz, plagioclase, muscovite and K-feldspar with biotite, chlorite, ankerite, pyrite, magnetite, hematite and gold. Metamorphism of the feldspar to muscovite, often referred to as alteration, is commonly observed within the mineralized zones. Mica defines the foliation, and in hand sample, the foliation appears continuous to zonal. In thin section this appears a bit messier, with anastomosing foliation defined by very fine grained mica within altered feldspar crystals and large grained muscovite crystals. Quartz crystals are sometimes elongated (or flattened) and exhibit undulose extinction. Quartz veins occur but they are affected by ductile deformation exhibiting undulose extinction and irregular grain boundaries. In hand sample and outcrop these quartz veins are rarely straight.

The main ore zones at Hammond Reef are the A zone and 41 zone which strike northeast adjacent to Marmion Lake. The approximate sampling area can be seen in Fig. 1.3.2, with sample details listed in Appendix D.

Samples ranging from well mineralized to poorly mineralized were collected from the A zone and 41 zone for thin section analysis. These samples were collected along strike of the deposit at varying depths within the ore zone. To better understand the metamorphic mineral assemblage XRD analysis was conducted on two samples to identify the very fine-grained white mica alteration (Appendix E).

3.3.1: Feldspar alteration (XRD results)

As observed in thin section and hand sample, much of the quartzofeldspathic schist from Hammond Reef is sericitized. Sericitic alteration is common in felsic rocks, most commonly characterized by feldspar alteration to very fine grained muscovite (Vernon and Clarke 2008 and references therein). This type of alteration is considered a hydration-dominant reaction because the main reactant is H^+. In such hydration-dominant reactions hydrogen ions are exchanged for other cations. For sericitic-type alterations the mass change may include loss of Na and Ca or loss of K and Si with the gain of H_2O with F, and S commonly associated (Vernon and Clarke 2008 and references therein).

The addition of H_2O and F is clear as the reaction from feldspar to the more hydrous mineral muscovite is widespread. Similarly the presence of pyrite implies the addition of sulfur. The replacement of feldspar by muscovite can be seen in Fig. 3.3.1, where in sample 749-438, feldspar has almost completely altered to muscovite. The muscovite appears as the fine grained matrix with quartz grains completely intact. Note the foliation, defined by the muscovite in this sample and how it anastomoses around the larger more competent quartz crystals.

XRD analysis was undertaken on two samples representative of highly sericitized quartzofeldspathic schist to determine the mineralogy of the white mica. The results of these analyses can be seen in Figs. 3.3.2 and 3.3.3. For both of these samples the dominant mineralogy was determined to be quartz, muscovite and albite, with all other peaks too close to the background to identify with confidence.

Due to the fine grained nature of the highly altered samples diffusive mass transfer may have been an active deformation mechanism. Diffusive mass transfer is not associated with clear

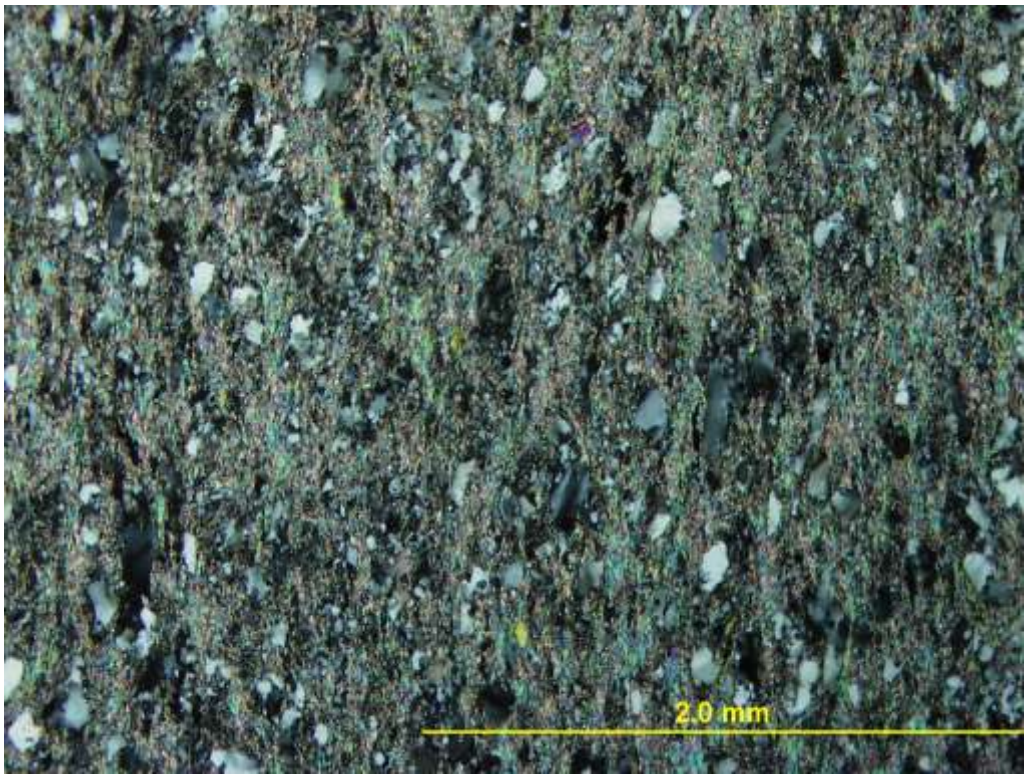

Figure 3.3.1 Sample 749-438 (438-005). This is a highly altered sample were nearly all the feldspar has reacted to form muscovite. Muscovite defines the foliation and appears as the fine grained matrix with larger quartz crystals. Notice how the muscovite anastomoses around the larger quartz porphyroclasts. The quartz is elongated parallel to the foliation and exhibits undulose extinction, irregular grain boundaries and subgrains.

microstructural evidence but it is common in fine grained rocks with grain boundary fluids present (Schmid et al. 1977; Behrmann 1983; Stunitz and Fitz Gerald 1993; Paterson 1995; Fliervoet et al. 1997; Kruse and Stunitz 1999).

The protolith for the quartzofeldspathic schist is considered to be mainly tonalite but can range to granodiorite. The major components of the igneous rock tonalite are plagioclase (oligoclase and andesine), quartz and K-feldspar (IUGS classification scheme). The XRD analysis shows albite

as the plagioclase member present in these samples. Albite is the most common plagioclase feldspar to find at greenschist facies metamorphism (Winter 2010), which is the presumed facies of metamorphism on the Hammond Reef property. Albite is the Na-rich end-member of the plagioclase group, and the protolith tonalite has more Ca-rich plagioclase compositions of oligoclase and andesine (An_{10-50}). The extra Ca from the initial plagioclase would not be used during metamorphism by either of the other two minerals but may be the source for the carbonate veins nearby.

Another interesting result of this analysis is that in these highly altered samples no K-feldspar remains. This is not entirely surprising because K-feldspar is a reactant in the metamorphic reaction to produce muscovite from a tonalitic protolith. In a tonalite K-feldspar would have originally made up less than 10% of the rock, so it is reasonable to assume that all the K-feldspar was consumed by reaction (Winter 2010). There is little evidence to support major changes due to metasomatism because of the simple mineralogy observed.

3.3.2: Pyrite

The pyrite content in Lithology 3, the quartzofeldspathic schist at Hammond Reef, varies but seems to be associated with gold mineralization. Pyrite is the most common sulfide mineral at Hammond Reef. Pyrite grains most commonly appear euhedral to subhedral, but also pyrite occurs brecciated and strung out, looking almost stringer-like. In hand sample this brecciated pyrite appears vein-like, but in thin section it is apparent that the "veins" are made up of aligned fractured, subhedral pyrite crystals. Pyrite is a competent mineral which is high on the crystalloblastic series, because of this, pyrite commonly appears in a euhedral cubic shape in metamorphic rocks. High strain rates in metamorphic rocks can cause the pyrite crystals to appear subhedral, fractured or even elongated.

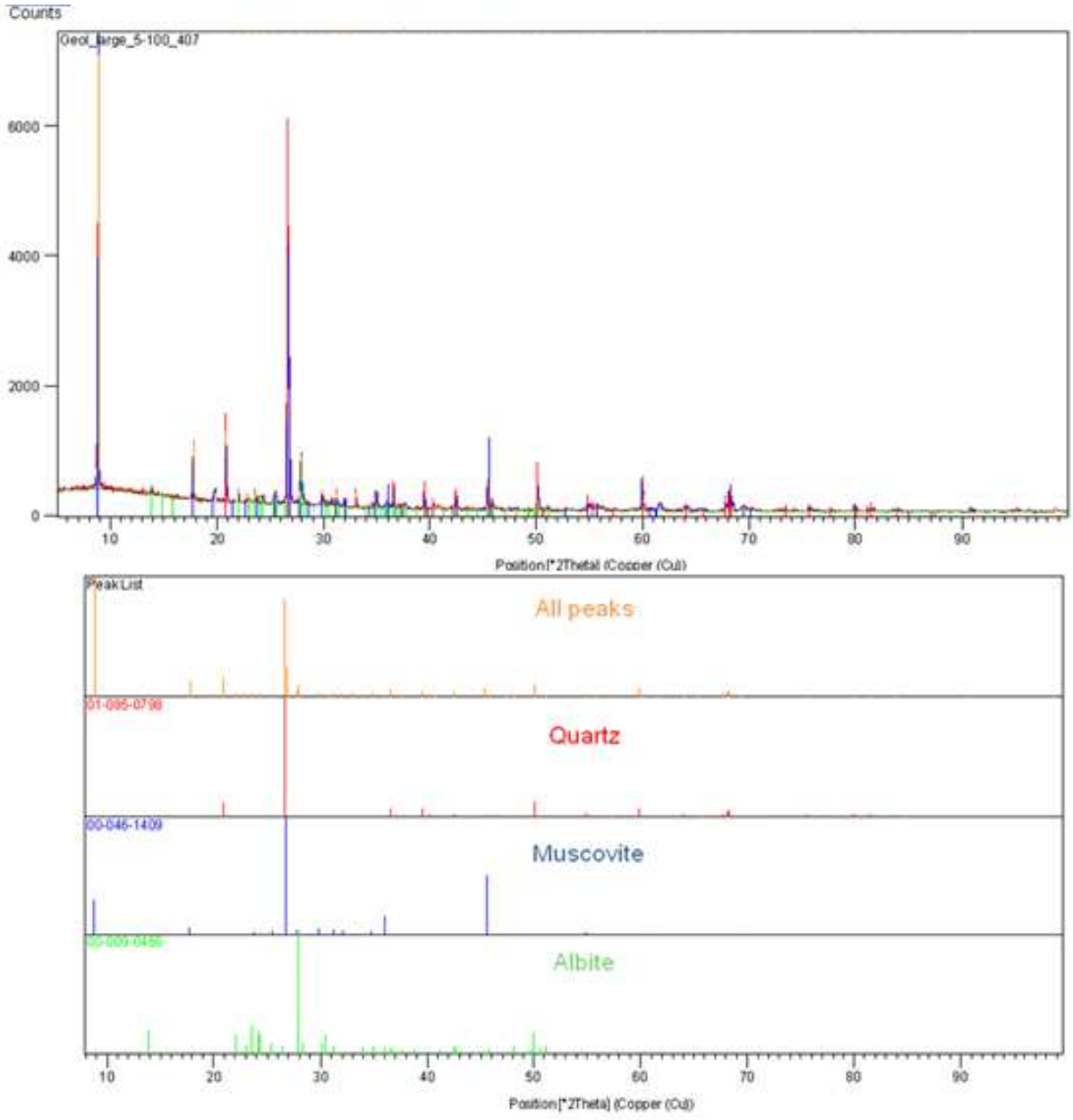

Figure 3.3.2 XRD results for sample 749-407. Top spectrum shows all peaks from the sample with peaks of matching minerals in different colors. The bottom chart breaks down the busy top spectrum into separate spectra giving all sample peaks first with matching mineral peaks separately (each of these are labeled). Three minerals fit the peaks and constitute the majority of the rock sample; those minerals are quartz, muscovite and albite.

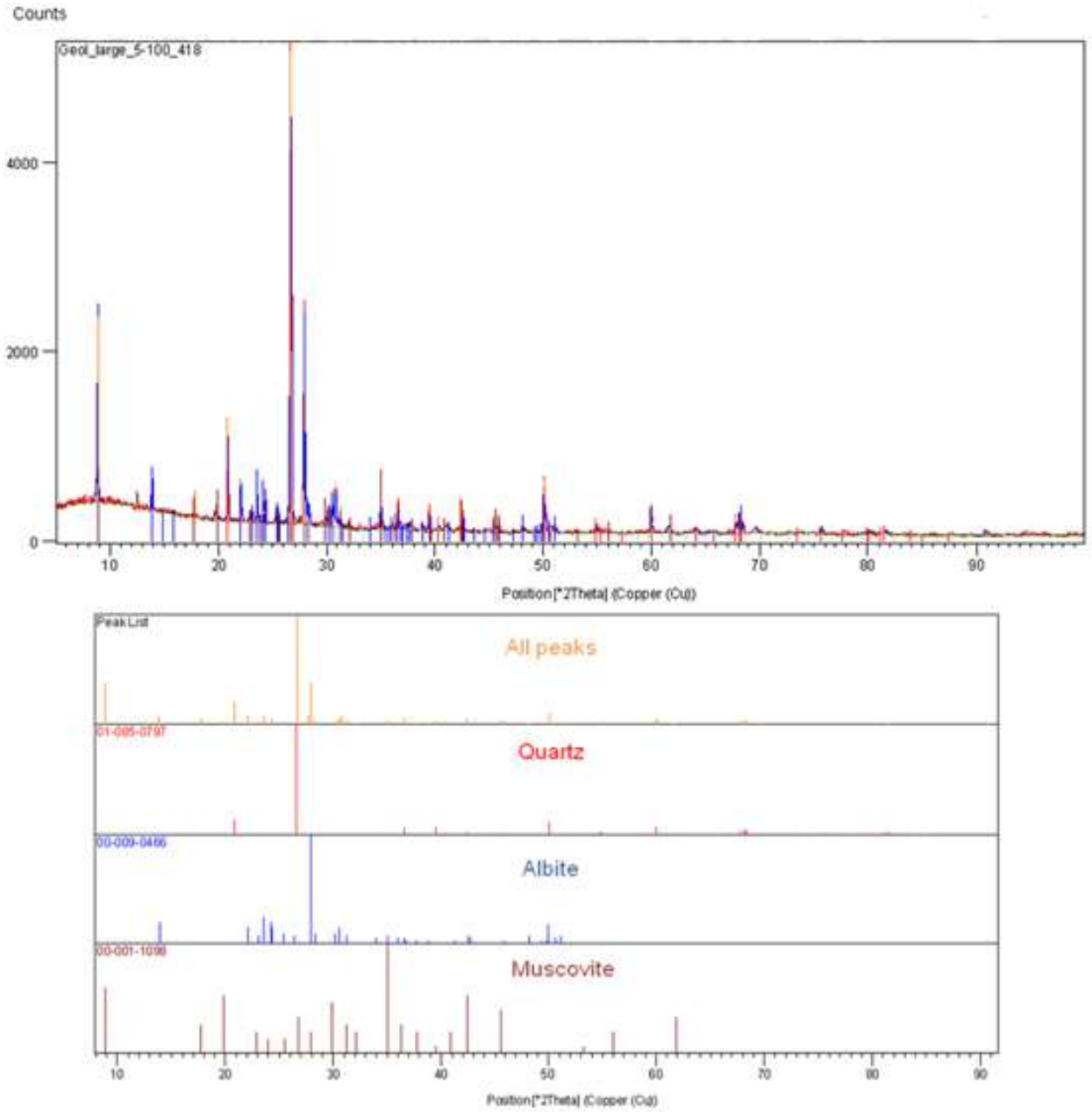

Figure 3.3.3 XRD results for sample 749-418. Top spectrum shows all peaks from the sample with peaks of matching minerals in different colors. The bottom chart breaks down the busy top spectrum into separate spectra giving all sample peaks first with matching mineral peaks separately (each of these are labeled). Three minerals fit the peaks and constitute the majority of the rock sample; those minerals are quartz, albite and muscovite.

3.3.2a: Pyrite etching

Etching can be used to see zoning in pyrite otherwise invisible under microscopic investigation. This etching technique was used to seek a relationship between growth zones and gold mineralization. Etching of pyrite was attempted for 10 samples in this study. None of these samples showed zoning. This may be due to the metamorphic condition in which these pyrite crystals grew. This technique is more commonly used on pyrite crystals in low temperature environments to see growth zoning. Etching indicates no signs of growth zoning in the Hammond Reef pyrite crystals.

3.3.3: Other features

In this study, only typical examples from the most common lithology at Hammond Reef were examined. The Marmion batholith is host to many other lithologies as well as pegmatites and many veins. These were not part of this study because they comprise a small amount of the ore-hosting rock.

3.4: Summary and comparison of lithologies

3.4.1 Musselwhite Mine

Both Lithologies 1 and 2 from Musselwhite Mine are metamorphosed banded iron formation. A clastic input can be interpreted from the aluminum-rich metamorphic mineral assemblage of Lithology 1, the garnet-grunerite schist. Aluminum-rich minerals such as garnet and biotite are not found in Lithology 2, the grunerite schist, because this metamorphosed iron formation does not have this clastic input. But both lithologies from Musselwhite Mine share common minerals typical of metamorphosed iron formation such as grunerite, magnetite and pyrrhotite.

Both Lithologies 1 and 2 have a spaced foliation, defined by minerals like grunerite and biotite in specific bands. The foliation for both Lithologies 1 and 2 range from smooth to rough and parallel to anastomosing. With the main gold-hosting lithology the garnet-grunerite schist (Lithology 1) a trend between foliation style and gold mineralization occurs. Gold more commonly occurs where the foliation is not smooth and parallel. For Lithology 1 from Musselwhite Mine, the more the foliation diverts from smooth and parallel, the more likely it will host gold mineralization. For Lithology 2, the grunerite schist from Musselwhite Mine, no such relationship can be deduced.

These two lithologies from Musselwhite Mine differ mineralogically, but in both cases gold appears most commonly within bands of complex mineralogy. For Lithology 1, the garnet-grunerite schist, gold mineralization appears most commonly in garnet-amphibole and garnet-amphibole-biotite bands, with 39 of the 52 documented gold occurrences for Lithology 1 occurring in these garnet-bearing bands. Similarly in Lithology 2, the grunerite schist, gold

appears commonly in the carbonate-grunerite-rich bands. In the 107 documented gold occurrences, 46 occur in carbonate-grunerite-rich bands.

3.4.2: Hammond Reef

At Hammond Reef, Lithology 3, the quartzofeldspathic schist is fairly simple. The main ore-hosting lithology is composed of quartz, feldspar and muscovite. The presence of muscovite is common to the gold-hosting rock, and indicates a hydrous metamorphic reaction. This muscovite is pervasive and defines the foliation in Lithology 3. Pyrite is associated with gold mineralization at Hammond Reef, with 79 of the 103 documented gold occurrences for Lithology 3 occurring as inclusions and in fractures in pyrite.

3.4.3: Comparison of Musselwhite Mine and Hammond Reef

Musselwhite Mine and Hammond Reef are shear-zone-hosted gold deposits. Musselwhite Mine is adjacent to the North Caribou-Totogan Lake shear zone while Hammond Reef is adjacent to the Marmion Lake shear zone. Both of these shear zones are major regional shear zones and separate rocks of different age domains (Stott et al. 2007 and Stone 2009). At Musselwhite Mine the North Caribou-Totogan Lake shear zone separates the Island Lake Domain to the north from the North Caribou Terrane to the south (Stott et al. 2007) (Fig. 1.3.1). Recent work by Stone (2009) separated the Central Wabigoon area also known as the Marmion Terrane into many different age domains. Most importantly to Hammond Reef is the separation of the Central Wabigoon Domain from the Marmion Domain which occurs along the Marmion shear zone adjacent to the property (Chapter 1; Figs. 1.3.2 and 1.3.3).

Both of these deposits are associated with regional metamorphism. Musselwhite Mine has been determined to have metamorphosed to amphibolite facies (Hall and Riggs 1986, Breaks et al.

2001, Ottto 2002, Stinson 2010). Hammond Reef on the other hand is inferred to have metamorphosed to greenschist facies (Tomlinson et al. 2003, Easton 2000) which is consistent with the textures observed in samples from this study.

Although these deposits have been affected by different metamorphic temperatures, both deposits show evidence of dominantly ductile deformation. Rocks from both deposits are foliated with microstructures supporting only minor brittle deformation.

Chapter 4: Gold Mineralization

4.1: Lithology 1, Musselwhite Mine, garnet-grunerite schist

Gold mineralization is observed to be associated with a number of different minerals and textures (Appendix A.5). The following discusses the observed gold occurrences in Lithology 1.

4.1.1: Gold mineralization associated with garnet crystals

4.1.1a: Gold as inclusions

Gold mineralization appears as inclusions within the competent mineral garnet in 13 documented gold occurrences. These gold inclusions come in a variety of shapes. Some inclusions were likely trapped during garnet growth while others exhibit an irregular shape and are more likely to have originated in fractures which healed over during progressive metamorphism.

4.1.1b: Gold in fractures

In 16 documented gold occurrences, gold appears within fractures in the competent garnet crystals. In many of these cases, the fractures are filled with other minerals like pyrrhotite or grunerite. Lithology 1 is rich with garnets. These garnets fracture due to their resistance to ductile deformation. The deformation of garnet has been studied with respect to understanding the mantle because garnet is found in eclogite. Storey and Prior (2005) concluded that garnet can plastically deform at a temperature of 700 °C and high strains, like those found in a high temperature ductile shear zone. This agrees with the work of others (e.g. Ando et al. 1993; Voegele et al. 1998a; Wang and Ji 1999; Ji et al. 2003; Mainprice et al. 2004; Storey and Prior 2005), but those temperatures are much higher than those interpreted for metamorphism at

Musselwhite Mine. Even in research of this high temperature deformation, strain partitioning is thought to accommodate much of the deformation (e.g. Mainprice et al. 2004).

Because garnet is much more competent than the other minerals present in Lithology 1, the garnet-grunerite schist (Musselwhite Mine), microfractures are commonly observed in this mineral. Also gold mineralization is commonly observed within these microfractures in garnet crystals. Gold mineralization within garnet crystals and in fractures is consistent with the observations of other researchers (Hill et al. 2006).

4.1.1c: Gold mineralization in strain shadows

Garnet has also been associated with gold mineralization in a less direct way than inclusions and fracture filling.. Gold occurs in strain shadows from Lithology 1, the garnet-grunerite schist. Because garnet is a competent mineral it is often the "core" mineral that nucleates strain shadows (Passchier and Trouw 2005). Gold blebs neighbor a large garnet crystal in sample 310-637 (Fig. 4.1.1), the gold occurs within the strain shadow to the right of the garnet crystal. Outside the strain shadow, grunerite defines a foliation but the gold appears within the disorderly grunerite in the strain shadow area. In sample 909-007 gold mineralization is found between three garnet crystals in a complex strain shadow (Fig. 4.1.2). The gold in this example is found within a strain shadow where biotite and quartz are randomly oriented despite the foliation which is defined outside the shadow structure.

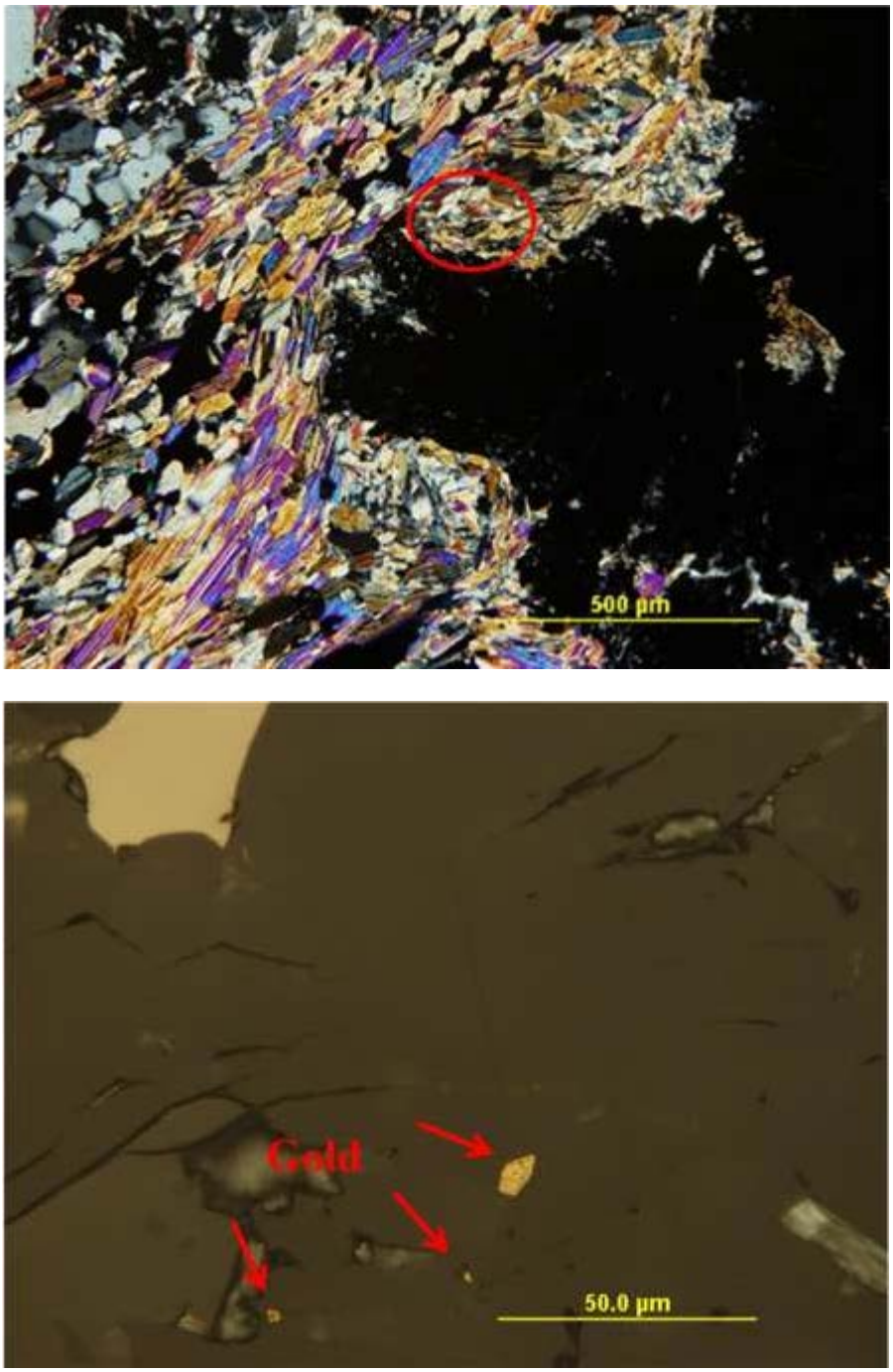

Figure 4.1.1 Sample 310-637 (637-001). Large opaque garnet is the "core" mineral causing a strain shadow seen in the top photomicrograph in cross-polarized transmitted light. Gold occurs within the circled area of the strain shadow, notice that the foliation defined by grunerite does not occur in this area. Gold can be seen at higher magnification in the bottom photomicrograph in plane polarized reflected light.

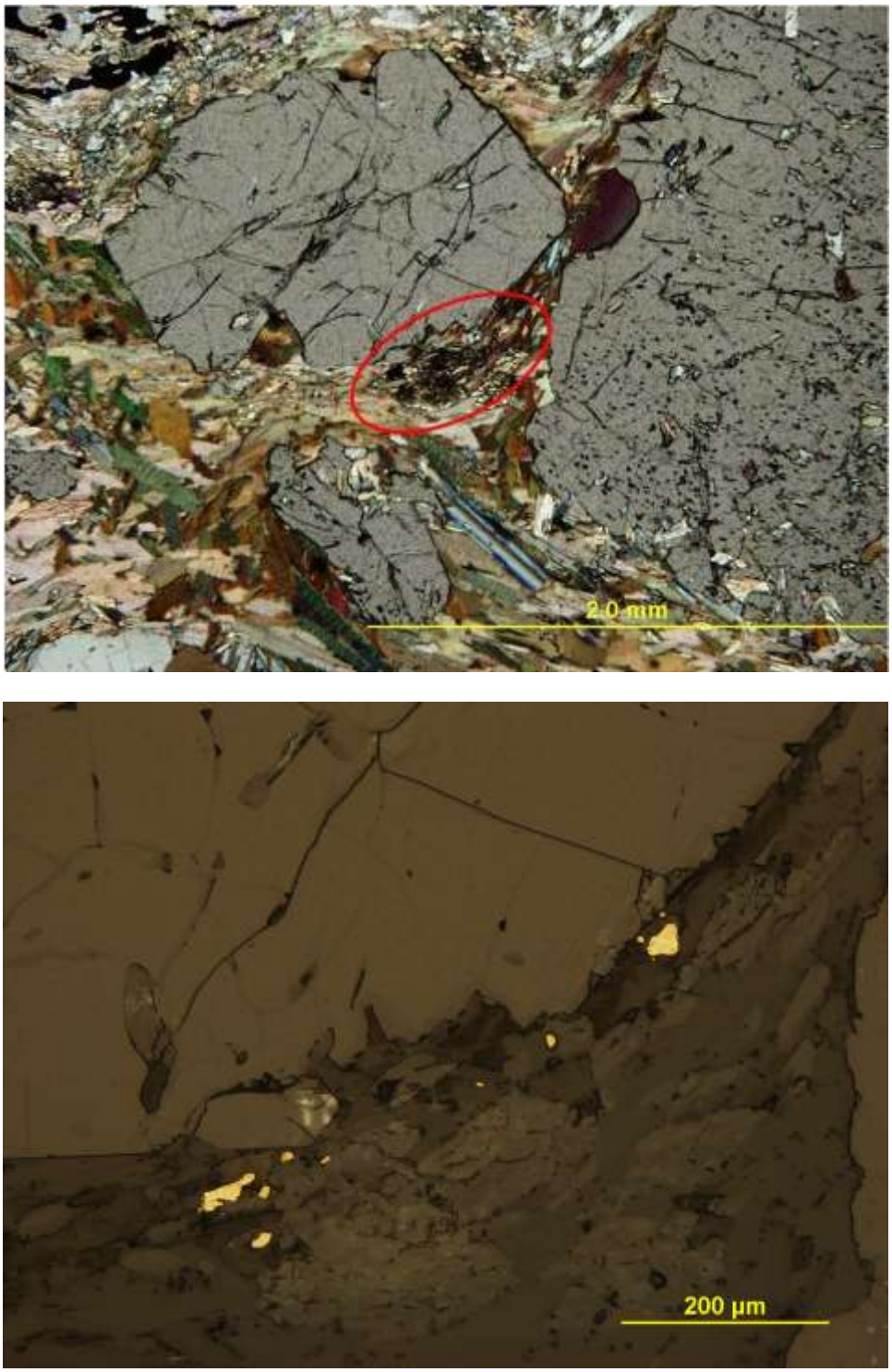

Figure 4.1.2 Sample 909-007 (007-003). In the top photomicrograph seen in cross polarized transmitted light, a strain shadow exists between the extinct garnet crystals. This strain shadow hosts gold mineralization. The bottom photomicrograph is at higher magnification and in plane-polarized reflected light; note the gold blebs, the large gangue mineral to the top left is garnet.

4.1.2: Gold as inclusions and fracture filling in other minerals

Garnet is not the only mineral to host gold inclusions in this lithology; gold occurs as inclusions within hornblende, grunerite, quartz, pyrrhotite and arsenopyrite in Lithology 1. Sample 808-113 is rich with gold inclusions within garnet as well as grunerite; gold also appears within fractures in the garnet (Fig. 4.1.3). A single gold inclusion appears within hornblende in Fig. 4.1.4. In some cases, inclusions of gold are associated with other inclusions within garnet crystals, such as pyrrhotite, grunerite and quartz. This occurs in sample 909-002, where gold and quartz appear as inclusions in garnet (Chapter 3; Fig. 3.1.5). Garnet crystals at Musselwhite Mine are often rich with inclusions, for example sample 909-001 (Chapter 3; Fig. 3.1.6).

4.1.3: Gold mineralization on plane defects

Plane defects occur where the crystal structure is different across a plane. Plane defects include; grain boundaries, subgrains and twin planes (Perkins 2002). In Lithology 1, gold commonly appears along grain boundaries, which is the most common plane defect. Gold mineralization on grain boundaries appears between like minerals for example on quartz-quartz boundaries as well as unlike mineral boundaries. One example of gold mineralization on unlike mineral grain boundaries occurs in sample 310-630 where gold is on the boundary between carbonate and quartz (Fig. 4.1.5). Gold mineralization also appears on twin planes in grunerite. In sample 310-624 gold appears as inclusions and on grain boundaries but one speck of gold also occurs on a twin plane in grunerite (Fig. 4.1.6).

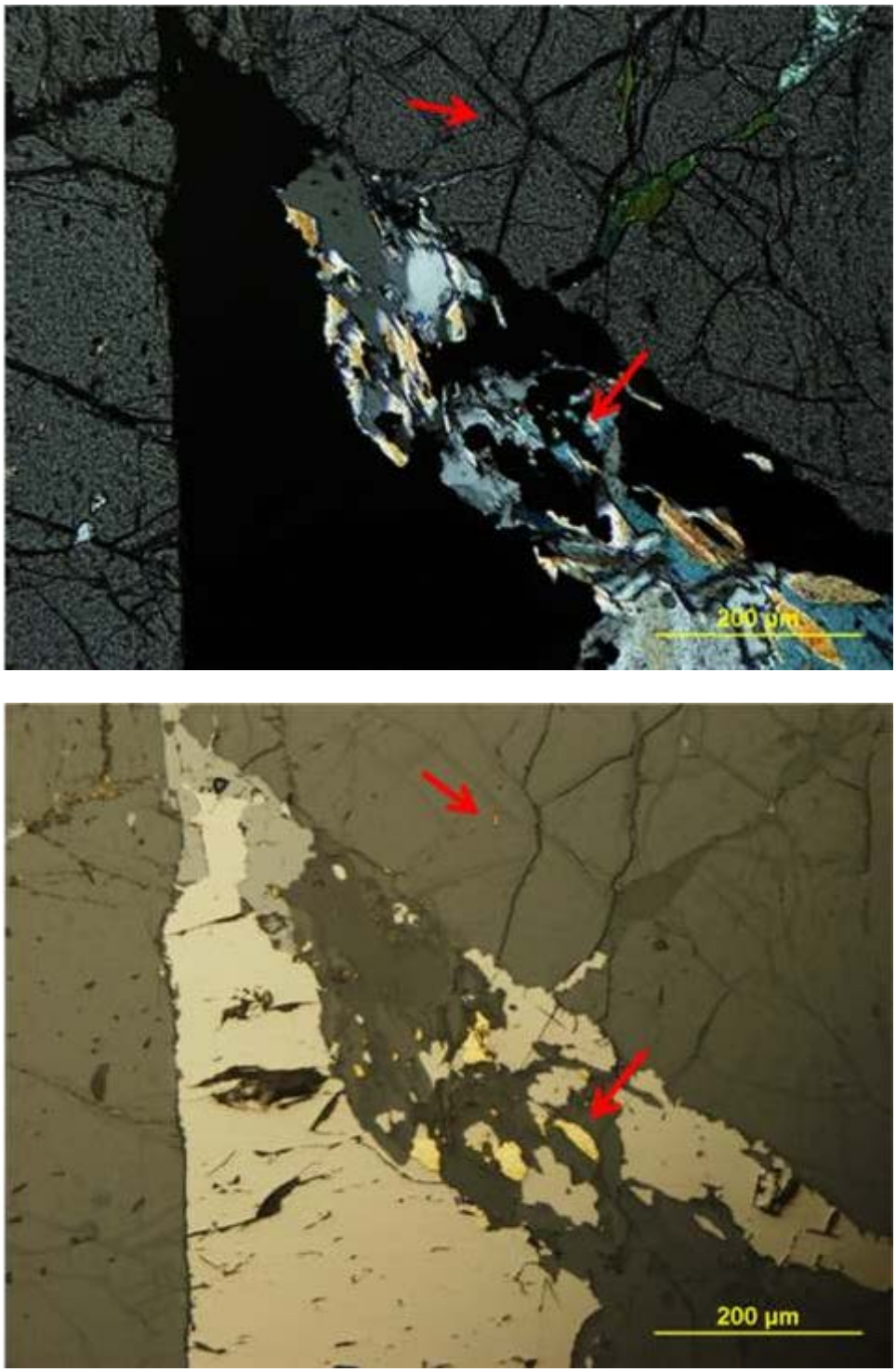

Figure 4.1.3 Sample 808-113 (113-001): This sample is rich with gold as inclusions in garnet and grunerite (see red arrows). Gold is also within fracture in garnet, best seen in bottom photomicrograph (plane polarized reflected light) at the top left corner. The rest of the gold appears on grain boundaries.

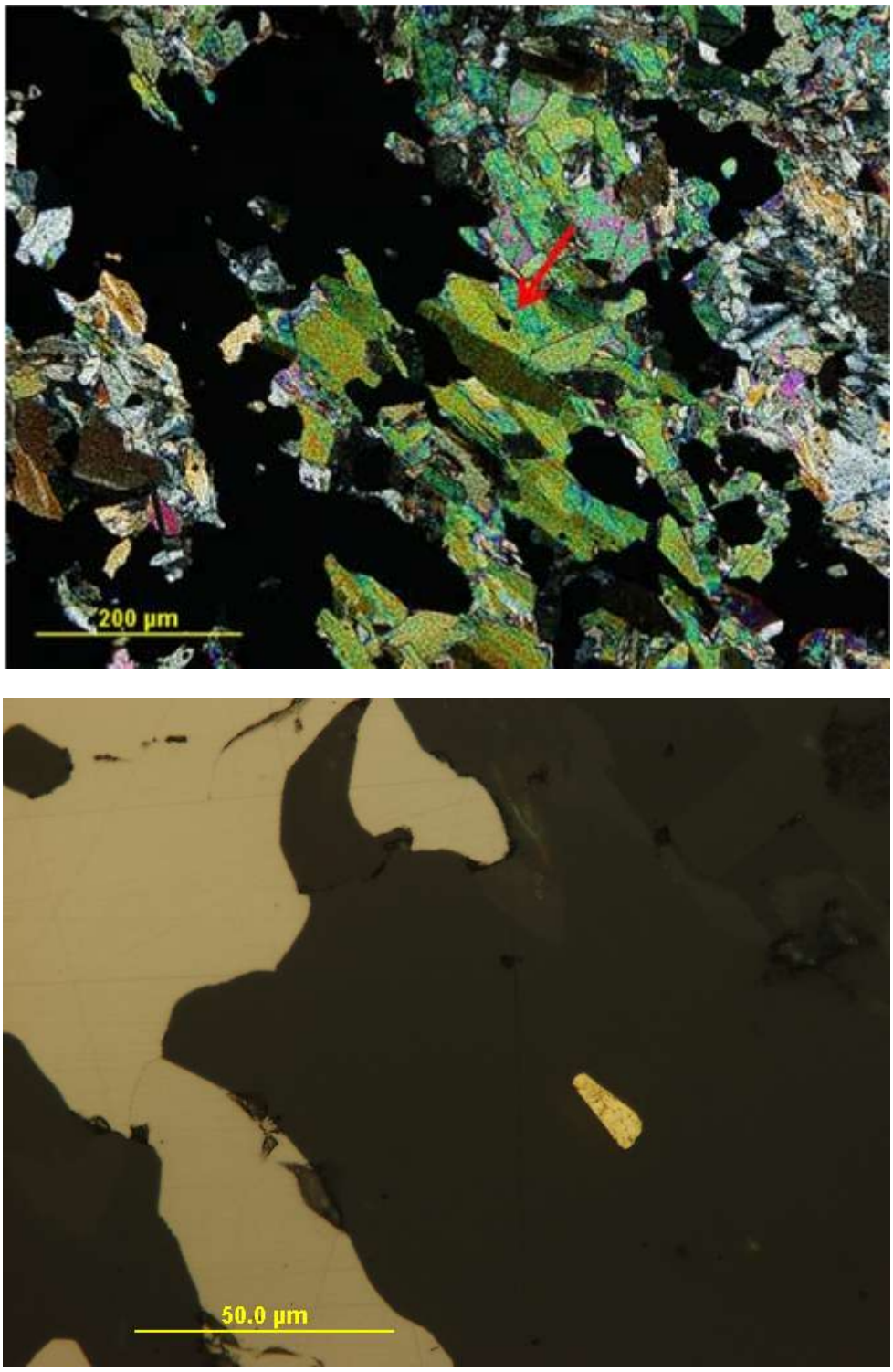

Figure 4.1.4 Sample 310-611 (611-001). Gold occurs as an inclusion within hornblende. Red arrow shows the location of the gold bleb in the top photomicrograph in cross-polarized transmitted light. The bottom photomicrograph is at higher magnification in plane-polarized reflected light.

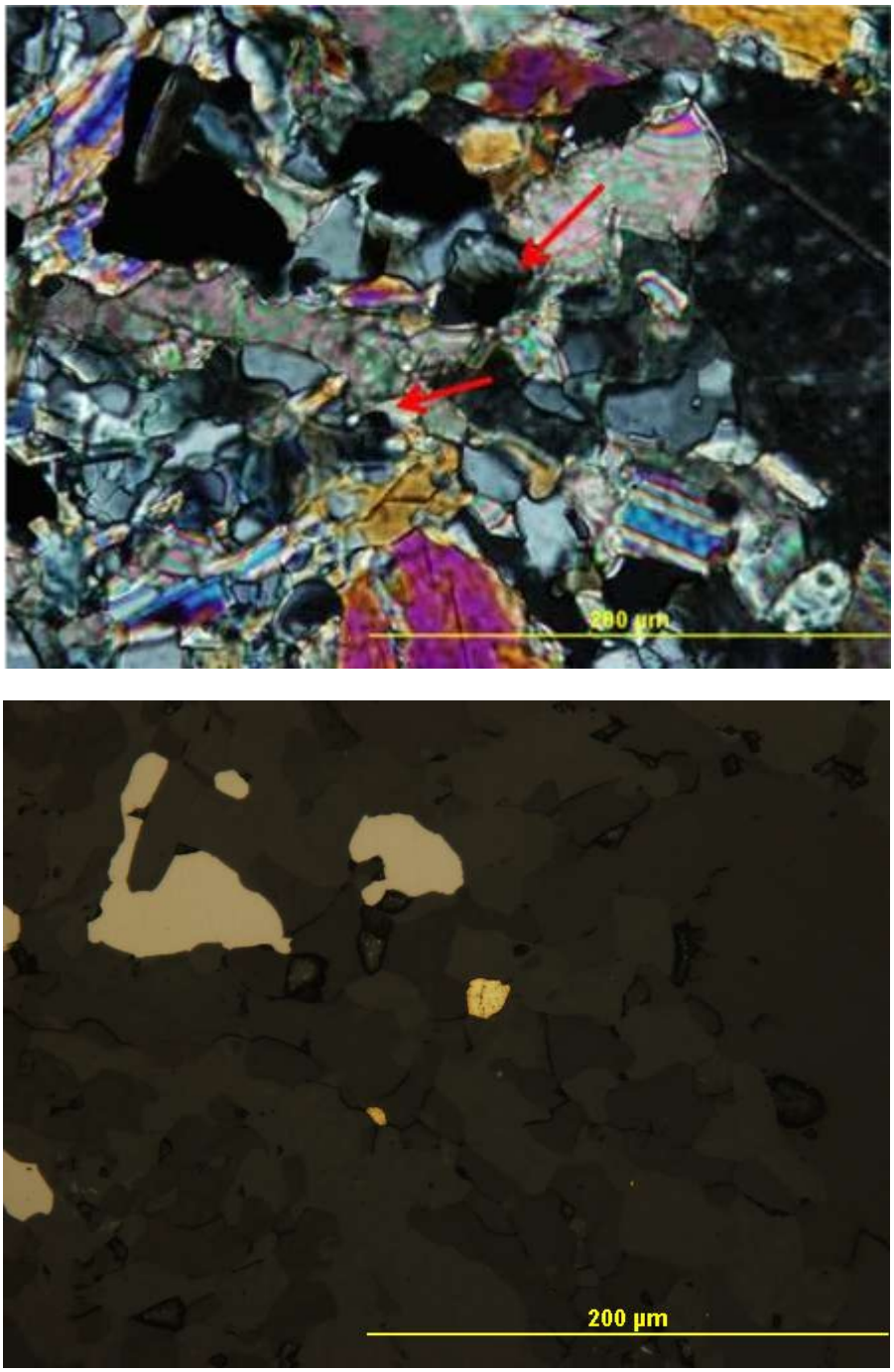

Figure 4.1.5 Sample 310-630 (630-001) The red arrows in the top photomicrograph (cross-polarized transmitted light) point out the opaque gold blebs which occur on the grain boundaries between quartz and carbonate. The bottom photomicrograph depicts the same area at the same magnification but in plane polarized reflected light. The gold blebs can be seen in the bottom photomicrograph.

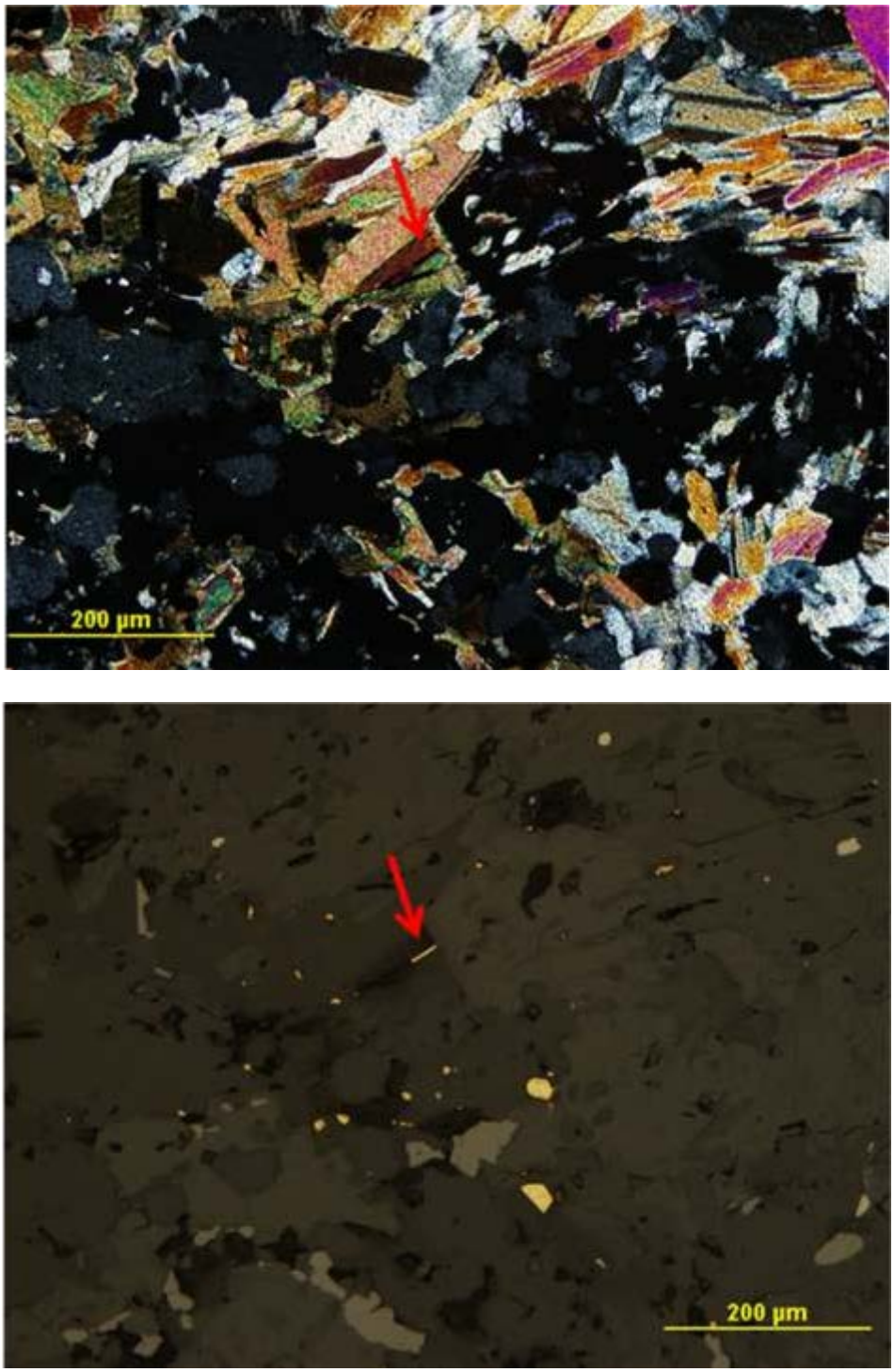

Figure 4.1.6 Sample 310-624 (624-001). There are many gold blebs in this example which can be seen in the bottom photomicrograph (in plane-polarized reflected light). Most of the gold blebs occur as inclusions or on grain boundaries. The red arrow in both photomicrographs highlights one specific speck of gold which occurs on the twin boundary of a grunerite crystal. The twin boundary can be observed best from the top photomicrograph in cross-polarized transmitted light.

4.1.4: Gold associated with polymineralic ductile deformation

Two examples of gold mineralization from Lithology 1 are associated with polymineralic ductile deformation. Deformation of polymineralic rocks is thought to be less efficient, than in monomineralic rocks, which causes textural change in unlike neighboring minerals (Tullis 2002). Lithology 1 from Musselwhite Mine is banded iron formation with quartz bands commonly occurring. In a quartz band area containing only quartz, it will deform as monomineralic rocks and exhibit typical textures of quartz deformed at amphibolite facies metamorphism. If this quartz band contains another mineral phase like biotite, for example, the texture of the quartz crystals will be affected when adjacent to the biotite crystals. The quartz adjacent to the biotite crystals will have a smaller grain size than the quartz completely surrounded by other quartz crystals. Gold appears in two such examples in Lithology 1.

In the first example gold appears in a quartz band along strike from a thin stringer of grunerite crystals as in sample 808-111 (Fig. 4.1.7). This gold mineralization is interpreted to be associated with the heterogeneous response to strain by the quartz and grunerite. In this sample along strike from the grunerite stringer, the neighboring quartz grain-size is reduced. A similar example occurs in sample 909-007 where scattered biotite crystals are present in a quartz-rich band. The quartz grains are finer grained in the biotite-rich portion of the band than where the biotite is absent. Where the quartz is biotite-free, the quartz exhibits textures typical of quartz at amphibolite facies metamorphism, which are less apparent in the biotite-rich area. The gold mineralization occurs within a quartz crystal in the biotite-rich area of the quartz band (Fig. 4.1.8).

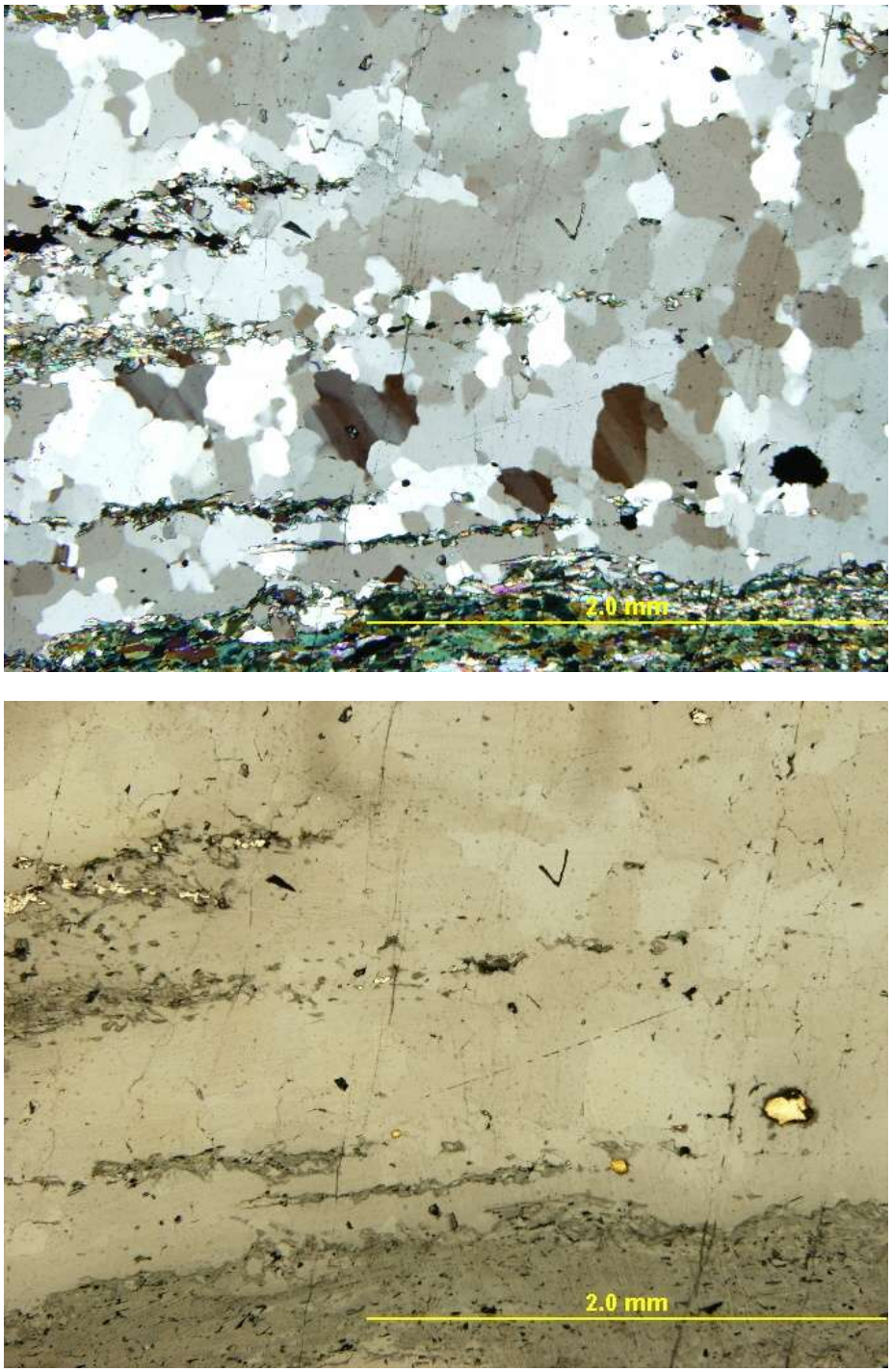

Figure 4.1.7 Sample 808-111 (111-001). Gold appears in a quartz band along strike from a thin band of grunerite crystals. The gold can be seen in bottom photomicrograph (plane-polarized reflected light). Notice in the top photomicrograph (cross-polarized transmitted light) the smaller grain size of the quartz bordering the grunerite stringer. This textural difference is likely related to heterogeneous response to strain between the neighboring quartz and grunerite crystals.

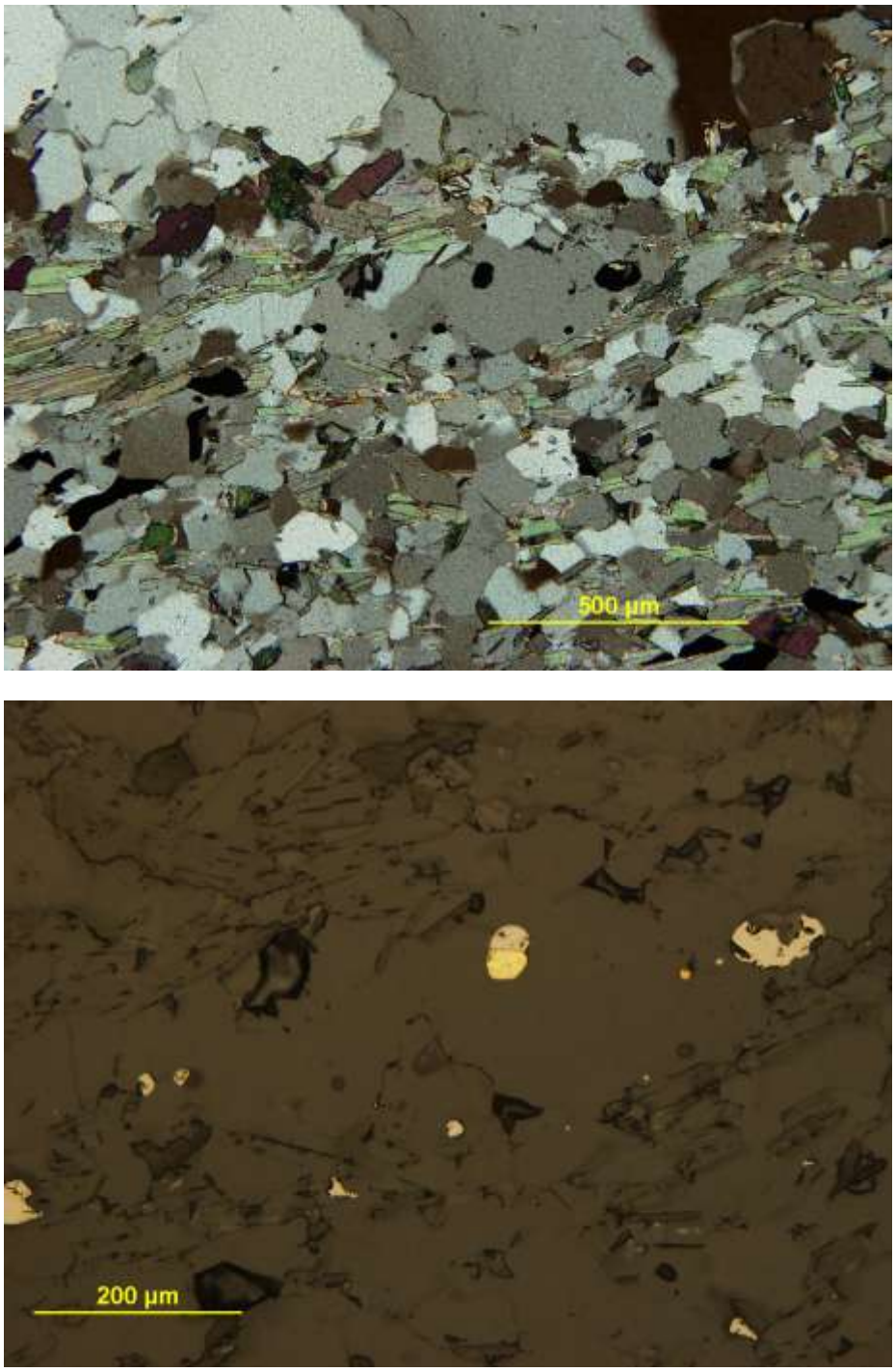

Figure 4.1.8 Sample 909-007 (007-002). In top photomicrograph (cross-polarized transmitted light) scattered biotite crystals appear in a quartz-rich band. The quartz grains are finer in the biotite-rich portion of the band than where the biotite is absent. Where the quartz is biotite-free, the quartz exhibits textures typical of quartz at amphibolite facies metamorphism, less apparent in the biotite-rich band. The gold mineralization occurs within a quartz crystal in the biotite-rich band which can be seen in bottom photomicrograph (plane-polarized reflected light).

Table 4.1.1: Summary of documented gold occurrences for Lithology 1, Musselwhite Mine, garnet-grunerite schist

Summary of documented gold occurrences	**Totals**
Total number of occurrences documented:	52
Gold inclusions in metamorphic minerals:	31
Gold inclusions within garnet:	13
Gold inclusions within grunerite:	15
Gold inclusions within hornblende:	3
Gold within fractures:	16
Gold within fractures in garnet:	16
Gold within strain shadows:	8
Gold within strain shadows of garnet:	8
Gold occurring on plane defects:	15
Gold within quartz-rich bands:	5
Quartz-rich band with other minerals:	4
Quartz-rich band without other minerals:	1
Gold associated with sulfide minerals:	17
Gold in contact with pyrrhotite:	13
Gold within arsenopyrite:	4
Other:	2
Gold within carbonate:	2

*Many of the gold occurrences fall into more than one group in this table.

4.2 Lithology 2: Musselwhite Mine, grunerite schist

Like Lithology 1 from Musselwhite Mine, gold mineralization is observed in many different minerals and textures in Lithology 2, all of these listed in Appendix B.5, with a summary of the gold occurrences documented in Lithology 2 at the end of this section.

4.2.1 Gold mineralization associated with arsenopyrite

Pyrrhotite is the most common sulfide mineral at Musselwhite Mine, but in Lithology 2, arsenopyrite is important because of its physical relationship with gold mineralization. Arsenopyrite crystals are found associated with pyrrhotite of all textures, most commonly stringer-like pyrrhotite and the massive poikiloblastic pyrrhotite. These pyrrhotite textures are discussed earlier in section 3.2.5. Gold occurs as inclusions in arsenopyrite crystals as well as in fractures. In sample 210-304 gold appears as rounded blebs within arsenopyrite (Fig. 4.2.1). Arsenopyrite is known for its distinct habit; crystals observed in this study are euherdal to subhedral. Often even ragged looking crystals have a distinct shape like the arsenopyrite crystal in Fig. 4.2.2. In Fig. 4.2.2, gold is included in arsenopyrite but gold has an irregular and jagged shape. This gold is most likely filling a fracture, where the rest of the fracture has either healed or cannot be seen at this orientation.

4.2.2 Gold occurring in clinopyroxene

In the carbonate-grunerite-rich bands of Lithology 2 (the grunerite schist at Musselwhite Mine) clinopyroxene also hosts gold as inclusions and in fractures. This is comparable to the arsenopyrite in this lithology and to the garnet crystals from Lithology 1 (the garnet-grunerite schist from Musselwhite Mine) discussed in section 4.1.1. The clinopyroxene crystals

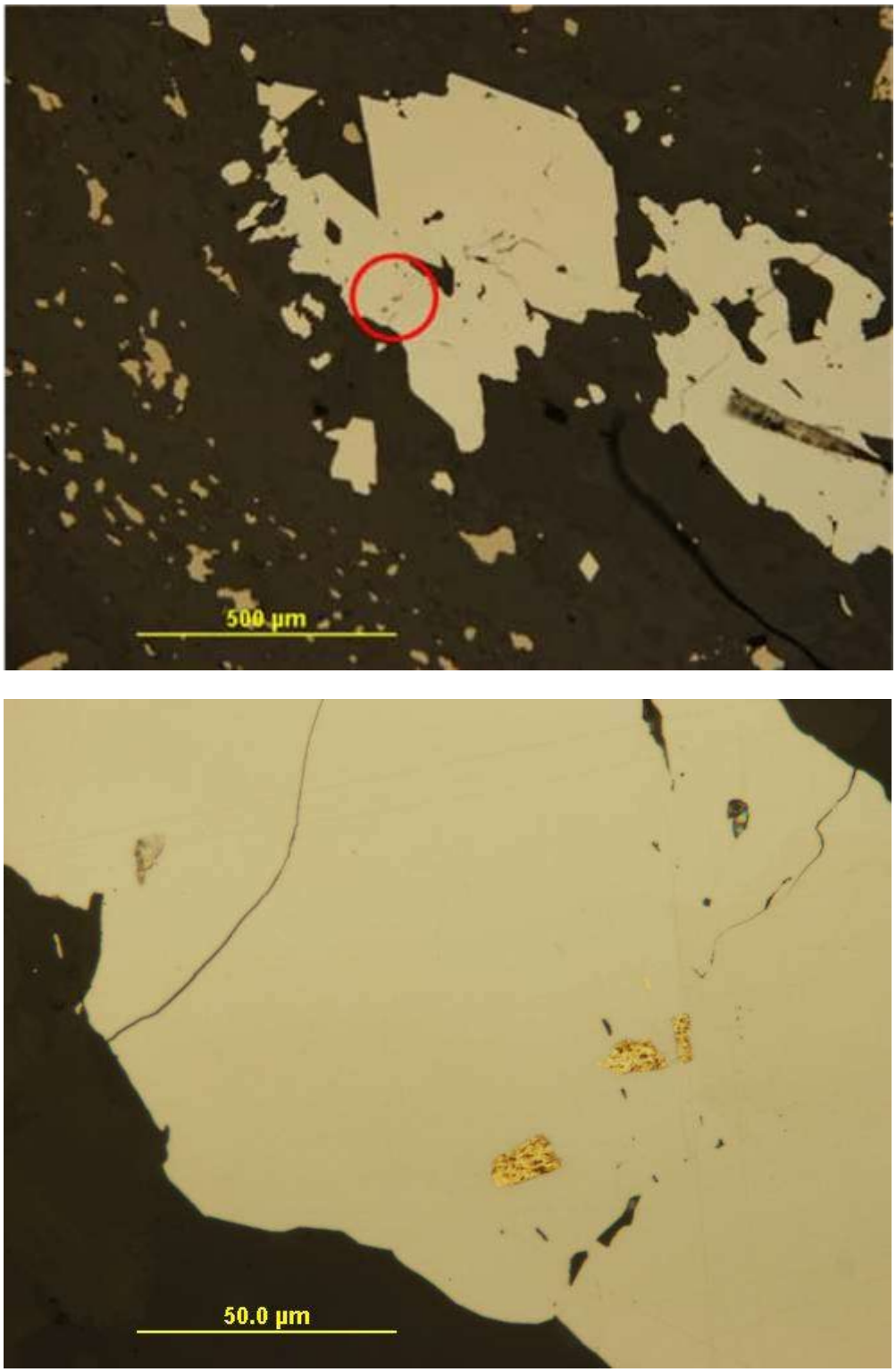

Figure 4.2.1 Sample 210-304 (304-003). Gold inclusions appear within a subhedral arsenopyrite crystal. Red circle depicts area where gold inclusions occur in the top photomicrograph which can be seen at higher magnification in bottom photomicrograph (both in plane polarized reflected light).

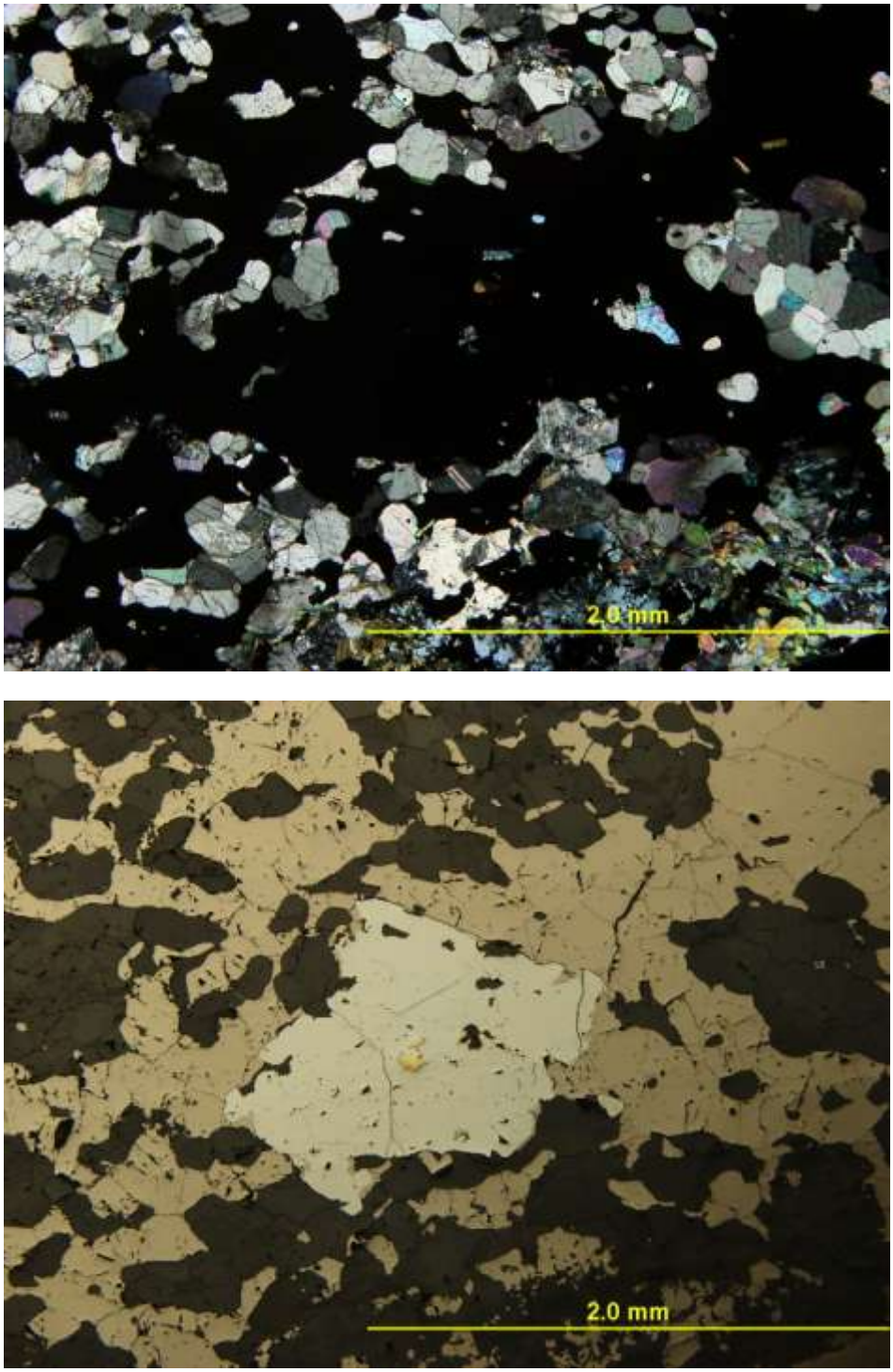

Figure 4.2.2 Sample 210-320 (320-001). In bottom photomicrograph (plane polarized reflected light) gold occurs in a ragged arsenopyrite crystal. Gold is an irregular and jagged shape likely due to gold filling fracture. The related fracture cannot be seen; it may have healed or occur at a perpendicular orientation. Notice the poikiloblastic texture created by the pyrrhotite. Pyrrhotite appears opaque wrapping around carbonate crystals in top photomicrograph (cross polarized transmitted light).

(hedenbergite) act as competent minerals in Lithology 2. Hedenbergite is an iron and calcium rich pyroxene often associated with iron formation metamorphosed to amphibolite facies. It also occurs at the Lupin gold deposit (Geusebroek, personal communication 2010).

These clinopyroxene crystals are highly fractured and some appear brownish-orange in plane polarized light, likely due to iron staining. Gold occurs as a rounded inclusion in a brownish-orange stained hedenbergite crystal of sample 210-238 in Fig. 4.2.3. It is more common to see gold within fractures in clinopyroxene like in sample 210-509 (Fig. 4.2.4).

4.2.3 Other examples of gold mineralization

In the carbonate-grunerite-rich bands of Lithology 2 gold mineralization also occurs as inclusions in carbonate and amphibole. The carbonate in this rock could be attributed to two possible sources: it may have been present in the protolith or the carbonate could be the product of metamorphic reaction with the introduction of volatiles. The amphiboles present in grunerite schist are typically grunerite with lesser ferrotschermakite and ferroactinolite. Gold is included near the edge of a grunerite crystal in sample 210-313 (Fig. 4.2.5). Sample 210-534 (Fig. 4.2.6) is an example of gold included in ferroactinolite as well as on the grain boundary between the amphibole and quartz. Gold mineralization on plane defects is not uncommon in this lithology; it has also been observed on grain boundaries like the example in Fig. 4.2.6 and twin boundaries of many minerals. Gold seems to appear more commonly on grain boundaries between different mineral phases, but in sample 210-239 gold is found on quartz-quartz grain boundaries (Fig. 4.2.7). A less common example of gold mineralization is on subgrain boundaries in feldspar and quartz. Gold appears to occur on the subgrain boundary in feldspar in sample 210-534 (Fig. 4.2.8).

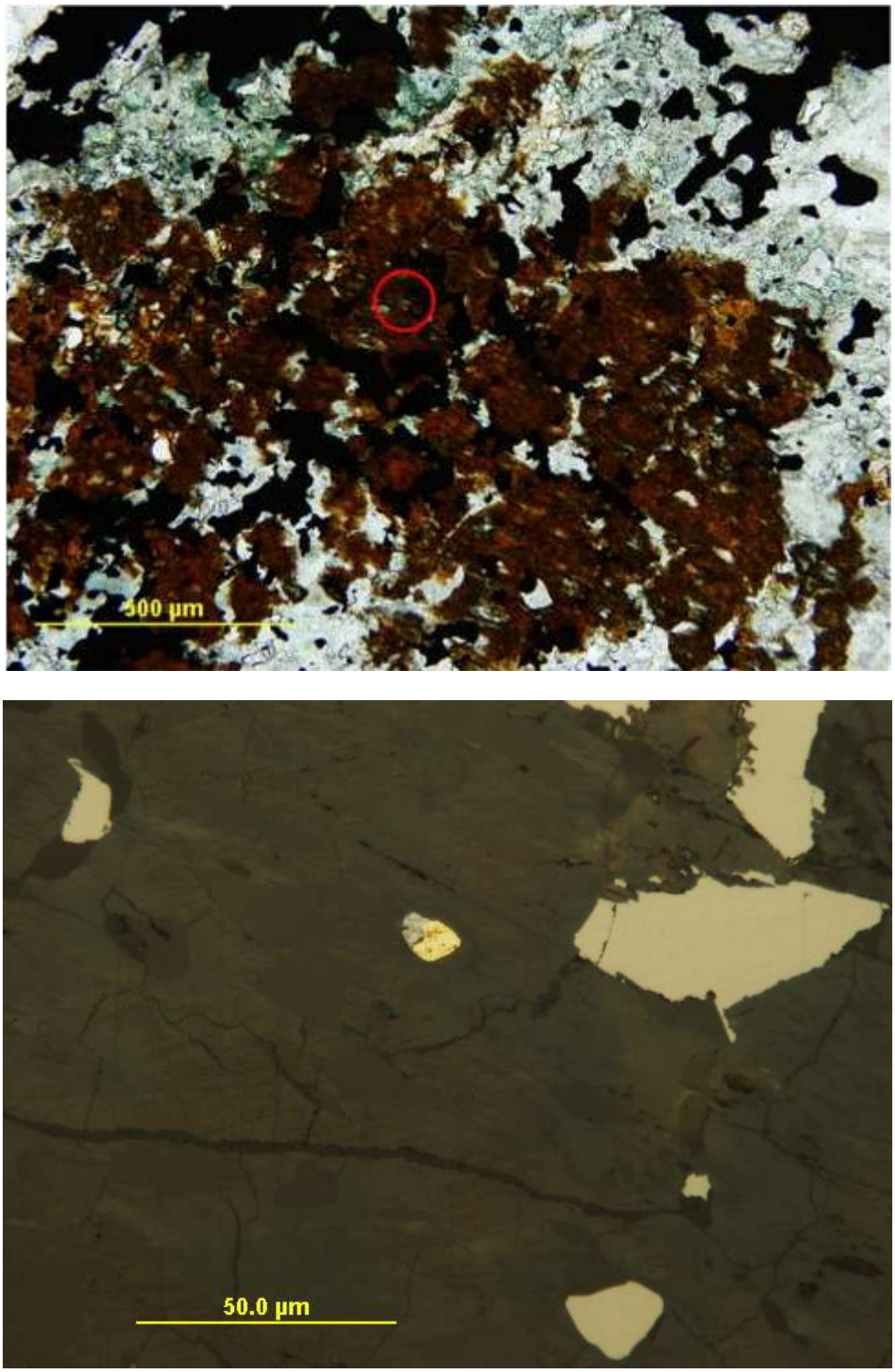

Figure 4.2.3 Sample 210-238 (238-010). In the top photomicrograph brownish-orange stained clinopyroxene stands out in plane polarized transmitted light. This large crystal hosts gold inclusion which can be seen at higher magnification in the bottom photomicrograph in plane polarized reflected light.

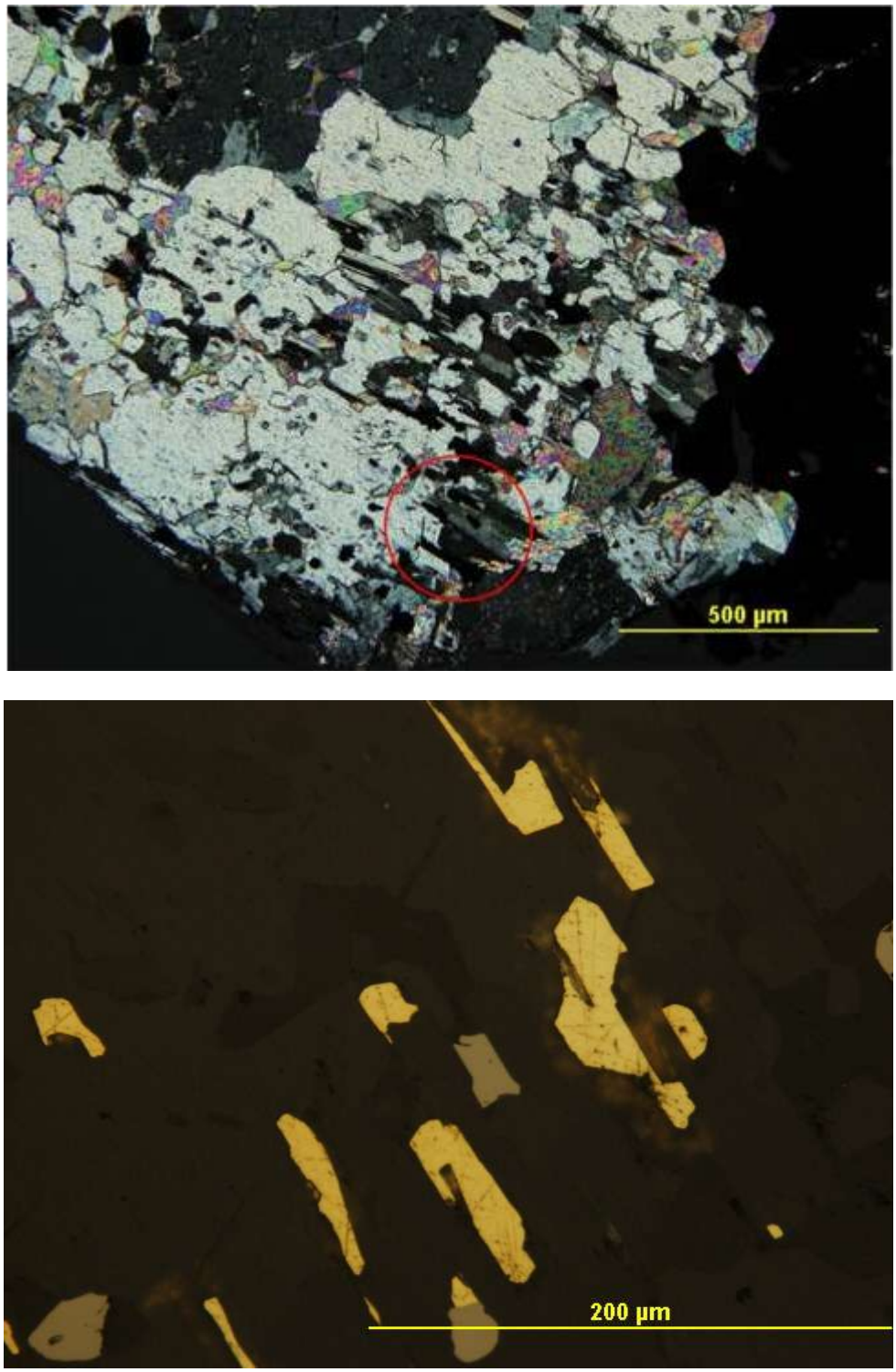

Figure 4.2.4 Sample 210-509 (509-001). The red circle in the top photomicrograph (in cross-polarized light) highlights the fractured area of the clinopyroxene crystal which hosts gold mineralization. At higher magnification and in plane polarized reflected light the bottom photomicrograph captures this fracture filling gold mineralization.

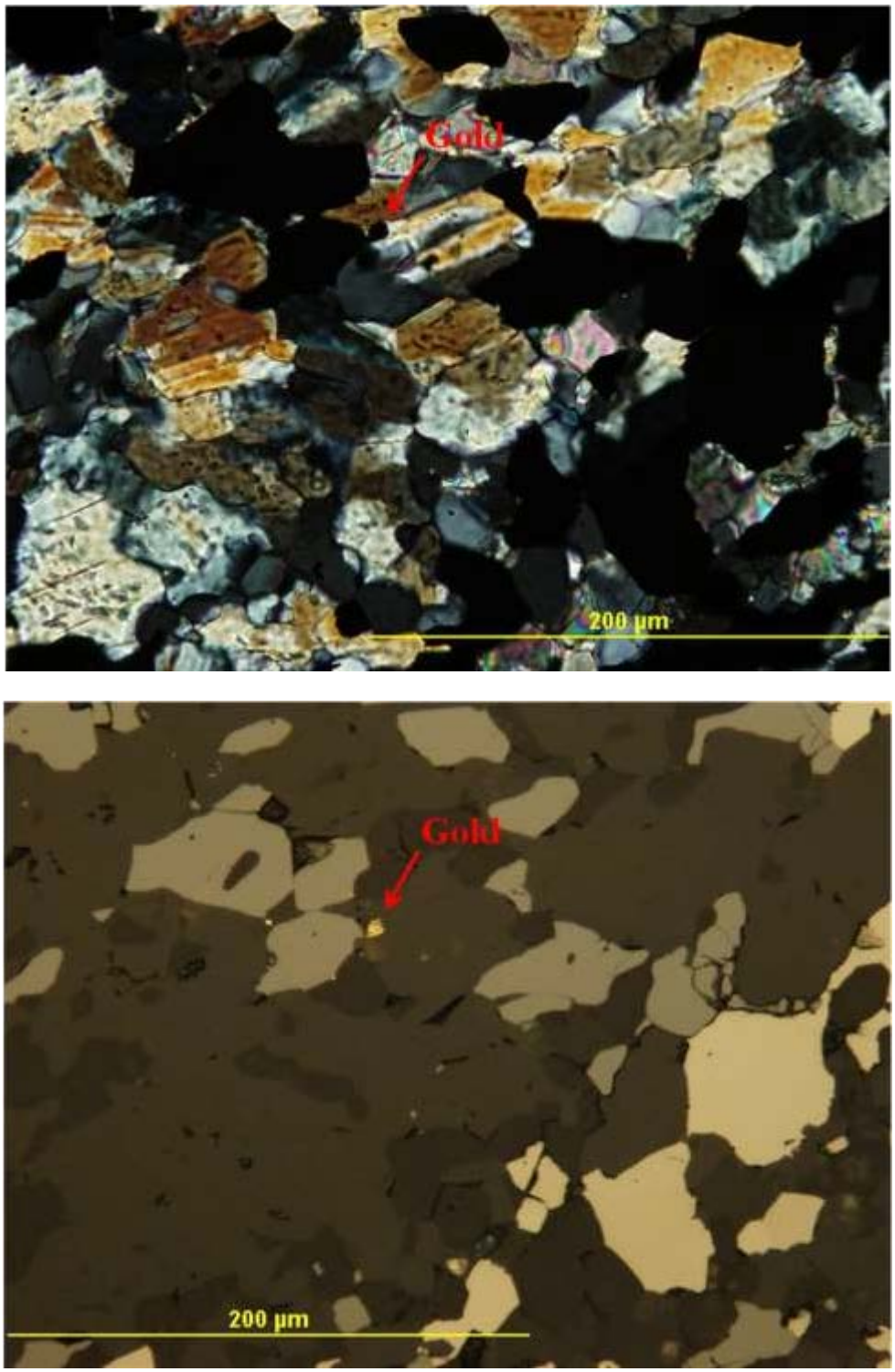

Figure 4.2.5 Sample 210-313 (313-007). Gold appears as an inclusion within grunerite. In the top photomicrograph grunerite crystals can be seen mixed with quartz and carbonate in cross polarized transmitted light. The bottom photomicrograph is of the same area in plane polarized reflected light. In reflected light gold, magnetite and pyrrhotite can be seen.

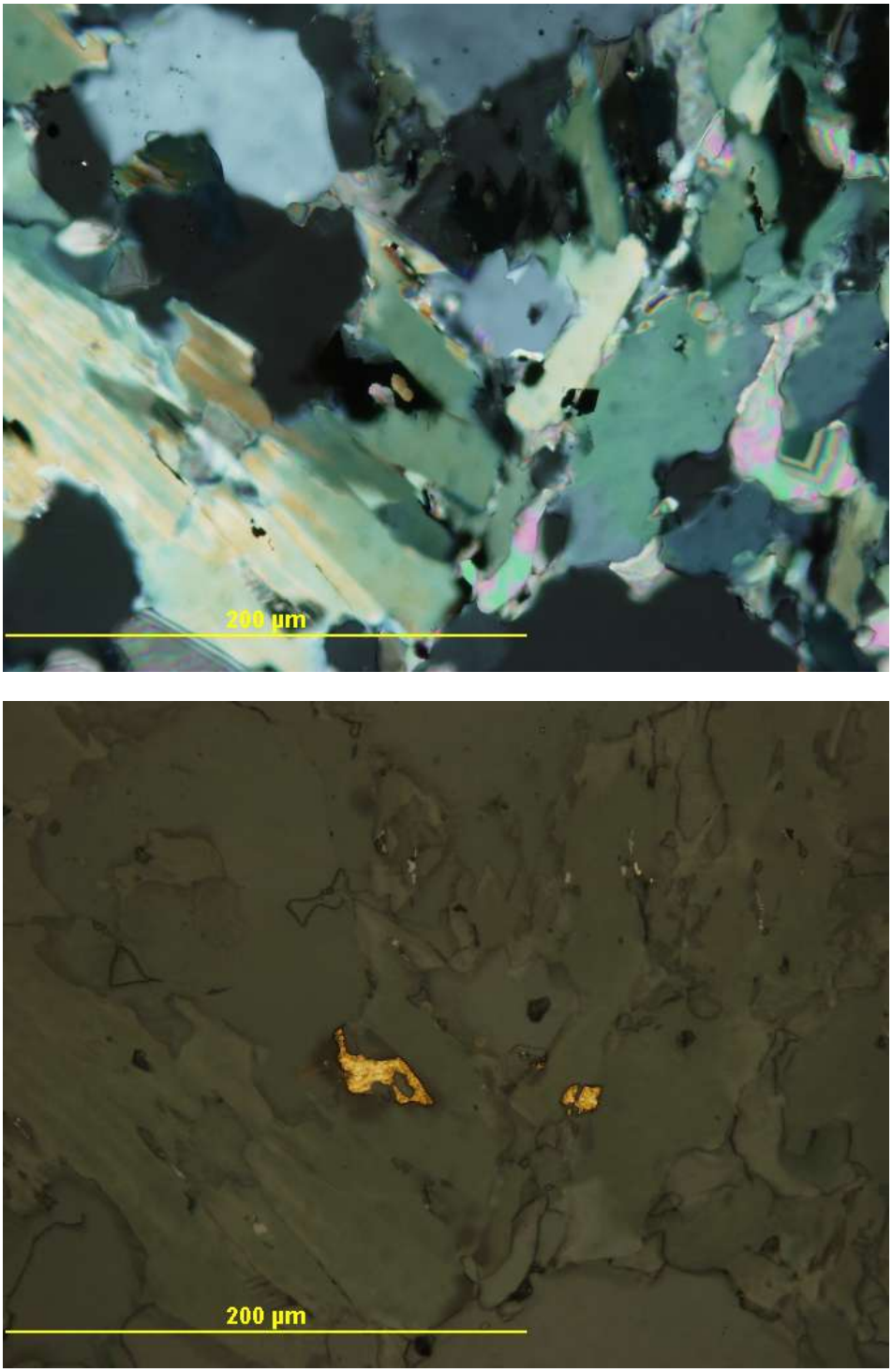

Figure 4.2.6 Sample 210-534 (534-007). In the top photomicrograph in cross polarized transmitted light the ferroactinolite appears green. The opaque mineral is gold which can be seen in the bottom photomicrograph in plane- polarized reflected light take in the same area. Gold occurs included in ferroactinolite to the right side of the photo as well as on the grain boundary between the amphibole and quartz to the left side of the photo.

Figure 4.2.7 Sample 210-239 (239-004). The red arrow in the top photomicrograph depicts the location of gold mineralization on a quartz-quartz grain boundary seen in cross polarized transmitted light. At higher magnification and in plane polarized reflected light (bottom photomicrograph) gold sits right on this grain boundary.

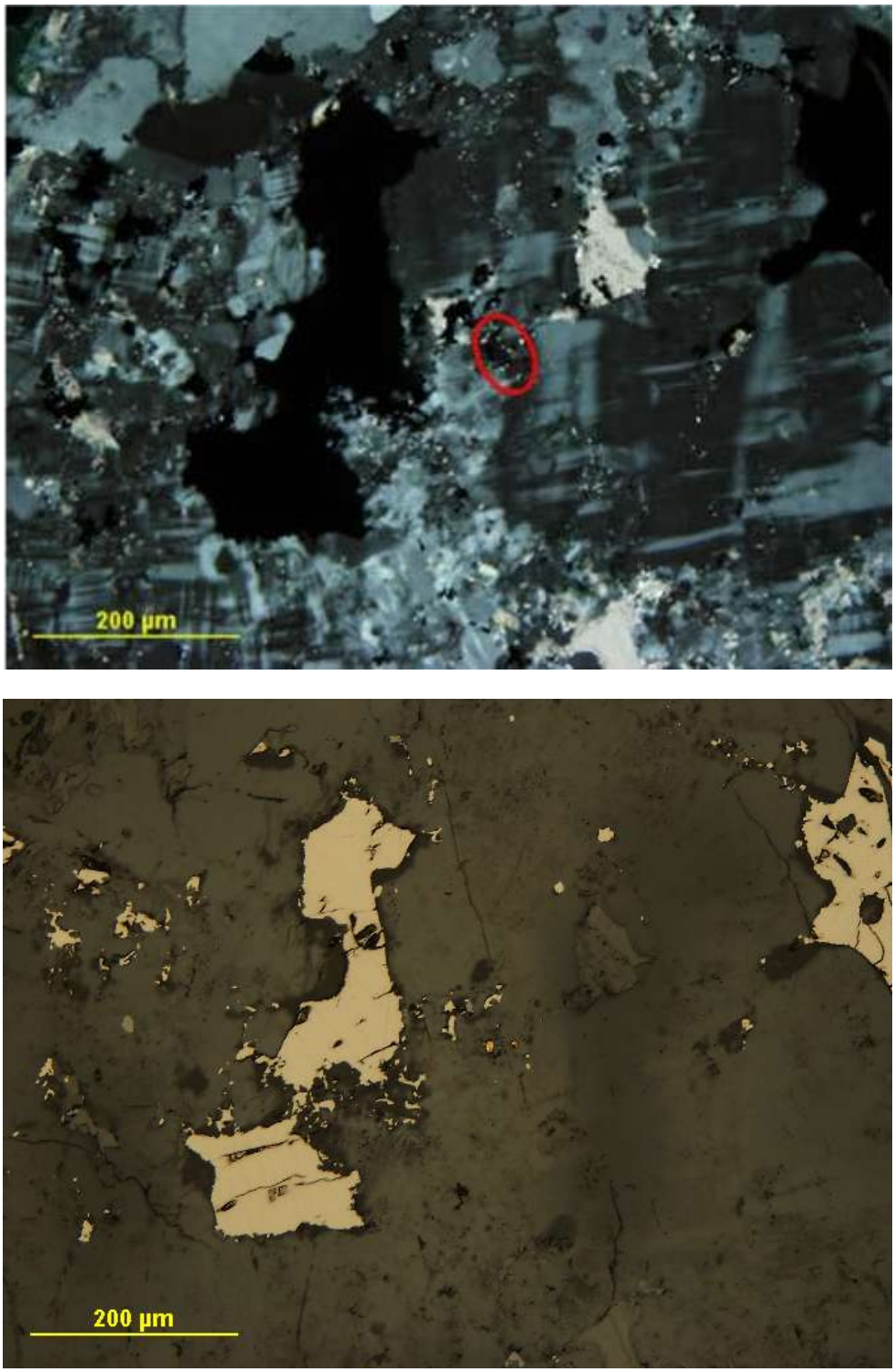

Figure 4.2.8 Sample 210-534 (534-002). Subgrain boundaries of feldspar can be observed in the top photomicrograph. The red circle highlights a subgrain boundary which hosts gold mineralization. The gold can be seen in the bottom photomicrograph taken in plane-polarized reflected light.

Table 4.2.1: Summary of documented gold occurrences for Lithology 2, Musselwhite Mine, grunerite schist

Summary of documented gold occurrences	Total
Total number of documented gold occurrences:	107
Gold inclusions in metamorphic minerals:	22
Gold inclusions within hedenbergite:	17
Gold inclusions within amphiboles:	5
Gold within fractures:	20
Gold within fractures in arsenopyrite:	15
Gold within fractures in hedenbergite:	4
Gold within fractures in feldspar:	1
Gold within strain shadows:	0
Gold on plane defects:	29
Gold within quartz-rich bands:	15
Gold within quartz-rich bands which included other minerals:	8
Gold within quartz-rich bands which did not include other minerals:	7
Gold associated with sulfides:	53
Gold inclusions within arsenopyrite:	27
Gold in contact with pyrrhotite:	9
Gold within arsenopyrite which was surrounded by poikiloblastic pyrrhotite:	17
Other:	22
Gold inclusions within quartz:	5
Gold inclusions within carbonate:	9
Gold inclusions within feldspar:	8

*Many of the gold occurrences fall into more than one group in this table

4.3: Lithology 3, Hammond Reef, quartzofeldspathic schist

At Hammond Reef, gold mineralization correlates with pyrite content (Madon, personal communication 2010); this is supported by the gold mineralization documented in this study. Sericitic alteration also seems to be associated with gold mineralization; in all samples where gold appears, feldspars are highly to moderately altered. This trend can be seen in Table 4.3.1 and Appendix C.5. Note that gold is not related to either one or the other, instead gold appears only in samples which are highly to moderately altered and also include pyrite. Even where gold is not directly related to pyrite, each thin section contains at least some pyrite crystals.

4.3.1: Gold associated with pyrite

With so much of the gold at Hammond Reef associated with pyrite, documenting the relationship between pyrite and gold is important. Microstructural examination in this study shows physically how gold and pyrite are related.

4.3.1a: Gold inclusions and fracture filling in pyrite

Gold occurs as inclusions and filling fractures in pyrite crystals. Gold is often seen as rounded inclusions within pyrite, like in sample 740-419 (Fig. 4.3.1). In some examples, gold inclusions appear associated with fractures as in sample 749-402 (Fig. 4.3.2). In sample 749-402 a gold bleb appears in a highly fractured pyrite crystal with fractures approaching the gold bleb, yet the bleb itself is slightly rounded and is much larger than these fractures. In other samples, gold more definitively appears to fill fractures like in sample 749-418 (Fig. 4.3.3) and sample 749-416 (Fig. 4.3.4).

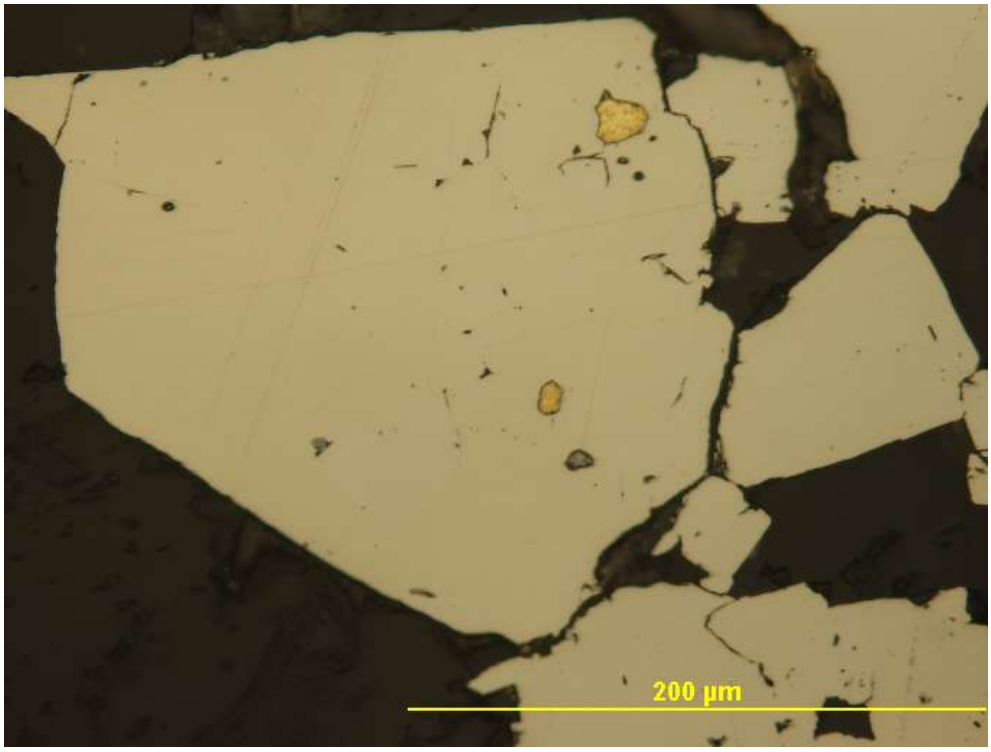

Figure 4.3.1 Sample 749-419 (419-005). Gold inclusions within subhedral pyrite cyrstal.

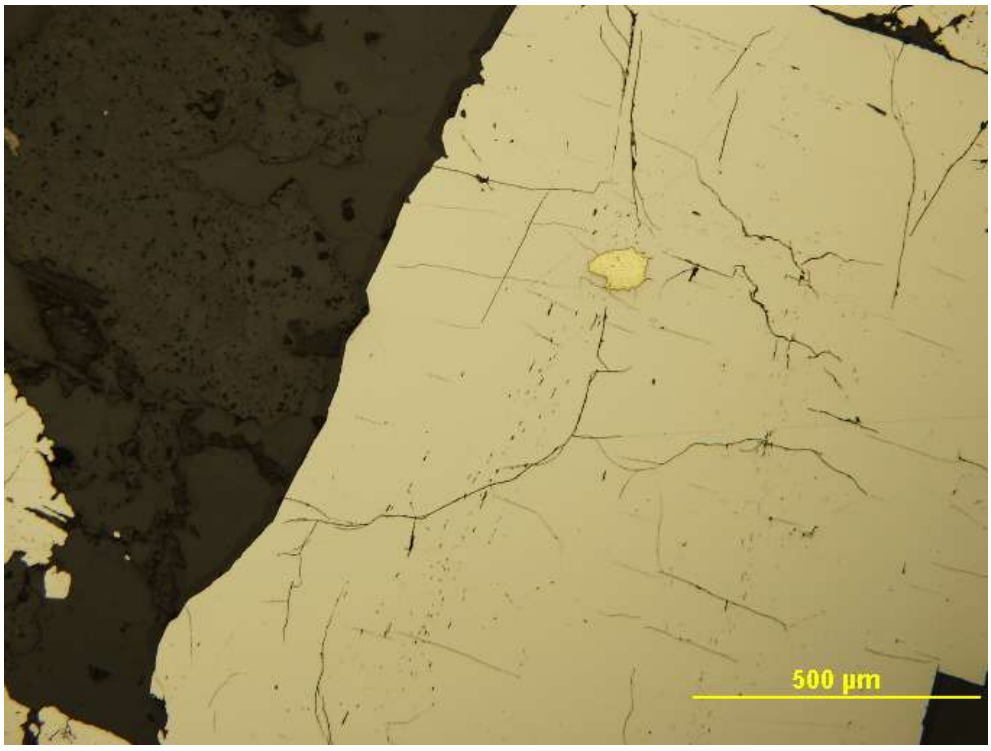

Figure 4.3.2 Sample 749-402 (402-002). Gold mineralization occurs within a subhedral pyrite crystal with many fractures.

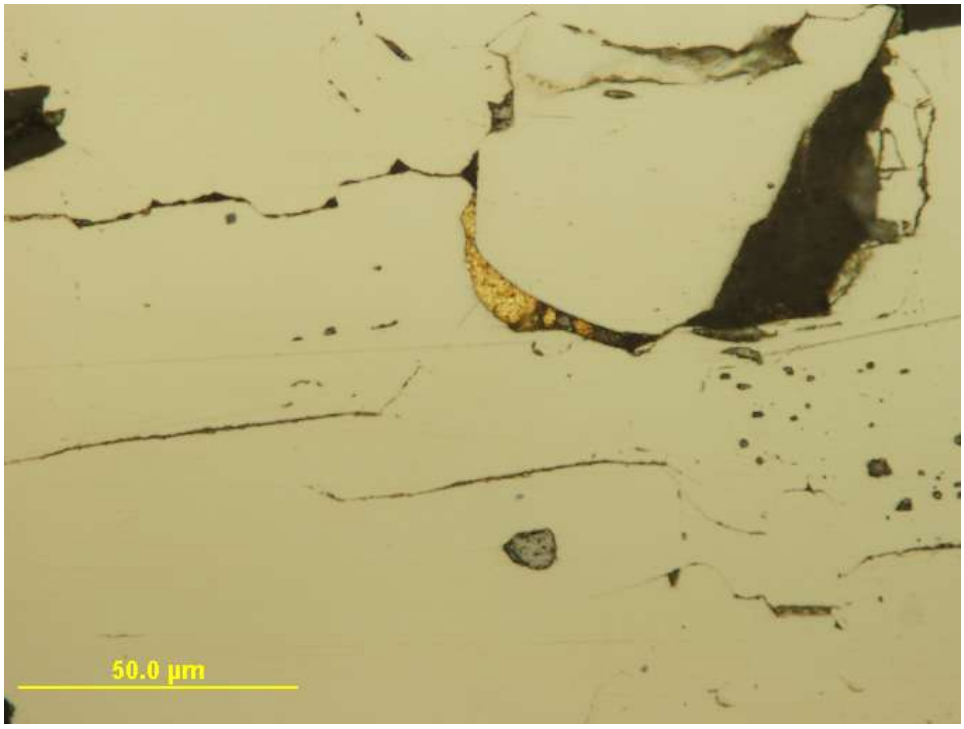

Figure 4.3.3 Sample 749-418 (418-009). Gold appears filling a fracture within pyrite.

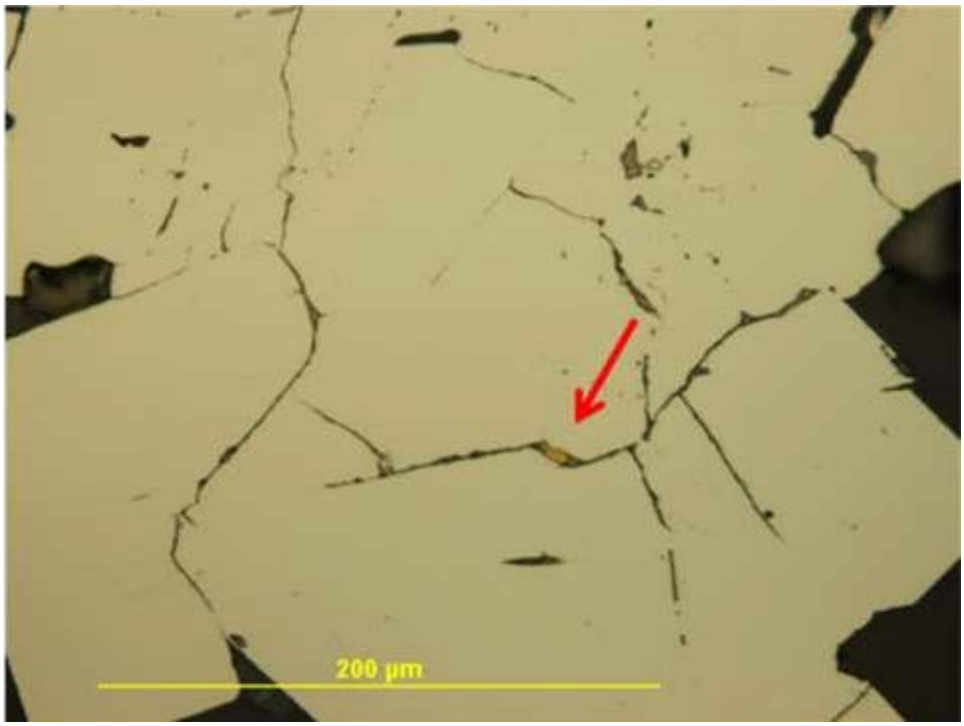

Figure 4.3.4 Sample 749-416 (416-008). The red arrow points to gold mineralization filling a fracture within pyrite.

Pyrite crystals are commonly euhedral to subhedral. In hand sample, pyrite sometimes appears stringer or vein-like, but on microscopic investigation, pyrite is actually brecciated. The pyrite is highly fractured, but euhedral to subhedral growth shapes can still be discerned. These crystals appear to have been affected by the deformation which gives this strung out, brecciated texture. Note that the pyrite crystals are not elongated although they are highly fractured and appear aligned together along strike. With higher temperature and/or increased strain rate, pyrite may have become elongated in spite of being high on the crystalloblastic series (Winter 2010).

Gold inclusions occur in euhedral pyrite, subhedral pyrite and in the brecciated pyrite which appears stringer-like. Also gold mineralization appears almost every time the pyrite crystals are brecciated and appear stringer-like. In Fig. 4.3.5, gold mineralization appears associated with fractures where pyrite has this brecciated texture.

Pyrite is a competent mineral especially when compared to the matrix minerals at Hammond Reef. Quartz, feldspar and muscovite make up the bulk of the rock at Hammond Reef. Quartz exhibits evidence of ductile deformation by dislocation creep, with undulose extinction, irregular grain boundaries and subgrains typical of quartz deformed at greenschist facies metamorphic conditions. The feldspar at Hammond Reef participated in metamorphic reaction to produce the white mica (muscovite), causing some reaction softening allowing them to respond more ductilely. Feldspar crystals do not show evidence for dislocation creep which is consistent with greenschist facies metamorphic conditions. Muscovite ductilely deforms easily at greenschist facies metamorphic conditions. There would be a major competency contrast between the ductilely deforming matrix and the competent pyrite crystals.

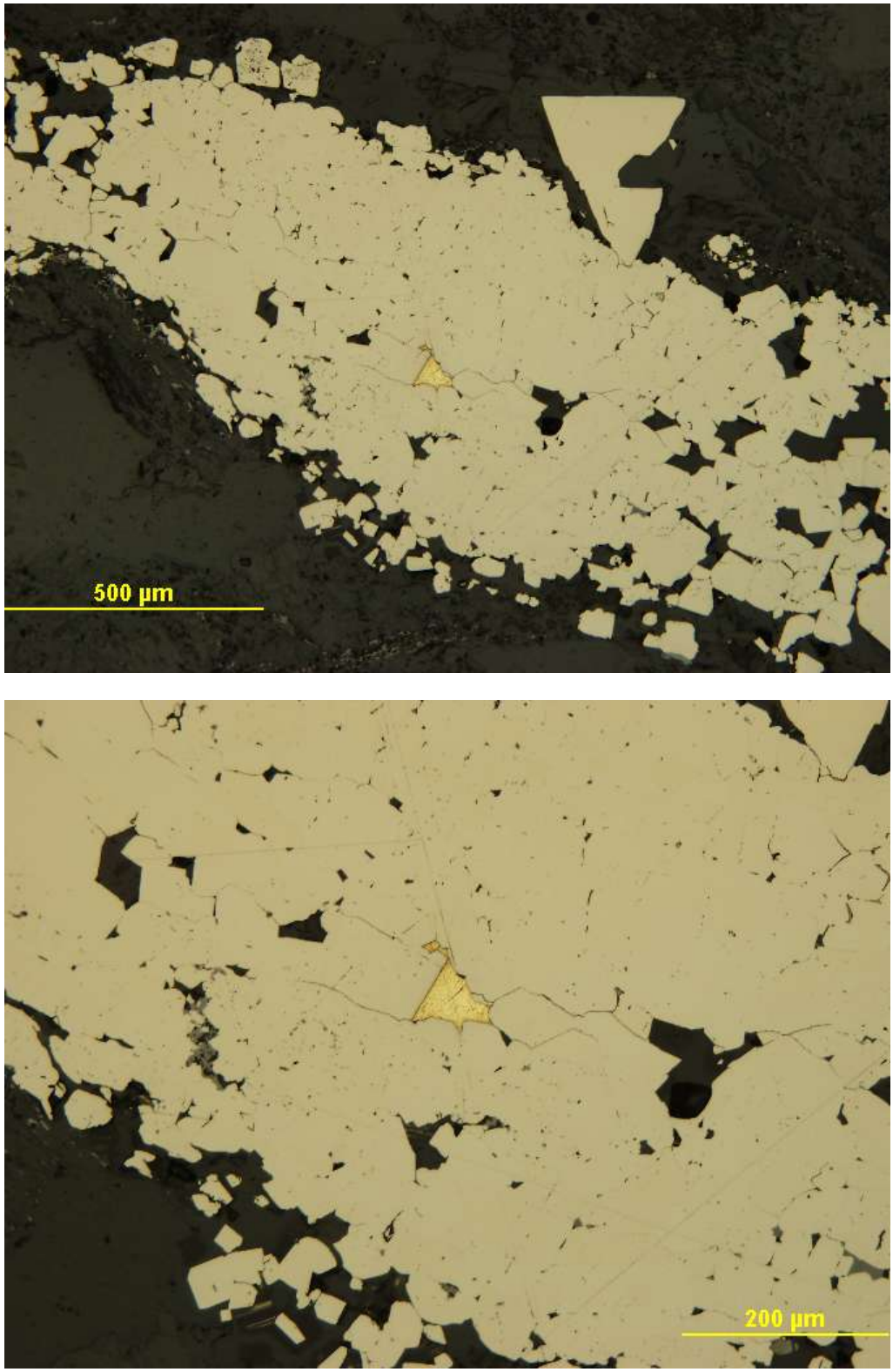

Figure 4.3.5 Sample 749-414 (414-007). Gold mineralization occurs associated with fractures in pyrite. Note the brecciated nature of the pyrite in the top photomicrograph.

4.3.1b Gold mineralization in strain shadows

Gold is hosted in the fibrous variety of strain shadows called strain fringes at Hammond Reef. At Hammond Reef the pyrite acts as the "core" mineral for the fibrous strain shadow or strain fringe. Strain fringes are unlike the typical strain shadows where the minerals that normally define the foliation are randomly orientated in the shadow of the competent "core" mineral. In strain fringes, the mineral defining the shadow grows in a fibrous manner in the shadow of the competent "core" mineral. At Hammond Reef the strain fringes are most commonly defined by quartz; the fibrous growth of the quartz in these fringe structures creates a "stripe-like" pattern. Gold mineralization occurs within one of these strain fringes in sample 749-415 (Fig. 4.3.6).

These strain fringes stand out due to the unusual pattern created by the fibrous quartz. The quartz in these fringe structures does not exhibit the same texture as quartz seen outside strain fringes. Deformed quartz throughout the Hammond Reef samples shows undulose extinction and irregular grain boundaries which are typical textures of quartz deformed by dislocation creep (e.g. Stipp et al. 2002, Tullis 2002). Fringe structures which have been undisturbed by ongoing deformation keep their fibrous texture. In this study strain fringes range from fibrous to completely recrystallized, indicating that deformation and metamorphism continued to affect some of these strain fringes but not others. In sample 749-417 the strain fringe hosting gold has been completely recrystallized, the quartz exhibits undulose extinction and irregular grain boundaries comparable to the quartz textures which occur in the matrix (Fig. 4.3.7).

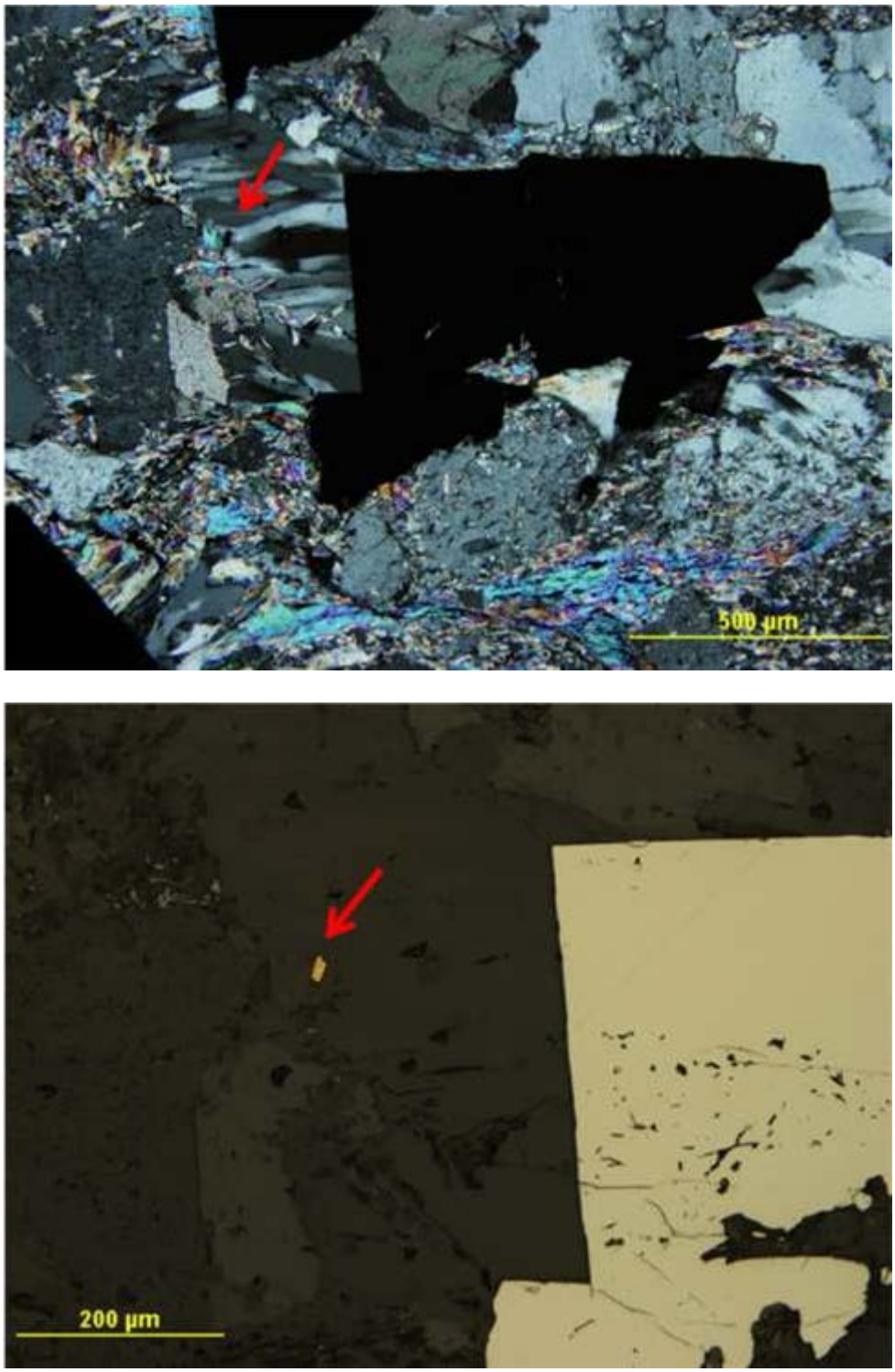

Figure 4.3.6 Sample 749-415 (415-001). Gold mineralization appears within a strain fringe. Note the fibrous nature of the quartz in top photomicrograph; the red arrow indicates the location of the gold bleb, which can be seen in plane-polarized reflected light in the bottom photomicrograph, again located by the red arrow.

Figure 4.3.7 Sample 749-417 (417-005) Gold mineralization within recrystallized strain fringe and as inclusions within pyrite crystal. Note the irregular grain boudaries and undulose extinction of the quartz in the fringe structure and how it matches the texture of the nearby quartz crystals (top photomicrograph in transmitted cross-polarized light). At higher magnification, gold blebs can be seen (bottom photomicrograph plane-polarized reflected light).

These strain fringes can be compared to the strain shadows which occur in Lithology 1, the garnet-grunerite schist from Musselwhite Mine (discussed in section 4.1.1). Gold mineralization occurs in the fibrous strain shadows in Lithology 3, at Hammond Reef as well as the strain shadows in Lithology 1, at Musselwhite Mine.

4.3.2: Other examples of gold mineralization

The importance of pyrite seems to go beyond these examples where pyrite is physically related to gold mineralization. On inspection of all the other gold occurrences in Lithology 3, it was found that every thin section sample which hosts gold mineralization also contains pyrite. One example where gold is not physically related to pyrite is sample 749-438. In this sample, gold occurs in muscovite adjacent to a pyrite crystal (Fig. 4.3.8). Gold also occurs on grain boundaries just like discussed in the two lithologies from Musselwhite Mine. Gold appears on the boundary between quartz and carbonate in sample 749-402 (Fig. 4.3.9) as well as on the boundary between carbonate and pyrite in sample 749-437 (Fig. 4.3.10). In sample 749-437, gold also occurs as inclusions within this pyrite crystal (Fig. 4.3.10).

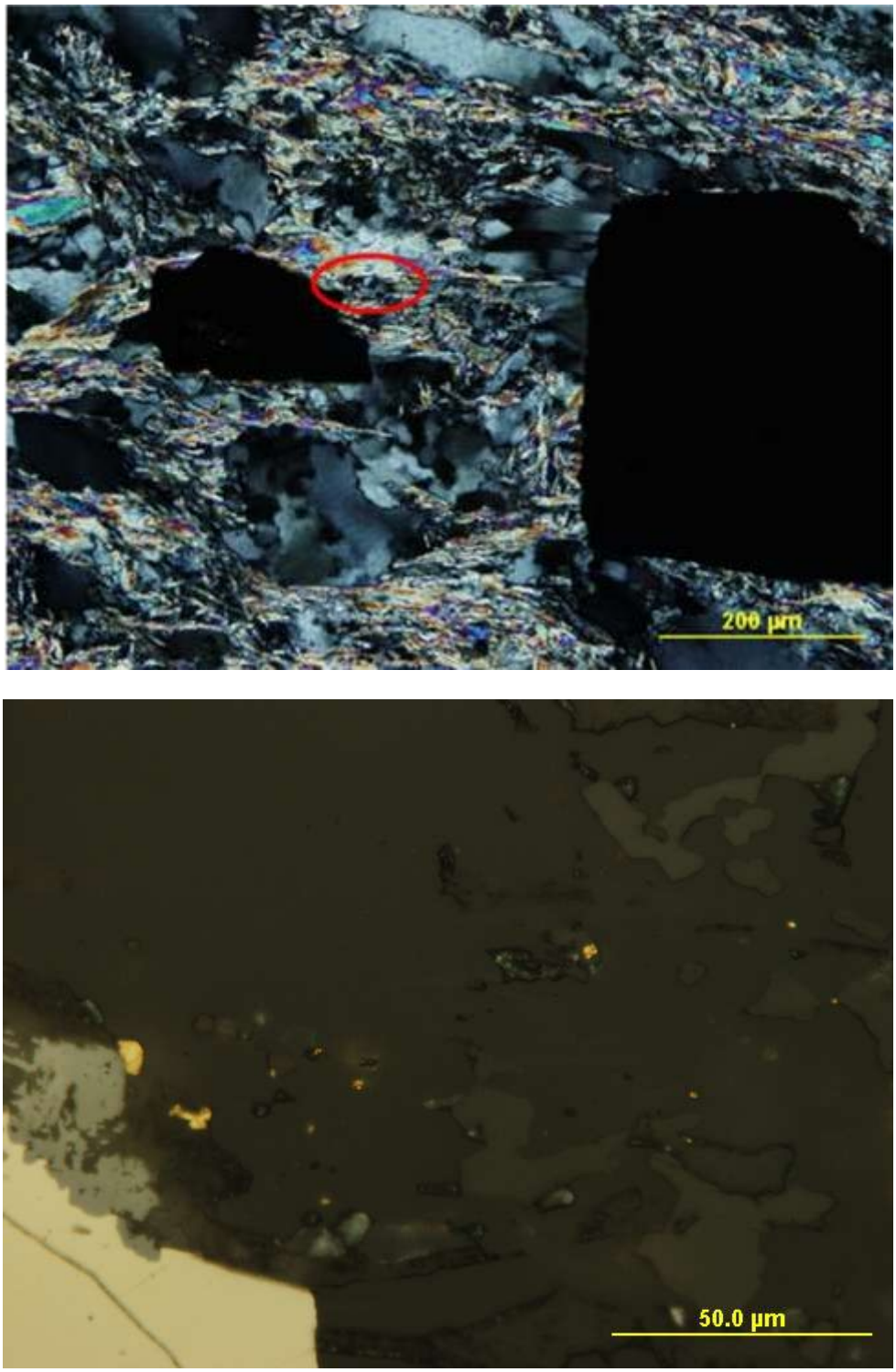

Figure 4.3.8 Sample 749-438 (438-010). Gold mineralization appears in muscovite within the red circled area in the (top photomicrograph, cross-polarized transmitted light). At higher magnification, gold appears on the boundary of magnetite. Gold also occurs as tiny blebs included in muscovite (bottom photomicrograph, plane-polarized reflected light).

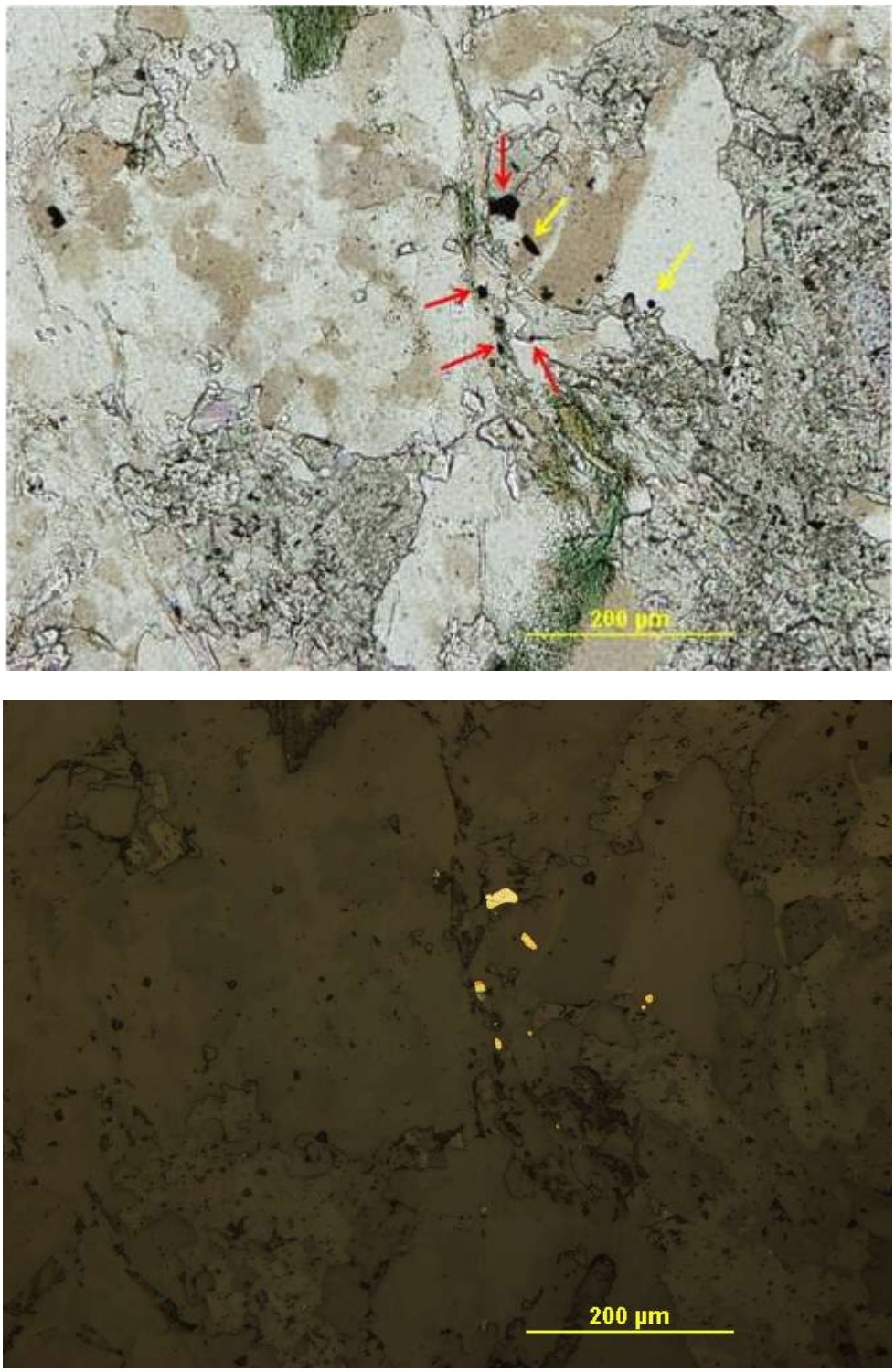

Figure 4.3.9 Sample 749-402 (402-004). Gold mineralization occurs on grain boundaries between quartz, carbonate and chlorite areas as indicated by red arrows (top photomicrograph, plane-polarized transmitted light). This example also hosts gold as inclusions in quartz shown by the yellow arrows. The gold blebs can be seen in the bottom photomicrograph (plane-polarized reflected light).

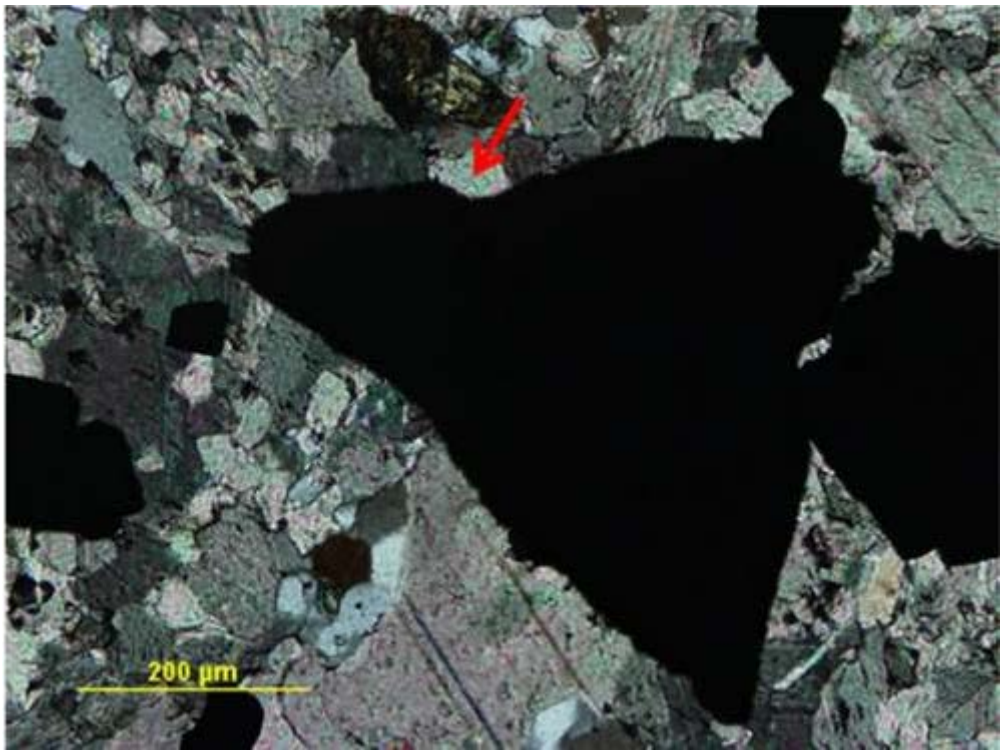

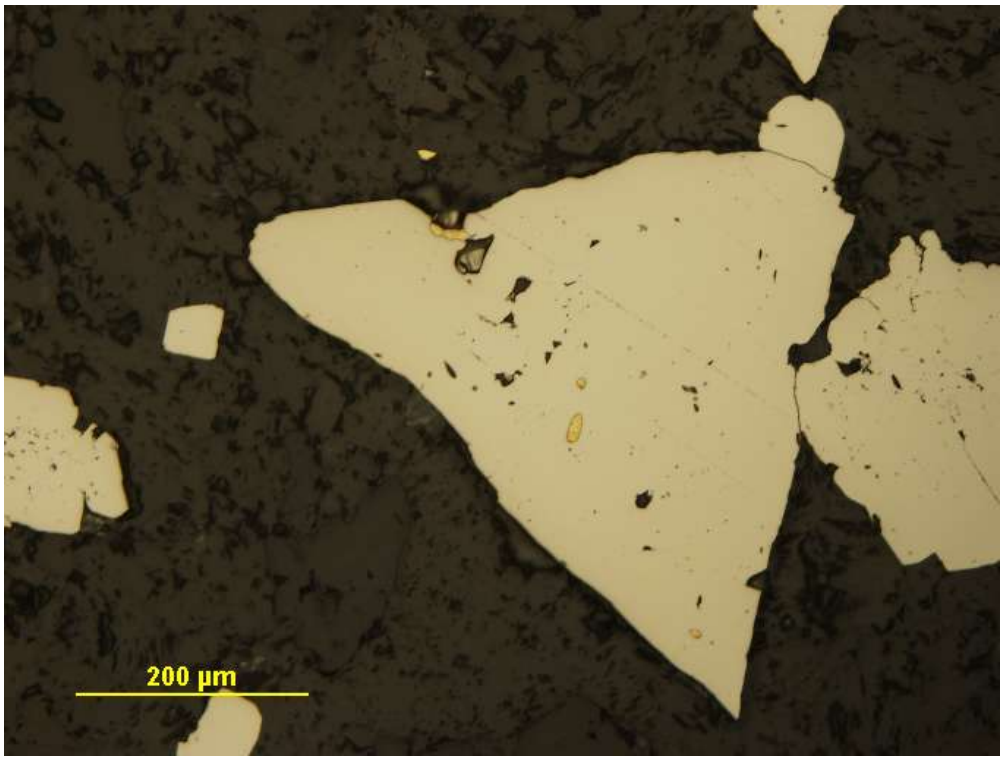

Figure 4.3.10 Sample 749-437 (437-003). The red arrow highlights gold mineralization occurring on the boundary between carbonate and pyrite (top photomicrograph cross polarized transmitted light). Gold also appears as rounded inclusions (bottom photomicrograph, plane polarized reflected light).

Table 4.3.1: Summary of documented gold occurrences for Lithology 3, Hammond Reef, quartzofeldspathic schist

Summary of documented gold occurrences	Total
Total number of documented gold occurrences:	103
Gold inclusions in metamorphic minerals:	4
Gold inclusions within highly altered feldspars:	3
Gold inclusions within muscovite:	1
Gold within fractures:	35
Gold within fractures in pyrite:	35
Gold within strain shadows:	10
Gold on plane defects:	9
Gold associated with sulfides:	55
Gold inclusions within pyrite:	55
Other:	17
Gold inclusions within quartz:	8
Gold inclusions within carbonate:	9

*Some of the gold occurrences fall into more than one group in this table.

4.4: Summary and comparison of gold mineralization

4.4.1: Musselwhite Mine

Gold mineralization is associated with similar textures and microstructures for both Lithology 1, the garnet-grunerite schist and Lithology 2, the grunerite schist from Musselwhite Mine. Gold occurs as inclusions and in fractures in competent minerals for both lithologies at Musselwhite Mine. Gold inclusions occur in many different minerals at Musselwhite Mine like quartz, feldspar, amphibole, garnet and others. Gold mineralization is hosted in fractures at Musselwhite Mine; garnet is the competent mineral hosting gold in fractures for Lithology 1, the garnet-grunerite schist, while arsenopyrite and clinopyroxene are the competent minerals hosting gold in fractures in Lithology 2, the grunerite schist. Although both Lithology 1 and 2 from Musselwhite Mine host gold mineralization within fractures and as inclusions within competent minerals, only the competent garnet crystals from Lithology 1 create strain shadows which host gold mineralization. Lithology 2 does contain the competent minerals arsenopyrite and clinopyroxene, but no strain shadows appear around these minerals.

Much of the gold at Musselwhite Mine is found on plane defects. Grain boundaries are the most common plane defect associated with gold mineralization. Sometimes gold mineralization is on a boundary between grains of the same mineral, like in Fig. 4.2.6, where gold mineralization occurs on grain boundaries in a quartz-rich band. Other examples of gold mineralization occur on the boundaries between different minerals. Gold appears on the grain boundary between carbonate and quartz grains in Fig. 4.1.4.

4.4.2: Hammond Reef

Observations show gold mineralization at Hammond Reef to always be associated with pyrite. This association can be directly as inclusions in the pyrite crystals or within fractures in pyrite. But gold mineralization also occurs within strain shadows behind pyrite crystals and along the boundary between pyrite and matrix minerals. Gold blebs occur on the edge of a pyrite crystal, between pyrite and the matrix in Fig. 4.3.5.

4.4.3: Comparison of gold mineralization at Musselwhite Mine and Hammond Reef

When comparing gold mineralization from Musselwhite Mine and Hammond Reef, many similarities stand out, especially the microstructural control on mineralization provided by competent minerals. The most common control is the gold mineralization within fractures in competent minerals which occurs at both deposits in all three lithologies. Gold fills fractures in garnet in Lithology 1, the garnet-grunerite schist (Musselwhite Mine), arsenopyrite and clinopyroxene in Lithology 2, the grunerite schist (Musselwhite Mine) and pyrite in Lithology 3, the quartzofeldspathic schist (Hammond Reef).

The competent minerals garnet and pyrite share another common feature: strain shadows. Gold appears in non-fibrous strain shadows around garnet crystals in Lithology 1, the garnet-grunerite schist (Musselwhite Mine) like that in Fig. 4.1.3. Lithology 3, the quartzofeldspathic schist from Hammond Reef, hosts gold in fibrous strain shadows like the example in Fig. 4.3.2.

Also gold occurs on plane defects at both deposits; examples appear in all three lithologies. In Fig. 4.1.1, an example from Lithology 1, the garnet-grunerite schist from Musselwhite Mine, gold occurs on the boundary between grunerite and quartz. Similarly, gold appears on the boundary between quartz and carbonate in Lithology 3, the quartzofeldspathic schist from

Hammond Reef, sample 749-402 (Fig. 4.3.6). Gold also appears on boundaries between grains of the same minerals for both deposits; one example is gold on amphibole boundaries in sample 210-534, from Musselwhite Mine‟s gɲunerite schist (Lithology 2).

Chapter 5: Interpretation of results

Gold mineralization appears in many similar microstructures and textures at Musselwhite Mine and Hammond Reef. A comparison of these gold occurrences can be found in Table 5.1.1.

5.1: Gold inclusions in metamorphic minerals:

Gold mineralization occurs as inclusions within metamorphic minerals in all three lithologies examined in this study, seen in Table 5.1.1 (part A). At Musselwhite Mine, gold inclusions are formed within such metamorphic minerals as grunerite, garnet and hedenbergite, while at Hammond Reef, gold appears within highly altered areas in feldspar grains as well as muscovite. The presence of gold inclusions within metamorphic minerals indicates that gold mineralization occurred before and/or during metamorphism.

5.2: Gold associated with heterogeneous strain

In this study, gold was most commonly associated with textures and structures caused by heterogeneous strain, due to competence contrast in the polymineralic rocks. This heterogeneous strain is expressed as fractures, strain shadows and the evidence for different deformation mechanisms between different mineral phases.

5.2.1: Gold mineralization within fractures in competent minerals

Gold sometimes occurs in veins and fractures in the rocks at both Musselwhite Mine and Hammond Reef, but in this study, gold was most commonly observed in microfractures within competent minerals, see Table 5.1.1 (part B). These microfractures do not extend into the matrix;

they only affect the competent minerals while the matrix exhibits evidence of ductile deformation.

In Lithology 1 from Musselwhite Mine, the competent garnet crystals commonly host gold in microfractures. For Lithology 2, the grunerite schist also from Musselwhite Mine, both arsenopyrite and clinopyroxene (hedenbergite) host gold in microfractures. At Hammond Reef pyrite plays the same role hosting gold mineralization within microfractures. These minerals are more competent than the matrix which surrounds them. This competency contrast causes heterogeneous strain allowing both ductile and brittle deformation to occur simultaneously in response to the stress.

Most often competence contrast is considered at the macroscopic scale. For example Duuring et al. (2001) examined heterogeneous deformation along the margin of a small pluton associated with gold mineralization in the Tarmoola gold deposit of Australia. Similarly, in this study, gold mineralization was related to heterogeneous strain caused by competence contrast, but on the microscopic scale. Instead of gold occurring along the margin of a competent pluton, gold appears in strain shadows of competent minerals like garnet and pyrite as well as within fractures in these competent minerals.

Gold appearing in fractures of competent minerals indicates that gold mineralization had to occur during and/or after deformation. Because gold also appears as inclusions in metamorphic minerals from both deposits it can be inferred that gold mineralization, metamorphism and deformation were occurring at the same time.

This interpretation of synchronous gold mineralization, metamorphism and deformation has been concluded in previous work on Lithology 1 from Musselwhite Mine (Hill et al. 2006), but in this

study similar examples have been documented for Lithology 2 (a secondary gold-hosting lithology at Musselwhite Mine) as well as at Hammond Reef, a deposit in a very different rock type and hosted by rocks of a different metamorphic grade.

There is also a correlation between competent minerals hosting gold not only in fractures but as inclusions. In Table 5.1.1 (part E) the number of gold occurrences relating to competent minerals, whether as inclusions or filling fractures, accounts for 186 of the 262 total documented gold occurrences in this study. When considering only the gold occurrences which appear in fractures of competent minerals the number is much lower, 71 gold occurrences. In detailed examination of the inclusions within competent minerals, they are often irregularly shaped. It is possible that some of these irregularly shaped inclusions originated as gold in fractures in the competent minerals which later healed during ongoing metamorphism.

5.2.2: Gold mineralization associated with heterogeneous ductile deformation

Heterogeneous deformation seems important as gold mineralization was observed commonly in microfractures in competent minerals where the matrix minerals showed only evidence of ductile deformation. Examples of gold mineralization associated with only ductile heterogeneous deformation also occur.

5.2.2a: Gold mineralization in strain shadows

Gold mineralization within strain shadows was observed in Lithology 1, the garnet-grunerite schist from Musselwhite Mine and Lithology 3, the quartzofeldspathic schist from Hammond Reef. Garnet at Musselwhite Mine is the “core” mineral for strain shadows in Lithology 1 with pyrite as the competent “core” mineral for the fibrous variety of strain shadows found in Lithology 3 at Hammond Reef. The fact that gold mineralization is associated with these strain

shadows in both deposits is another indicator of the importance of heterogeneous strain for gold mineralization. Strain shadows are formed during deformation, and because these structures host gold mineralization, they support the interpretation that gold mineralization occurred during deformation.

At Hammond Reef, the fibrous strain shadows, called strain fringes, which host gold can have various textures. Some of the gold-hosting strain fringes appear very fibrous with a striped pattern in cross-polarized light while other gold hosting strain fringes appear completely recrystallized. The recrystallized strain fringes formed during deformation and continued to be affected by ongoing deformation which can be seen by the subgrains, irregular grain boundaries and undulose extinction. Gold appearing in both very fibrous strain fringes as well as recrystallized strain fringes indicates progressive gold mineralization during ongoing deformation.

5.2.2b: Gold mineralization associated with polymineralic heterogeneous ductile deformation

The most subtle example of heterogeneous strain associated with gold mineralization comes from samples where polymineralic deformation causes noticeable differences in texture. Tullis (2002) suggests this change in texture is caused by less efficient deformation in polymineralic rocks than monomineralic rocks. There are two examples from Lithology 1 where this is evident and associated with gold mineralization (in Table 5.1.1 these are listed in part B under "other").

In monomineralic rocks, the deformation mechanism dislocation creep is more effective than in polymineralic rocks (Jordan 1987; Handy 1989,1992; Bons 1993; Handy et al. 1999; Stunitz and Tullis 2001; Tullis 2002). In this study, textural differences were observed on boundaries of monomineralic bands where interaction with other minerals occurred. Grain size appeared

smaller in bands nearby where the minerals were bounded by unlike minerals than when bounded by like minerals, for example, within a large quartz vein where a stringer of amphibole appears. The quartz grains bounding this amphibole band are smaller than the other nearby quartz crystals which are completely surrounded by other quartz crystals. This textural difference indicates that the ductile deformation mechanism dislocation creep worked more efficiently in the monomineralic areas than the polymineralic areas.

Gold mineralization occurred in two similar examples: one with biotite in quartz and the other with amphibole in quartz. It is unclear how this heterogeneous ductile deformation aids or promotes gold mineralization, but in these two cases, gold appears where monomineralic bands are infiltrated with another mineral phase. These observations indicate some relationship between the heterogeneous ductile deformation and gold mineralization.

Table 5.1.1: Comparison of gold occurrences for all lithologies

A

Gold inclusions in metamorphic minerals: *for all lithologies*	**57**	**262**
Lithology 1: Musselwhite Mine, garnet-grunerite schist	31	52
Lithology 2: Musselwhite Mine, grunerite schist	22	107
Lithology 3: Hammond Reef, quartzofeldspathic schist	4	103

B

Gold associated with heterogeneous strain: *for all lithologies*	**91**	**262**
Gold inclusions within fractured minerals: *for all lithologies*	**71**	**262**
Lithology 1: Musselwhite Mine, garnet-grunerite schist	16	52
Lithology 2: Musselwhite Mine, grunerite schist	20	107
Lithology 3: Hammond Reef, quartzofeldspathic schist	35	103
Gold in strain shadows: *for all lithologies*	**18**	**262**
Lithology 1: Musselwhite Mine, garnet-grunerite schist	8	52
Lithology 2: Musselwhite Mine, grunerite schist	0	107
Lithology 3: Hammond Reef, quartzofeldspathic schist	10	103
Other: *for all lithologies*	**2**	**262**
Lithology 1: Musselwhite Mine, garnet-grunerite schist	2	52
Lithology 2: Musselwhite Mine, grunerite schist	0	107
Lithology 3: Hammond Reef, quartzofeldspathic schist	0	103

C

Gold on plane defects: *for all lithologies*	**53**	**262**
Lithology 1: Musselwhite Mine, garnet-grunerite schist	15	52
Lithology 2: Musselwhite Mine, grunerite schist	29	107
Lithology 3: Hammond Reef, quartzofeldspathic schist	9	103

D

Gold inclusions in sulfides: *for all lithologies*	**86**	**262**
Lithology 1: Musselwhite Mine, garnet-grunerite schist	4	52
Lithology 2: Musselwhite Mine, grunerite schist	27	107
Lithology 3: Hammond Reef, quartzofeldspathic schist	55	103

E

Gold inclusions and gold in fractures of competent minerals: *for all lithologies*	**186**	**262**
Lithology 1: Musselwhite Mine, garnet-grunerite schist	33	52
Lithology 2: Musselwhite Mine, grunerite schist	63	107
Lithology 3: Hammond Reef, quartzofeldspathic schist	90	103

*Shaded column indicates total number of all documented gold occurrences for the specific lithology or the group of lithologies.

*Competent minerals include: garnet, arsenopyrite, hedenbergite and pyrite.

Chapter 6: Discussion and Summary

Though Musselwhite Mine and Hammond Reef are both shear-zone-hosted gold deposits, they differ fundamentally in that they are hosted by completely different rock types. Yet even with this fundamental lithologic difference, many microstructural similarities were found in gold mineralization at these deposits.

6.1: Gold mineralization associated with heterogeneous strain

Through the observations of this study, it can be concluded that heterogeneous strain is important to gold mineralization at both Musselwhite Mine and Hammond Reef. Microstructures indicating heterogeneous strain were associated with 91 out of the 262 examples of gold mineralization from the three study lithologies.

The most common example of gold mineralization associated with heterogeneous strain is gold within fractures of competent minerals. This type of gold mineralization occurred in all three lithologies studied. Because these fractures are exclusively within the competent minerals and do not extend into the matrix, they represent the heterogeneous deformation which occurred in these polymineralic rocks. The competent minerals which host gold in their fractures include garnet, clinopyroxene, arsenopyrite at Musselwhite Mine and pyrite at Hammond Reef.

The number of gold occurrences associated with heterogeneous strain does not include the gold inclusions within competent minerals. Many of the gold inclusions within competent minerals are irregularly shaped and may have originated as gold-filling fractures in the competent minerals such as garnet, arsenopyrite, clinopyroxene and pyrite. Although it cannot be distinguished with certainty which inclusions are associated with heterogeneous deformation, 186 out of the 262 total gold occurrences documented in this study are within competent

minerals. Also of the competent minerals in this study, two are sulfide minerals: arsenopyrite and pyrite. It may be argued whether gold mineralization in these sulfide minerals is related to sulfidization of the wall rock or the heterogeneous deformation. But the observations in this study indicate that heterogeneous deformation definitely plays a role in the gold mineralization in these competent minerals. That is not to say that gold precipitation due to sulfidization is completely ruled out, only that both heterogenous deformation and sulfidization contribute to gold mineralization. Table 5.1.1 (part D) lists gold inclusions in sulfide minerals for each of the study lithologies. In Lithology 3, the quartzofeldspathic schist at Hammond Reef, more than half of the gold mineralization occurred within the sulfide mineral pyrite. At Musselwhite Mine, although gold inclusions occurred within arsenopyrite in both Lithology 1, the garnet-grunerite schist, and Lithology 2, the grunerite schist, it was much less common (4 out 52 examples for Lithology 1 and 27 out of 107 examples for Lithology 2). The documentation of gold mineralization associated with both heterogeneous deformation in both silicate and sulfide minerals indicate its importance to gold mineralization.

Another example of gold mineralization related to heterogeneous deformation is gold mineralization within strain shadows. Strain shadows are created by heterogeneous strain. Gold mineralization within strain shadows of competent minerals occurred in Lithology 1 from Musselwhite Mine and Lithology 3 from Hammond Reef. Gold was also observed associated in areas where subtle textural changes occurred due to heterogeneous strain associated with polymineralic ductile deformation.

In Chapter 3 the relationship between the style of foliation and the likelihood of gold mineralization was discussed for Musselwhite Mine. In Lithology 1, the garnet-grunerite schist, gold mineralization is less commonly associated with smooth and parallel foliation. The more the

foliation deviates from this smooth and parallel foliation, the more likely it will host gold mineralization. Smooth and parallel foliation indicates efficient ductile deformation, where the heterogeneity between different minerals has been overcome by strain, usually aided by metamorphism and grain size reduction. Where the foliation is rough and anastomosing, deformation is more heterogeneous, which from the examples in this study is linked to gold mineralization. McCuaig and Kerrich (1998) also discuss gold mineralization to be more likely associated with secondary structures because the primary structures are usually defined by well foliated talc and/or mica schist. This well foliated talc and/or mica schist is analogous with the gold mineralization being less likely to occur in smooth and parallel foliated (well foliated) Lithology 1 from Musselwhite Mine. This supports the conclusion that gold is related to heterogeneous deformation and therefore less likely to occur in well foliated or smooth and parallel foliated rocks.

In Chapter 3, the complex strain partitioning of Lithology 2, the grunerite schist from Musselwhite Mine was discussed. In outcrop and drill core Lithology 2 and the quartz-magnetite iron formation are commonly adjacent to one another. The amphibole grunerite is formed by the hydrous metamorphic reaction between quartz and magnetite. The quartz-magnetite iron formation is the less metamorphosed equivalent to the grunerite schist, Lithology 2. The missing component to cause the existence of grunerite in the quartz-magnetite iron formation is the introduction of fluid during metamorphism. Due to the inter-mixed nature of the grunerite schist and the quartz-magnetite iron formation, they can be hard to differentiate as stratigraphic units. The reason for this is because of the way the units formed through metamorphic reaction where hydrous fluid was introduced in some places but not others. Perhaps detailed mapping of these

two units could help us to better understand the nature of the fluid introduction and possible movement.

The heterogeneity between the grunerite schist and the quartz-magnetite iron formation may have caused strain partitioning on a large scale in this iron formation. The heterogeneous nature of this iron formation would have contributed to the anastomosing shear zone. Strain partitioning and anastomosing foliation occur in this study at the microscopic scale. Other researchers (e.g. Clark and Fisher 1994; Bell et al. 2004; Sullivan and Law 2007) apply strain partitioning on the macroscopic scale which could be useful for understanding gold mineralization in Lithology 2, the grunerite schist at Musselwhite Mine.

6.2: Relative timing of gold mineralization

Using the microstructures observed to be associated with gold mineralization in this study, conclusions can be made about the relative timing of gold mineralization in these two shear-zone-hosted gold deposits. Microstructures indicate timing of gold mineralization as a continuum throughout the metamorphism and deformation, with structures indicating possible pre-peak-metamorphism to post-deformation gold mineralization.

Gold inclusions within metamorphic minerals at both Musselwhite Mine and Hammond Reef indicate that gold mineralization had to begin before or during the growth of these minerals. Also mineralization within healed fractures of competent minerals implies gold mineralization during ongoing deformation and metamorphism, while gold mineralization along “open” fractures could have mineralized during or after deformation. The gold mineralization appearing within strain shadows in Lithology 1 from Musselwhite Mine and Lithology 3 from Hammond Reef, indicates that gold mineralization was occurring during deformation.

6.3: Gold mineralization occurring on planar defects

Observations from this study imply an important relationship between planar defects and gold mineralization. Many examples of gold occur on grain boundaries as well as sub-grain boundaries and twin compositional planes.

Researchers such as Beach and Fyfe (1972), Etheridge et al. (1983), Vernon and Clarke (2008) have postulated that gold may be transported along grain boundaries deep in the crust where open spaces are almost nil. Geraud et al. (1995) were able to demonstrate that porosity is somewhat increased in shear zones which can help support this theory. The documented examples of gold mineralization on grain boundaries in this study strengthen the case for at least atom mobility on grain boundaries. But the simple explanation for the number of occurrences of gold on grain boundaries may also be due to the unsatisfied bonds. Because gold mineralization was also observed associated with other planar defects like twins and sub-grains, it seems highly likely that these defects serve as reaction sites for the nucleation of gold. This implies atomic movement on grain boundaries but to what extent is unknown. Although the process by which gold mineralization occurs on plane defects is unclear, the large number of occurrences documented in this study stresses the importance of better understanding this relationship.

6.4: Summary

Samples from Musselwhite Mine and Hammond Reef were compared microstructurally to investigate the importance of metamorphism and deformation in shear-zone-hosted gold deposits. Both Musselwhite Mine and Hammond Reef are located adjacent to regional shear zones, have undergone regional metamorphism and are dominated by ductile deformation, but the deposits are hosted by completely different lithologies. Because the rock types of these

deposits differ so completely, attention to the physical similarities between the microstructures hosting gold is important. For both deposits, the relative timing of gold mineralization was determined to be synchronous with metamorphism and deformation. Similar microstructures host gold at both Musselwhite Mine and Hammond Reef.

Gold occurs as inclusions within metamorphic minerals like grunerite and garnet at Musselwhite Mine and muscovite at Hammond Reef. Gold inclusions within these metamorphic minerals indicate gold mineralization occurred before or during metamorphism.

Commonly, gold mineralization is associated with microstructures indicative of heterogeneous deformation for both deposits. Gold mineralization often appears within fractures occurring in competent minerals not extending into the surrounding matrix. This type of heterogeneous response to strain is common in polymineralic rocks. Gold mineralization appears in fractures in the competent minerals garnet, arsenopyrite and clinopyroxene at Musselwhite Mine as well as in pyrite at Hammond Reef. Other deformation induced microstructures host gold mineralization at Musselwhite Mine and Hammond Reef. For example, strain shadows of competent garnet and pyrite host gold mineralization at both deposits. Gold associated with deformation induced microstructures indicates gold mineralization occurred during and/or after deformation. Also at both Musselwhite Mine and Hammond Reef, gold commonly appears on plane defects such as grain boundaries. This common observation implies an important role for these defects.

Through the documented microstructures associated with gold, constraint on the relative timing of gold mineralization at Musselwhite Mine and Hammond Reef can be made. Gold inclusions within metamorphic minerals must have existed before or during the metamorphism to be included. Similarly, gold mineralization associated with deformation features must have occurred during or after ongoing deformation. This implies that gold mineralization occurs together with

metamorphism and deformation at Musselwhite Mine and Hammond Reef; could this be the case for other shear-zone-hosted gold deposits?

References:

Ando, J., Fujino, K. and Takeshita, T., 1993, Dislocation microstructures in naturally deformed silicate garnets: Physics of the Earth and Planetary Interiors, v. 80, p. 105-116.

Barber, D.J. and Wenk, H.R., 1991, Dauphine twinning in deformed quartzites: implications of an in-situ TEM study of the α-β-phase transformation: Physics and Chemistry of Minerals, v. 17, p. 492-502.

Beach, A., and Fyfe, W.S., 1972, Fluid transport and shear zones at Scourie, Sutherland: evidence of overthrusting: Contributitions in Mineralogy and Petrology, v. 36, p. 175-180.

Behrmann J.H., 1983, Microstructure and fabric transition in calcite tectonites from the Sierra Alhamilla (Spain): Geologische Rundschau, v. 72, p. 605-618.

Bell, T.H., Ham, A.P. and Kim, H.S., 2004, Partitioning of deformation along an orogen and its effects on porphyroblasts growth during orogenesis: Journal of Structural Geology, v. 26, p. 825-845.

Bell, I.A., Wilson, C.J.L., McLaren, A.C. and Etheridge, M.A.,1986; Kinks in mica: role of dislocations and (001) cleavage: Tectonophysics, v. 127, p. 49-65.

Bell, T.H., 1985, Deformation partitioning and porphyroblasts rotation in metamorphic rocks: a radical reinterpretation: Journal of Metamorphic Geology, v. 3, p. 109-118.

Berger, A. and Stunitz, H., 1995, Deformation mechanisms and reaction of hornblende: examples from Bergell tonalite (Central Alps): Tectonophysics, v.257, p.149-174.

Bons,P.D. and Urai, J.L., 1994, Experimental deformation of two-phase rock analogues: Materials Sceince and Engineering , v. 175, p. 221-229.

Bouller, A.M. and Gueguen, Y., 1975; SP-mylonites produced by superplastic flow: Controbutions to Mineralogy and Petrology, v. 50, p. 93-104.

Breaks, F.W., Osmani, I.A. and deKempt, E.A., 2001, Geology of the North Caribou Lake area, Northwestern Ontario: Ontario Geological Survey Open File Report 6023, 80 p.

Card, K.D., 1990, A review of the Superior Province of the Canadian Shield, a product of Archean accretion: Precambrian Research, v. 48, p. 99-156.

Carter, N.L., Christie, J.M. and Griggs, D. T., 1964, Experimental deformation and recrystallization of quartz: Geology, v. 72, p. 687-733.

Chattopadhyay, A. and Ghosh, N., 2007, Polyphase deformation and garnet growth in pelitic schists of Sausar Group in Ramtek area, Maharashtra, India: A study of porphyoblast-matrix relationship: Journal of Earth System Science, v. 116, p. 423-432.

Clark, M.B. and Fisher, D.M., 1994, Strain partitioning and crack-seal growth of chlorite-muscovite during progressive noncoaxial strain: an example from the slate belt of Taiwan: Journal of Structural Geology, v. 17, p. 461-474.

Craig, J.R. and Vaughan, D.J., 1994, Ore microscopy and ore petrography 2nd edition, John Wiley and Sons Inc., 434p.

Culshaw, N. and Fyson, W., 1984, Quartz ribbons in high grade gneiss: modifications of dynamically formed quartz c-axis preffered orientations by oriented grain growth: Journal of Structural Geology , v. 6, p. 663-668.

Duuring, P., Hagemann, S. G., and Love, R. J., 2001, A thrust ramp model for gold mineralization at the Archean trondjemite-hosted Tarmoola deposit: The importance of heterogeneous stress distribution around granitoid contacts: Economic Geology, v. 96, p. 1379-1396.

Drury, M.R., Humphreys, F.J. and White, S.H., 1985, Large strain deformation studies using polycrystalline magnesium as a rock analogue. Part II: dynamic recrystallization mechanisms at high temperatures: Physics of the Earth and Planetary Interiors, v. 40, p. 208-222.

Easton, R. M., 2000, Metamorphism of the Canadian Shield. Ontario, Canada. The Superior Province: The Canadian Mineralogist, v. 38, p. 287-317.

Eggleton R.A. and Buseck P.R. 1980, The orthoclase-microcline inversion: a high-resolution transmission electron microscope study and strain analysis: Contributions to Mineralogy and Petrology, v. 74, p. 123-133

Egydio-Silva, M. and Mainprice, D., 1999, Determination of stress directions form plagioclase fabrics in high grade deformed rocks (Alem Paraiba shear zone, Ribeira fold belt, southeastern Brazil): Journal of Structural Geology, v. 21, p. 1751-1771.

Eisenlohr, B.N., Groves, D. and Partington, G.A., 1989, Crustal-scale shear zones and their significance to Archean gold mineralization in Western Australia: Mineralium Deposita, v. 24, p.1-8.

Etheridge, M.A., Wall, V.J. and Vernon, R.H., 1983, Journal of Metamorphic Geology, v. 1, p. 205-226.

Fettes, D. and Desmons, J. editiors, 2007, Metamorphic Rocks, A Classification and Glossary of Terms: Cambridge University Press, 244 p.

Fliervoet, T.F., White, S.H. and Drury, M.R., 1997, Evidence for dominant grain-boundary sliding deformation in greenschist- and amphibolite-grade polymineralic ultramylonites from the Redbank Deformed Zone, Central Australia: Journal of Structural Geology, v. 19, p. 1495-1520.

Geraud, Y., Caron, J.M. and Faure, P., 1995, Porosity of a ductile shear zone: Journal of Structural Geology, v. 17, p. 1757-1769.

Gleason, G.C. and Tullis, J., 1995, A flow law for dislocation creep of quartz aggregates determined with the molten salt cell: Tectonophysics, v. 247, p. 1-23.

Gregg, W.J., 1985, Microscopic deformation mechanisms associated with mica film formation in cleaved psammitic rocks: Journal of Structural Geology, v. 7, p. 45-56.

Groves, D.I., 1993, The crustal continuum model for late-Archaean lode-gold deposits of the Yilgarn Block, Western Australia: Mineral Deposita, v. 28, p. 366-374.

Guillope, M. and Poirier, J.P., 1979, Dynamic recyrstallization during creep of single-crystallin halite: an experimental study: Journal of Geophysical Research, v. 84, p. 5557-5567.

Hall, R.S., and Riggs, D.M., 1986, Geology of the West Anticline zone, Musselwhite prospect, Opapimiskan Lake, Ontario, Canada: Proceedings of Gold‟86, Konsult International, Toronto, Ontario, p. 124-136.

Handy, M.R., Wissing, S.B. and Streit, L.E., 1999, Frictional-viscous flow in mylonite with varied bimineralic composition and its effect on lithospheric strength: Tectonophysics, v. 303, p. 175-191.

Handy, M.R., 1992, Correction and addition to “The solid-state flow of polymineralic rocks”: Journal of Geophysical Research, v. 97, p. 1897-1899.

Handy, M.R., 1990, The solid-state flow of polymineralic rocks: Journal of Geophysical Research, v. 95, p. 8647-8661.

Handy, M.R., 1989, Deformaiton regimes and the rheological evolution of fault zones in the lithosphere- the effects of pressure, temperature, grain size and time: Tectonophysics, v. 163, p. 119-152.

Hill, M.L., Cheatle, A., and Liferovich, R., 2006, Musselwhite Mine: An orogenic gold deposit in the Western Superior Province: Geological Association of Canada Abstracts, v. 31, p. 67.

Hippertt, J., Rocha, A., Lana, C., Egydio-Silva, M. and Takeshita, T., 2001, Development of crystal morphology during unitaxial growth in a progressively widening vein: II. Numerical simulations of evolution of antitaxial fibrous veins: Journal Structural Geology, v. 23, p. 873-885.

Hirth, G., Teyssier, C. and Dunlap, W.J., 2001, An evaluation of quartzite flow laws based on comparisons between experimentally and naturally deformed rocks: International Journal of Earth Sciences, v. 90, p. 77-87

Hirth, G. and Tullis, J., 1992, Dislocation creep regimes in quartz aggregates: Journal of Structural Geology, v. 14, p. 145-159.

Hollings, P. and Kerrich, R., 1999, Trace element systematic of ultramafic and mafic volcanic rocks from the 3 Ga North Caribou greenstone Belt, Northwestern Superior Province: Precambrian Research, v. 93, p. 257-279.

Holyoke, C.W. and Tullis, J., 2006a, Mechanisms of weak phase interconnection and the effects of phase strength contrast on fabric development: Journal of Structural Geology, v. 28, p. 621-640.

Holyoke, C.W. and Tullis, J., 2006b, The interaction between reaction and deformation: an experimental study using a biotite + plagioclase + quartz gneiss: Journal of Metamorphic Geology, v. 24, p.724-762.

Ji, S. Saruwatari, K., Mainprice, D., Wirth, R., Xu, Z. and Xia, B., 2003, Microstructures, petrofabrics and seismic properties of ultra high-pressure eclogites from Sulu region, China: implications for rheology of subducted continental crust and origin of mantle reflections: Tectonophysics, v. 370, p. 49-76.

Jordan 1987, The deformational behavior of bimineralic limestone- halite aggregates: Tectonophysics, v. 135, p. 185-197.

Kruse, R. and Stunitz, H., 1999, Deformation mechanisms and phase distribution in mafic high-temperature mylonites from the Jotun Nappe, southern Norway: Tectonophysics, v. 303, p. 223-249.

Lagoeiro, L. Hippertt and Lana, C., 2003, Deformation partitioning during folding and transposition of quartz layers: Tectonophysics, v. 361, p. 171-186.

Lapworth, T., Wheeler, J. and Prior, D.J., 2002, The deformation of plagioclase investigated using electron backscatter diffraction crystallographic preferred orientation data: Journal of Structural Geology, v. 24, p. 387-399.

Mackinnin, P., Fueten, F. and Robin, P.Y., 1997, A fracture model for quartz ribbons in straight gneisses: Journal of Structural Geology, v. 19, p. 1-14.

Mainprice, D., Bascou, J., Cordier, P., and Tommasi, A., 2004, Crystal preferred orientations of garnet:comparision between numerical simulations and electron back-scattered diffraction (EBSD) measurements in naturally deformed eclogites: Journal of Structural Geology, v. 26, p. 2089-2102.

Marshall, D.B. and McLaren, A.C., 1977, Deformation mechanism in experimentally deformed plagioclase feldspars: Physics and Chemistry of Minerals, v. 1, p. 351-370.

McCuaig T.C. and Kerrich R., 1998, P-T-t-deformation –fluid characteristics of lode gold deposits: evidence for alteration systematic: Ore Geology Reviews, v. 12, p. 381-453.

Mikucki, E.J., 1998, Hydrothermal transport and depositional processes in Archean lode-gold systems: A review: Ore Geology Special Issue, v. 13, p. 307-321.

Moran, P., 2008, Lithogeochemistry of the sedimentary stratigraphy and metosomatic alteration in the Musselwhite Gold Deposit, North Caribou Lake Belt, Superior Province Canada: Implications for deposition and mineralization [Masters Thesis]: Lakehead University, 347 p.

Nishikawa, O., Saiki, K. and Wenk, H.R., 2004, Intra-granular strains and grain boundary morphologies of dynamically recrystallized quartz aggregates in a mylonite: Journal of Structural Geology, v. 26, p. 127-141.

Nishikawa, O. and Takeshita, T., 2000, Progressive lattice misorientation and microstructural development in quartz veins deformed under subgreenschist conditions: Journal of Structural Geology, v. 22, p. 259-276.

Nishikawa, O. and Takeshita, T., 1999, Dynamic analysis and two types of kink bands in quartz veins deformed under subgreenschist conditions: Tectonophysics, v. 301, p. 21-34.

Osmani, I.A. and Stott, G.M., 1988, Regional-Scale Shear Zones in Sachigo Subprovince and their Ecomomic Significance; in Summary of Field Work and Other Activities 1988, Ontario Geological Survey, Miscellaneous Paper 141, p. 53-67.

Otto, A., 2002, Ore forming processes in the BIF-hosted gold deposit Musselwhite Mine, Ontario, Canada [Masters thesis]: Freiberg University of Mining and Technology, Institute of Mineralogy, Department of Economic Geology and Leibniz Laboratory for Applied Marine Research, 86 p.

Passchier,C. and Trouw, R., 2005, Microtectonics, Springer-Verlag Berlin Heidelberg, 366 p.

Paterson, M. S., 1995, A theory for granular flow accommodated by material transfer via an intergranular fluid: Tectonophysics, v. 245, p. 135-151.

Percival, J.A., Sanborn-Barrie, M., Skulski, T., Stott, G.M., Helmstaedt, H., and White, D.J., 2006, Tectonic Evolution of the Western Superior Province from NATMAP and Lithoprobe Studies: Canadian Journal of Earth Science, v.43, p. 1085-1117.

Perkins, D., 2002, Mineralogy (2nd edition), Prentice Hall Inc., 483 p.

Post, A.D., Tullis, J. and Yund, R. A., 1996, Effects of chemical environment on dislocation creep of quartzite: Journal Geophysical Research, v. 101, p. 22143-22155.

Rayner, N. and Stott, G.M., 2005, Discrimination of Archean domains in the Sachigo Subprovince: Ontario Geological Survey, poster, in Northeast Mines and Mineral Symposium, Timmins Ontario, April 12-13, 2005.

Rahimi-Chakdel, A., Boyle, A.P., and Prior, D.J., 2006, Quartz deformation mechanisms during Barrovian metamorphism: Implications from crystallographic orientation of different generations of quartz in pelites: Tectonophysics, v. 427, p. 15-34.

Rutter, E.H. and Brodie, K. H., 2004, Experimental intracrystalline plastic flow in hot-pressed synthetic quartzite prepared from Brazilian quartz crystals: Journal of Structural Geology, v. 26, p. 259-270.

Rybacki, E. and Dresen, G., 2004, Deformation mechanism maps for feldspar rocks: Tectonophysics, v. 382, p.173-187.

Schmid, S.M., Boland, J.N. and Paterson, M.S., 1977, Superplastic flow in fine grained limestone: Tectonophysics, v. 43, p. 257-291.

Shigematsu, N., 1999, Dynamic recrystallization in deformed plagioclase during progressive shear deformation: Tectonophysics, v. 305, p. 437-452.

Stinson, V.R., 2010, Metamorphism at Musselwhite Mine, Western Superior Province, Canadian Shield [Honours Thesis]: Lakehead University, 50 p.

Stipp, M., Stunitz, H., Heilbronner, R., and Schmid, S., 2002, The eastern Tonale fault zone: a „natural laboratory" for crystal plastic deformation of quartz in temperature range from 250° to 700°C. Journal of Structural Geology, v. 24, p. 1861-1884.

Stone, D., 2009, The Central Wabigoon Area: Ontario Geological Survey, poster, *in* Northwest Ontario Mines and Mineral Symposium, Thunder Bay, Ontario, April 7-8, 2009.

Stone, D., 2010, Precambrian geology of the central Wabigoon Subprovince area, northwestern Ontario: Ontario Geological Survey, Open File Report 5422, 130p.

Storey C.D. and Prior D.J., 2005, Plastic deformation and recrystallization of garnet: a mechanism to facilitate diffusion creep: Journal of Petrology, v. 45, p. 2593-2613.

Stott, G., Corkery, T., Leclair, A., Boily, M., and Percival, J.A., 2007, A revised terrane map for the Superior Province as interpreted from aeromagnetic data: *in* Institute on Lake Superior Geology Proceedings, 53rd Annual Meeting, Lutsen, Minnestota, Abstract, v.53, part 1, p. 74–75.

Stunitz, H. and Tullis, J., 2001, Weakening and strain localization produced by syn-deformational reaction of plagioclase: International Journal of Earth Sciences, v. 90, p. 136-148.

Stunitz, H. and Fitz Gerald, J. D., 1993, Deformation of granitoids at low metamorphic grade, II. Granular flow in albite-rich mylonites: Tectonophysics, v. 221, p. 299-324.

Sullivan, W.A. and Law, R.D., 2007, Deformation path partitioning within the transpressional White Mountain shear zone, California and Nevada: Journal of Structural Geology, v. 29, p. 583-598.

Thurston, P.C., Osmani, I.A. and Stone, D., 1991, Northwestern Superior Province Review and Terrane Analysis, Geology of Ontario, Ontario Geological Survey, 144 p.

Tomlinson, K.Y., Davis, D.W., Stone, D., and Hart, T., 2003, New U-Pb and Nd isotopic evidence for crustal recycling and Archean terrane development in the south-central Wabigoon Subprovince, Canada: Contributions to Mineralogy and Petrology, v. 144, p. 684-702.

Tomlinson, K.Y., Stott, G., Percival, J., and Stone, D., 2004, Basement terrane correlations and crustal recycling in the western Superior Province: Nd isotopic character of granitoid and felsic volcanic rocks in the Wabigoon subprovince, N. Ontario, Canada: Precambrian Research, v. 132, p. 245-274.

Tullis, J. 2002. Deformation of granitic rocks: experimental studies and natural examples: Reviews in mineralogy and geochemistry, v. 51, part 1, p. 51-95

Tullis, J. and Yund, R.A., 1985, Dynamic recrystallization of feldspar: a mechanism for ductile shear zone formation: Geology, v. 13, p. 238-241.

Urai, J., Means, W.D. and Lister, G.S., 1986, Dynamic recrystallization of minerals: *In* Heard H.C., and Hobbs, B.E. (editors) Mineral and rock deformation: laboratory studies, the Paterson volume, American Geophysics Union, Washington D.C., v. 36, p. 161-200.

Vernon, R. H., and Clarke, G. L., 2008, Principles of Metamorphic Peterology, Cambridge University Press, 343 p.

Voegele, V., Ando, J.I., Cordier, P., and Liebermann, R.C., 1998a, Plastic deformation of silicate garnets I. High-pressure experiments: Physics of the Earth and Planetary Interiors, v. 108, p. 305-318.

Voegele, V., Cordier, P., Sautter, V., Sharp, T.G., Lardeaux, J.M. and Marques, F.O., 1998b, Plastic deformation of silicate garnets II. Deformation microstructures in natural samples: Physics of the Earth and Planetary Interiors, v. 108, p. 319-338.

Wang, Z. and Ji, S., 1999, Deformation of silicate garnets: brittle-ductile transition and its geological implications: The Canadian Mineralogist, v. 37, p. 525-541.

White, J.C. and Barnett, R.L., 1990, Microstructural signatures and glide twins in microcline, Hemlo, Ontario. Canadian Mineralogist, v. 28, p. 757-769.

Winter, J.D., 2010, Principles of Igneous and Metamorphic Petrology (2nd edition), Prentice Hall Inc., 693 p.

Wu and Groshang 1991, Low temperature deformation of sandstone, southern Appalachian fold-thrust belt: Geological Society of America Bulletin, v. 103, p. 861-875

.

Appendices:

Appendix A: Lithology 1, Musselwhite Mine, garnet-grunerite schist

A.1: Sample locations (Lithology 1, Musselwhite Mine, garnet-grunerite schist)

Number	hole #:	Ore-body	from (m)	to (m)	X	Y	Z
310-601	06-PQU-016	a-block (a1)	172.5	172.7	8824.8	11300.48	4583.47
310-602	06-PQU-017	c-block	125.8	126	8784.51	11300	4616.42
310-603	06-pqu-016	c-block	128.6	128.7	8783.24	11300.03	4595.99
310-604	06-pqu-017	c-block	127.3	127.5	8786.37	11300	4616.13
310-605	05-pqe-020	c-block	59.05	59.2	8747.34	11580.48	4585.93
310-606	03-pqu-022	a-block (a1)	106.25	106.4	8795.1	11491.99	4638.97
310-607	03-pqu-022	a-block (a1)	113.6	113.8	8796.87	11491.29	4631.08
310-608	05-pqe-020	c-block	57	57.2	8746.76	11589.52	4586.83
310-610	07-pqe-009	c-block	88.5	88.7	8722.58	11924.2	4524.54
310-611	06-pqe-107	c-east	130.6	130.75	8744.54	11797.31	4506.88
310-612	07-pqe-088	c-east	159.3	159.45	8731.65	12098.7	4442.87
310-613	09-del-064	c-block	40	40.15	8737.4	11700	4530.09
310-614	07-pqe-089	c-block	95.2	95.4	8701.35	12104.07	4500.99
310-615	09-pqe-030	d-block	174	174.2	8654.74	12416.94	4394.95
310-616	09-pqe-062	c-block	150.2	150.4	8633.85	12462.02	4413
310-618	09-pqe-030	c-block	154	154.1	8641.61	12416.81	4411.47
310-619	09-pqe-056	c-block	172.2	172.3	8612.85	12505.48	4355.17
310-620	08-pqe-006	c-block	114.6	114.7	8673.24	12211.52	4458.27
310-624	08-pqe-029	d-block	172.9	173.1	8648.8	12278.55	4384.9
310-625	04-pqu-120	a-block (a1)	224.85	225	8841.9	11201.3	4607.03
310-627	06-pqe-107	c-block	117.1	117.3	8736.86	11799.96	4517.08
310-630	05-pqe-013	a or c-east?	125.3	125.5	8785.03	11574.2	4530.5
310-631	09-pqu-001	d-block	40.2	40.5	8704.83	11929.77	4451.26
310-632	07-pqe-009	a-block (a1)	147	147.1	8756.96	11924.2	4476.52
310-633	07-pqe-009	a-block (a1)	147.5	147.6	8756.96	11924.2	4476.52
310-634	09-del-134	a-block (a1)	26.5	26.65	8772.3	11726.96	4507.91
310-635	09-del-134	c-east	11.7	11.9	8758.02	11727.46	4512.26
310-636	09-del-113	c-east	55.6	55.7	8740.19	11893.66	4468.55
310-637	07-pqe-065	a-block (a1)	154.8	155	8737.58	12075.81	4449.7
310-638	07-pqe-065	a-block (a1)	158.8	159	8739.7	12075.85	4446.62

Number	hole #:	Ore-body	from (m)	to (m)	X	Y	Z
310-640	07-pqe-086	d-block	130.6	130.7	8699.38	12106.22	4456.75
310-642	08-pqe-007	a-block (a1)	113.2	113.3	8722.48	12277.02	4503.42
310-645	09-del-047	c-east	15.9	16	8765.04	11675.36	4530.91
808-111	MWMS2	a-block (a1)	n/a	n/a	n/a	n/a	n/a
808-112	MWMS3a	a-block (a1)	n/a	n/a	n/a	n/a	n/a
808-113	4EAPM0565C	n/a	n/a	n/a	n/a	n/a	n/a
909-001	09-TAN-042A	moose	239.5	239.6	8483.54	12409.93	4304.65
909-002	09-TAN-042B	moose	181	181.1.5	8499.35	12413.08	4358.62
909-003	09-TAN-017a	moose	209.3	209.4	8502.93	12325	4366.22
909-004	09-TAN-017b	moose	208.2	208.35	8503.48	12314.09	4367.09
909-005	08-TAN-022A	moose	223.5	223.55	8516.36	12217.79	4363.89
909-006	08-TAN-022B	moose	214.5	214.6	8520.46	12218.33	4371.03
909-007	08-TAN-012	moose	199.5	199.6	8537.58	12115.13	4399.37
909-008	07-TAN-007	moose	185.5	185.65	8550.41	12018.83	4418.05
909-009	08-TAN-029A	moose	184.3	184.4	8565.54	11958.61	4431.83
909-010	08-TAN-029B	moose	185.5	185.6	8565	11958.61	4430.95
909-017	08-tan-014	moose	220.4	220.55	8534.12	12109.32	4377.98
909-022	09-tan-016	moose	231.7	231.9	8502.94	12320.55	4340.45
909-023	09-tan-021	moose	226.1	226.2	8495.16	12381.43	4341.63

A.2: Sample descriptions

Number	Sample Description (HS- hand sample, TS- thin section):	Foliation/texture:	Gold observed:
310-601	HS: Grunerite and garnet dominate this sample, and are found together in bands with grunerite wrapping around and filling space between garnet crystals. TS: A spaced foliation is defined by the grunerite. Green-amphibole wisps can be seen along the edge of these grunerite-garnet bands.	spaced, smooth, parallel, discrete	No
310-602	HS: Bands are mainly garnet and grunerite-rich with quartz-rich bands between. TS: Garnets appear rich with inclusion in this sample. Grunerite defines the foliation, magnetite blebs occur within this foliated grunerite.	spaced, smooth, parallel, discrete	No
310-603	HS: This sample has large garnet crystals with minor grunerite and pyrrhotite wrapping around them. Quartz makes up the rest of the sample. TS: Garnet crystals make up most of this sample and host many inclusions of grunerite and quartz.	n/a	No
310-604	HS: This sample is composed of iron-rich bands and quartz-rich bands. Iron-rich bands include garnet, grunerite, hornblende, minor biotite and pyrrhotite. Amphiboles and pyrrhotite appear wispy. TS: Foliation defined by amphiboles which anastomoses around the large garnet porphyroblasts.	smooth, parallel to anastomosing, discrete	Yes
310-605	HS: This sample is nearly half quartz with a wriggly Fe-Al-rich band of in the center. Pyrrhotite can be seen wispy to stringer-like in the iron-rich portion as well as the quartz-rich. TS: Garnet appears cracked with inclusions. Foliation is defined by wisps bands of amphiboles and biotite. The foliation anastomoses around large 1 cm diameter garnet porphyroblasts.	rough to smooth, parallel to anastomosing, discrete	Yes
310-606	HS: Fe-bands are magnetic, but appear to be mainly garnet, biotite and grunerite. Garnet is small mm diameters. TS: Folaition is defined by amphiboles in this sample, but is rich with magnetite. Garnets are ragged and have inclusions of magnetite.	rough to smooth, anastomosing to parallel	No

Number	Sample Description (HS- hand sample, TS- thin section):	Foliation/texture:	Gold observed:
310-607	HS: Sample included garnet-biotite-amphibole bands with quartz bands separating them. Garnet has a diameter of 2mm and appears with biotite. TS: Sample is made up of ragged looking garnet. Biotite and amphiboles are well foliated. About half of the Fe-rich bands in this sample are made up of grunerite and magnetite.	smooth, parallel, discrete	No
310-608	HS: Al-Fe-rich bands are separated by thin quartz bands. Note the overall anastomosing appearance to the foliation. TS: Subhedral garnet crystals (1 cm diameter) appear with grunerite and sometimes biotite anastomosing around them.	spaced, anastomosing to parallel, discrete bands, smooth	No
310-610	HS: Half of this sample is dominated by garnet-amphibole bands with pyrrhotite wisps (note that these bands are magnetic). TS: Strain shadows occur around garnet porphyroblasts defined by grunerite and green amphibole with wispy pyrrhotite parallel to the foliation.	rough, parallel to anastomosing	Yes
310-611	HS: This sample is dominated by quartz, with ragged, wispy bands of pyrrhotite, green amphibole, grunerite and garnet. Garnet crystals can be up to 1 cm in diameter. TS: Garnets appear cluster together with amphiboles and biotite anastomosing around these porphyroblasts.	ragged, rough at best	Yes
310-612	HS: Quartz defines portions of this sample but they are not nicely banded instead it appears blotchy and distorted. Pyrrhotite appears as blebs, wisps and stringers. The amphiboles and biotite define a spaced, rough, anastomosing foliation. TS: Garnet porphyroclasts appear in this sample with biotite and amphiboles anastomosing around them. Note that carbonate clusters occur within the amphibole-rich area.	rough to wriggly, anastomosing, discrete	No

Number	Sample Description (HS- hand sample, TS- thin section):	Foliation/texture:	Gold observed:
310-613	HS: Grunerite and garnet dominate this sample, they are found together in bands with grunerite wrapping around and filling space between garnet crystals. TS: Strain shadows occur around garnet porphyroblasts in this sample. Also note that some of the garnet crystals are flattened or elongated.	spaced, smooth, parallel, discrete	No
310-614	HS: The foliation is hard to distinguish in this sample; it appears ragged and folded. The amphibole in this sample appears dark green in color. Garnet crystals have about 1 cm diameter. This sample is rich with pyrrhotite. TS: Stringers of poikiloblastic pyrrhotite appear in this sample and include amphibole crystals. Amphiboles also anastomose around large garnet crystals which make up about half the sample.	folded.	Yes
310-615	HS: It is hard to make out a foliation in this sample because the bands are so distorted and pinched out. The fabric is rough. Dark-green amphibole can be seen with grunerite, minor biotite and garnet (.5cm). Pyrrhotite also appears as irregular wispy veinlets. TS: The textures appear ductile, bands are not continuous. Amphiboles appear fine grained mixed with quartz, where amphiboles are neighboring garnet their grain size is larger and quartz is not present.	rough at best, anastomosing to the point that it can't be made out	Yes
310-616	HS: Sample is banded with quartz-rich bands and Al-Fe-rich bands. The Fe-rich bands are dark green in color. Garnet grain size varies from band to band. TS: Clinopyroxene and amphibole wisps occur within the quartz-rich area. Amphiboles and pyrrhotite wrap around the large garnet crystal in the corner of the thin section.	smooth, parallel	Yes
310-618	HS: Typical garnet-biotite-amphibole-rich bands with quartz between them. Foliation is defined by the biotite and amphiboles, note some folding of these bands is also present. TS: Foliation anastomoses around garnet porphyroblasts in the garnet-biotite-amphibole-rich portion of the sample. Quartz bands make up the rest of the sample, note these are not continuous.	smooth , folded to parallel	No

Number	Sample Description (HS- hand sample, TS- thin section):	Foliation/texture:	Gold observed:
310-619	HS: Garnet in this sample varies from large 1cm diameter to small 2mm diameter size. The small garnet is found with grunerite wrapping around it in a grunerite-garnet band. The large garnet is found within garnet-biotite-amphibole bands. TS: Sample is well foliated; amphiboles and biotite anastomose around large garnet porphyroblasts. Also quartz-grunerite bands appear in this sample.	smooth, anastomosing, discrete	No
310-620	HS: This sample is banded with quartz-rich, garnet-amphibole, and garnet-biotite-amphibole bands. Garnet is fairly euhedral and ranges from 2mm-1cm in diameter. Quartz makes up more than half of the sample. There are thin amphibole wisps within the quartz-rich areas. TS: Discontinuous quartz bands appear in this sample. Garnet crystals contain many fractures and inclusions.	rough to smooth, parallel to anastomosing, discrete	No
310-624	HS: Quartz dominates this sample with amphibole wisps scattered throughout. Garnet and amphiboles appear on the edge of the quartz-rich area and make up the rest of the sample. TS: Amphiboles define the foliation which anastomoses around garnet porphyroblasts. These amphiboles also anastomose around quartz-rich clusters within the garnet-amphibole bands.	fairly smooth, anastomosing, discrete	Yes
310-625	HS: This sample is well foliated. It appears as thin bands (1-2mm) quartz-rich, garnet-biotite-amphibole, and grunerite-rich. TS: Quartz and amphiboles are very fine grained in this sample. Garnets look ragged with many inclusions. Magnetite and pyrrhotite appear as wisps scattered throughout this sample.	fairly smooth, nearly parallel, discrete	No
310-627	HS: Garnet porphyroblasts are scattered through the sample. Amphiboles, biotite, and pyrrhotite appear as wispy thin discontinuous bands. TS: The foliation defined by amphiboles and biotite anastomoses around garnet porphyroblasts. Quartz appears as discontinuous bands which sometimes contain stringers of amphibole.	rough to smooth, anastomosing, discrete	No

Number	Sample Description (HS- hand sample, TS- thin section):	Foliation/texture:	Gold observed:
310-630	HS: This sample has garnet-biotite-amphibole bands with quartz-rich bands separating them. Pyrrhotite occurs as wisps and irregular shaped blebs mainly in the garnet-biotite-amphibole bands. TS: Garnets are rich with inclusions. Bands are not easy to make out in this sample because they are very discontinuous and anastomosing.	smooth to rough, anastomosing, discrete	No
310-631	HS: This sample has a ragged appearance. Garnet-biotite-amphibole bands are not continuous making the foliation hard to distinguish in this sample. TS: In this sample garnets appear elongated or flattened. Pyrrhotite has a poikiloblastic texture enveloping quartz and amphibole crystals.	ragged, rough at best	No
310-632	HS: The foliation appears ragged and rough defined by garnet-biotite-amphibole bands. Quartz-rich bands separate the Al-rich bands and are often discontinuous. Pyrrhotite occurs as wisps and blebs throughout the sample. TS: Amphiboles anastomose around ragged garnet crystals rich with inclusions.	rough, anastomosing	No
310-633	HS: Sample is made up of quartz-rich and garnet-biotite-amphibole bands. It is hard to make out the foliation in this sample due to the abundance of garnet and quartz. TS: Large garnet porphyroblasts (5mm) appear in this sample with amphiboles anastomosing around them. In thin section a quartz-rich portion of also exists, amphibole wisps occur in this quartz-rich portion.	N/A	No
310-634	HS: The quartz bands are very discontinuous in this sample; they appear between distorted garnet-amphibole bands. This sample is pyrrhotite-rich. TS: Sample is dominated poikiloblastic pyrrhotite with amphiboles surrounded by pyrrhotite. Amphiboles define the foliation but due to the abundance and texture of garnet and quartz this foliation is often rough.	smooth to rough, anastomosing and discrete	Yes
310-635	HS: This sample has quartz-rich bands as well as garnet-amphibole bands. Pyrrhotite wisps mainly occur within the garnet-amphibole bands but can be seen within the quartz as well. These bands are smooth to wriggly (some even appear rough). TS: Foliation anastomoses around garnet porphyroblasts as well as discontinuous quartz bands.	smooth to wriggly (rough at times), anastomosing and discrete	No

Number	Sample Description (HS- hand sample, TS- thin section):	Foliation/texture:	Gold observed:
310-636	HS: The foliation is defined by amphibole in this sample. Stringers of amphibole appear within quartz-rich areas. Pyrrhotite wisps occur scattered throughout the sample. TS: The amphiboles anastomose around garnet crystals in this sample. Garnet is rich with inclusions and appears ragged. Note also that clinopyroxene and carbonate occurs neighboring green amphibole.	Foliation more is continuous to zonal in this sample than in most others.	No
310-637	HS: Garnet-amphibole-rich areas appear ragged and distorted (pinched to folded). Garnet crystals are fractured. Pyrrhotite as irregular shaped wisps and blebs with minor arsenopyrite crystals. TS: Garnet porphyroblasts dominate this sample, some appear slightly ragged with many inclusions while others are nearly inclusion free though fractured.	ragged, rough at best, discrete	Yes
310-638	HS: Garnet-amphibole bands make up this sample with quartz-rich bands between. The garnet appears fractured. Pyrrhotite occurs as blebs and wisps. TS: Sample is rich with large garnet porphyroblasts (about 1 cm). The garnets are fractured and often have inclusion accompanying these fractures. Amphiboles surrounding the garnet defines the foliation.	rough to smooth, anastomosing to parallel, discrete	Yes
310-640	HS: This sample is magnetite-rich with thin pyrrhotite wisps. A few scattered garnet crystals occur within the grunerite-magnetite-rich bands. TS: Most of this sample is fine grained grunerite foliated and mixed with quartz and magnetite, yet large grunerite crystals appear within massive magnetite.	smooth, parallel, nearly continuous	No
310-642	HS: This sample appears ragged or distorted with little garnet. Fe-rich bands mainly grunerite with lesser green amphibole and magnetite. TS: Thin section was taken in garnet-rich portion of the sample. The large garnet porphyroblasts are accompanied by pyrrhotite with amphiboles foliated around them.	rough to smooth, anastomosing	Yes
310-645	HS: This sample is banded but the bands are not straight, instead they are randomly folded and pinched. There is a quartz-rich and garnet-grunerite-green amphibole-rich band. TS: Garnets appear ragged with many inclusions of magnetite occurring within them.	n/a	No

Number	Sample Description (HS- hand sample, TS- thin section):	Foliation/texture:	Gold observed:
808-111	HS: Sample is rich with quartz although garnet-biotite-amphibole bands also occur. TS: Wispy thin bands of amphiboles appear throughout the quartz-rich portion of this sample. The biotite and amphiboles define the foliation. Where garnet porphyroblasts exist the foliation anastomoses around them.	rough to smooth, parallel to anastomosing, discrete	Yes
808-112	HS: Sample is banded with quartz-rich bands as well as garnet-amphibole bands. TS: Foliation anastomoses around large garnet crystals. Hornblende and biotite stringers occur within the quartz-rich portions.	rough to smooth, nearly parallel, discrete	Yes
808-113	HS: Unable to find handsample. TS: Wispy bands of biotite and grunerite occur within the quartz-rich portion of this sample. Biotite and grunerite define the foliation and anastomose around garnet crystals.	rough, anastomosing, discrete	Yes
909-001	HS: This sample is banded with quartz-rich, biotite-rich and garnet-biotite-rich bands. Garnets have 1 to 3 cm diameter. The quartz is clear to grey in color. The quartz bands are often pinched out where large garnet crystals appear to disrupt the biotite foliation and quartz band. TS: Staurolite appears within the garnet-biotite bands. Biotite wraps around the fractures and inclusion-rich garnet crystals. In the biotite-rich bands quartz is elongated or flattened in many cases and is found scattered throughout the biotite. Also where the biotite dominates it is exhibiting crenulated cleavage.	rough to smooth, anastomosing, discrete	No
909-002	HS: This sample is biotite rich with large garnet crystals. The biotite defines the foliation and wraps around the garnet crystals. Thin (less than a cm) quartz bands follow the foliation but are often pinched out. Pyrrhotite appears wispy and also is orientated following along foliation. TS: Garnet porphyroblasts are about 1cm in diameter. The garnets in this sample are very broken up and are rich with inclusions. In the quartz-rich areas biotite and grunerite can be seen as scattered stringers.	rough to smooth anastomosing, discrete	Yes
909-003	HS: Discontinuous quartz bands occur between the garnet-biotite-amphibole-rich areas. TS: Sample is garnet-rich with biotite and amphiboles defining the foliation around the garnet crystals. Sometimes the foliation becomes wriggly. Pyrrhotite stringers occur throughout and often have a poikiloblastic texture.	rough at best, anastomosing to the point that it can't be made out	Yes

Number	Sample Description (HS- hand sample, TS- thin section):	Foliation/texture:	Gold observed:
909-004	HS: Sample is banded with quartz-rich bands as well as garnet-biotite-grunerite bands. Pyrrhotite appears as stringers orientated parallel to the foliation. TS: The thin section is completely dominated by garnet. Grunerite appears pinched between crystals.	smooth to rough, parallel to anastomosing, discrete	No
909-005	HS: This sample is differentiated into bands which are very wavy and rough. Garnet-biotite-amphibole bands, garnet-amphibole bands and quartz-rich bands make up this sample. This sample is very pyrrhotite-rich, pyrrhotite occurs as wisps and blebs but also massive pyrrhotite-rich areas where poikiloblastic texture can be seen on the hand sample scale. TS: This thin section has two large garnet crystals just over 1 cm in width. The foliation is defined mainly by grunerite with biotite and hornblende.	rough to wriggly, anastomosing, discrete	No
909-006	HS: This sample is distinctly banded with quartz bands, garnet-amphibole bands, and garnet-biotite bands. The bands are not perfectly straight but instead wavy. The quartz bands appear dark in color. TS: The garnet-amphibole bands are fine grained about one mm wide. These bands are dominated by grunerite. Garnet crystals are large in the garnet-biotite bands (1cm).	rough to wriggly, anastomosing, discrete	No
909-007	HS: This sample can be broken into quartz-rich or aluminum and iron-rich areas. The garnets in this sample range from very large to medium grain (2mm-1cm). The quartz is dark grey in color. Biotite and grunerite define the foliated but it is wavy and anastomoses around garnet crystals. TS: Larger garnet crystals appear broken. The cracks appear to be filled with pyrrhotite, grunerite and biotite.	smooth to rough, anastomosing, discrete	Yes
909-008	HS: The bands in this sample are often wavy and discontinuous. It is made up of garnet-biotite-amphibole bands and quartz-rich bands. Biotite and amphibole define the foliation. Pyrrhotite appears as wisps and is orientated parallel to the foliation. This sample contains little magnetite and in only slightly magnetic. Quartz is clear to grey in color. TS: Garnets are large 1 cm diameter.	rough to wriggly, anastomosing, discrete	No

Number	Sample Description (HS- hand sample, TS- thin section):	Foliation/texture:	Gold observed:
909-009	HS: Sample is made up of quartz-rich and garnet-amphibole-rich bands. These bands are discontinuous. TS: Pyrrhotite appears as stringers orientated with the foliation. Pyrrhotite has poikiloblastic texture.	rough to smooth nearly parallel	Yes
909-010	HS: The sample is banded with quartz-rich bands, garnet-biotite-rich bands and garnet-grunerite-rich bands. TS: Pyrrhotite appears as stringers orientated with the foliation which often exhibit poikiloblastic texture incasing quartz and grunerite . Sample is very rich with grunerite which defines the foliation.	rough tot smooth, nearly parallel with some folding	Yes
909-017	HS: Bands in this sample appears ragged and discontinuous. Bands are garnet-biotite-amphibole-rich with lesser biotite and green amphibole. TS: Foliation anastomoses around large garnet crystals (1cm). Hornblende and biotite stringers occur within the quartz-rich portion.	rough to smooth, anastomosing	Yes
909-022	HS: Garnet amphibole bands (dominantly grunerite). Pyrrhotite occurs as wisps in these bands and is orientated parallel to the foliation. Quartz separates these bands. TS: This sample is dominated by garnet porphyroblasts (5mm) which are full of inclusions.	smooth and parallel	No
909-023	HS: Garnet amphibole bands (dominantly grunerite). Pyrrhotite occurs as wisps in these bands and is orientated parallel to the foliation. Quartz separates these bands. TS: This sample is dominated by garnet porphyroblasts (5mm) which are full of inclusions.	smooth, parallel	No

A.3: Modal percent based on petrography (Lithology 1, Musselwhite Mine, garnet-grunerite schist)

Sample number:	quartz:	biotite:	garnet:	grunerite:	hornblende:	pyrrhotite:	magnetite:	other:
310-601	10	15	40	20	7	5	3	
310-602		minor	40	35	minor	trace	25	
310-603	15		45	25	5	10		minor chlorite
310-604	15	7	40	30	5	3	minor	minor chlorite
310-605	10	10	40	15	15	5		minor chlorite
310-606	10		15	30	15	5	5	carbonate: 10
310-607	20	20	20	30	10	minor	minor	trace carbonate
310-608	25	minor	40	30	minor	5	minor	
310-610	35	5	20	30	5	5		minor pyroxene
310-611	40	15	25	15	minor	5		
310-612	30	5	30	10	17	minor		carbonate: 3, pyroxene: 5
310-613	15		37	20	25	3		minor carbonate and pyroxene
310-614	15	5	30	15	25	10		minor pyroxene
310-615	40	10	10	20	10	10		
310-616	40		20	10	15	10		minor carbonate, pyroxene: 5
310-618	30		35	15	15	5		
310-619	25	minor	30	20	25	minor		
310-620	20	20	30	15	5	5	5	
310-624	45	5	20	20	8	3		
310-625	5	20	35	25	15	minor	minor	
310-627	32	10	33	10	10	5		
310-630	25	25	20	25	minor	5		
310-631	20		10	30	10	10	15	carbonate: 5

Sample number:	quartz:	biotite:	garnet:	grunerite:	hornblende:	pyrrhotite:	magnetite:	other:
310-632	45		15	30	10	minor	minor	minor pyroxene, minor carbonate
310-633	20	10	50	10	8	2		minor staurolite and chlorite
310-634	30		15	20	20	15		
310-635	35		15	20	25	5		minor carbonate and pyroxene
310-636	30		10	25	25	10		minor carbonate and pyroxene
310-637	10		66	20	minor	4		minor arsenopyrite, trace carbonate
310-638	25	15	40	20		minor		trace carbonate and pyroxene
310-640	25		15	25	10	minor	25	
310-642	20		35	20	10	15	minor	minor carbonate and pyroxene
310-645	10		35	35	5		15	minor carbonate
808-111	60	12	10	10	3	5	minor	
808-112	28	5	38	20	5	2	2	
808-113	50	10	20	10	5	5		
909-001	50	30	13	5	minor	minor	2	
909-002	30	20	35	12	minor	3	minor	
909-003	20	5	30	5	24	15	1	
909-004	5	5	80	5	minor	5	minor	
909-005	40	10	20	10	10	10	minor	
909-006	15	15	40	25	minor		5	

Sample number:	quartz:	biotite:	garnet:	grunerite:	hornblende:	pyrrhotite:	magnetite:	other:
909-007	30	35	35	minor		minor	minor	
909-008	20	30	30	15	minor	5	minor	
909-009	45		minor	25	20	10	minor	minor arsenopyrite
909-010	15	10	15	45		10	5	
909-017	37	5	30	25	minor	3		
909-022	15	5	58	20	trace	2	minor	
909-023	68		10	15		2	5	

*minor indicate less than 5%

*trace indicates less than 1%

A.4: Bands and textures (Lithology 1, Musselwhite Mine, garnet-grunerite-biotite schist)

Sample number	garnet-biotite bands	garnet-amphibole bands	garnet-amphibole-biotite bands	grunerite-magnetite bands		pyrrhotite stringers	poikiloblastic-stringer pyrrhotite	pyrrhotite blebs	vein-like or fracture-filling sulfides	magnetite-rich		quartz only bands	quartz with other minerals	quartz with minor other minerals
310-601			X			X		X						
310-602		X		X						X				
310-603		X						X	X			X		
310-604		X						X	X					X
310-605		X							X					X
310-606		X						X		X			X	
310-607			X										X	
310-608		X	X					X	X				X	
310-610			X			X						X		X
310-611			X				X	X					X	
310-612			X					X						X
310-613		X					X		X				X	
310-614			X				X	X	X				X	
310-615			X			X	X						X	
310-616		X					X	X	X				X	
310-618		X					X	X					X	
310-619		X	X					X					X	
310-620			X				X	X					X	X
310-624			X			X						X		X
310-625	X			X					X				X	
310-627			X				X	X	X			X		X
310-630			X			X		X					X	
310-631		X		X			X	X					X	X
310-632		X						X					X	
310-633			X						X					X
310-634		X					X					X	X	
310-635		X				X	X	X					X	X

Sample number	garnet-biotite bands	garnet-amphibole bands	garnet-amphibole-biotite bands	grunerite-magnetite bands		pyrrhotite stringers	poikiloblastic-stringer pyrrhotite	pyrrhotite blebs	vein-like or fracture-filling sulfides	magnetite-rich		quartz only bands	quartz with other minerals	quartz with minor other minerals
310-636		X					X	X					X	
310-637		X							X				X	X
310-638			X				X							X
310-640		X		X						X		X	X	
310-642		X					X	X	X				X	
310-645				X						X				
808-111		X	X			X	X	X						
808-112		X						X	X				X	
808-113		X	X			X		X	X				X	X
909-001		X											X	
909-002		X												
909-003		X	X				X	X	X				X	X
909-004			X					X	X					
909-005			X				X	X					X	X
909-006	X	X								X			X	
909-007	X					X		X					X	
909-008	X		X				X	X					X	
909-009		X					X	X					X	
909-010			X	X			X	X	X				X	
909-017		X	X				X	X	X				X	X
909-022		X	X					X	X					
909-023		X		X				X		X			X	X

A.5: Gold occurrences (Lithology 1, Musselwhite Mine, garnet-grunerite schist)

Sample number:	Gold occurrence number:	Description:
310-604	604-001	Gold occurs as inclusions within garnet. One of the gold inclusions is in contact with pyrrhotite while the other is adjacent to a bleb of magnetite both also included within the garnet crystal
310-605	605-001	Pyrrhotite and gold fill a fracture which extends across a garnet crystal.
310-605	605-002	Gold bleb occurs within a fracture filled with both silicate and metallic minerals. The fracture extends only through a garnet crystal and not into the matrix
310-605	605-003	Gold bleb occurs within a pyrrhotite-filled fracture in a garnet crystal. Note that the garnet crystal hosts inclusions of grunerite.
310-605	605-004	Gold blebs occur in fractures within garnet crystal. Some of the blebs appear in a fracture which seems to have healed while the others appear in a fracture is filled with pyrrhotite.
310-610	610-001	Gold filling fracture in garnet crystal. This fracture is also filled by silicates and pyrrhotite
310-610	610-002	Gold filling fractures in garnet crystal.
310-610	610-003	Gold appears filling a fracture in garnet as well as several gold blebs create an inclusion trail in the same garnet crystal.
310-610	610-005	Gold associated with fracture as well as pyrrhotite inclusion within garnet crystal.
310-610	610-006	Gold inclusions within garnet crystal associated with inclusions of magnetite and grunerite.
310-610	610-007	Gold filling fractures in garnet crystal as well as along boundary of grunerite inclusions within garnet.
310-610	610-008	Gold mineralization along boundary between pyrrhotite and garnet crystal as well as blebs of gold within fracture in the same garnet crystal.
310-611	611-011	Gold inclusion within hornblende.

Sample number:	Gold occurrence number:	Description:
310-614	614-001	Gold bleb within ragged arsenopyrite crystal which is surrounded by pyrrhotite and within a highly fractured garnet crystal.
310-615	615-001	Gold bleb occurs on the edge of larger pyrrhotite bleb which is located within a quartz-rich band. A stringer of grunerite runs through this quartz dominated area, along the opposite side of the pyrrhotite bleb as the gold is positioned.
310-615	615-002	Gold located within quartz and grunerite, in an area where quartz is filled with fine-grained grunerite as well as pyrrhotite blebs.
310-615	615-003	Gold inclusion within quartz. Note that this quartz band includes many inclusions of grunerite, hornblende and pyrrhotite.
310-615	615-004	Gold blebs occur in fractures within garnet crystal. Some of the gold blebs are alone filling tiny fractures while the others are in contact with pyrrhotite filling fractures.
310-616	616-001	Gold bleb appears on grain boundary in hornblende.
310-616	616-003	Gold bleb occurs within chalcopyrite, which is surrounded by web-like pyrrhotite stringer. The pyrrhotite surrounds the grunerite and quartz.
310-624	624-001	Gold blebs occur on grain boundaries within grunerite-dominated area. Some gold blebs occur on grunerite-grunerite boundaries while others occur on grunerite-garnet boundaries and grunerite-quartz boundaries.
310-630	630-001	Gold blebs occur on grain boundaries between grunerite, carbonate and quartz in this quartz-dominated band.
310-630	630-002	Gold bleb appears with pyrrhotite within fracture in a garnet crystal. This garnet crystal is rich with inclusions of pyrrhotite, grunerite and quartz.
310-630	630-003	Gold appears as an inclusion within a garnet crystal, this crystal is rich with inclusions of grunerite with minor pyrrhotite inclusions as well.
310-630	630-004	Gold blebs occur on grain boundaries between grunerite and quartz with one gold bleb on a quartz-quartz grain boundary.
310-634	634-001	This gold bleb occurs on hornblende-hornblende grain boundaries.

Sample number:	Gold occurrence number:	Description:
310-637	637-001	Gold occurs in a complex strain shadow of a garnet crystal. The gold itself appears between grunerite crystals in the grain boundary.
310-637	637-002	Gold blebs occur within a complex garnet strain shadow. Two gold blebs appear on grunerite-grunerite grain boundaries, with one inclusions of gold within a grunerite crystal.
310-637	637-003	Gold appears on the grain boundary of garnet. The boundaries vary between garnet-garnet and garnet-grunerite. One bleb of gold occurs as an inclusion in grunerite on what appears to be a plane defect.
310-637	637-004	Gold occurs in a strain shadow between two garnet crystals. This bleb of gold is an inclusion within the randomly orientated grunerite. The twinning of the grunerite which hosts the gold mineralization is curious and may be deformation twinning or a deformed growth twin, with the gold inclusion in this area.
310-637	637-005	This gold bleb occurs on the boundary between garnet and grunerite which defines a strain shadow.
310-637	637-006	Four blebs of gold appear on the boundary of grunerite inclusions within garnet. Three other gold blebs appear on the edge of the garnet crystal, with two of those adjacent to a fracture. All of these examples occur adjacent to a large garnet crystal which appears broken up on the side where these gold occurrences take place.
310-637	637-007	Irregular shape gold blebs occur within an arsenopyrite crystal. This arsenopyrite crystal is surrounded by pyrrhotite which appears on the edge of a large garnet crystal. The garnet appears ragged with many grunerite and pyrrhotite inclusions.
310-637	637-008	Gold appears within arsenopyrite which is surrounded by garnet. The arsenopyrite may be a large inclusion in one garnet crystal or it may separate two garnet crystals. Pyrrhotite rims the arsenopyrite crystal but does not completely surround it.
310-638	638-001	Gold occurs on the boundary between hornblende and quartz.
310-638	638-002	Gold blebs appear on the edge of a garnet crystal, on a garnet-grunerite boundary. This area is part of a strain shadow where garnet appears to have broken apart.

Sample number:	Gold occurrence number:	Description:
310-638	638-003	Two gold blebs occur on the edge of a garnet crystal on the boundary with grunerite. This area is part of the strain shadow of a large competent garnet crystal. Another gold bleb appears as an inclusion within the garnet crystal. The gold is neighboring grunerite also included in the garnet crystal.
310-638	638-004	This gold inclusion occurs within a ragged garnet crystal rich with inclusions. The gold bleb itself is in contact with pyrrhotite and grunerite which are also included in the garnet crystal.
310-642	642-002	Gold occurs included in a garnet crystal, pyrrhotite and magnetite are also observed as inclusions within this garnet crystal.
808-111	111-001	Gold blebs occur in quartz-rich band. Note that there is a stringer of hornblende and the quartz grain size is reduced neighboring this stringer, also the gold blebs are along strike of this stringer.
808-112	112-001	Gold occurs as an inclusion in biotite neighboring another small inclusion of quartz.
808-112	112-002	An inclusion of gold occurs within a ragged garnet crystal which also has inclusions of pyrrhotite.
808-113	113-001	This example is rich with gold blebs, some as inclusions in garnet with other small blebs associated with fractures in garnet. Gold also appears within grunerite and quartz which defines a strain shadow of the nearby gold-hosting garnet. Some of these gold blebs are completely included by grunerite while others are on grain boundaries.
909-002	002-001	Gold occurs in a fracture within a garnet crystal.
909-002	002-002	Gold occurs within a garnet crystal and is in contact with pyrrhotite. Fractures in the garnet crystal extend to the pyrrhotite neighboring the gold bleb.
909-002	002-003	Gold bleb occurs within garnet crystal and neighbors quartz inclusion, the gold itself borders both garnet and quartz.
909-003	003-001	A tiny trail of gold blebs occurs included within a quartz crystal, note fluid inclusions are also present in nearby quartz crystals.

Sample number:	Gold occurrence number:	Description:
909-007	007-002	Gold blebs are included within quartz, this quartz is part of a band which has foliated scattered biotite crystals throughout. Note the grain size of the quartz is smaller in this biotite-rich area then above where quartz occurs biotite-free.
909-007	007-003	Gold blebs occur in biotite within a strain shadow.
909-009	009-001	Irregular shape gold blebs occur within an arsenopyrite crystal. This arsenopyrite crystal is in an area of massive web-like pyrrhotite which surrounds grunerite crystals and includes some magnetite.
909-010	010-003	Gold blebs are included in a garnet crystal associated with a fracture
909-017	017-001	Tiny gold blebs appear on the boundary between a quartz-rich and grunerite-rich area. It is impossible to distinguish whether these blebs are included or on grain boundaries.

Appendix B: Lithology 2, Musselwhite Mine, grunerite schist

B.1: Sample locations (Lithology 2, Musselwhite Mine, grunerite schist)

Sample number	Hole number	from (m)	to (m)	x	y	z
210-201	03-RAN-024	136.7	136.8	9230.73	7602.58	5193.58
210-202	03-RAN-024	139.5	139.6	9228.63	7602.62	5191.38
210-203	03-RAN-024	134.1	134.25	9229.98	7602.59	5192.79
210-204	03-RAN-024	137.4	137.55	9232.09	7602.56	5195.01
210-205	03-RAN-023	173.4	173.58	9160.73	7649.45	5171.96
210-207	03-RAN-022	231.3	231.4	9580.59	7700	4500
210-209	03-RAN-022	45.7	45.8	9214.95	7699.75	5281.35
210-210	03-RAN-017	103.2	103.4	9128.26	8000.23	5208.44
210-211	03-RAN-017	104	104.15	9127.67	8000.23	5207.56
210-212	03-RAN-015	76	76.1	9120.33	8050.06	5232.93
210-214	03-RAN-015	78.8	78.9	9119.14	8050.07	5231.21
210-215	03-RAN-014	138	138.1	9126.54	8101.82	5190.88
210-216	03-RAN-014	162.5	162.6	9110.06	8102.2	5173.12
210-217	03-RAN-014	160.3	160.4	9110.54	8102.18	5174.69
210-218	03-RAN-014	161.3	161.5	9110.68	8100	5173.81
210-219	03-RAN-014	162	162.1	9110.06	8102.2	5173.12
210-220	03-RAN-014	162.35	162.5	9110.06	8102.2	5173.12
210-221	03-RAN-013	69.3	69.44	9137.33	8099.59	5234.94
210-222	03-RAN-013	69	69.12	9137.33	8099.59	5234.94
210-223	03-RAN-013	66.6	66.7	9138.37	8099.61	5236.9
210-224	03-RAN-012	8.9	8.9	9140.42	8100.47	5289.47
210-226	03-RAN-012	10.9	11.1	9139.4	8100.56	5287.56
210-227	03-RAN-011	113.1	113.3	9102.69	8152.95	5201.65
210-230	03-RAN-008	52.2	52.3	9125.82	8249.76	5252.26
210-232	03-RAN-008	118.3	118.4	9094.88	8249.56	5194.43
210-233	03-RAN-004	161.7	162	9096.14	8408.57	5158.3
210-234	03-RAN-001	79.31	79.5	9081.08	8451.78	5230.81
210-235	03-RAN-001	80.4	80.6	9081.08	8451.78	5230.81
210-236	03-RAN-001	80	80.15	9081.08	8451.78	5230.81
210-237	03-RAN-013	66.7	66.85	9138.27	8099.61	5236.71
210-238	03-RAN-015	51.8	51.9	9134.04	8050	5252.79
210-239	03-ran-005	21.6	21.8	9128.23	8350.17	5277.59
210-241	03-ran-008	88.4	88.5	9108.73	8249.65	5220.17
210-242	03-RAN-024	134.1	134.25	9229.98	7602.59	5192.79
210-301	03-RDW-003	205.3	205.4	9099.45	8697.01	5129.68
210-302	03-RDW-003	201.4	201.6	9101.13	8697.08	5133.35

Sample number	Hole number	from (m)	to (m)	x	y	z
210-303	03-RDW-003	204.6	204.7	9099.9	8697.03	5130.65
210-304	03-RDW-003	223.4	223.6	9091.68	8696.7	5112.9
210-305	03-RDW-023	298.3	298.4	9078.49	10326.09	4842.9
210-306	03-RDW-024	308.3	308.5	9126.88	10324.8	4979.44
210-307	03-RDW-024	308.9	309.5	9126.88	10324.8	4979.44
210-308	03-RDW-024	311.4	311.6	9128.7	10324.59	4979.42
210-309	03-RDW-026	283.2	283.28	9091.87	10437.8	4954.94
210-310	03-RDW-026	283	283.2	9091.87	10437.8	4954.94
210-312	03-RDW-029	305.9	306	9090.35	10530.78	4905.81
210-313	03-RDW-029	300.2	300.36	9084.65	10531.43	4906.92
210-314	03-RDW-031	297	297.1	9075.08	10630.37	4990.85
210-315	03-rdw-032	294	249.2	9059.92	10650	4959.07
210-316	03-rdw-032	296.5	296.65	9062.97	10634.09	4959.24
210-317	03-RDW-035	302.2	302.4	9079.04	10628.58	4910.24
210-318	03-rdw-028	289.2	289.3	9082.19	10549.7	4939.91
210-320	03-rdw-023	297	297.15	9076.88	10350	4843.74
210-321	03-rdw-023	273.1	273.2	9053.79	10329.23	4855.86
210-501	07-the-006	207.8	207.9	8874.47	11918.77	4650.87
210-502	07-the-006	206.6	206.68	8873.49	11925	4650.87
210-503	07-the-006	208.1	208.3	8875.47	11918.74	4651.12
210-504	07-the-006	221.4	221.6	8887.95	11918.39	4654.22
210-506	08-the-013	287.6	287.75	8905.87	12123.01	4694.39
210-507	08-the-014	276.95	277.1	8911.58	12114.49	4643.36
210-508	08-the-014	215.8	216	8853.25	12118.31	4627.96
210-509	08-the-014	277.3	277.5	8912.39	12114.43	4643.57
210-510	08-the-025	201.9	202	8894.81	12175	4641.82
210-511	08-the-025	135.55	135.75	8832.95	12172.97	4617.77
210-512	08-the-025	205.3	205.5	8898.07	12177.56	4643.04
210-513	08-the-028	181.6	181.7	8857.94	12175	4667.88
210-516	08-the-005	293.2	293.4	8913.78	12232.69	4625.72
210-517	08-the-005	295.1	295.18	8915.75	12232.69	4626.1
210-518	08-the-005	294.05	294.15	8814.71	12232.66	4625.9
210-519	08-the-005	204.7	204.8	8826.61	12230.34	4608.12
210-520	08-the-005	205.2	205.35	8827.25	12230.36	4608.26
210-521	08-the-004	293.2	293.4	8911.17	12241.36	4634.3
210-523	08-the-001	245.7	245.9	8852.99	12235.03	4661.12
210-525	08-the-001	244.9	245	8852.99	12235.03	4661.12
210-526	08-the-012	260.95	261	8891.06	12126.05	4656.16
210-531	08-the-018	244.65	244.7	8845.27	12269.16	4659.3
210-532	08-the-018	241.8	242	8843.04	12269.28	4658.31

Sample number	Hole number	from (m)	to (m)	x	y	z
210-533	08-the-020	290.5	290.55	8880.08	12275.7	4693.94
210-534	08-the-020	290.55	290.75	8880.08	12275.7	4693.94
210-536	08-the-023	307.8	307.97	8890.88	12330.55	4684.97
210-537	08-the-023	242.75	242.95	8831.83	12331.13	4657.94
210-539	08-the-023	243.3	243.45	8832.43	12331.13	4658.21
210-540	08-the-023	307.6	307.8	8890.88	12330.55	4684.97
210-542	08-the-018	246.7	246.8	8846.93	12269.08	4660.04
210-543	08-the-003	267.8	267.9	8882.33	12232.87	4643.25
210-544	08-the-003	271	271.15	8885.16	12232.95	4644.03
210-545	07-the-013	244.7	244.8	8869.04	12124.05	4671.88
210-546	08-the-021	260.9	261	8863.74	12341.82	4622.73

B.2: Sample descriptions (Lithology 2, Musselwhite Mine, grunerite schist)

Sample #	Sample description (HS: hand sample, TS: thin section)	Foliation/texture:	gold observed:
210-201	HS: This sample is dominated by quartz. Thin bands of grunerite define the foliation (about 1mm) with quartz-rich bands between. TS: Quartz-rich bands contain fine grain carbonate, magnetite and grunerite.	smooth, parallel, discrete	No
210-202	HS: This sample is dominated by quartz with thin magnetite and grunerite bands. Quartz in this sample is grey to white in color. Massive arsenopyrite and pyrrhotite at lower end of sample. TS: Boundinage structures occur in the quartz and have been overprinted by continued ductile deformation. Thin wavy discontinuous bands of magnetite and grunerite wrap around these quartz boudins.	rough to smooth, anastomosing, discrete	Yes
210-203	HS: This sample is dominated by massive poikiloblastic pyrrhotite. Where the sample is not dominated by pyrrhotite, it appears foliated made up of grunerite-rich, grunerite-magnetite-rich and quartz-rich. The foliation defined by grunerite ranges from parallel to anastomosing. Sometimes pyrrhotite and arsenopyrite are found along boundaries of grunerite wisps in the grunerite-rich portion of the sample. TS: Round pockets of quartz occur within the poikiloblastic pyrrhotite as well as individual grunerite, carbonate and quartz crystals. Arsenopyrite crystals also occur within the pyrrhotite dominated area.	smooth to wriggly, parallel to anastomosing, discrete	No
210-204	HS: This sample is dominated by quartz-rich bands with wisps of other minerals. Pyrrhotite fills in cracks in quartz bands. Smooth nearly parallel foliation is defined by grunerite-rich bands. TS: The wisps within the quartz-rich bands are defined by carbonate-grunerite, grunerite and pyrrhotite. The grunerite-rich bands can be nearly all grunerite or a combination of carbonate and grunerite.	smooth, nearly parallel, discrete	Yes
210-205	HS: This sample is made up of quartz-rich bands and grunerite-magnetite bands. The foliation in this sample is nearly parallel and smooth defined by thick bands of grunerite and magnetite. TS: Pyrrhotite is found as tiny wisps within the grunerite-magnetite bands. Although the bands appear to be grunerite-magnetite dominated carbonate-rich bands do occur.	smooth, parallel, discrete	Yes

Sample #	Sample description (HS: hand sample, TS: thin section)	Foliation/texture:	gold observed:
210-207	HS: This sample is made up of thin bands of light green grunerite alternating with bands of magnetite and quartz. Boundinage structures occur across these different bands. TS: The grunerite-rich bands in this sample range from all grunerite to grunerite-quartz rich and grunerite-carbonate rich. Pyrrhotite stringers have a poikiloblastic texture including grunerite, magnetite and quartz crystals.	smooth, parallel, discrete	Yes
210-209	HS: This sample is grunerite rich with thin bands of quartz and magnetite with boudinage structures crossing all bands. There is also a 2cm thick broken up carbonate vein which has been ductilely deformed. TS: Grunerite defines the foliation in this sample. Where the sample is quartz-rich fine-grained grunerite and carbonate can be seen among the quartz crystals.	smooth, parallel, discrete	No
210-210	HS: Light green grunerite bands define the foliation in this sample, but folding of these bands can also be seen. Grunerite surrounds quartz boudinage structures seeming to wrap around the boudins. Pyrrhotite fills in cracks within the quartz-rich areas. TS: Sample is made up of grunerite-magnetite-rich and quartz-rich bands. Quartz rarely occurs free of fine grained grunerite. Blebs and Poikiloblastic pyrrhotite appears as wisps and stringers within the grunerite-rich areas.	rough to smooth, parallel to anastomosing, discrete	No
210-211	HS: Bands of grunerite, magnetite and quartz are folded in this sample. Quartz bands are boudinaged with pyrrhotite filling in cracks. TS: Sample is made up of two types of bands; quartz-rich bands with fine grained grunerite, carbonate and pyrrhotite as well as grunerite-rich bands with carbonate, magnetite and pyrrhotite.	folded	Yes
210-212	HS: The foliation in this sample defined by thin bands of grunerite. Sample is almost half quartz and half grunerite. TS: The quartz-rich bands are full of inclusions along with very-fine-grained grunerite and carbonate. Grunerite-rich bands include carbonate as well as magnetite.	smooth, parallel, discrete	No

Sample #	Sample description (HS: hand sample, TS: thin section)	Foliation/texture:	gold observed:
210-214	HS: Magnetite–rich bands with thin bands of grunerite (less than 1mm) occur at the upper portion of the sample. Quartz makes up the rest of the sample. Cracks within the quartz-rich areas are filled with magnetite and grunerite. TS: Jagged fragments of pyrrhotite, magnetite, carbonate and grunerite and minor clinopyroxene occur within the quartz-rich area.	smooth, parallel, discrete	No
210-215	HS: Sample is made up of think bands (2cm). Magnetite, quartz and grunerite make up this sample. Quartz boudins appear overprinted by continued ductile deformation. TS: Sample is made up of quartz-rich and carbonate-grunerite bands. The quartz-rich area contains scattered carbonate and grunerite often as thin stringers. One of the grunerite-carbonate bands neighboring poikiloblastic pyrrhotite.	fairly smooth, nearly parallel, discrete	No
210-216	HS: Sample is made up of grunerite-rich bands with minor magnetite and quartz rich bands. Pyrrhotite fills in cracks as well as appears as wisps and/or stringers orientation parallel to foliation. TS: The thin section is carbonate-rich, dominated by carbonate with grunerite. Some twinned plagioclase and round shaped quartz clusters occurs surrounded by poikiloblastic pyrrhotite.	rough to smooth, anastomosing, discrete	Yes
210-217	HS: Grunerite defines the foliation and can be seen lining magnetite bands. Quartz bands are boudinaged and appear ductilely overprinted. Pyrrhotite occurs as wisps and filling cracks in quartz. TS: This thin section is separated into complex groups not bands. Clusters of quartz grains are observed as well as plagioclase. Grunerite is found throughout the thin section. Pyrrhotite appears as veins but poikiloblastic stringers occur with carbonate and grunerite crystals within the pyrrhotite.	rough to smooth, anastomosing, discrete	No
210-218	HS: This sample is banded with half magnetite-rich and grunerite-rich bands. Minor folding and boudinage structures. TS: The thin sectioned area is dominated by foliated grunerite with discontinuous quartz-rich, magnetite-rich and carbonate-rich areas scatted through the grunerite dominated area.	smooth, parallel, discrete	No

Sample #	Sample description (HS: hand sample, TS: thin section)	Foliation/texture:	gold observed:
210-219	HS: Bands of magnetite are rimmed by grunerite are folded with quartz bands mixed in with boundinage structures. Pyrrhotite fills in cracks in the quartz. Pyrrhotite also occurs with the magnetite massive to web-like. TS: Sample is made up of two parts: quartz-rich band with fragments of grunerite, carbonate and pyrrhotite, the other is dominated by grunerite with carbonate, magnetite and pyrrhotite.	folded	No
210-220	HS: Quartz dominates this sample. Discontinuous light green to yellow grunerite bands appear throughout the sample (they appear almost wispy in hand sample). Pyrrhotite fills cracks within the quartz-rich areas. TS: The grunerite-rich bands are made up of grunerite and carbonate. Pyrrhotite occurs as veins and stringers which often occur along the boundaries between different minerals.	n/a	No
210-221	HS: Grunerite occurs as thin discontinuous bands which define the rough foliation. Pyrrhotite stringers occur parallel to the foliation. Quartz makes up the rest of the sample. TS: In thin section some of the grunerite-rich bands were found to be mainly clinopyroxene and carbonate-rich with some grunerite and blue-green amphibole. Note that clinopyroxene appears very ragged and altered. The quartz-rich areas contain very fine grained carbonate and other minerals.	rough to wriggly, anastomosing, discrete	Yes
210-222	HS: This sample is dominated by light green grunerite and light grey quartz. Grunerite occurs as thin discontinuous bands which define the foliation. TS: Quartz demonstrates boudinage structures which the grunerite-rich bands wrap around. In this thin section the grunerite-rich bands surrounding the quartz boudins where defined by carbonate, clinopyroxene, blue-green amphibole and grunerite. Pyrrhotite occurs as poikiloblastic stringers which include quartz, carbonate and grunerite grains.	rough, anastomosing, discrete	Yes
210-223	HS: Quartz in this sample is light grey and makes up most of the sample. Yellow-green grunerite-rich bands are thin and discontinuous. Some of these bands have a darker green color and often pyrrhotite stringers occur parallel to the foliation. TS: The grunerite-rich bands are mainly composed of grunerite and carbonate but they also include chlorite and some blue-green amphibole.	rough, anastomosing, discrete	Yes

Sample #	Sample description (HS: hand sample, TS: thin section)	Foliation/texture:	gold observed:
210-224	HS: Quartz bands in this sample are very discontinuous; it appears that earlier boudinage structures were later ductilely deformed. Grunerite-rich bands define the foliation. TS: The thin section is dominated by a quartz-rich band which includes very fine grained grunerite and carbonate. Pyrrhotite appears vein-like and as stringers. Grunerite and carbonate occur along pyrrhotite-quartz boundaries.	wriggly, anastomosing, discrete	No
210-226	HS: Bands are thin and discontinuous; they are made up mainly of grunerite, quartz and magnetite. A pyrrhotite-rich portion occurs in this sample. TS: Stringers of pyrrhotite run through this sample which includes subhedral arsenopyrite crystals. The pyrrhotite is poikiloblastic with clusters which are feldspar-rich and quartz-rich surrounded by pyrrhotite.	smooth, parallel to anastomosing, discrete	Yes
210-228	HS: This sample is almost completely made up of quartz. Fractures in quartz are filled with pyrrhotite. There thin discontinuous bands of grunerite with magnetite (2mm). TS: The thin section is quartz-rich with stringers of pyrrhotite.	rough to smooth, parallel to anastomosing, discrete	Yes
210-230	HS: Sample is made up of thick (1 cm) quartz bands with thin discontinuous grunerite bands. Quartz bands are often boudinaged. Magnetite occurs within the grunerite bands in the upper portion of the sample. TS: Tiny blebs of magnetite are scattered throughout the quartz-rich areas which also contain fine grained grunerite and carbonate. Pyrrhotite fills in cracks in the quartz bands.	smooth, parallel to anastomosing, discrete	No
210-232	HS: Well foliated grunerite occurs in the upper portion of the sample. The sample is dominated by quartz with fractures filled by pyrrhotite. Thin light green grunerite-rich discontinuous bands occur. TS: The grunerite-rich portion is more carbonate-rich with stringer and blebs of pyrrhotite and arsenopyrite.	smooth, parallel, discrete	No
210-233	HS: Quartz bands are pinched off with many boundins. Pyrrhotite occurs as wisps and veins filling the boundin structures. Boundin structures appear ductilely deformed, often with grunerite-rich bands wrapping around them. TS: This sample is made up of two parts: quartz-rich (which contains some carbonate) and carbonate-grunerite-rich. In thin section there is one main vein of pyrrhotite and small stringers of pyrrhotite within the carbonate-grunerite-rich areas.	smooth, anastomosing to parallel, discrete	No

Sample #	Sample description (HS: hand sample, TS: thin section)	Foliation/texture:	gold observed:
210-234	HS: Grunerite-rich bands define the foliation in this sample. The upper portion of the sample has thin grunerite- magnetite rich bands with pyrrhotite wisps. A large quartz-rich area makes up the bulk of the sample with minor wisps of grunerite, pyrrhotite and arsenopyrite crystals within in it. The lower portion is grunerite-rich with pyrrhotite and arsenopyrite in veins and stringers near the contact with the quartz-rich area. TS: In thin section grunerite and carbonate surround arsenopyrite crystals.	smooth to rough, anastomosing, discrete	Yes
210-235	HS: This sample is made up of grunerite-rich, quartz-rich and pyrrhotite-rich areas. The grunerite-rich bands define the foliation. These grunerite bands are thin and discontinuous in the more quartz-rich portions of the sample. Pyrrhotite is wispy to massive and sometimes poikiloblastic. TS: Pyrrhotite appears as wisps or stringers scattered through the grunerite as well as massive and poikiloblastic where is surrounds large rounded clusters of quartz crystals up to 2mm across.	smooth, anastomosing, discrete	No
210-236	HS: This sample is dominated by quartz, with pyrrhotite veins. Thin discontinuous grunerite-rich bands define the foliation in this sample. TS: Quartz-rich areas include irregular shaped blebs of pyrrhotite which appear to be ductilely deformed. Magnetite and carbonate sometimes occur within the grunerite-rich bands.	smooth to wriggly, anastomosing, discrete	No
210-237	HS: Bands in this sample are commonly discontinuous. Quartz-rich boundins and veins occur. The texture is indicative of ductile deformation. TS: Quartz-rich areas are separate from the grunerite-carbonate-rich areas. The areas rich with grunerite and carbonate also include clinopyroxene and blue-green amphibole.	rough, anastomosing, discrete	No
210-238	HS: Grunerite-rich bands define the foliation. These bands are often thin and discontinuous. This sample is pyrrhotite-rich, the pyrrhotite occurs most often as stringers which are orientated parallel to the foliation. TS: The grunerite-rich areas are also carbonate-rich. Large clinopyroxene crystals are cracked and altered with carbonate surrounding them in the grunerite-carbonate-rich bands. Pyrrhotite often appears between grunerite-carbonate-rich and quartz-rich areas but also appears as large poikiloblastic stringers in the more carbonate-rich sections.	rough, anastomosing, discrete	Yes

Sample #	Sample description (HS: hand sample, TS: thin section)	Foliation/texture:	gold observed:
210-239	HS: Sample is made up of quartz-rich bands and grunerite-rich bands. Grunerite-rich bands are smooth or continuous. TS: Quartz-rich bands often have boundinage structures filled with pyrrhotite. Also fine grained carbonate and pyrrhotite crystals commonly occur on quartz grain boundaries in the quartz-rich areas in this sample. Carbonate-rich area separates this thin section in half, this area is dominated by carbonate but chlorite over prints in a radiating "flower-like" texture, among the carbonate crystals foliated grunerite can be seen in patches.	smooth, nearly parallel, discrete	Yes
210-241	HS: This sample is made up of quartz-rich and grunerite-rich areas. It is pyrrhotite-rich. Foliation is defined by thin, discontinuous grunerite-rich bands. TS: This thin section is dominated by carbonate-grunerite-rich areas. The pyrrhotite most often occurs within the carbonate-grunerite-rich portions or along the boundary with quartz-rich areas.	rough, anastomosing, discrete	Yes
210-242	HS: This sample is dominated by massive poikiloblastic pyrrhotite. Where the sample is not dominated by pyrrhotite, it appears foliated made up of grunerite-rich, grunerite-magnetite-rich and quartz-rich. Sometimes pyrrhotite and arsenopyrite are found along boundaries of grunerite wisps in the grunerite-rich portion of the sample TS: In thin section thin, discontinuous grunerite-rich bands define a foliation.	smooth, parallel to anastomosing, discrete	Yes
210-301	HS: This sample is made up of green grunerite-rich and thick quartz-rich bands. Pyrrhotite can be seen as wisps within the grunerite-rich bands. TS: This sample is dominated by grunerite-carbonate-rich areas which include clinopyroxene, grunerite and blue-green amphibole. Blue-green amphiboles occur as elongate clusters commonly near clinopyroxene crystals. Clusters of quartz and feldspar can be found scattered through the carbonate-rich area. Pyrrhotite occurs as stringers in the carbonate-rich areas.	rough to smooth, anastomosing, discrete	No
210-302	HS: Quartz in this sample is dark grey quartz. The sample has a wriggly or wavy appearing foliation. The quartz and grunerite-rich bands are thin and discontinuous. TS: The thin section is dominated by carbonate and grunerite, with small discontinuous quartz bands scattered throughout. Pyrrhotite is associated mainly with carbonate-grunerite areas and bounds areas between quartz-rich and the carbonate-grunerite-rich areas. Pyrrhotite and arsenopyrite crystals occur in this sample.	wriggly, anastomosing, discrete	Yes

Sample #	Sample description (HS: hand sample, TS: thin section)	Foliation/texture:	gold observed:
210-303	HS: Sample is made up of quartz and wispy grunerite. Pyrrhotite also appears wispy along boundaries between grunerite and quartz. Foliation is rough and anastomosing. TS: Quartz-rich bands or areas make up much of this thin section. Grunerite -rich bands make up the rest with minor carbonate and magnetite associated.	rough, anastomosing, discrete	No
210-304	HS: Foliation is defined by thin, discontinuous grunerite-rich bands. Pyrrhotite is wispy, tiny arsenopyrite crystals can be see within the grunerite-rich areas. TS: Small quartz-rich discontinuous bands occur although this thin section is dominated by carbonate, grunerite and clinopyroxene. Most quartz-rich areas include fine grained carbonate and grunerite crystals scattered throughout, especially triple-junction grain boundaries.	smooth to wriggly, anastomosing, discrete	Yes
210-305	HS: This sample is quartz-rich with thin discontinuous bands of grunerite defining the rough foliation. Pyrrhotite appears as wisps orientated with the foliation. Sometimes pyrrhotite also occurs as blebs and small veins. TS: This thin section is mainly carbonate. A plagioclase dominated section occurs where large crystals are bounded by pyrrhotite. The pyrrhotite has a poikiloblastic texture here but the plagioclase crystals are much larger then typically observed with pyrrhotite of this texture at Musselwhite. The pyrrhotite separates the plagioclase from the carbonate-rich area. Note also that grunerite crystals appear between the pyrrhotite-plagioclase area and the carbonate-rich area.	rough, anastomosing, discrete	Yes
210-306	HS: This sample is quartz-rich discontinuous grunerite bands defining the rough foliation. Pyrrhotite occurs as wisps and blebs throughout this sample. A carbonate vein occurs at the upper portion of this sample. TS: Poikiloblastic stringers of pyrrhotite occur in the carbonate-grunerite-rich portions of the sample. In these portions clinopyroxene and blue-green amphibole also occur.	rough, anastomosing, discrete	No
210-307	HS: This sample is quartz-rich with thin, discontinuous light green grunerite bands defining the rough foliation. Pyrrhotite is wispy and occurs orientated with the foliation. TS: Radial chlorite appears overgrown on some of the grunerite-carbonate-rich bands, especially the larger ones which also contain pyrrhotite.	rough, anastomosing, discrete	Yes

Sample #	Sample description (HS: hand sample, TS: thin section)	Foliation/texture:	gold observed:
210-308	HS: Quartz makes up most of this sample with thin, discontinuous grunerite-rich bands defining a rough but parallel foliation. Pyrrhotite appears as wisps and has similar orientation to the grunerite. There are small minor carbonate vein with a similar orientation. TS: In the thin section the grunerite-rich bands also include clinopyroxene, carbonate and blue-green amphibole. Also fine grained carbonate, grunerite and pyrrhotite crystals occur in quartz-rich areas. Where the quartz is accompanied by carbonate, grunerite and pyrrhotite it is finer grained.	rough, parallel, discrete	No
210-309	HS: Thin, discontinuous grunerite bands define the wriggly anastomosing foliation. Pyrrhotite occurs as wisps and stringers. It is found along boundaries between grunerite-rich and quartz-rich bands. TS: This sample is dominated by quartz with fine grained grunerite is often among the quartz crystals. There are very few areas where quartz is alone and inclusion free. Minor magnetite appears in the grunerite-rich bands.	wriggly, anastomosing, discrete	No
210-310	HS: Quartz bands appear boudinaged and overprinted by continued ductile deformation. Grunerite-rich bands define the foliation. TS: The majority of quartz in this sample is fine grained with very fine grained carbonate and grunerite crystals scattered throughout. The rest of the thin section is grunerite-carbonate-rich with lesser amounts of clinopyroxene and blue-green amphibole. Poikiloblastic pyrrhotite contains quartz crystals, and occurs within the grunerite-rich areas.	wriggly, anastomosing, discrete	No
210-312	HS: This sample is grunerite-rich. The foliation is continuous where thick grunerite bands dominate. Pyrrhotite appears as wisps and small veins oriented with the foliation. TS: Quartz-rich area has thin bands of discontinuous grunerite. On the edge of the thin section massive chlorite appears with broken flattened or elongate garnet.	smooth, parallel to anastomosing, discrete	No
210-313	HS: Foliation in this sample is fairly parallel with minor folding in one area where pyrrhotite wisps can be seen. Pyrrhotite is also in blebs and as veins near boudin structures. This sample is magnetite-rich with much more magnetite then quartz. TS: Much of the quartz in this sample is mixed with fine very fine grained grunerite and magnetite inclusions. Poikiloblastic pyrrhotite runs through the center of the thin sections. Inclusions of grunerite, carbonate and quartz occur within this pyrrhotite.	smooth, parallel, discrete	Yes

Sample #	Sample description (HS: hand sample, TS: thin section)	Foliation/texture:	gold observed:
210-314	HS: Foliation is defined by thin discontinuous grunerite-rich bands with pyrrhotite along boundaries and as blebs scattered throughout. White to grey quartz bands separate the grunerite-rich bands. TS: Quartz-rich areas in this sample are full of inclusions with fine grained grunerite, magnetite and carbonate crystals scattered throughout. Grunerite-rich bands are well foliated and some contain carbonate.	rough, anastomosing, discrete	No
210-315	HS: Foliation is defined by fairly continuous bands of grunerite. Quartz bands are also fairly continuous with a few boundinage structures. Pyrrhotite veins run parallel to the quartz and grunerite bands. TS: Quartz-rich bands in this sample contain inclusion and fine grained crystals of grunerite, magnetite and carbonate. Where there are large stringers of pyrrhotite it is poikiloblastic.	smooth, parallel, discrete	No
210-316	HS: Pyrrhotite-rich sample with dark black bands and quartz-rich bands making up the rest of the sample. Chunks of carbonate veins can also be seen in this sample. TS: Massive poikiloblastic pyrrhotite makes up most of this sample with inclusions which are made of many grains, and could possibly be chucks of rock. The dark black bands are made up of foliated grunerite and biotite with magnetite and quartz.	N/A	No
210-317	HS: Grey-white quartz makes up the majority of the sample. Thin discontinuous grunerite-rich bands define the foliation. Minor pyrrhotite cross cuts the foliation. A carbonate vein cuts through the center of the sample but it is boudinaged and therefore not continuous. TS: Quartz-rich areas have many tiny inclusions of carbonate, grunerite and magnetite.	rough, parallel, discrete	No
210-318	HS: Sample is made up of grunerite-rich bands and quartz-rich bands. Boundinage structures appear in the quartz bands. Pyrrhotite occurs as wisps and as veins filling boundinage structures. TS: Quartz in this sample contains many inclusions of carbonate, grunerite, and magnetite. Grunerite-carbonate-rich bands are thin and discontinuous.	smooth, nearly parallel, discrete	No
210-320	HS: Thin, discontinuous grunerite-rich bands define the foliation. Pyrrhotite stingers and wisps are also orientated with the foliation. Quartz bands are also discontinuous and irregularly shaped. TS: Pyrrhotite is poikiloblastic with carbonate crystals included. In thin section only minor grunerite and arsenopyrite occur.	rough, parallel to anastomosing, discrete	Yes

Sample #	Sample description (HS: hand sample, TS: thin section)	Foliation/texture:	gold observed:
210-321	HS: This sample appears to be banded with quartz-rich, grunerite-rich and magnetite-rich bands. Grunerite-rich bands are thin and discontinuous. These bands define the rough foliation. Pyrrhotite stringers are orientated with the anastomosing foliation. TS: The quartz-rich band appears boudinaged with a pyrrhotite and arsenopyrite vein cross cutting the thin section. Note that the quartz in this thin section has fluid inclusions.	rough, anastomosing, discrete	No
210-501	HS: This sample is quartz-rich with blebs and stringers of pyrrhotite. Grunerite makes up thin, discontinuous bands which define the rough anastomosing foliation. TS: This thin section is made up mainly of quartz with a large pyrrhotite vein. The pyrrhotite is poikiloblastic with inclusions of grunerite and carbonate. The quartz-rich area hosts inclusions (especially of carbonate) but this becomes more prevalent near the pyrrhotite vein.	rough, anastomosing, discrete	No
210-502	HS: This sample is banded made up of magnetite-rich and quartz-rich bands. With minor grunerite occurring between these bands. TS: Magnetite bands in this sample are rimmed by grunerite separating them from quartz-rich bands. All quartz-rich bands include fine grained magnetite and grunerite crystals.	smooth, parallel, discrete	No
210-503	HS: Quartz makes up wide (1-7cm) bands with grunerite-rich bands between. The grunerite-rich bands define the foliation. Wispy to stringer-like pyrrhotite can be seen in grunerite-rich bands. Pyrrhotite also occurs as veins cross cutting the quartz bands. TS: This sample is mainly quartz with thin discontinuous grunerite-rich bands and veins of pyrrhotite. The quartz contains tiny inclusions.	smooth, parallel, discrete	No
210-504	HS: This sample is pyrrhotite-rich, matrix is dark grey. Pyrrhotite is massive and poikiloblastic. TS: This sample differs because it contains biotite. In thin section dark bands appear as mylonitic bands of feldspar, biotite and quartz. Pyrrhotite also occurs as stringers which also have a poikiloblastic texture surrounding quartz, feldspar and some biotite.	N/A	No

Sample #	Sample description (HS: hand sample, TS: thin section)	Foliation/texture:	gold observed:
210-506	HS: The majority of this sample is made up of poikiloblastic pyrrhotite surrounding blebs of light green and beige. The upper portion of the sample is well foliated thin (1 mm) bands of magnetite, grunerite and quartz. Boundinage structures cross cut all of these bands. The contact between the pyrrhotite portion and the foliated bands is very sharp but is not a straight surface, it is irregular and wavy. TS: About half the thin section is taken up by massive poikiloblastic pyrrhotite which surrounds clusters and individual crystals of carbonate, grunerite and quartz. The rest of the thin section is made up of very fine grained grunerite, carbonate with lesser magnetite.	smooth, nearly parallel, discrete	Yes
210-507	HS: Poikiloblastic pyrrhotite appears massive in upper portion of this sample. But pyrrhotite appears as stringers and wisps in grunerite-rich and quartz-rich portions of the sample. TS: Poikiloblastic pyrrhotite includes carbonate, but the majority of the thin section is made up of clinopyroxene with carbonate and pyrrhotite between these crystals.	smooth, parallel, discrete	Yes
210-508	HS: This sample is quartz-rich with thin, discontinuous light green grunerite bands defining the foliation. Most of the pyrrhotite occurs within quartz. The pyrrhotite is wispy, orientated cross cutting the foliation. The discontinuous quartz-rich bands are likely boundinage structures which have undergone continued ductile deformation. TS: This thin section consists of quartz-rich areas and clinopyroxene-rich areas. The clinopyroxene is associated with carbonate, grunerite and blue-green amphibole.	rough, anastomosing, discrete	No
210-509	HS: Green bands define the foliation. Quartz bands are very discontinuous and irregular in this sample. Pyrrhotite occurs as blebs and wisps within the quartz-rich areas. Poikiloblastic pyrrhotite is seen within some of the green bands. TS: The green bands are clinopyroxene-rich. Clinopyroxene occurs in half of the thin section with carbonate occurring with cracks and filling the space between grains. The quartz-rich areas also include fine grained carbonate.	smooth, parallel, discrete	No

Sample #	Sample description (HS: hand sample, TS: thin section)	Foliation/texture:	gold observed:
210-510	HS: Sample is mostly quartz with thin grunerite-rich bands and pyrrhotite stringers. Foliation is defined by the grunerite-rich bands. TS: This sample is banded with various types of bands. Quartz-only quartz-rich bands occur as well as quartz-rich bands with fine-grained grunerite. A chlorite dominated band occurs adjacent to green-amphibole band. Clinopyroxene-rich bands also occur with carbonate, green amphibole and grunerite associated.	smooth, nearly parallel, discrete	No
210-511	HS: Sample is made up of quartz-rich and grunerite-rich discontinuous bands. Pyrrhotite appears wispy in grunerite-rich band and occurs as veins in quartz-rich bands. TS: Quartz makes up most of this thin section with an area rich with grunerite and carbonate which includes minor clinopyroxene crystals. Pyrrhotite appears as odd shaped blebs and veins.	rough to smooth, anastomosing, discrete	No
210-512	HS: This sample is dominated by glassy quartz with very wispy, thin, discontinuous bands of grunerite defining the foliation. Pyrrhotite is found within the grunerite-rich bands. TS: Thin bands of grunerite, carbonate and pyrrhotite occur through the quartz-rich thin section. One large band is made up of clinopyroxene surrounded by grunerite, carbonate and blue-green amphibole.	rough, anastomosing, discrete	No
210-513	HS: The grunerite-rich bands which define the foliation in this sample are thin and discontinuous. The bulk of the sample is made up of quartz. Pyrrhotite appears as wisps wit arsenopyrite as subhedral blebs. TS: Sulfides in this sample occurs neighboring clinopyroxene-green amphibole-carbonate-grunerite-rich areas more commonly then within quartz-rich areas.	rough, anastomosing, discrete	Yes
210-516	HS: This sample is mostly quartz with thin, discontinuous grunerite-rich bands. These bands contain small pyrrhotite and magnetite crystals. TS: This sample is dominated by quartz with clustered of small carbonate and amphibole crystals.	n/a	No
210-517	HS: This sample is made up of grunerite-rich and quartz-rich bands. Quartz-rich areas commonly contain black specks. The grunerite-rich bands define the rough foliation. TS: The quartz-rich areas in this thin section are pure quartz as well as quartz with fine grained grunerite. Grunerite-rich areas also contain carbonate and altered clinopyroxene.	rough, anastomosing, discrete	No

Sample #	Sample description (HS: hand sample, TS: thin section)	Foliation/texture:	gold observed:
210-518	HS: This sample is almost entirely made up of quartz with tiny, thin discontinuous bands of grunerite and carbonate and blebs of magnetite. Pyrrhotite appears as odd shaped blebs within the quartz. TS: This thin section is made up of large quartz crystals and large carbonate crystals in quartz-rich and carbonate-rich areas. A vein of pyrrhotite occurs in the quartz-rich area.	smooth, fairly parallel, discrete	No
210-519	HS: Grunerite-rich bands make up the majority of this sample and define the foliation. Tiny specks of magnetite can be seen within the grunerite-rich areas. The bands in this sample are very discontinuous, likely from boudinage and continuous ductile deformation. Pyrrhotite occurs as wisps and in cross cutting veins. TS: This thin section is dominated by clinopyroxene with carbonate, pyrrhotite, and amphiboles filling space between. There are a few quartz-rich discontinuous bands (likely small boundins).	wriggly, anastomosing, discrete	Yes
210-520	HS: Dark green and grunerite-rich bands define the foliation in this sample. There is a large boudinage structure which cross cuts many of the thin (1mm) bands which alternate between dark green, quartz-rich and pyrrhotite-rich bands. TS: In the center of this thin section runs a band of massive magnetite adjacent to pyrrhotite. This magnetite and pyrrhotite cuts the sample in half. On either side of this grunerite can be seen orientated in the same way as this magnetite-pyrrhotite band. Past that moving out from the center perpendicularly orientated bands of amphibole which seem to vary from green-amphibole to grunerite with minor carbonate exist.	smooth, parallel, discrete	No
210-521	HS: This sample is dominated by quartz. Thin, wispy, discontinuous bands of grunerite define an anastomosing, rough foliation. Pyrrhotite appears much like the grunerite. Quartz is rich with tiny inclusions of magnetite and grunerite. TS: Quartz makes up most of this thin section but radial "flower-like" texture chlorite also occurs.	rough, parallel, discrete	No
210-523	HS: This sample is pyrrhotite-rich. Poikiloblastic stringers of pyrrhotite are orientated with the foliation and host inclusions of carbonate. TS: This sample is dominated by carbonate with minor grunerite, green amphibole and clinopyroxene. Pyrrhotite also is found in the carbonate-rich area. A quartz vein splits the thin section, note that the clinopyroxene only occurs adjacent to this vein.	smooth, nearly parallel, discrete	Yes

Sample #	Sample description (HS: hand sample, TS: thin section)	Foliation/texture:	gold observed:
210-525	HS: This sample is made up of thin (1 mm) bands of grunerite and quartz with minor magnetite bands. Grunerite-rich bands define the foliation. TS: This sample is dominated by fine-grained quartz with foliated thin discontinuous bands of grunerite and magnetite. Thin bands of grunerite also occur.	smooth, parallel, discrete	No
210-526	HS: Thin discontinuous grunerite-rich bands are wriggly to rough and define the foliation. Pyrrhotite appears as stringers orientated with the foliation. Quartz makes up the rest of the sample. Pyrrhotite also occurs as veins which cross cut the quartz-rich bands. Boudinage structures occur in many of the quart-rich bands. TS: Clinopyroxene occurs in clusters with blue-green amphibole, carbonate and some grunerite.	rough to wriggly, anastomosing, discrete	No
210-531	HS: Thin quartz-rich, magnetite-rich and pyrrhotite-rich bands make up the upper portion of sample. Massive poikiloblastic pyrrhotite makes of the rest of the sample. TS: This thin section is made up of carbonate with stringers of pyrrhotite orientated the same direction as these bands. The poikiloblastic pyrrhotite dominated area hosts inclusions of carbonate and larger oval shaped clusters of carbonate and green-amphibole.	smooth, parallel, discrete	No
210-532	HS: Grunerite-rich bands define the foliation in this sample. Most of the sample is made up of quartz. Pyrrhotite is wispy and commonly occurs on boundaries between quartz and grunerite. Pyrrhotite also appears as wisps within the quartz-rich bands. TS: Clinopyroxene, blue-green amphibole, carbonate and grunerite-rich areas occur.	smooth, parallel to anastomosing, discrete	No
210-533	HS: Foliated grunerite-rich bands make up the upper portion of this sample. Pyrrhotite stringers and wisps occur within this portion orientated with the foliation. The lower portion is dominated by massive poikiloblastic pyrrhotite with blebs of carbonate. TS: The massive poikiloblastic pyrrhotite contains clusters of carbonate and grunerite. The rest of the sample is a mix of grunerite, carbonate and quartz with lesser pyrrhotite.	fairly smooth, nearly parallel, discrete	No

Sample #	Sample description (HS: hand sample, TS: thin section)	Foliation/texture:	gold observed:
210-534	HS: Thin (1mm) discontinuous light green grunerite-rich bands define foliation of this sample with thin magnetite-rich and quartz-rich bands between. The quartz-rich bands are sometimes think (1 cm) and include ductile boudinage structures.. TS: Poikiloblastic pyrrhotite occurs in the thin section and includes carbonate and grunerite. Also in thin section a chaotic area of carbonate, green-amphibole, grunerite and clinopyroxene occurs. A band of quartz cross cuts a pyrrhotite vein in the center of the thin sections. This band is cut off by a microcline-rich area which hosts gold. The rest of the thin section is made up of quartz with short thin, discontinuous bands of grunerite and carbonate. Fine grain arsenopyrite crystals are disseminated through sample.	wriggly, anastomosing, discrete	Yes
210-536	HS: This sample is made up of green amphibole-rich, grey quartz-rich and carbonate-rich bands. The amphibole-rich bands define the foliation. Wisps and thin discontinuous bands of grunerite occur in the dark grey quartz. The sample is overall dark grey in color. TS: Most of this sample is very fine grained with the exception of large carbonate and grunerite crystals which make grunerite-carbonate-rich bands. Green amphibole makes up much of the thin section. Blebs of magnetite are scattered throughout with minor pyrrhotite as well.	smooth, parallel to anastomosing, discrete	No
210-537	HS: This sample is made up of grunerite-magnetite-rich bands and quartz-rich bands. The grunerite-rich bands define the foliation. Pyrrhotite appears along boundaries of bands and in veins which cross cut the foliation. TS: The bands in this thin section anastomose through each other in a tangled mess. Quartz-rich bands and bands of carbonate, grunerite, clinopyroxene with stringer-like magnetite occur. A pyrrhotite vein cuts through the center of this thin section.	wriggly, nearly parallel, discrete	No
210-539	HS: Magnetite-rich and quartz-rich bands dominate this sample. The bands are nearly parallel and smooth except where they have been boudinaged and/or folded. Pyrrhotite appears as odd shaped blebs. TS: Quartz bands are fine-grained with very-fine grain grunerite and magnetite crystals. These are often adjacent to thin grunerite bands which bound magnetite bands. Some of these magnetite bands are adjacent to pyrrhotite bands and both have a poikiloblastic texture including grunerite and carbonate crystals.	smooth, nearly parallel, discrete	No

Sample #	Sample description (HS: hand sample, TS: thin section)	Foliation/texture:	gold observed:
210-540	HS: This sample is made up of quartz-rich, carbonate-rich, magnetite-rich and grunerite-rich bands. Poikiloblastic pyrrhotite occurs in the carbonate and grunerite bands. Pyrrhotite occurs as veins filling fractures in the quartz-rich areas. TS: This thin section is dominated by carbonate and pyrrhotite. Poikiloblastic pyrrhotite surrounds individual grains as well as clusters of crystals.	fairly smooth, anastomosing, discrete	Yes
210-542	HS: Sample is made up of quartz-rich and grunerite-rich areas. Pyrrhotite appears as stringers and wisps. TS: This thin section is quartz-rich and clinopyroxene-rich. Carbonate, minor grunerite and green-amphibole occur with the clinopyroxene. Pyrrhotite appears commonly within pyroxene-rich areas and on the boundary of quartz-rich and pyroxene-rich areas.	rough to smooth, parallel to anastomosing, discrete	Yes
210-543	HS: Quartz bands in this sample are very discontinuous and irregular. Pyrrhotite veins occur in some of the boundinage structures in these quartz bands. The rest of the sample is made up of thin discontinuous light green grunerite-rich bands with wisps of pyrrhotite. TS: Minor carbonate and green amphibole occur within the grunerite-rich portion of the thin section.	rough to smooth, anastomosing, discrete	No
210-544	HS: This sample is banded with quartz-rich and iron-rich bands. The quartz-rich bands show boundinage texture, the pinched off areas are commonly filled in with pyrrhotite. Poikiloblastic pyrrhotite also appears with inclusions of quartz and grunerite. Iron-rich bands are light green in color, grunerite in these bands defines the foliation. The bands are wavy and often slightly displaced where the quartz bands are pinched. TS: The iron-rich bands include grunerite, clinopyroxene, carbonate and green amphibole.	smooth, nearly parallel, discrete	No
210-545	HS: Sample is made up of quartz-rich and grunerite-rich discontinuous bands. Pyrrhotite appears as stringers and wisps. Boundinage structures appear in the quartz-rich areas. TS: The thin section is quartz-rich and clinopyroxene-rich. Carbonate is associated with the clinopyroxene. Pyrrhotite appears mainly within clinopyroxene-rich areas or on the boundary of quartz-rich and pyroxene-rich areas.	smooth to rough, parallel to anastomosing, discrete	No
210-546	HS: Sample is quartz-rich with bands and boundinage structures. Pyrrhotite fills in the boundinage structures and appears as stingers and wisps orientated with the foliation. The foliation is defined by grunerite. TS: A pyrrhotite vein cross cuts the quartz-rich portion of this thin section. The majority of the sample is then dominated by clinopyroxene, grunerite and carbonate. Pyrrhotite also occurs associated with the pyroxene-grunerite-carbonate areas.	fairly smooth, anastomosing, discrete	No

B.3: Modal percent based on petrography (Lithology 2, Musselwhite Mine, grunerite schist)

Sample number	quartz	magnetite	grunerite	carbonate	blue-green amphibole	clinopyroxene	pyrrhotite	arsenopyrite	Other:
210-201	45		45	10			minor		
210-202	30	5	23	7			20	15	
210-203	15	5	5	5			70		
210-204	95	minor					5	minor	
210-205	20	20	35	20			5		
210-207	15	10	35	10			30		
210-209	10	20	67	3			minor		
210-210	25	20	35	minor			20		
210-211	40	10	35	5			10		
210-212	40	15	40	5			trace		
210-214	80	5	5	5		minor	5		
210-215	70		10	10			10		
210-216	5	5	20	55	minor		15		
210-217	5	20	40	10	minor		25		
210-218	10	10	75	5			trace		
210-219	10	10	60	10	minor		10		
210-220	55	5	20	10			10	minor	
210-221	46		4	20	5	15	10	minor	
210-222	30		15	20	10	15	10		
210-223	70		10	8	2		5		chlorite: 5
210-224	75	minor	10	5			10		
210-226	40	minor	15	15			15	10	feldspar 5
210-228	82	minor		3			15		
210-230	65	10	15	5			5		
210-232	38		15	25			20	2	
210-233	40	trace	20	25			15		
210-234	75		10	5				10	
210-235	10		40	10			30	10	
210-236	85		5	5			5		

Sample number	quartz	magnetite	grunerite	carbonate	blue-green amphibole	clinopyroxene	pyrrhotite	arsenopyrite	Other:
210-237	30		10	15	10	10	10		chlorite: 15
210-238	25		20	15	3	15	22		
210-239	70		5	10			5		chlorite: 10
210-241	20		30	40			10		
210-242	45	10	20	2			15	8	
210-301	10		20	30	10	15	10		feldspar:5
210-302	25		30	30	2	3	5	5	
210-303	57		35	5			3		
210-304	10		30	28	5	20	5	2	
210-305	5		10	65	5		10		plagioclase:5
210-306	40		minor	20	10	15	15	minor	
210-307	83		5	5	2		5		
210-308	72		5	10		10	3		
210-309	50	minor	30	15			5		
210-310	46		20	20	minor	4	10		
210-312	37		18	5	3	2	5		chlorite: 20, garnet:10
210-313	50	5	25	10			10	minor	
210-314	48	2	37	10			3		
210-315	30	5	40	10			10		chlorite: 5
210-316	25	5	20				50	minor	biotite: minor
210-317	73	2	15	5		minor	2		chlorite:3
210-318	50	trace	30	15			5	trace	
210-320			5	45	minor		47	3	
210-321	45	20	20	trace			10	5	
210-501	70		5	5			20		
210-502	34	33	33						
210-503	95		5	minor			minor		
210-504	30						30		biotite:35, feldspar: 5
210-506	10	15	15	15			45	minor	
210-507			10	10	5	55	20		
210-508	45		10	5	10	20	10		
210-509	60			10		10	20		

Sample number	quartz	magnetite	grunerite	carbonate	blue-green amphibole	clinopyroxene	pyrrhotite	arsenopyrite	Other:
210-510	40		10	10	15	10	5		chlorite:10
210-511	80		5	5		minor	10		
210-512	45		5	5	5	30	10		
210-513	50			5	5	25	5	10	
210-516	85		5	5			5		
210-517	20	2	50	20		5	3		
210-518	60			35			5		
210-519	5		5	5	3	72	10		
210-520		15	10	5	50		20		
210-521	60		10				5		chlorite: 25
210-523	15		5	60	5	5	10		
210-525	52	10	30	5			3		
210-526	50		minor	minor	10	30	10		
210-531				60	5		35		
210-532	40		5	5	15	15	20		
210-533	5	minor	20	20		minor	55	minor	
210-534	30	minor	15	15	5	5	25		microcline:5
210-536	25	15	15	15	30	minor	minor		
210-537	40	5	30	10		5	10		
210-539	30	20	25	10			15	minor	
210-540	5	minor		75		minor	20	minor	galena: minor
210-542	30		minor	10	minor	50	10		
210-543	40	minor	40	5	minor		15	minor	
210-544	30	5	26	10	4	20	5		
210-545	45			5	minor	35	15		
210-546	45		15	15		15	10		

*minor indicate less than 5%

*trace indicates less than 1%

B.4: Bands and textures (Lithology 2, Musselwhite Mine, grunerite schist)

Sample Number	grunerite-rich bands	grunerite with minor carbonate or magnetite	carbonate-grunerite bands	carbonate-grunerite-pyroxene-green amphibole	carbonate		massive poikiloblastic pyrrhotite	poikiloblastic stringer pyrrhotite	pyrrhotite blebs	vein-like sulfides	magnetite-rich		quartz only bands	quartz with carbonate-magnetite-grunerite
210-201	X													X
210-202			X					X		X				
210-203							X						X	
210-204	X		X						X					X
210-205	X	X	X											X
210-207	X		X					X						X
210-209	X	X									X			X
210-210		X						X			X		X	X
210-211			X					X		X				X
210-212		X	X								X			X
210-214				X				X						X
210-215			X					X						X
210-216			X					X		X			X	
210-217	X		X					X					X	
210-218	X	X									X			X
210-219		X						X						X
210-220			X					X		X			X	
210-221				X										X
210-222				X				X					X	X
210-223			X					X					X	X
210-224			X							X				X
210-226			X					X						X
210-228										X			X	
210-230	X										X			X
210-232			X					X	X	X			X	
210-233			X					X		X				X
210-234			X											X
210-235	X		X				X	X						X

Sample Number	grunerite-rich bands	grunerite with minor carbonate or magnetite	carbonate-grunerite bands	carbonate-grunerite-pyroxene-green amphibole	carbonate		massive poikiloblastic pyrrhotite	poikiloblastic stringer pyrrhotite	pyrrhotite blebs	vein-like sulfides	magnetite-rich		quartz only bands	quartz with carbonate-magnetite-grunerite
210-236			X							X				X
210-237				X				X						X
210-238				X				X					X	
210-239			X		X					X			X	X
210-241			X					X					X	
210-242	X	X			X			X						X
210-301				X				X					X	
210-302			X					X					X	X
210-303		X								X			X	X
210-304				X				X						X
210-305	X				X			X						
210-306				X	X			X					X	X
210-307			X					X					X	X
210-308				X	X			X					X	X
210-309		X						X						X
210-310				X				X						X
210-312	X							X						X
210-313		X	X				X	X						X
210-314	X		X					X						X
210-315	X	X	X				X	X		X				X
210-316		X					X							
210-317			X					X						X
210-318			X					X		X				X
210-320					X		X							
210-321		X								X			X	
210-501										X			X	X
210-502	X	X									X			X
210-503	X									X			X	X
210-504								X						X
210-506		X					X				X			
210-507				X			X	X						

Sample Number	grunerite-rich bands	grunerite with minor carbonate or magnetite	carbonate-grunerite bands	carbonate-grunerite-pyroxene-green amphibole	carbonate		massive poikiloblastic pyrrhotite	poikiloblastic stringer pyrrhotite	pyrrhotite blebs	vein-like sulfides	magnetite-rich		quartz only bands	quartz with carbonate-magnetite-grunerite
210-508				X				X	X					X
210-509				X						X				X
210-510				X				X					X	X
210-511				X					X	X			X	X
210-512				X				X	X					X
210-513				X				X		X			X	X
210-516			X					X						X
210-517				X					X				X	X
210-518					X					X			X	
210-519				X				X					X	
210-520	X	X					X			X	X			
210-521														X
210-523				X	X		X	X					X	
210-525		X												X
210-526				X				X	X				X	X
210-531					X		X	X						
210-532				X				X		X				X
210-533	X		X		X		X	X	X					
210-534				X			X	X		X			X	X
210-536				X					X		X			X
210-537				X				X		X				X
210-539		X						X			X			X
210-540					X		X						X	
210-542				X				X					X	X
210-543	X									X				X
210-544				X				X					X	
210-545				X				X		X			X	X
210-546				X				X		X			X	X

B.5: Gold occurrences (Lithology 2, Musselwhite Mine, grunerite schist)

Sample number:	Gold occurrence number:	Description:
210-202	202-001	Gold appears in a fracture in arsenopyrite. Surrounding the arsenopyrite is some pyrrhotite within a quartz-rich area.
210-202	202-002	Inclusion of gold within arsenopyrite crystal. The arsenopyrite is included as part of web-like stringer of pyrrhotite.
210-202	202-004	Gold occurs in a fracture in arsenopyrite included in a web-like stringer of pyrrhotite.
210-205	205-004	Gold inclusion within feldspar neighboring blebs of pyrrhotite. The gold appears near the plane of a twin in this plagioclase crystal.
210-205	205-005	Gold is included within a plagioclase crystal. Note that this crystal is surrounded by web-like pyrrhotite.
210-207	207-004	Scattered blebs of gold within fine grained grunerite and carbonate. Some gold blebs occur on grain boundaries while others appear as inclusions.
210-207	207-005	One gold inclusion appears within magnetite. With scattered tiny blebs included in grunerite and on boundaries between grunerite and carbonate.
210-216	216-003	Gold bleb appears on the boundary between magnetite, pyrrhotite and quartz.
210-221	221-002	Gold inclusion within carbonate which occurs included in a clinopyroxene crystal.
210-221	221-003	Gold occurs within carbonate.
210-222	222-005	Gold appears along the edge of grunerite crystal bordering the quartz. This area is quartz-rich with scattered amphibole crystals.
210-223	223-005	Gold bleb occurs on quartz grain boundary, in a quartz-rich band.
210-226	226-001	Irregular shaped inclusions of gold within arsenopyrite. Surrounding the arsenopyrite is ragged looking pyrrhotite (somewhere between blebs and stringers).
210-226	226-002	Rectangular shaped inclusions of gold within arsenopyrite. Arsenopyrite is surrounded by pyrrhotite. The pyrrhotite has a stringer-like appearance.
210-226	226-003	Rounded gold inclusions within arsenopyrite crystal, surrounded by stringer-like pyrrhotite.
210-228	228-001	Gold inclusion within quartz, in quartz-rich area.

Sample number:	Gold occurrence number:	Description:
210-228	228-002	Gold blebs occur on the boundary between quartz and carbonate. The carbonate appears around magnetite and pyrrhotite blebs/stringers in otherwise quartz-rich area.
210-228	228-003	Gold blebs occur on grain boundaries between quartz crystals as well as on boundaries between quartz and magnetite. With one bleb occurring on boundary between quartz and pyrrhotite.
210-229	229-001	Irregularly shaped gold inclusions within arsenopyrite. Some of these inclusions appear associated with fractures while others do not. Arsenopyrite crystal is surrounded by pyrrhotite.
210-229	229-002	Gold inclusions filling fractures in arsenopyrite, which is surrounded by pyrrhotite.
210-229	229-003	Gold inclusions within elongate arsenopyrite crystal surrounded by pyrrhotite and carbonate.
210-229	229-004	Angular gold inclusions within arsenopyrite crystal as well as gold filling fracture in arsenopyrite. Pyrrhotite surrounds most of the arsenopyrite crystal.
210-231	231-001	Gold appears as an inclusion within arsenopyrite.
210-234	234-001	Somewhat angular gold inclusion within arsenopyrite crystal.
210-234	234-002	Angular gold inclusion within arsenopyrite crystal with nearby gold filling fractures in arsenopyrite. Arsenopyrite crystal appears with grunerite in a quartz-rich area.
210-234	234-003	Gold blebs border the edge of carbonate inclusions and the host arsenopyrite crystal. Pyrrhotite borders part of the arsenopyrite crystal.
210-234	234-004	Long angular gold inclusions appear within an arsenopyrite crystal lined with pyrrhotite within grunerite-rich area.
210-238	238-005	Gold blebs appears within clinopyroxene crystal, some seem to fall on fractures while others appear as inclusions.
210-238	238-006	Gold bleb appears on the boundary between clinopyroxene and grunerite.
210-238	238-007	Gold bleb occurs on fracture within clinopyroxene.
210-238	238-008	Gold blebs occur in fractures in clinopyroxene and as inclusions in clinopyroxene.
210-238	238-009	Gold blebs occur within carbonate which is surrounded completely by web-like pyrrhotite.
210-238	238-010	Inclusion of gold within clinopyroxene.
210-238	238-011	Gold bleb occurs in a fracture in clinopyroxene.

Sample number:	Gold occurrence number:	Description:
210-239	239-004	Gold bleb occurs on the grain boundary between quartz crystals, in a quartz-rich area.
210-239	239-005	Gold bleb occurs on the grain boundary between carbonate grains in a carbonate-grunerite-rich area.
210-239	239-006	Gold bleb appears on the boundary between quartz crystals in a quartz-rich area.
210-241	241-001	Gold bleb appears on the boundary between quartz crystals in a quartz-rich area.
210-242	242-001	Angular inclusion of gold within arsenopyrite crystal surrounded by blebs/stringers of pyrrhotite.
210-242	242-002	Gold bleb within fractured arsenopyrite crystal which neighbors both magnetite and pyrrhotite.
210-242	242-003	Gold occurs in fractures in arsenopyrite with nearby stinger of pyrrhotite.
210-242	242-004	Gold inclusion within arsenopyrite.
210-242	242-005	Angular gold inclusion appears within arsenopyrite which neighbors stringer and blebs of magnetite and pyrrhotite.
210-242	242-007	Gold occurs in fractures in arsenopyrite with nearby blebs of pyrrhotite and magnetite.
210-242	242-008	Gold occurs in fractures in arsenopyrite with nearby blebs of pyrrhotite and magnetite.
210-242	242-009	Gold appears in a fracture in arsenopyrite. Surrounding the arsenopyrite is some pyrrhotite and magnetite.
210-242	242-010	Angular gold inclusion appears within arsenopyrite which neighbors stringer and blebs of magnetite and pyrrhotite.
210-302	302-001	Gold appears on grain boundary between quartz grains in quartz-rich area.
210-302	302-002	Gold inclusion within arsenopyrite.
210-302	302-003	Gold inclusions within arsenopyrite crystal neighboring pyrrhotite which creates large sulfide-rich area.
210-302	302-004	Irregular shaped inclusions of gold within arsenopyrite neighboring pyrrhotite.
210-304	304-003	Gold inclusions within arsenopyrite.
210-305	305-001	Gold inclusion within plagioclase.
210-305	305-002	Gold bleb occurs on the subgrain boundary of a feldspar crystal.
210-305	305-003	Gold bleb on a fracture in feldspar crystal.
210-305	305-004	Gold bleb neighboring pyrrhotite included in feldspar crystal.

Sample number:	Gold occurrence number:	Description:
210-307	307-005	Gold blebs appear on grain boundaries of carbonate as well as between carbonate and quartz. One small bleb occurs as an inclusion in carbonate.
210-313	313-003	Gold inclusion within quartz, in quartz-rich area.
210-313	313-005	Gold bleb appears on the boundary between pyrrhotite and quartz grains. Note chalcopyrite appears within the pyrrhotite in this example.
210-313	313-006	Gold blebs occur within pyrrhotite. Note that grunerite appears to cross cut the pyrrhotite.
210-313	313-007	Gold blebs appear neighboring a magnetite crystal. One gold bleb is included within amphibole.
210-313	313-008	A gold bleb occurs neighboring magnetite within grunerite.
210-313	313-009	Gold blebs appear along a fracture in arsenopyrite.
210-320	320-001	Irregular angular shaped inclusion of gold appears within arsenopyrite.
210-331	331-007	Irregular shaped gold appears on fracture within arsenopyrite.
210-506	506-001	Irregular shaped gold inclusion in arsenopyrite. Note the fracture which appears on either side of the gold bleb.
210-507	507-001	Gold appears on the boundary between carbonate and grunerite and as an inclusion within grunerite.
210-507	507-002	Gold blebs appear on the boundary between magnetite and carbonate and/or quartz.
210-509	509-004	Gold appears as rounded and angular inclusions within clinopyroxene. The elongate gold blebs are likely fracture filling.
210-513	513-001	Irregular shaped gold inclusions within arsenopyrite.
210-513	513-002	Irregular shaped gold blebs occur within arsenopyrite crystal, some of which appear on fractures.
210-513	513-003	Gold appears as an inclusion within clinopyroxene.
210-513	515-004	Gold blebs appear within clinopyroxene.
210-513	515-005	Gold occurs on the grain boundaries
210-519	519-001	Gold blebs occur in clinopyroxene.
210-519	519-002	Gold appears neighboring pyrrhotite, as inclusions within clinopyroxene.
210-519	519-003	Gold inclusion occurs in carbonate which occurs within clinopyroxene. The gold bleb neighbors pyrrhotite which is also included within the carbonate.

Sample number:	Gold occurrence number:	Description:
210-523	523-001	Gold bleb appears surrounded mainly by pyrrhotite with part neighboring carbonate.
210-523	523-002	Gold appears on the boundary of carbonate crystals.
210-523	523-003	Gold blebs appear on grain boundaries and twin boundaries in grunerite, with one bleb in contact with pyrrhotite.
210-523	523-004	Gold blebs occur included within carbonate.
210-532	532-001	Gold inclusion within clinopyroxene.
210-532	532-002	Gold blebs included within clinopyroxene as well as within inclusions of carbonate in the same clinopyroxene crystal.
210-532	532-003	Gold blebs within carbonate which occurs between pyrrhotite and quartz-rich area.
210-532	532-004	. Inclusion of gold within clinopyroxene.
210-532	532-005	. Gold inclusions within clinopyroxene, note fractures near these gold blebs.
210-533	533-001	Angular gold inclusions within arsenopyrite.
210-533	532-002	Gold blebs appear on subgrain of feldspar and as inclusions.
210-533	533-003	Gold appears within a fracture of arsenopyrite.
210-533	533-004	Gold bleb within arsenopyrite. Note the fracture which radiates away from the gold bleb at the top. This arsenopyrite appears surrounded by pyrrhotite.
210-533	533-005	Gold blebs within arsenopyrite which appears surrounded by pyrrhotite
210-534	534-001	Gold blebs occur within feldspar, some appear on subgrain boundaries and others appear near altered area in feldspar. Two blebs of gold occur neighboring pyrrhotite also included in the feldspar.
210-534	534-002	Gold blebs appear on and neighboring subgrain boundaries in feldspar.
210-534	534-003	Gold bleb appears on subgrain boundary in feldspar.
210-534	534-004	Gold blebs appear as inclusions within feldspar.
210-534	534-005	Gold blebs appear as inclusions within feldspar.
210-534	534-006	Gold inclusion within quartz grain, in a quartz-rich area.
210-534	534-007	Gold bleb appears on the twin boundary (compositional plane) in amphibole. Another bleb appears within neighboring amphibole with one edge of the gold bleb neighboring quartz.

Sample number:	Gold occurrence number:	Description:
210-540	540-003	Irregular shaped gold inclusions within arsenopyrite which appears in web-like stringer of pyrrhotite. This arsenopyrite and pyrrhotite is surrounded by carbonate.
210-540	540-005	Gold bleb appears on the grain boundary between carbonate crystals.
210-540	540-006	Gold blebs appear within carbonate with magnetite nearby. Note this area in the carbonate appears altered in some way.
210-540	540-007	Gold blebs appear in quartz which is full of inclusion mainly of pyrrhotite blebs.
210-542	542-011	Gold inclusion appears within clinopyroxene.
210-542	542-012	Gold inclusion appears within clinopyroxene.
210-542	542-013	Thin elongate gold inclusion within clinopyroxene, likely filled a now healed fracture.
210-542	542-014	Gold inclusion appears within clinopyroxene.
210-542	542-015	Gold inclusion appears within clinopyroxene.

Appendix C: Scanning Electron Microscope results

C.1 Confirmation of visual gold identification

Samples used for confirmation of visual gold identification

Sample Number	Gold occurrence	Spectrum Number	Description:
909-002	002-001	01-10-001	Gold within fracture in garnet
808-011	011-001	01-10-002	Gold inclusion in quartz
210-509	509-004	06-10-003	Gold in fractures of clinopyroxene
210-509	509-004	06-10-004	Gold inclusion in clinopyroxene
749-402	402-002	06-10-005	Gold inclusion in pyrite
749-414	414-007	06-10-006	Gold in fracture in pyrite

Spectra: 01-10-001

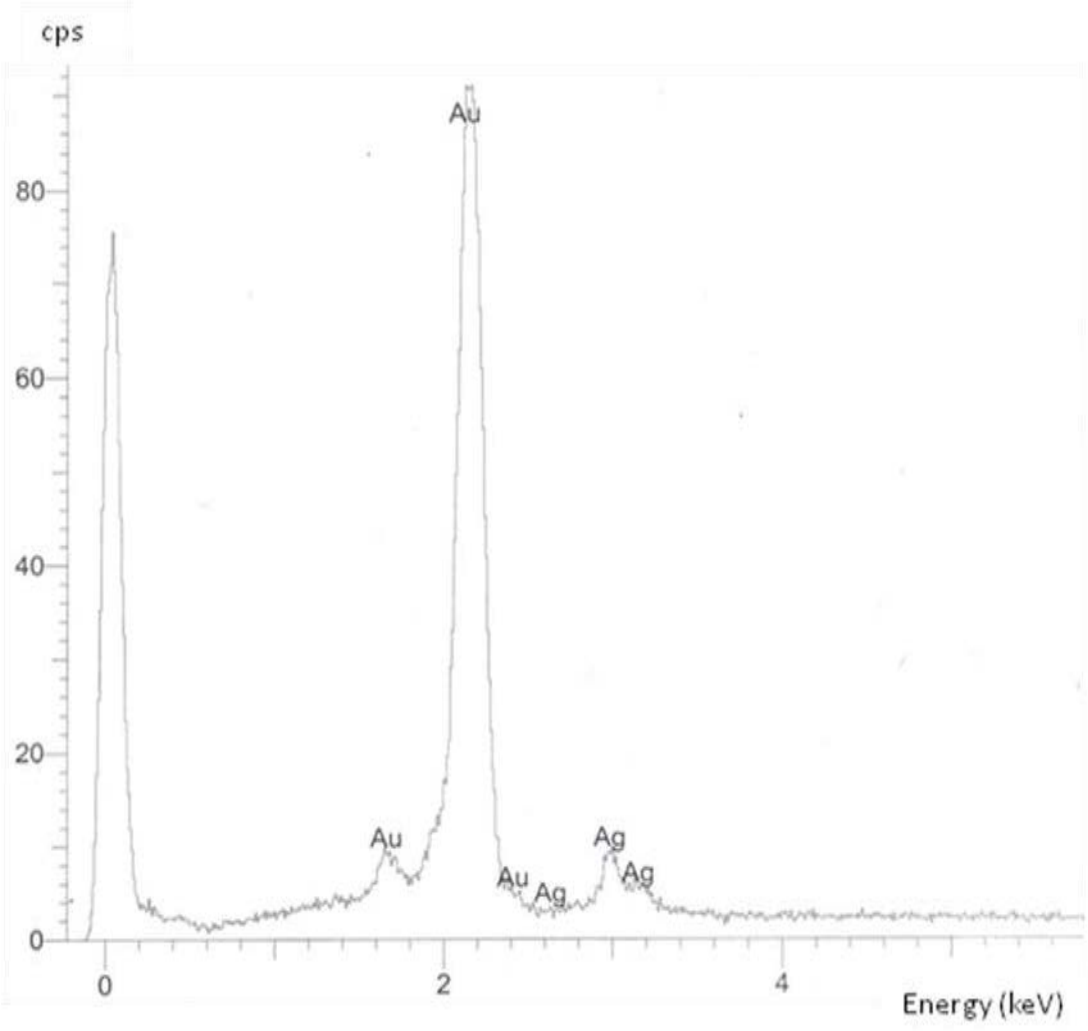

Spectra: 01-10-002

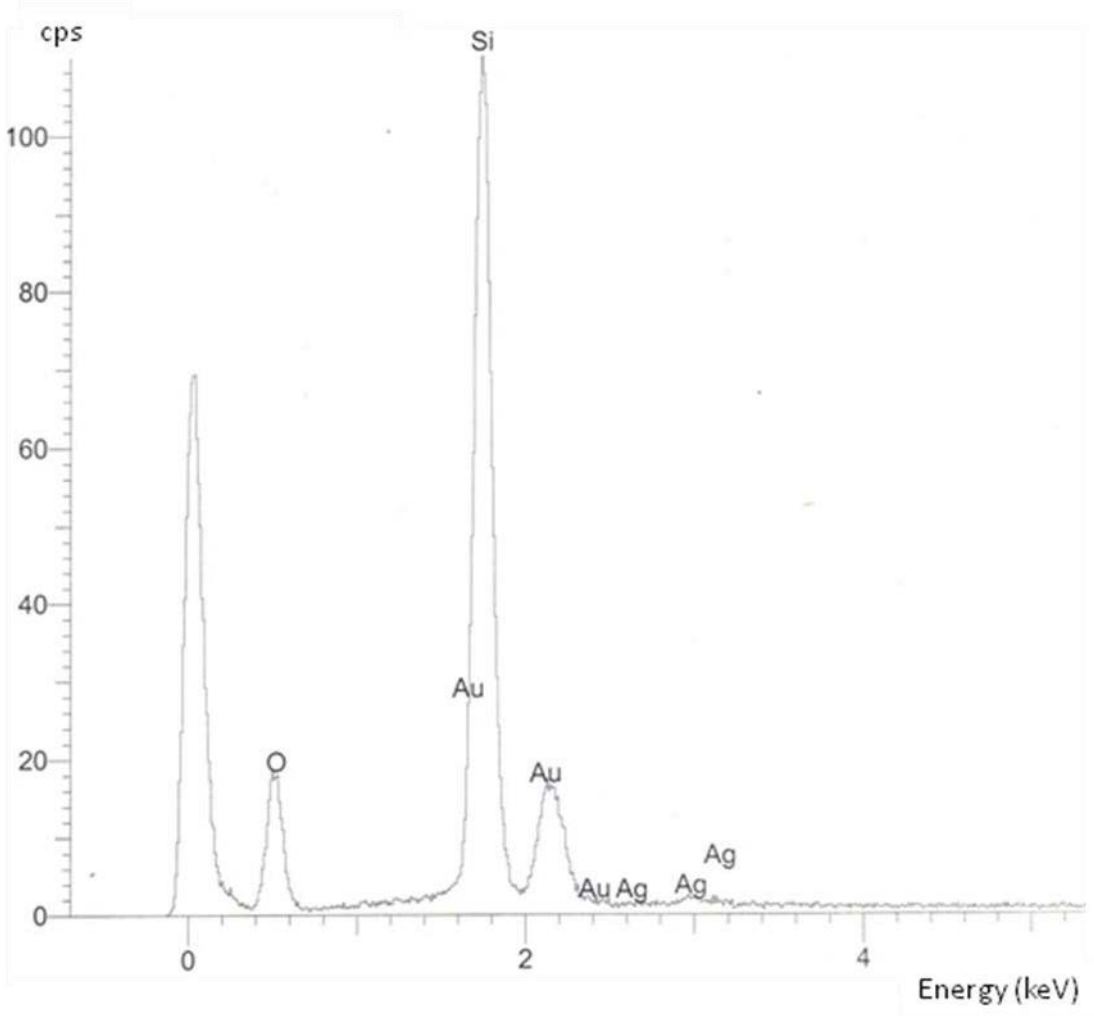

Spectra: 06-10-003

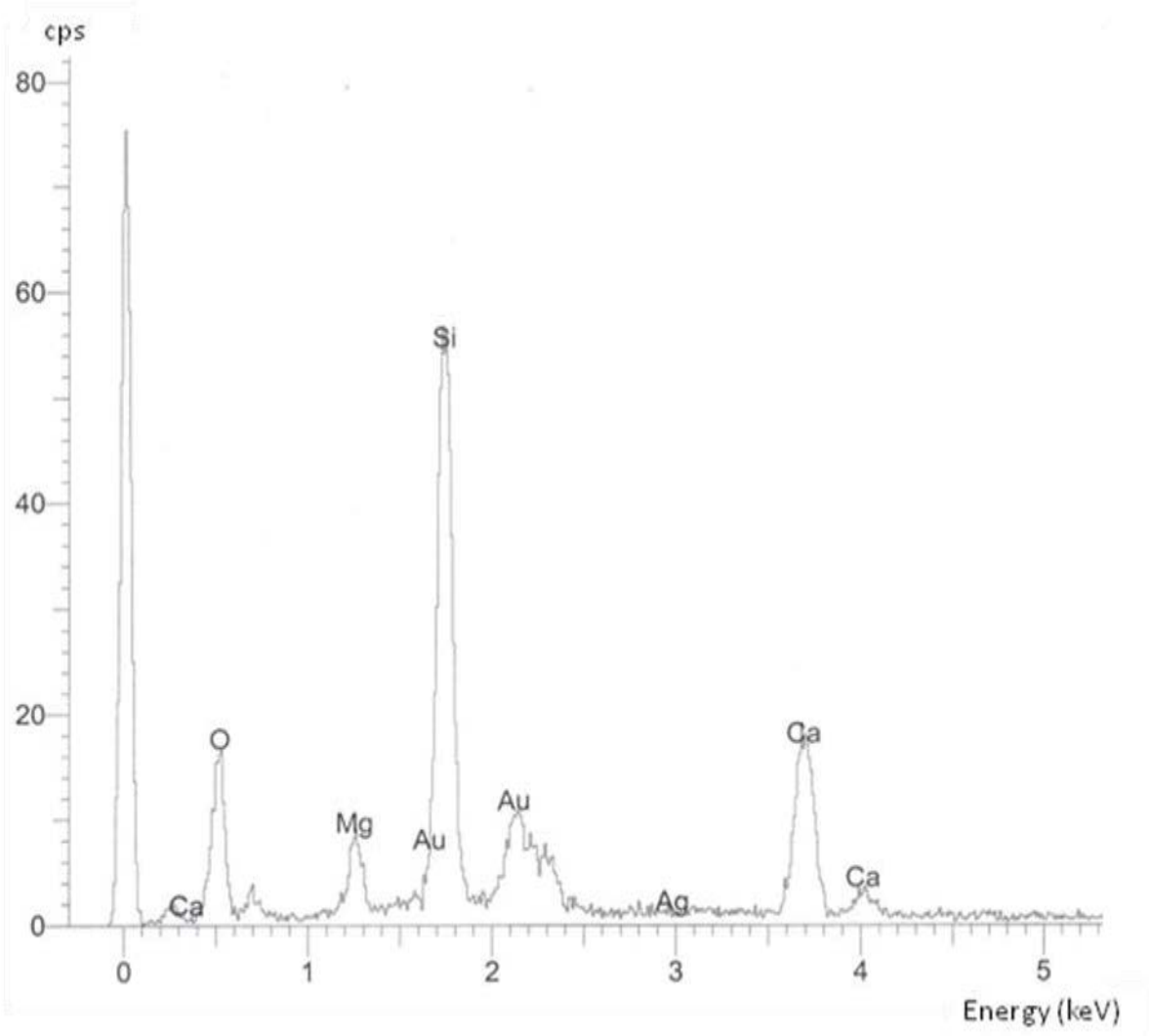

Spectra: 06-10-004

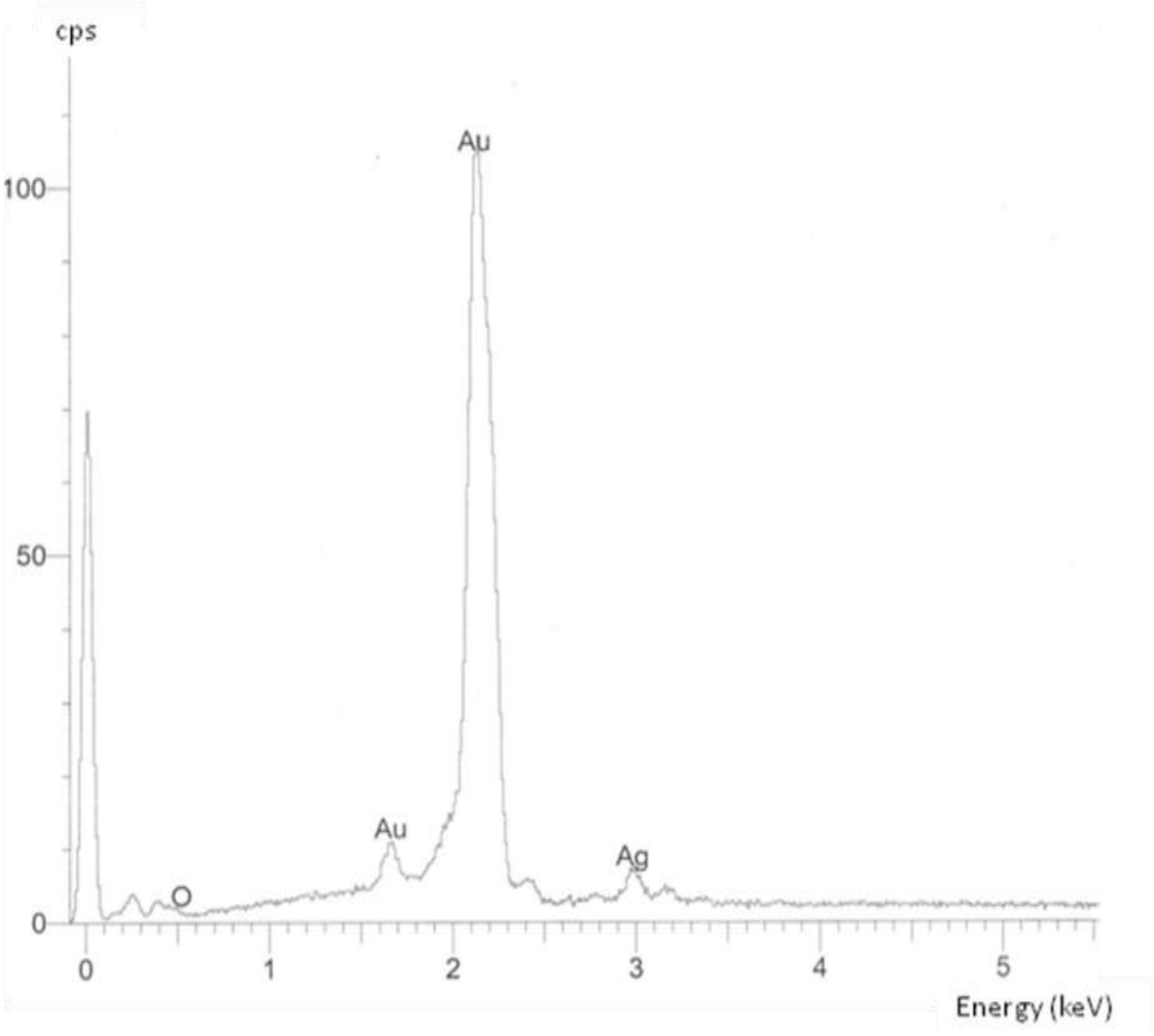

Spectra: 06-10-005

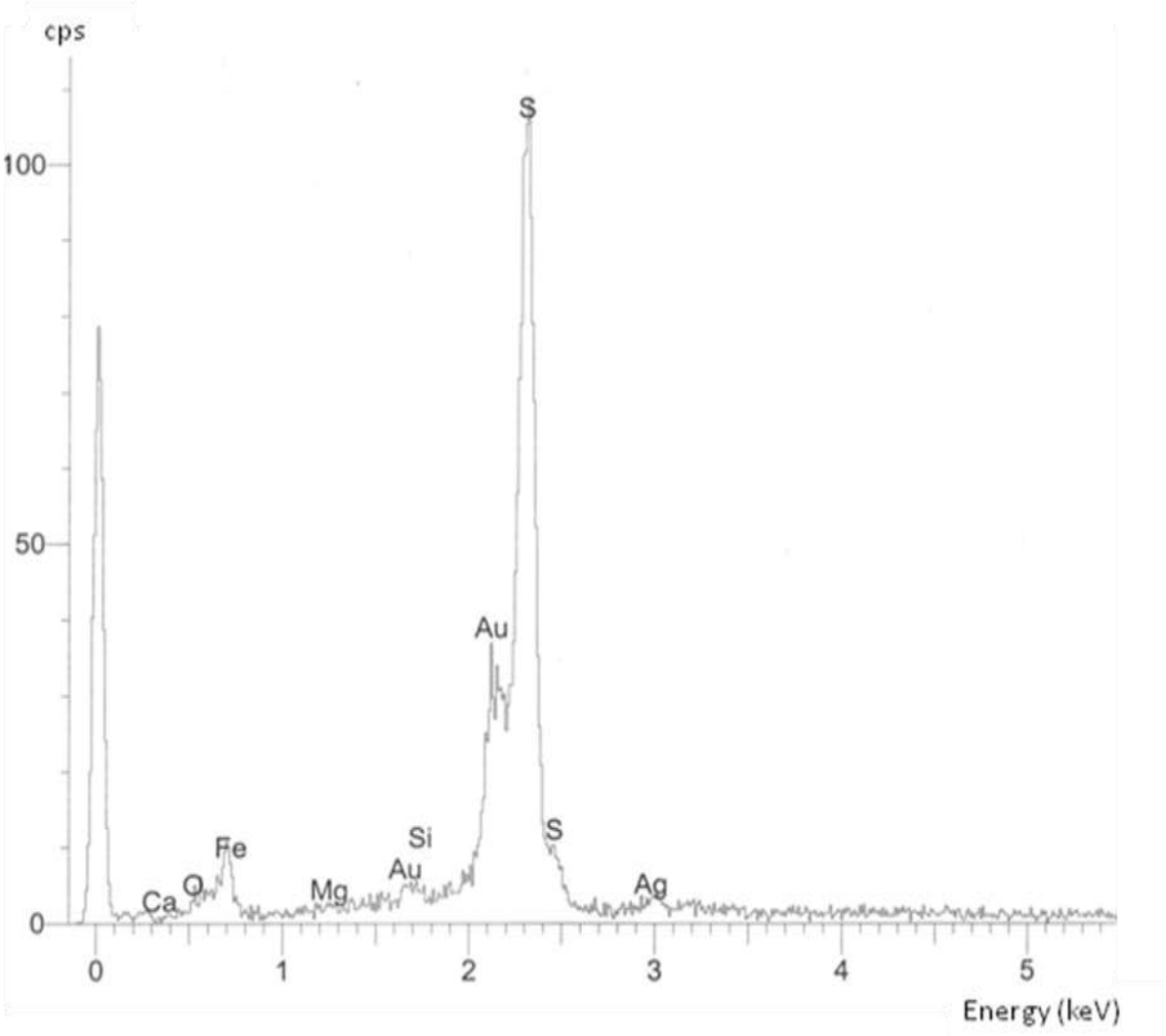

Spectra: 06-10-006

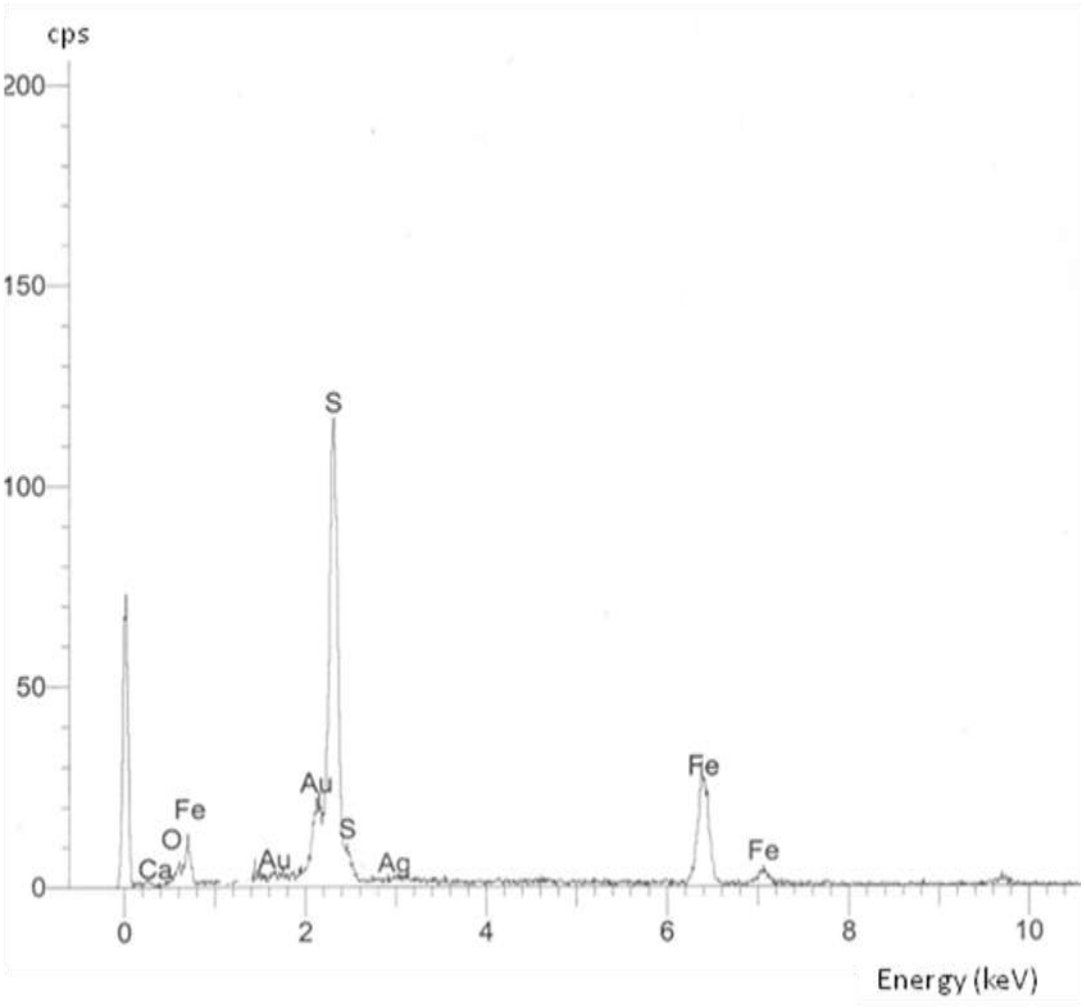

C.2 Clinopyroxene identification

Samples used for Clinopyroxene identification:

Sample Number	Photomicrograph Number	SEMQuant Number
210-308	308-001	05-10-007
210-308	308-001	05-10-008
210-238	238-001	05-10-009
210-238	238-001	05-10-010

SEM analysis of clinopyroxene:

Oxide percentages from SEM anlysis:

Oxide %	05-10-007	05-10-008	05-10-009	05-10-010
SiO2	52.52	52.91	51.72	51.74
Al2O3	1.5	0.75	<mdl	<mdl
FeO	29.01	29.34	36.82	36.82
MnO	<mdl	0.59	1.22	1.17
MgO	5.23	5.37	6.98	6.83
CaO	9.86	11.54	1.51	1.48

Stoichiometric conversion:

Si	1.611239	2.081073	2.106904	2.111475
Al	0.108466	0.034766		
Fe	1.488352	0.964944	0.836148	1.256431
Mn		0.019652	0.042089	0.040435
Mg	0.478349	0.314848	0.423868	0.415487
Ca	0.648121	0.486261	0.065901	0.064705

The SEM analysis indicates the unknown clinopyroxene to be hedenbergite. Hedenbergite is an iron-rich pyroxene. The hedenbergite in this study is commonly weathered and iron-stained, which is reflected in the totals reported by the SEM analysis.

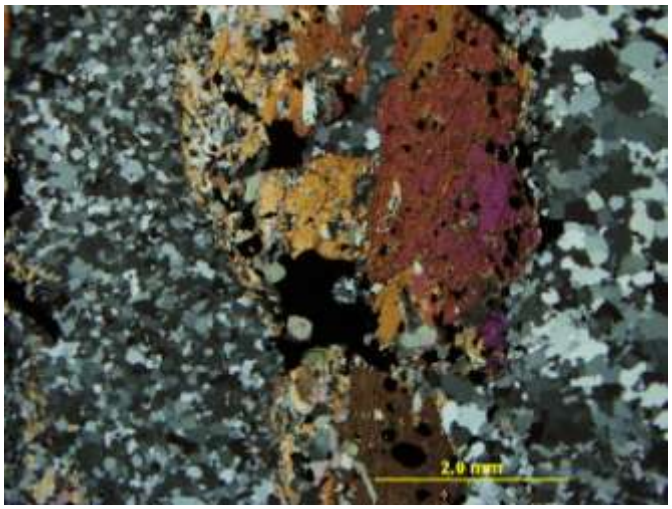

Sample 210-308 (308-001)

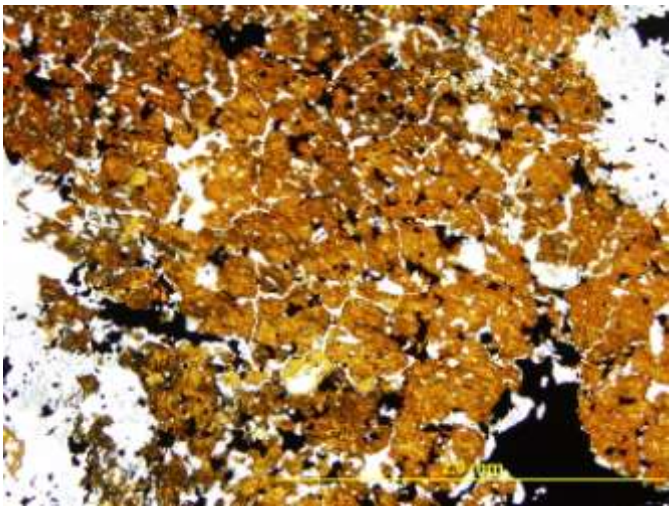

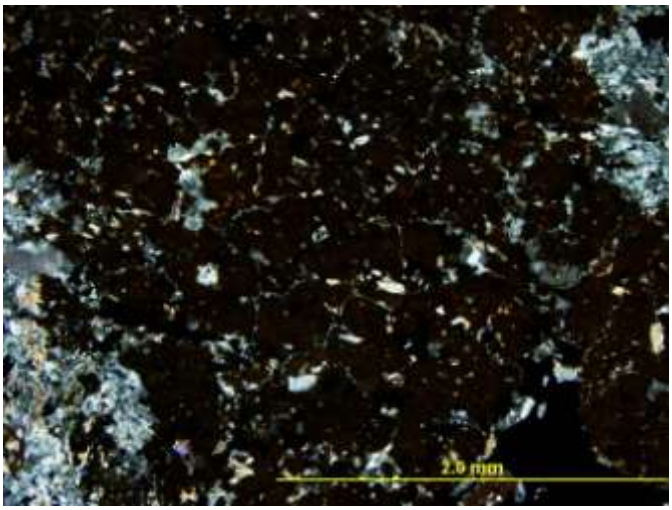

Sample 210-238 (238-001)

C.3 Amphibole identification

Samples used for amphibole identification:

Sample Number	Photomicrograph Number	SEMQuant Number
210-510	510-002	06-10-011
210-510	510-002	06-10-012
210-513	513-016	06-10-013
210-513	513-016	06-10-014

SEM analysis of blue-green amphibole:

Oxide percentages from SEM anlysis:

Oxide %	06-10-011	06-10-012	06-10-013	06-10-014
SiO2	45.76	45.87	44.53	51.54
Al2O3	5.98	5.93	7.8	1.01
FeO	30.79	30.92	30.25	30.65
MnO	0.51	0.47	0.72	0.59
MgO	4.34	4.52	4.36	6.02
CaO	10.93	11.14	10.82	12.02
Na2O	0.81	1.05	0.86	
K2O	0.5	0.37	0.64	

Stoichiometric conversion:

Si	7.443088	7.418274	7.216933	8.092933
Al	1.146326	1.130234	1.489822	0.186906
Fe	4.187641	4.181251	4.099378	4.024247
Mn	0.07025	0.06437	0.09882	0.078456
Mg	1.052288	1.089658	1.053329	1.40908
Ca	1.904588	1.930069	1.878628	2.021993
Na	0.127702	0.164593	0.135097	
K	0.051866	0.038161	0.066149	

The SEM analysis indicates the unknown blue-green amphiboles are ferrotschermakite and ferroactinolite. Both of these are iron-calcium-rich amphiboles. These differ from the iron-rich grunerite which is the most common amphibole in Lithology 2 (grunerite schist) from Musselwhite Mine.

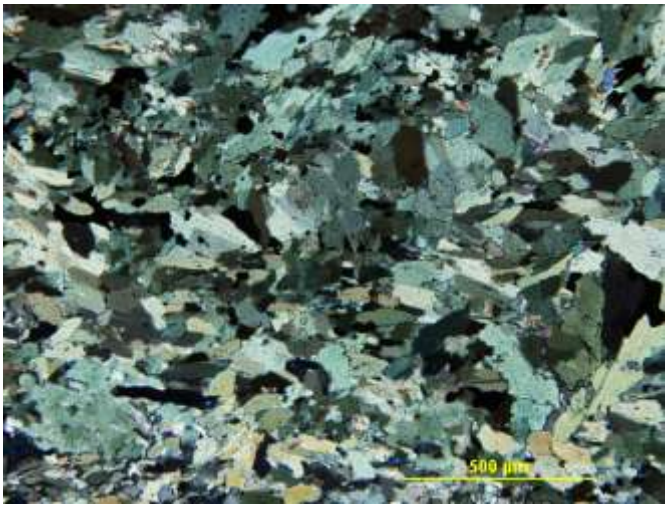

Sample 210-510 (510-002)

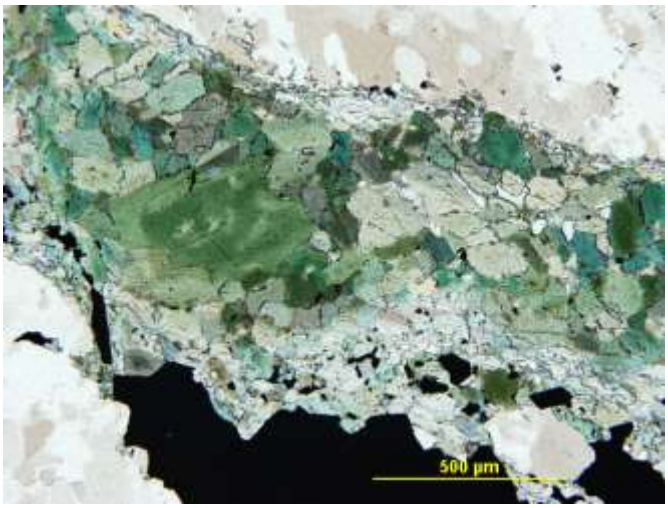

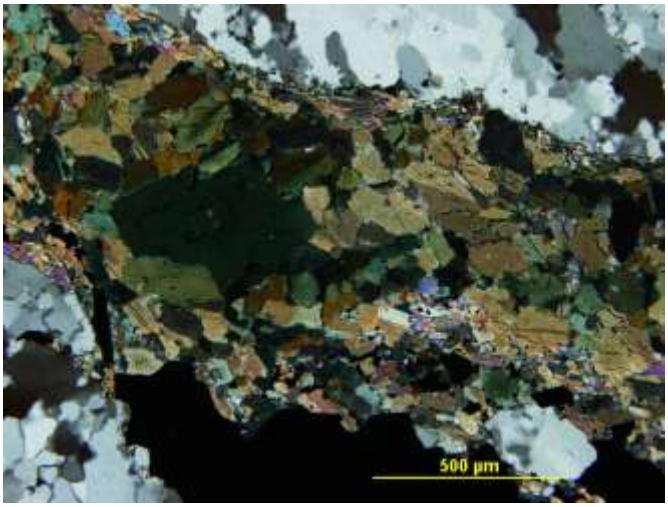

Sample 210-513 (513-016)

Appendix D: Lithology 3, Hammond Reef, quartzofeldspathic schist

D.1: Sample locations (Lithology 3, Hammond Reef, quartzofeldspathic schist)

Sample number:	Drill hole name:	from (m):	to (m):
749-401	br-23	90	90.1
749-402	br-23	64.45	64.5
749-404	br-23	175.5	175.65
749-405	br-122	229.9	230
749-406	br-122	230.3	230.4
749-407	br-29	111.1	111.2
749-409	br-29	116	116.1
749-411	br-117	195	195.1
749-413	br-115	174.9	174.95
749-414	br-98	357.5	357.6
749-415	br-93	107.5	107.6
749-416	br-93	107.7	107.75
749-417	br-38	160.9	160.95
749-418	br-34	51	51.1
749-419	br-34	54	54.1
749-421	br-14	16.5	16.55
749-422	br-79	46.9	46.95
749-423	br-26	99.3	99.4
749-424	br-62	250	250.1
749-426	br-47	171.1	171.2
749-427	br-47	175	175.1
749-432	br-82	124.9	125
749-437	br-19	176.5	176.6
749-438	br-31	153.9	153.95
749-439	br-31	151.93	152
749-441	br-37	19	19.1
749-442	br-125	194.4	194.5
749-445	br-23	90	90.1
749-446	br-98	357.5	357.6
603-451	N/A	N/A	N/A
603-452	N/A	N/A	N/A
603-454	N/A	N/A	N/A
603-455	N/A	N/A	N/A
603-456	N/A	N/A	N/A
603-458	N/A	N/A	N/A

Sample number:	Drill hole name:	from (m):	to (m):
603-459	N/A	N/A	N/A
603-460	N/A	N/A	N/A
603-461	N/A	N/A	N/A
603-462	N/A	N/A	N/A
603-463	N/A	N/A	N/A
603-464	N/A	N/A	N/A
603-465	N/A	N/A	N/A
603-468	N/A	N/A	N/A
603-469	N/A	N/A	N/A
603-470	N/A	N/A	N/A
603-471	N/A	N/A	N/A
603-472	N/A	N/A	N/A
603-473	N/A	N/A	N/A

D.2: Sample descriptions (Lithology 3, Hammond Reef, quartzofeldspathic schist)

Sample:	Sample description (HS: handsample, TS: thin section)	Foliation/ texture:	Gold observed:
749-401	HS: This sample is overall light green in color. Foliation anastomoses around small quartz crystals. There are white to grey quartz veins. Pyrite appears in the darker quartz veins but also occur in the light green matrix close to the quartz vein. TS: The feldspar in this sample has been almost completely altered to muscovite making the matrix a mix of fine grained mica and feldspar. In thin section muscovite defines the foliation with fine grain micas anastomosing around leftover tiny feldspar crystals as well as larger quartz grains. Quartz strain fringes appear around the many of the pyrite crystals, especially the large pyrite crystals (1-2mm).	strong	Yes
749-402	HS: Sample is pink in color distinct feldspar and quartz crystals can be made out. Fine grained mica appears pale green in color and anastomoses through the sample and defines the foliation. TS: A stringer-like cluster of large (1-2mm) brecciated pyrite crystals occur with strain shadows. Carbonate and chlorite can be seen associated with these pyrite clusters. Feldspars are altered but can still be made out, in some even twinning is preserved.	weak	Yes
749-404	HS: This sample is light in color (pink and green). It is well foliated with orange wisps scattered throughout. Pyrite is subhedral appears scattered throughout. Pyrite also appears as stringer orientated with the foliation. TS: Feldspars are altered but in some cases twinning can be observed. Also carbonate appears in this thin section.	moderate	No
749-405	HS: Part of this sample is pale green with very fine grained foliated matrix and cubic pyrite crystals. The rest of the sample appears much less altered; it is pink and pale green in color. TS: In the thin section feldspars are highly altered to mica. Carbonate occurs in the highly altered areas. Strain shadows around pyrite crystals in this sample are made up of both quartz and chlorite	moderate	No

Sample:	Sample description (HS: handsample, TS: thin section)	Foliation/ texture:	Gold observed:
749-406	HS: This sample is very fine grained and foliation is hard to discern. It is light green and pink in color. Ductilely deformed quartz veins can be seen. Alteration varies from looking pervasive to anastomosing around larger (1mm) grains of quartz and feldspar. TS: Feldspars are highly altered to white mica in this thin section. Pyrite appears as stringer-like clusters of pyrite crystals and brecciated pyrite crystals.	weak	Yes
749-407	HS: Sample is pale green to pink in color with grains of quartz and feldspar which appear pink and beige. Very fine grained matrix defines the foliation. Pyrite cubes are scatted through the sample. TS: Feldspars are highly altered but can still be made out. Pyrite appears subhedral and has strain shadows. Note pyrite crystals host inclusions of quartz, feldspar and muscovite.	moderate	No
749-409	HS: Sample is pale green in color with ductilely deformed quartz veins and boudins throughout. Pyrite appears scattered through the sample often nearby quartz veins. TS: Feldspars are almost completely altered to white mica. Pyrite cubes occur stringer-like made up of brecciated and subhedral pyrite crystals aligned with the foliation. The pyrite commonly has quartz strain fringes.	strong	No
749-411	HS: Quartz veins appear ductilely deformed in this sample. Remnants of pegmatite are present in this sample with a large K-feldspar crystal (2cm diameter). Alteration is prevalent in this sample as well and anastomoses around visible quartz grains (1 mm). TS: Feldspar crystals are fairly altered yet twinning can still be made out in many of the plagioclase crystals. Only minor pyrite occurs in this sample.	very weak	No
749-413	HS: This sample is reddish-pink with thick light green to black colored wisp which define the foliation. Pyrite can be seen near the light green to black wisps and is subhedral to anhedral. TS: Only minor stringer-like (cluster of brecciated pyrite aligned with the foliation) and cubic pyrite occur in this thin section. Both quartz and chlorite make up the fringes structures around these pyrite crystals. Feldspars in this thin section are almost completely altered to mica.	moderate	Yes

Sample:	Sample description (HS: handsample, TS: thin section)	Foliation/ texture:	Gold observed:
749-414	HS: Sample is overall pale green in color with areas which appear pink and beige. The very fine grained matrix defines the foliation. Pyrite cubes are scatted through the sample. TS: Feldspars are almost completely altered to mica. Strain fringes of pyrite crystals are fibrous as well as recrystallized.	moderate	Yes
749-415	HS: Sample is pale green to pink in color with quartz and carbonate veins. Subhedral pyrite crystals appear scatted through the sample. TS: Some feldspar crystals remain intact yet most are highly altered. Strain fringe structures commonly occur around the pyrite crystals.	strong	Yes
749-416	HS: Sample is pale green to pink in color with boudins of quartz, quartz veins and carbonate veins scattered through the sample. TS: Stringer-like brecciated pyrite runs through the center of this sample. Feldspars are highly altered in this sample. The fine grained mica defines the foliation.	moderate	Yes
749-417	HS: Sample is pale green to pink in color, very fine grained and well foliated. The sample is rich with cubic pyrite crystals. TS: Strain fringes around pyrite crystals appear fibrous and recrystallized. Feldspars are highly altered sample.	strong	Yes
749-418	HS: Sample is pale green in color with ductilely deformed quartz veins and boudins throughout. Pyrite appears scattered through the sample often nearby quartz. A large quartz vein cuts through this sample and pyrite lines one edge of this vein. TS: Pyrite appears brecciated and clustered near quartz vein in this thin section. Feldspars are highly altered though distinct grains can still be defined.	moderate	Yes
749-419	HS: This sample is overall light green in color. There appears to be many generations of ductilely deformed quartz veins along with likely remnant of pegmatite. Pyrite is subhedral to anhedral and seems to be associated with quartz veins as it appears along the edge of the quartz vein. TS: Feldspar crystals in this sample are highly altered. Stringer-like brecciated and clustered of pyrite occur aligned parallel to the foliation.	moderate	Yes

Sample:	Sample description (HS: handsample, TS: thin section)	Foliation/ texture:	Gold observed:
749-421	HS: Sample is pale green in color, fine grained and well foliated. A pegmatitic area occurs in the center of the sample with very large feldspar and quartz crystals. Euhedral pyrite crystals are scattered throughout the pale green portion of the sample. TS: Highly altered area with larger less altered plagioclase crystals included (likely remnant of pegmatite. Although the feldspar crystals are highly altered some twinned plagioclase is still present.	strong	No
749-422	HS: This sample contains porphyroclasts of quartz and feldspar in the grey to pale green colored matrix. Pyrite occurs stringer-like and in clusters. TS: Most of the pyrite crystals neighbor carbonate in this sample. Also pyrite crystals are subhedral.	no	Yes
749-423	HS: Sample is mostly pale green in color with scattered areas of quartz and feldspar white to beige in color. Foliation is defined by the fine grained mica. Scattered clusters of pyrite occur commonly near quartz. Orange colored veins are likely weathered ankerite. TS: Most of the feldspar crystals are highly altered while others can still be made out and in more rare cases even twinning can be seen.	moderate	Yes
749-424	HS: This sample is well foliated and is overall light green in color. Very fine grained mica defines the foliation which anastomoses around the tiny (1 mm) quartz crystals. Quartz and anchorite veins are present and often appear ductilely deformed. There is an orange color to the sample likely caused by the anchorite weathering. Specks of pyrite can be seen throughout the sample except within the quartz and anchorite veins. TS: Feldspars are almost completely altered to white mica. Subhedral to anhedral pyrite crystals occur scattered through the sample.	moderate	Yes
749-426	HS: Sample is made up of large unaltered areas with other light green altered areas. Subhedral pyrite appears scatted through the altered areas of the sample. Note some of the green areas appear to be chlorite-rich. TS: Chlorite appears in strain shadows of pyrite crystals in this sample, as well as in matrix with muscovite.	no	Yes

Sample:	Sample description (HS: handsample, TS: thin section)	Foliation/ texture:	Gold observed:
749-427	HS: Sample is well foliated with scatted clusters of pyrite. This matrix is very fine grained and pale green to pink in color. TS: Pyrite has many inclusions of carbonate, altered feldspars and mica. Feldspars are highly altered in this sample but some twinning can be seen in plagioclase.	no	Yes
749-432	HS: This sample is pink and dark green in color. It is chlorite rich with clusters of feldspar. TS: Feldspars are highly altered in thin section. Carbonate occurs with the chlorite in thin section.	no	No
749-437	HS: This sample is well foliated with many ductilely deformed white to light grey quartz veins present. Also there are grey veins which are associated with pyrite. Pyrite is abundant but small. It appears commonly as specks throughout the sample and commonly near quartz veins. TS: Sample is very rich in muscovite. Nearly all of the feldspar has been altered to mica. A carbonate vein appears at one end of the sample with chlorite stringers running through it. Pyrite appears subhedral to euhedral in this sample.	weak	Yes
749-438	HS: Sample is pale green in color with quartz veins which appear ductilely deformed. Pyrite crystals appear in clusters sometimes stringer-like orientated parallel to the foliation. This sample is strongly foliated. Feldspars are highly altered and sample appears mica-rich. TS: This sample is a mylonlite with significantly smaller grain size then most other samples. Quartz even appears flatted of elongated and fine grained. Pyrite crystals appear with strain shadows in this sample.	strong	Yes
749-439	HS: This sample is pink and green with irregular shape boudins or orange anchorite-rich areas. Sample is foliated anastomosing around quartz grains. There is no visible pyrite. TS: This sample is mylonitic, rich with fine grained white mica. Quartz appears fine grained; more so than in most other samples but quartz does not appear flattened in this thin section. Nearly all pyrite crystals in this thin section have strain fringes.	strong	No

Sample:	Sample description (HS: handsample, TS: thin section)	Foliation/ texture:	Gold observed:
749-441	HS: Sample contains rounded porphyroclasts of quartz and feldspar with foliated pale green to pink colored matrix anastomosing around the porphyroclasts. TS: Feldspar crystals are highly altered yet appear as distinct crystals in this sample. Only one small pyrite cube appears in this thin section.	weak	No
749-442	HS: Sample is quartz-rich boudins or clusters. The sample is pale green and sometimes pink in color. Foliation can be made out in the feldspar-mica-rich portions. TS: Feldspar crystals are moderately altered yet some twins are preserved. In this thin section only tiny scattered pyrite crystals occur.	no	No
749-445	HS: This sample is light green in color. Foliation anastomoses around small quartz crystals. There are white to grey quartz veins in this sample. The pyrite appears in the darker quartz veins and some occurs in the light green area, although this pyrite is still near quartz veins. TS: Feldspars are highly altered to white mica. Pyrite occur in stringer-like texture with small (<1mm) subhedral crystals aligned parallel to the foliation.	weak	Yes
749-446	HS: Sample is overall pale green in color with pink and beige areas. The very fine grained matrix defines the foliation. Pyrite crystals are scatted through the sample. TS: Pyrite crystals appear as large subhedral crystals as well as stringer-like in brecciated clusters aligned nearly parallel to the foliation. Strain fringes are fibrous as well as recrystallized.	moderate	Yes
603-451	HS: Sample is light pink in color. Grains appear equalgranular (2-3mm). TS: Feldspars are less altered in this sample; twinning can still be made out in many of the crystals.	no	No
603-452	HS: Samples is fine grained. It appears black and white in color. TS: This sample is rich with biotite, quartz and feldspar. The feldspar is only slightly altered in this sample twinning can still be made out in many of the crystals.	no	No

Sample:	Sample description (HS: handsample, TS: thin section)	Foliation/ texture:	Gold observed:
603-454	HS: Sample is made up of quartz and feldspar grains (2mm) with fine grain matrix appearing pale green, pink and black in color. TS: Feldspars in this thin section are fairly altered. Minor epidote appears in this thin section.	weak	No
603-455	HS: Sample appears pink to pale green in color. Feldspars crystals appear altered to white mica which defines a weak foliation. TS: Although feldspars are altered in this sample twinning can still be made out in some of the plagioclase crystals.	weak	No
603-456	HS: This sample is nearly all quartz with tiny grey blebs appearing in bunches. TS: Minor galena occurs in thin section.	no	No
603-458	HS: Sample is orange to pink in color. It appears highly weathered yet some feldspar crystals can still be made out. TS: Iron straining occurs in this thin section. Feldspars are highly altered though distinct crystals can still be determined.	weak	No
603-459	HS: Sample is pink in color. It is fine grained made up mainly of quartz, feldspar and muscovite. TS: Although feldspars are altered in this sample some twinning can still be made out in a few plagioclase crystals.	no	No
603-460	HS: Sample is pink in color rounded quartz and feldspar porphyroclasts appear. TS: This sample is moderately altered. The feldspar crystals can still be made out with some twinning even preserved in plagioclase. Only minor small pyrite crystals occur in this thin section.	no	No
603-461	HS: Sample is highly weathered and orange in color. Unweathered quartz-rich areas also appear. TS: Iron straining from weathering appears in this sample. Feldspars are almost completely destroyed from alteration and weathering.	moderate	No
603-462	HS: Sample is orange in color and highly altered cubic holes appear with some remnants of pyrite left behind. TS: Feldspar crystals are highly altered in this sample, weathering is apparent throughout the sample even pyrite crystals are weathered.	Strong	No

Sample:	Sample description (HS: handsample, TS: thin section)	Foliation/ texture:	Gold observed:
603-463	HS: Sample is pink-orange and pale green in color. It is very well foliated. Fine grained pyrite appears in a dark colored stringer. TS: Sample is highly weathered, iron straining occurs and pyrite crystals have been almost completely weathered away.	Strong	No
603-464	HS: Sample is well foliated with white rounded grains of quartz appearing in a pink matrix. Wispy pale green micas define the foliation. TS: In this sample feldspar crystals can still be made out and even twinning is preserved in some plagioclase crystals.	moderate	No
603-465	HS: Sample is dark in color with small round pink and white grains in a grey to green matrix. TS: Sample is weathered, but feldspar crystals can still be made out.	no	No
603-468	HS: Matrix is pink to green in color. It is very fine grained and foliated. Rounded feldspar and quartz porphyroclasts appear throughout. TS: Feldspar crystals are moderately altered yet distinct crystals can still be made out in this thin section.	moderate	No
603-469	HS: This sample is highly weathered and appears orange in color. Porphyroclasts and veins of quartz occur. TS: Feldspar crystals can still be made out some twinning is even preserved in the plagioclase crystals.	moderate	No
603-470	HS: This sample is highly weathered. It is light orange in color with fractures throughout. TS: Ankerite-rich with quartz veins. Iron-straining appearing throughout the sample. Feldspar crystals are highly altered or weathered.	no	No
603-471	HS: Sample is well foliated and very weathered. It is orange in color and rich with euhedral to subhedral pyrite crystals. TS: Ankerite-rich with quartz veins and Fe-straining appearing throughout the sample. Pyrite crystals are also weathered.	strong	No
603-472	HS: This sample is very well foliated. It is black and white in color. It does not appear altered or weathered. TS: Sample is biotite-rich, feldspars are not very altered twinning can be made out in many of the crystals.	strong	No
603-473	HS: Sample is highly weathered. It is light orange in color with fractures throughout. TS: This sample is ankerite-rich. Feldspar crystals are almost completely destroyed.	moderate	No

D.3: Modal percent based on petrography (Lithology 3, Hammond Reef, quartzofeldspathic schist)

Sample:	Quartz:	Feldspar:	Muscovite/ sericite:	Pyrite:	Carbonate	Chlorite:	Other:
749-401	47	20	30	3			
749-402	41	30	20	5	4	minor	
749-404	42	30	20	3	5	trace	
749-405	30	20	15	5	30	minor	
749-406	40	10	40	5	5	minor	
749-407	40	30	30	minor		trace	
749-409	50	20	30	minor			
749-411	50	30	20	minor			
749-413	40	20	35	5			
749-414	40	15	35	5	5	minor	
749-415	42	30	20	5	3		
749-416	40	25	25	10			
749-417	41	20	35	4			
749-418	50	15	30	5			
749-419	40	20	30	10	minor		
749-421	50	20	30	minor			
749-422	40	20	30	5	5	minor	
749-423	45	25	25	5		trace	
749-424	45	20	30	5	minor		
749-426	37	20	27	3	3	10	
749-427	20	45	20	5	10		
749-432	20	7	15	3	10	40	magnetite: 5
749-437	40	10	30	5	10	5	
749-438	40	15	40	5			
749-439	40	5	50	5			
749-441	45	25	25	minor		5	
749-442	50	30	20	trace			
749-445	50	20	30	minor			
749-446	40	15	35	5	5	minor	
603-451	45	45	10				
603-452	45	45	10				
603-454	40	29	25		4	2	
603-455	50	30	20				
603-456	95		5	trace			Galena: trace

Sample:	Quartz:	Feldspar:	Muscovite/ sericite:	Pyrite:	Carbonate	Chlorite:	Other:
603-458	40	25	35				
603-459	45	35	20				
603-460	50	30	20	minor			
603-461	50	10	40	minor			
603-462	15	20	45	10		10	
603-463	50	20	30	minor			
603-464	50	25	25				
603-465	37	30	30		3		
603-468	45	30	15		minor	10	
603-469	50	35	15				
603-470	10				90		
603-471	40	10	40	5	5		
603-472	45	45	10	trace			
603-473	20	minor	5		75		

*minor indicate less than 5%

*trace indicates less than 1%

D.4: Bands and textures (Lithology 3, Hammond Reef, quartzofeldspathic schist)

sample:	feldspars nearly completely altered to mica	no twinning but feldspar aren't completely destroyed	only plagioclase twinning preserved	microcline twinning preserved		strain shadows present	pyrite brecciated	Pyrite size		flattened or elongated quartz
749-401	X					X	X	0.5-2mm (with tiny as well)		X
749-402		X	X			X		1-2mm		
749-404		X	X			X		0.5-1mm		
749-405	X	X	X			X		0.5-1mm		
749-406	X						X	0.5-1mm		somewhat
749-407		X	X			X		1-2mm		
749-409	X					X		<0.5mm		X
749-411		X	X					tiny		
749-413	X	X						0.5-1mm		
749-414	X					X	X	0.5-2mm		
749-415		X	X			X		0.5-2mm		
749-416	X	X	X			X	X			
749-417	X					X		0.1-1.5mm		
749-418	X					X	X	1mm		
749-419	X					X	X	varies		
749-421	X		X			X		0.1-0.5mm		

sample:	feldspars nearly completely altered to mica	no twinning but feldspar aren't completely destroyed	only plagioclase twinning preserved	microcline twinning preserved		strain shadows present	pyrite brecciated	Pyrite size		flattened or elongated quartz
749-422	X									
749-423		X	X			X		0.5-1mm		
749-424	X					X		0.5mm		
749-426	X	X				X		1mm		
749-427		X	X					0.5-2mm		
749-432	X							0.1-0.5mm		
749-437	X	X						0.1-0.5mm		X
749-438	X					X	X	1mm		X
749-439	X					X		0.1-0.2mm		
749-441		X								
749-442			X					tiny		
749-445	X					X		tiny		
749-446	X					X	X			
603-451			X	X						
603-452			X	X						
603-454		X								
603-455		X	X							
603-456										
603-458	X	X								
603-459		X	X							
603-460			X					0.1-0.5mm		
603-461	X									
603-462	X									
603-463	X					X				

sample:	feldspars nearly completely altered to mica	no twinning but feldspar aren't completely destroyed	only plagioclase twinning preserved	microcline twinning preserved		strain shadows present	pyrite brecciated	pyrite size		flattened or elongated quartz
603-464		X	X							
603-465		X	X							
603-468		X								
603-469		X	X							
603-470	X									
603-471	X					X		0.5-2mm		X
603-472			X	X						
603-473	X									

D.5: Gold occurrences in Lithology 3, Hammond Reef, quartzofeldspathic schist

Sample number:	Gold occurrence number:	Description:
749-401	401-002	Gold appears as an inclusion within quartz, which neighbors a pyrite crystal.
749-401	401-003	Gold occurs in a recrystallized strain fringe; the core mineral is pyrite.
749-401	401-010	Gold appears within a fracture in pyrite.
749-401	401-011	Round gold inclusion appear within pyrite.
749-401	401-012	Gold appears within a fracture in pyrite.
749-401	401-013	Round gold inclusion appears within pyrite.
749-402	402-001	Gold occurs in a recrystallized strain fringe; the core mineral is pyrite.
749-402	402-002	Irregular shaped gold inclusions occur within pyrite with radiating fractures.
749-402	402-003	Gold blebs appear within quartz and carbonate and on the grain boundary between quartz and carbonate.
749-402	402-004	Gold inclusions occur within carbonate and quartz as well on grain boundaries between quartz-quartz and quartz-carbonate.
749-402	402-009	Gold appears on fracture within pyrite as well as an irregular shaped inclusion within pyrite.
749-406	406-001	Gold occurs as an irregular shaped inclusion within pyrite.
749-406	406-002	Gold bleb appears on quartz-quartz grain boundary as well as on the edge of a pyrite crystal surrounded by quartz and carbonate.
749-413	413-001	Gold appears on fracture within pyrite as well as an inclusion within pyrite. Pyrite appears subhedral and brecciated.
749-413	413-002	Round gold inclusion appear within brecciated pyrite.
749-413	413-003	Irregular shaped gold inclusions occur within pyrite which appears brecciated and subhedral
749-413	413-004	Rounded inclusions of gold appear within pyrite.
749-413	413-005	Gold appears within a fracture in pyrite.

Sample number:	Gold occurrence number:	Description:
749-413	413-006	Gold blebs appear within a fracture in brecciated pyrite.
749-413	413-007	Gold appears bordered on three sides by euhedral brecciated pyrite with quartz neighboring the other, the gold appears to fill a fracture in the edge of the pyrite crystal
749-413	413-009	Rounded inclusion of gold within euhedral shaped pyrite.
749-414	414-007	Angular gold bleb occurs within pyrite with radiating fractures on either side of the gold bleb. The pyrite is brecciated, appearing stringer-like though it is made up of many neighboring fractured pyrite crystals.
749-414	414-008	Irregular shaped gold appears within a fracture in subhedral pyrite.
749-414	414-009	Gold blebs appear near a pyrite crystal in a highly altered area.
749-414	414-010	Gold inclusions occur within pyrite.
749-414	414-011	Rounded gold inclusions occur within nearly euhedral pyrite.
749-414	414-012	Inclusion of gold appears in pyrite which occurs in a mass of fractured subhedral pyrite crystals.
749-415	415-001	Gold occurs in a recrystallized strain fringe; the core mineral is a subhedral pyrite crystal.
749-415	415-005	Gold inclusion appear within a nearly euhedral pyrite crystal which hosts inclusions of muscovite.
749-415	415-006	Rounded gold inclusion occurs within pyrite; neighboring the pyrite crystal blebs of gold appear within quartz and carbonate as well as on the grain boundary between quartz and carbonate.
749-415	415-007	Gold blebs appear neighboring magnetite in a very fine grained highly altered area.
749-415	415-008	Irregular shaped inclusion of gold appears within pyrite
749-415	415-009	Gold appears on fracture in pyrite.
749-415	415-010	Gold appears on fractures within subhedral brecciated pyrite.
749-415	415-011	Gold appears in a highly altered area within a small flake of muscovite.

Sample number:	Gold occurrence number:	Description:
749-415	415-012	Gold inclusions occur within a fairly altered plagioclase crystal.
749-416	416-008	Gold occurs within fractures in brecciated pyrite as well as an inclusion. This occurs within a large pyrite crystal neighboring brecciated pyrite crystals.
749-416	416-010	Angular and rounded gold inclusions appear within brecciated stringer-like pyrite.
749-416	416-011	Rounded inclusions of gold occur within pyrite.
749-416	416-012	Rounded inclusion of gold appears within pyrite.
749-416	416-013	Round gold inclusion occurs within brecciated stringer-like pyrite.
749-416	416-014	Gold inclusion appears within brecciated stringer-like pyrite.
749-416	416-015	Gold inclusion appears within brecciated stringer-like pyrite.
749-416	416-016	Gold inclusion within subhedral pyrite crystal.
749-416	416-017	Round gold inclusion occurs within brecciated stringer-like pyrite.
749-416	416-018	Gold inclusion occurs within brecciated stringer-like pyrite as well as gold appearing on fractures within this pyrite.
749-416	416-019	Gold inclusions appear within brecciated stringer-like pyrite.
749-416	416-020	Gold inclusion occurs within brecciated stringer-like pyrite as well as gold appearing on a fracture within this pyrite.
749-416	416-021	Irregular shaped gold inclusion appears within pyrite.
749-416	416-022	Round and irregular shape inclusions appear within pyrite as well as gold on a fracture in this brecciated stringer-like pyrite.
749-417	417-005	Gold appears in a recrystallized strain fringe as well as within the core pyrite crystal. Note that one of the gold blebs within the strain fringe touches the edge of the pyrite crystal.
749-417	417-006	Gold inclusion within subhedral pyrite crystal.
749-417	417-007	Gold inclusion within subhedral pyrite crystal.
749-418	418-007	Gold inclusion within stringer-like brecciated pyrite.

Sample number:	Gold occurrence number:	Description:
749-418	418-008	Gold bleb appears on fracture within stringer-like brecciated pyrite.
749-418	418-009	Gold bleb appears on fracture within stringer-like brecciated pyrite.
749-418	418-010	Gold inclusion within subhedral pyrite crystal.
749-418	418-013	Gold appears on grain boundaries of quartz in highly altered area where carbonate also appears.
749-418	418-017	Angular gold inclusion within stringer-like brecciated pyrite.
749-418	418-018	Gold bleb appears on fracture within stringer-like brecciated pyrite.
749-419	419-001	Gold inclusion within subhedral pyrite crystal.
749-419	419-002	Gold inclusion within pyrite, gold appears neighboring an inclusion of what appears to be galena.
749-419	419-003	Gold occurs as inclusion within pyrite and as a bleb on a fracture in this pyrite crystal.
749-419	419-004	Irregular shaped gold inclusion within pyrite.
749-419	419-005	Gold inclusions within stringer-like brecciated pyrite.
749-419	419-006	Gold appears within a fracture in stringer-like brecciated pyrite as well as an inclusion.
749-419	419-007	Gold inclusions appear within subhedral and fractured pyrite crystal.
749-419	419-008	Irregular shaped inclusions appear within pyrite. A gold bleb also occurs in the recrystallized strain fringe. The pyrite is stringer-like and brecciated, with many strain fringes appearing which are deformed to different degrees.
749-419	419-009	Gold inclusion appears within brecciated stringer-like pyrite.
749-419	419-010	Gold inclusion appears within brecciated stringer-like pyrite.
749-419	419-011	Gold blebs appear on fractures and as inclusions within stringer-like brecciated pyrite.
749-419	419-012	Gold inclusions appear within brecciated stringer-like pyrite.
749-419	419-013	Gold inclusion appears within pyrite; note there are many holes and fractures in this pyrite crystal.

Sample number:	Gold occurrence number:	Description:
749-419	419-014	Gold inclusions appear within brecciated stringer-like pyrite.
749-419	419-015	Gold blebs appear on fractures within stringer-like brecciated pyrite.
749-422	422-003	Gold inclusions appear within brecciated stringer-like pyrite.
749-422	422-004	Gold inclusions appear within subhedral pyrite crystal with holes and inclusions of carbonate and quartz.
749-422	422-006	Gold appears within a fracture in pyrite as well as inclusions.
749-422	422-015	Gold bleb appears on the edge of a pyrite crystal within quartz.
749-422	422-016	Gold inclusions appear within pyrite.
749-422	422-017	Gold inclusions appear within subhedral and fractured pyrite crystal.
749-423	423-001	Irregular shaped gold inclusion within pyrite cluster.
749-423	423-005	Gold bleb appears on the edge of a pyrite crystal within strain fringe.
749-423	423-009	Gold inclusions appear within pyrite, which appears in a cluster of pyrite crystals.
749-423	423-010	Gold appears within strain fringe between two pyrite crystals.
749-424	424-001	Gold appears on grain boundaries and as inclusions within carbonate.
749-426	426-011	Gold bleb appears with magnetite inclusions within subhedral pyrite.
749-426	426-012	Gold inclusion appears within quartz crystal.
749-426	426-013	Irregular shaped gold appears cross cutting a fracture in pyrite which also hosts gold mineralization.
749-427	427-006	Gold bleb appears within an altered feldspar crystal neighbored almost completely by muscovite.
749-437	437-001	Gold blebs appear as inclusions and neighboring fractures in a pyrite crystal. A gold bleb also occurs on the edge of this pyrite crystal surrounded by carbonate.
749-437	437-002	Round gold inclusion appears within subhedral pyrite crystal.

Sample number:	Gold occurrence number:	Description:
749-437	437-003	Gold appears as inclusions within sub-euhedral pyrite crystals. One gold bleb appears on the edge of the larger pyrite crystal surrounded by carbonate. Another gold bleb occurs nearby within the carbonate matrix.
749-437	437-004	Gold appears within fracture in stringer-like brecciated pyrite.
749-437	437-005	Gold inclusions occur within rounded pyrite crystal, one of which neighbors inclusion of galena. This pyrite appears near a cluster of brecciated stringer-like pyrite.
749-438	438-005	Irregular shaped gold inclusion appears within pyrite crystal rich with
749-438	438-006	Gold inclusions appear within stringer-like brecciated pyrite.
749-438	438-007	Gold inclusion appears within subhedral pyrite crystal which also contains other inclusions.
749-438	438-008	Gold inclusion appears within subhedral pyrite.
749-438	438-010	Gold appears within muscovite near a subhedral pyrite crystal.
749-438	438-011	Gold bleb appears within a strain fringe which appears offset, no longer in contact with pyrite but nearby. The strain fringe is identified by the fibrous nature of the quartz.
749-445	445-003	Round gold inclusion within subhedral pyrite.
749-446	446-003	Angular gold bleb occurs within pyrite with radiating fractures on either side of the gold bleb. The pyrite is brecciated appearing stringer-like.

Appendix E: X-ray Diffraction results

E.1: Sample 749-407

Peak List:

Pos. [°2Th.]	Height [cts]	FWHM [°2Th.]	d-spacing [Å]	Rel. Int. [%]	Tip width [°2Th.]	Matched by:
8.8574	6680.82	0.0768	9.9838	100	0.0921	00-046-1409
13.8602	152.12	0.0768	6.38942	2.28	0.0921	00-009-0466
17.7766	885.45	0.1023	4.98959	13.25	0.1228	00-046-1409
19.8384	184.8	0.1535	4.47544	2.77	0.1842	00-046-1409
20.8643	1079	0.0768	4.25766	16.15	0.0921	01-085-0798
22.0517	177.51	0.0768	4.03101	2.66	0.0921	00-009-0466
22.8562	128.13	0.0768	3.89091	1.92	0.0921	00-046-1409
23.5449	172.25	0.0768	3.77863	2.58	0.0921	00-046-1409; 00-009-0466
24.3268	124.92	0.0768	3.65893	1.87	0.0921	00-009-0466
25.4452	187.69	0.1535	3.50058	2.81	0.1842	00-046-1409; 00-009-0466
26.6392	5384.42	0.0768	3.34634	80.6	0.0921	01-085-0798; 00-046-1409
26.8312	1602.07	0.0768	3.32282	23.98	0.0921	00-046-1409
27.7165	304.6	0.0768	3.21867	4.56	0.0921	00-046-1409
27.9328	707.59	0.1279	3.19424	10.59	0.1535	00-046-1409; 00-009-0466
29.8195	222.24	0.1279	2.99629	3.33	0.1535	00-046-1409
30.7983	98.3	0.1535	2.90326	1.47	0.1842	
31.2049	207.89	0.1279	2.86635	3.11	0.1535	00-046-1409; 00-009-0466
31.9758	125.65	0.1791	2.79899	1.88	0.2149	00-046-1409; 00-009-0466
33.0258	224.15	0.1023	2.71236	3.36	0.1228	
34.969	243.88	0.2047	2.56596	3.65	0.2456	00-009-0466
36.0097	110.97	0.2047	2.49416	1.66	0.2456	00-046-1409; 00-009-0466
36.5277	396.55	0.0768	2.45997	5.94	0.0921	01-085-0798; 00-009-0466
37.6092	70.05	0.307	2.39168	1.05	0.3684	00-009-0466
39.446	273.33	0.0768	2.28444	4.09	0.0921	01-085-0798; 00-009-0466
40.27	164.04	0.0768	2.23958	2.46	0.0921	01-085-0798

40.7751	58.12	0.1535	2.21299	0.87	0.1842	
42.4336	332.29	0.0768	2.13026	4.97	0.0921	01-085-0798; 00-009-0466
45.4133	456.51	0.1535	1.99718	6.83	0.1842	00-046-1409; 00-009-0466
45.8487	99.52	0.1535	1.97922	1.49	0.1842	01-085-0798; 00-009-0466
47.3924	39.76	0.1535	1.91829	0.6	0.1842	
48.1171	29.27	0.307	1.89108	0.44	0.3684	00-009-0466
50.1207	703.75	0.0624	1.81858	10.53	0.0749	01-085-0798; 00-009-0466
51.1364	57.09	0.2047	1.78629	0.85	0.2456	00-009-0466
54.8703	142.04	0.1535	1.67324	2.13	0.1842	01-085-0798; 00-046-1409
55.7698	71.77	0.2558	1.64837	1.07	0.307	00-046-1409
59.9424	501.68	0.0936	1.54194	7.51	0.1123	01-085-0798
60.1141	235.91	0.0936	1.54177	3.53	0.1123	
61.6083	81.23	0.312	1.50418	1.22	0.3744	
64.0912	48.41	0.4992	1.45177	0.72	0.599	01-085-0798
65.4626	21.17	0.9984	1.42463	0.32	1.1981	
67.7269	208.19	0.0936	1.38241	3.12	0.1123	01-085-0798
68.1293	278.9	0.0936	1.37522	4.17	0.1123	01-085-0798
68.3087	274.25	0.0936	1.37204	4.11	0.1123	01-085-0798
69.4708	53.09	0.3744	1.35191	0.79	0.4493	00-046-1409
75.6362	71.59	0.1248	1.25628	1.07	0.1498	01-085-0798
79.8676	91.36	0.1248	1.20003	1.37	0.1498	01-085-0798
81.4627	73.7	0.156	1.18051	1.1	0.1872	01-085-0798
83.8987	22.78	0.9984	1.15233	0.34	1.1981	01-085-0798
90.7981	78.31	0.0936	1.08186	1.17	0.1123	
98.7153	45.1	0.1872	1.01517	0.67	0.2246	

Identified Patterns List:

Ref. Code	Score	Compound Name	Displacement [°2Th.]	Scale Factor	Chemical Formula
01-085-0798	67	Quartz	-0.01	0.795	Si O2
00-046-1409	43	Muscovite, vanadian barian	-0.044	0.302	(K , Ba , Na)0.75 (Al , Mg , Cr , V)2 (Si , Al , V)4 O10(O H , O)2
00-009-0466	35	Albite, ordered	0.008	0.094	Na Al Si3 O8

Spectrum can be found in Chapter 3, Figure 3.3.4.

E.2: Sample 749-418

Peak List:

Pos. [°2Th.]	Height [cts]	FWHM [°2Th.]	d-spacing [Å]	Rel. Int. [%]	Tip width [°2Th.]	Matched by:
8.8614	1968.48	0.1023	9.97936	39.5	0.1228	00-001-1098
12.5278	148.85	0.0768	7.06582	2.99	0.0921	
13.864	382.95	0.0768	6.38769	7.68	0.0921	00-009-0466
17.7756	261.24	0.0768	4.98987	5.24	0.0921	00-001-1098
19.8317	144.79	0.2047	4.47693	2.91	0.2456	00-001-1098
20.8726	1070.12	0.0768	4.25598	21.47	0.0921	01-085-0797
22.06	442.03	0.1023	4.02951	8.87	0.1228	00-009-0466
23.0814	122.55	0.1279	3.85346	2.46	0.1535	00-009-0466; 00-001-1098
23.5566	443.07	0.1023	3.77679	8.89	0.1228	00-009-0466
24.3213	314.89	0.0768	3.65975	6.32	0.0921	00-009-0466
25.4416	151.13	0.2047	3.50107	3.03	0.2456	00-009-0466; 00-001-1098
26.6501	4983.65	0.1023	3.34499	100	0.1228	01-085-0797; 00-001-1098
27.7154	431.32	0.0768	3.21879	8.65	0.0921	
27.9355	1965.75	0.1279	3.19393	39.44	0.1535	00-009-0466; 00-001-1098
28.3308	229.35	0.1023	3.15026	4.6	0.1228	00-009-0466
30.2101	211.37	0.1791	2.95844	4.24	0.2149	00-009-0466
30.5075	256.47	0.0768	2.93027	5.15	0.0921	00-009-0466
30.792	452.74	0.1279	2.90384	9.08	0.1535	
31.2279	226.09	0.1023	2.86429	4.54	0.1228	00-009-0466; 00-001-1098
32.0793	80.17	0.2047	2.79019	1.61	0.2456	00-009-0466; 00-001-1098
35.0026	216.84	0.2303	2.56357	4.35	0.2763	00-009-0466; 00-001-1098
36.5324	315.61	0.0768	2.45966	6.33	0.0921	01-085-0797; 00-009-0466
37.6437	59.51	0.5117	2.38957	1.19	0.614	00-009-0466; 00-001-1098
38.8471	50.17	0.1535	2.31827	1.01	0.1842	00-009-0466
39.4463	197.44	0.1023	2.28442	3.96	0.1228	01-085-0797; 00-009-0466; 00-001-1098
40.2791	125.21	0.0768	2.23909	2.51	0.0921	01-085-0797

41.0656	47.66	0.4093	2.19801	0.96	0.4912	
42.4554	310.46	0.0768	2.12922	6.23	0.0921	01-085-0797; 00-009-0466; 00-001-1098
45.4568	156.47	0.1535	1.99537	3.14	0.1842	00-009-0466; 00-001-1098
45.7834	189.72	0.0768	1.98189	3.81	0.0921	01-085-0797; 00-009-0466
48.1533	57.94	0.2047	1.88974	1.16	0.2456	00-009-0466
50.1249	560.5	0.0624	1.81843	11.25	0.0749	01-085-0797; 00-009-0466
51.1204	99.5	0.0768	1.78681	2	0.0921	00-009-0466
54.8662	144.43	0.0768	1.67336	2.9	0.0921	01-085-0797
59.9514	293.38	0.0936	1.54173	5.89	0.1123	01-085-0797
60.116	128.03	0.0936	1.54172	2.57	0.1123	
61.5801	59.28	0.3744	1.5048	1.19	0.4493	
64.0688	38.92	0.3744	1.45222	0.78	0.4493	01-085-0797
65.6604	14.62	0.9984	1.42082	0.29	1.1981	01-085-0797
67.7337	195.44	0.1248	1.38229	3.92	0.1498	01-085-0797
68.1321	206.69	0.0936	1.37517	4.15	0.1123	01-085-0797
68.3069	193.19	0.0936	1.37208	3.88	0.1123	01-085-0797
69.5517	54.72	0.3744	1.35053	1.1	0.4493	
75.6512	90.52	0.1248	1.25607	1.82	0.1498	01-085-0797
80.0248	24.99	0.7488	1.19806	0.5	0.8986	01-085-0797
81.4717	82.78	0.1248	1.1804	1.66	0.1498	01-085-0797
90.8079	53.22	0.2496	1.08177	1.07	0.2995	

Identified Patterns List:

Ref. Code	Score	Compound Name	Displacement [°2Th.]	Scale Factor	Chemical Formula
01-085-0797	65	Quartz	-0.007	0.746	Si O2
00-009-0466	54	Albite, ordered	0.034	0.425	Na Al Si3 O8
00-001-1098	27	Muscovite	-0.002	0.12	H2 K Al3 (Si O4)3

Spectrum can be found in Chapter 3, Figure 3.3.5.